Aspects of Karroo Vulcanicity in the Komatipoort area Lebombo

by

C.T. LOGAN

Submitted in partial fulfilment of the requirements for the Degree of Doctor of Philosophy in the Department of Geology, University of Natal.

Durban, 1979

I hereby declare that the dissertation entitled "Aspects of Karroo Vulcanicity in the Komatipoort Area" is my own work and has not been submitted as a thesis for any other degree.

C. T. Logan

December 1979.

ABSTRACT

The petrology, mineralogy and geochemistry of the Karroo-age basaltic and rhyodacitic volcanics present in the Lebombo Belt near Komatipoort, Eastern Transvaal, Republic of South Africa are described.

The volcanics comprise a succession of extrusives within the Komatipoort area, consisting of:

(3) Rhyodacitic lavas and tuffs

(2) Basalts

(1) Olivine Basalts.

These volcanics dip eastwards at angles between 10° and 40°, with dips increasing as the Eastern boundary of the area, the Mozambique border, is approached. Further Karroo-age volcanics, constituting the upper part of this succession, lie across the border in neighbouring Mozambique.

Various intrusives, similar in composition to the extrusives, are also present in the area, commonly as north-south trending dykes forming part of a large dyke-swarm. These, as elsewhere in the Lebombo, are considered to be feeders to the extrusives. Three relatively major intrusions occur in the area, the largest being the Komatipoort Intrusion, here interpreted as a 700m thick, sub-concordant, composite sheet-like body, consisting of five major lithological units. From the base upwards these are:- unit 1 - olivine gabbro, unit 2 - igneously laminated gabbro, unit 3- granophyric gabbro, unit 4 - granophyre, unit 5 - feldspathic gabbro. The olivine gabbro, the granophyre and the feldspathic gabbro appear to form separate intrusive bodies, but the igneously laminated gabbro and the granophyric gabbro, could represent the products of in situ differentiation. If so, the granophyric gabbro has suffered subsequent disturbance as shown by evidence including a homogeneous composition, reaction and corrosion textures and the presence of deformed pyroxene grains, which are described in detail.

Another major intrusive of probable Karroo age is the Crocodile River Intrusion, which occurs to the north-east of the main mapped, and represents the southern-most end of a north-

south trending line of mafic intrusives, which parallel the Lebombo for approximately 200 km. The intrusion here has a dyke-like form, and shows evidence of fractionation by crystal settling.

A smaller, obviously composite intrusion occurs near the base of the basaltic sequence in the Komatipoort area, (the Basal Intrusion).

Representative samples of a variety of extrusive and intrusive rock types have been analysed. These analyses include major and trace element determinations of a series of samples of the major units of the Komatipoort Intrusion. In addition, analyses of a number of minerals from several different rock types occurring in the Komatipoort Intrusion, are presented. The analytical data available for the Komatipoort volcanics confirms the previously known southward variation in the geochemistry of the basalts and the presence of both a high and a low-Mg basalt series in the Komatipoort area.

The majority of the basic rocks in the Komatipoort area belong to the low-Mg series. Compositional variation in this series may be explained largely by low-pressure fractionation of olivine and pyroxene only, despite the presence of abundant plagioclase phenocrysts. Some of the variation in the high-Mg series basalts can be explained by the fractionation of olivine, and what appear to be relatively highly fractionated rocks formed in this manner occur in the area.

The Lebombo volcanics in general display a bimodal silica distribution and rocks with an intermediate silica content are rare. In the Komatipoort area intermediate rocks do occur in the form of two classes of granophyre, (high and low silica varieties), present in the granophyre unit of the Komatipoort Intrusion. Liquid immiscibility is a possible mechanism for the formation of the two types of granophyre, and a widespread development of this process in intermediate magmatic liquids could provide an explanation for the scarcity of rocks of this composition in the Lebombo belt.

Relatively few analyses of the rhyolitic volcanics are presented in this study, but it appears possible that those available could be representative of two processes, firstly, partial melting of the

lower crust or upper mantle, and secondly, fractionation by crystallisation of the commonly observed phenocryst phases,(feldspar, pyroxene, quartz, magnetite), or addition of these phases to the magma.

TABLE OF CONTENTS

INDEX TO TABLES

INDEX TO FIGURES

PAGE NO.

INDEX TO PLATES

ASPECTS OF KARROO VULCANICITY IN THE KOMATIPOORT AREA, LEBOMBO

1 INTRODUCTION

The Komatipoort area lies approximately midway along the Lebombo tectonic-volcanic belt, a major geological feature in Southern Africa, consisting of easterly dipping, monoclinally flexured volcanic rocks and subordinate sediments of the Karroo Supergroup. This belt, approximately 50 km wide and 700 km in length extends along the eastern borders of the Republic of South Africa and Swaziland, in a roughly north-south direction, (fig 1), from a point just north of the town of Empangeni, in the south, to the Limpopo River in the north. In the north these rocks join the outcrops of the Nuanetsi area of Rhodesia and continue in a north-easterly direction to the Buzi Valley in Mozambique. According to du Toit (1954), the volcanics terminate against a major oblique fault in the south.

The lavas and intrusives present in the belt have been assigned to the Lebombo Stage of the Stormberg Series, (Stratten 1965), forming a part of the extensive Karroo volcanic province which is widely distributed in Southern Africa.

2 THE KARROO VOLCANIC ROCKS

The Karroo -age volcanics of the Stormberg Series, as described by Walker and Poldevaart, (1949), are the climax to a prolonged period of sedimentation in a large, gradually subsiding basin, centered approximately around Lesotho. During this period depositional conditions changed gradually from glacial through lacustrine and swampy until, towards the close of Karroo times, a period of general aridity occurred. Large thicknesses of Dwyka, Ecca and Beaufort sediments accumulated near the centre of the basin during the Karroo period and these are capped by the aeolian Cave Sandstones. Onto the Cave Sandstones in turn, the Stormberg volcanics were erupted. The thickness of all of the sediments however, decreases markedly to the north-east, where the margin of the basin is downfolded by the easterly-dipping monoclinal flexure which forms the Lebombo belt.

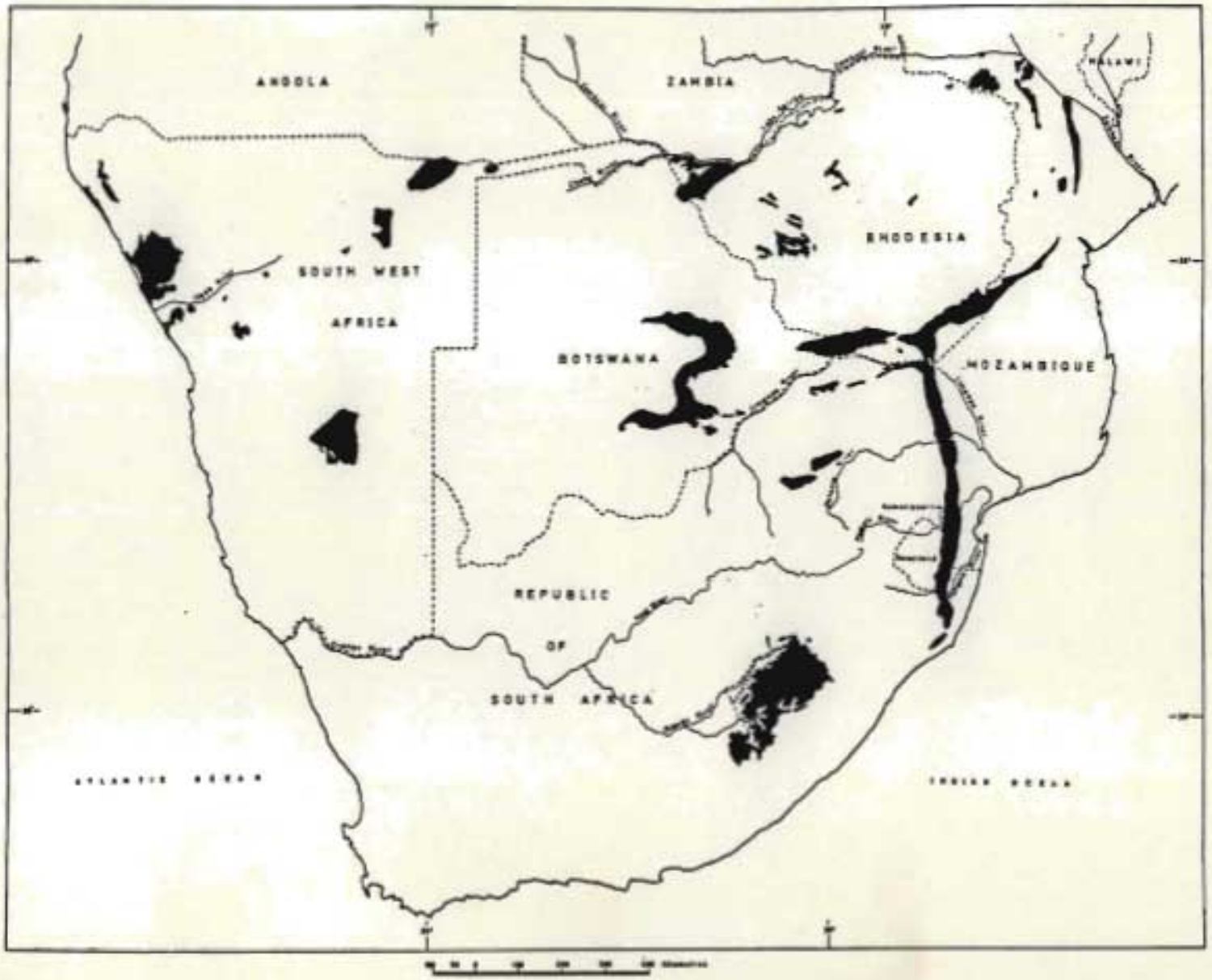

Figure 1 Distribution of Karroo Volcanics in Southern Africa.

A general stratigraphic table is shown in Table 1 and the present distribution of Karroo volcanics in Southern Africa is shown in fig. 1.

As may be expected from volcanics showing such a widespread distribution, variations in geochemistry have been noted. The volcanics present in the centre of the sub-continent are essentially tholeiitic flood basalts and show relatively minor variations in geochemistry, however, the Karroo volcanics occurring at both the western and eastern continental margins are more diverse in composition. In the monoclinally warped eastern part of the province, (the Lupata and Nuanetsi areas in Rhodesia and the Lebombo belt in Southern Africa), rock types ranging from nephelinites through olivine tholeiites to dacites and rhyolites, are developed in some abundance. General accounts of these rocks have been given by du Toit (1954), Walker and Poldervaart (1949), Haughton (1963) and latterly by Cox (1970), who summarised the sedimentary, tectonic and volcanic evolution of Southern Africa during the Karroo period.

These descriptions indicate that, within the Lebombo belt, the volcanics tend to form a triple series consisting of a lower tholeiitic succession, overlain by rhyolitic and dacitic lavas, which are themselves followed by a further basaltic sequence in places, In the northern part of the Lebombo belt an initial lower alkaline succession has been noted.

For example, Cox et al. (1965), have described the volcanic rocks in the Nuanetsi area, and south of this point near the Letaba river the succession has been described by du Toit (1929) and by Lombaard (1952). Additional investigation has been carried out by Saggerson and Logan (1970), on the volcanics of the adjacent Olifants river area. In each of these localities, early nepheline bearing rocks are followed by olivine-rich extrusive and hypabyssal rocks, which in turn are succeeded by olivine-free basalts and their intrusive equivalents. These are overlain by rhyolitic extrusives interbedded with subordinate tholeiitic flows and finally by a sequence of late tholeiitic basalts and associated intrusives. In the Nuanetsi area and again in the little Lebombo to the east in Mozambique, a late alkaline phase is also known (de Assunção et al. 1961).

TABLE 1

The Karroo Stratigraphic Succession*

Supergroup	Series	Sub-division	Rock type	European Equivalent
Karroo	Stormberg	Drakensberg Volcanics	Basalts, limburgites, rhyodacites, pyroclasts, granite	Rhaetic
		Cave Sandstone formation Red Bed Formation	Sandstone, shale, mudstone, marl	Late Triassic
	Beaufort		Shale, sandstone, mudstone, limestone	Late Permian to mid Triassic
	Ecca		Shale, sandstone, grit, coal	Early to mid Permian
	Dwyka		Tillite, sandstone, shale	Late Carboniferous

After Truswell, (1967) and King (1962)

*As no definite sub-division of the Karroo Supergroup has, as yet, been produced by the South African Committee for Stratigraphy, the traditional terminology is employed here.

In contrast, south of the Komatipoort area in Swaziland, members of the Swaziland Geological Survey (Urie and Hunter, 1963) have described the simpler tholeiitic basalt-rhyolite-tholeiitic basalt succession and a similar sequence was recorded by Stratten (1965) in the Natal Lebombo. In all these areas the upper part of the Karroo volcanic succession lies across the border in the neighbouring territory of Mozambique and usually includes a large portion of the rhyolitic sequence and the late tholeiitic extrusives.

At Komatipoort, du Toit (1929) has described the occurrence of tholeiitic and rhyolitic lavas only, which form a succession resembling that found in the southern Lebombo (Swaziland and Natal). Near the contact between the Stormberg basalts and sandstones, he does, however, mention finding a boulder of limburgite. In addition Lombaard (1952) has described doleritic and microgranitic dyke rocks from the Komatipoort area. The stratigraphic succession in the Komatipoort area, as determined during the present investigation is shown in Table 2.

The thickness of the Stormberg volcanic succession has been found to vary; in Lesotho for example, the lavas are only 500 m thick, but much greater thicknesses have been recorded in the Lebombo and Nuanetsi areas. Cox et al. (1965) indicate a minimum thickness of 8 500 m for the Karroo lavas in the Nuanetsi area and Cox (1970) has suggested that about 9 000 m of volcanics may be present in the Southern Lebombo.

Wachendorf (1971) has estimated a thickness of 12 600 m for the total volcanic succession in a cross-section from Northern Swaziland to Maputo.

Estimates of thickness of the lower basalts only, vary with position along the length of the Lebombo, ranging from 1 500 to almost 3 000 m. For the overlying acid lavas du Toit (1929) has suggested a thickness of 5 000 m. No estimates of thickness could be located for the discontinuous upper basalts, although an estimate made from the map presented by de Assunção et al. (1961) suggests a thickness of 2 000 to 3000 m.

TABLE 2

Stratigraphic Succession in the Komatipoort area

Age				Rock type	Approximate thickness meters	Intrusive rocks	
Karroo Super-group	Stormberg Series	Drakensberg Volcanics	Upper suite	Rhyolites, dacites and tuffs with interbedded basalts	500	Felsite and breccia dykes	Dolerite Dykes
			Conformable junction				
			Middle suite	Basalts with intercalated rhyolitic lava flows at the top	1 600	Felsite dyke Granophyre, basic intrusive masses	
				Olivine basalts	15		
			Conformable junction				
		Cave Sandstone formation		Yellow or buff fine-grained sandstones	30		

An examination of several traverses across the Lebombo by a joint expedition from the Swaziland, Mozambique and South African Geological Surveys (Haughton, 1963) indicated that the 5 000 m quoted above for the acid volcanics may be misleading due to the presence of basaltic flows interbedded with the acid volcanics. These interbedded basalts were considered to reduce significantly the volume of truly rhyolitic material.

3 PREVIOUS WORK IN THE KOMATIPOORT AREA

Several geologists have worked in the area previously, but no detailed account of the geology has been given. Earliest mentions of the Lebombo volcanics are made by Cohen (1875) who crossed the Lebombo some 20 km south of Komatipoort, and Molengraaff (1897) who briefly described the Komatipoort area, regarding the Karroo sediments as a downfaulted strip of the 'coal formation of the highveld'. Later Kynaston (1907), who was mainly concerned with the potential of the area as a coalfield, completed the first, small-scale geological map of the area between Komatipoort and the Swaziland border and provided a general description of the volcanics. A.L. du Toit (1929) summarised the salient features of the geology of the area, whilst describing the whole of the Lebombo belt. In his account of the structure of the area he discussed the petrography and origin of the basalts, rhyolites and dyke rocks, including with the latter a mention of the large gabbro intrusion at Komatipoort. In his description of the gabbro body, he notes an east-west variation from gabbro to diorite, and comments on vesicular varieties of the latter rock type. He suggested, both in the text and in the cross-section drawn east-west through Komatipoort, that the body was a multiple dyke, however, the present work offers a different interpretation.

Lombaard (1952) working on the Karroo lavas and intrusives in the Republic of South Africa, collected samples from the area and gave a broad summary of the mineralogy of the major local rock types, but did not concern himself with the gabbro body. Venter (1954) of the Geological Survey mapped the area between Komatipoort and Swaziland on a reconnaissance

basis and gave a brief description of the rock types in the area in an unpublished Geological Survey Report. Like du Toit, he concluded the gabbro body was more likely to be a multiple dyke than a differentiated sill. However, both he and du Toit, were engaged in work on a broad scale and neither attempted to map the body nor to give a detailed description of the rock types comprising it.

4 PRESENT INVESTIGATION

4.1 Field Study

One of the main objectives of this investigation was a detailed petrographical study of the intrusive gabbroic body noted by du Toit (1929) at Komatipoort. In addition the Komatipoort area was of interest because of the transitional nature of the basic lavas which occur there. The area lies virtually midway between the tholeiitic southern portion of the Lebombo belt and the northern extension of the range, where, in addition to tholeiitic basalts, alkali-rich rock types, are present.

Geological mapping of the area was carried out on a scale of 1:18 000 during a total period of five months spent in the field. Observations were recorded directly on aerial photographs of this scale and details of geology were subsequently transferred to a topo-cadastral map of the area which was then photographically reduced to a scale of 1:36 000. While mapping the area a representative suite of specimens was collected for laboratory study.

The gabbroic intrusion was systematically sampled, where possible at close intervals along continuous traverses designed to provide cross-sections of the intrusion, and these samples were examined in detail in the laboratory.

4.2 Laboratory Study

A total of approximately six hundred thin sections were prepared from

samples of volcanic rocks and these were examined by the usual microscope techniques. Thirty-seven new analyses for major elements were made of rocks from the area; of these thirty-two were analysed by the National Institute of Metallurgy in Johannesburg and the other five were performed by the author using a Tectron AA3 atomic absorption spectrometer. In addition, ten of the samples submitted to the National Institute for Metallurgy were analysed for Cu and Cr. A number of mineral grains were analysed by the National Institute for Metallurgy using an electron microprobe analyser, and at a late stage in the investigation U, Th, Rb, Sr, and K values for a representative series of rocks from the Komatipoort Intrusion were made available by Professor Erlank of the University of Cape Town.

Details of the various Laboratory techniques used in this study are given in Appendix 1.

5 THE KARROO VOLCANIC ROCKS IN THE KOMATIPOORT AREA

During the present investigation the sequence of lavas in the Komatipoort area was found to consist of:

		Thickness
(i)	Rhyo-dacites and interbedded tholeiites	500 m
(ii)	Andesine basalts and dacites	5 to 10 m
(iii)	Tholeiitic basalts	1000 to 1600 m
(iv)	Olivine basalts	5 to 20 m

Across the border in Mozambique a further thickness of rhyo-dacites occur together with a succession of overlying late tholeiitic extrusives which are associated with subordinate acid volcanics and alkaline lavas. These rocks were originally described by de Assunção et al.(1961) who do not give any estimate of the thickness of the succession however, more recently Wachendorf (1971) suggested a thickness of some 12 600 m.

The minor quantities of olivine-rich rocks present at the base of the volcanic succession at Komatipoort suggest that the area is transitional between the alkaline and olivine basalt-tholeiite-rhyolite-tholeiite sequence of the Northern Lebombo and the tholeiite-rhyolite-tholeiite succession that has been described from the Southern Lebombo.

5.1 The Olivine Basalts

The olivine basalts and their intrusive equivalents are confined to a narrow ill-defined band, extending north-south through the area directly above the contact between the Karroo volcanics and the underlying sedimentary series.

They are dense, black, fine-grained rocks, that weather freely, yielding poor exposures usually confined to man-made excavations. A thickness of the order of 5 to 20 m is suggested for the olivine basalts, although the accuracy of the estimate is probably low, due both to their poor

exposure and to the ill-defined nature of the sedimentary-volcanic contact.

5.1.1 Petrography

Variations in grain size and texture characterise the olivine basalts which range from glassy types bordering on limburgites, through variolites, to more coarsely crystalline varieties, indistinguishable in thin section from rocks composing the equivalent feeder dykes.

The olivine basalts usually consist of a subtranslucent to opaque, dark glassy groundmass in which abundant acicular plagioclase crystals (0,1-0,6 mm in length) are set. These crystals are frequently arranged in sub-radiating groups and thus many of the finer grained rocks may be described as variolitic. In the coarser-grained types, occasional large plagioclase or clinopyroxene phenocrysts may be present.

Scattered through the glassy groundmass are very small (up to 0,1 mm), euhedral crystals of clinopyroxene which sometimes occur in glomero-porphyritic clusters. Occasional large, (5 mm) , partly to completely altered olivine phenocrysts with a former subhedral to euhedral habit are also present (Plate 1, p 12).

Ore minerals of four types were observed in the olivine basalts viz., magnetite, ilmenite, pyrite, and chalcopyrite. Ilmenite is the most conspicuous of these minerals, usually forming comb-like structures or, less commonly, needle-like crystals, varying from 0,1 to 0,2 mm in length. Exsolution products are not present. Magnetite occurs as interstitial grains, set in the glassy groundmass commonly present in these rocks. Although the grains range from 0,05 to 0,15 mm in diameter the larger grains are not common. Pyrite and chalcopyrite occur as similar tiny, irregular, interstitial patches approximately 0,05 mm in diameter, with pyrite always present in excess of chalcopyrite. Amygdales are not common in the olivine basalts but a few small amygdales up to 0,5 mm in diameter

PLATE 1

1 Olivine Basalt. Large, partially altered olivine phenocryst set in a ground mass of euhedral to subhedral clinopyroxene grains, and acicular plagioclase crystals. Ore minerals (black) occur both as irregular patches and tiny needle-like crystals. (Transmitted light, X96.)

2 Basalt. Plagioclase phenocryst set in fine grained ground mass of plagioclase, clinopyroxene and ore minerals. (Transmitted light, X60.)

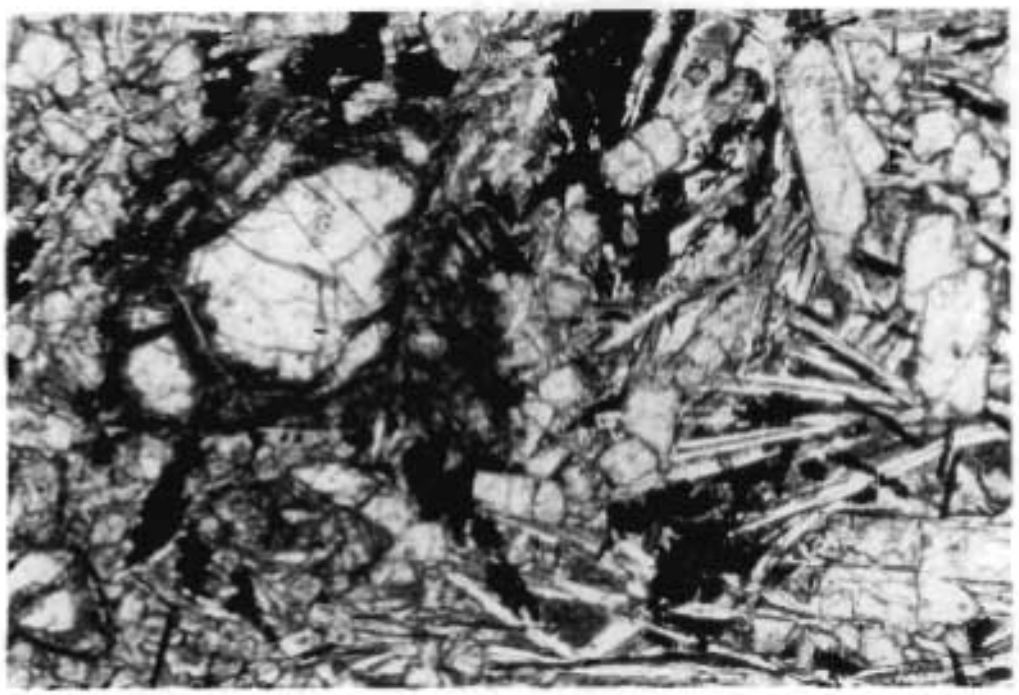

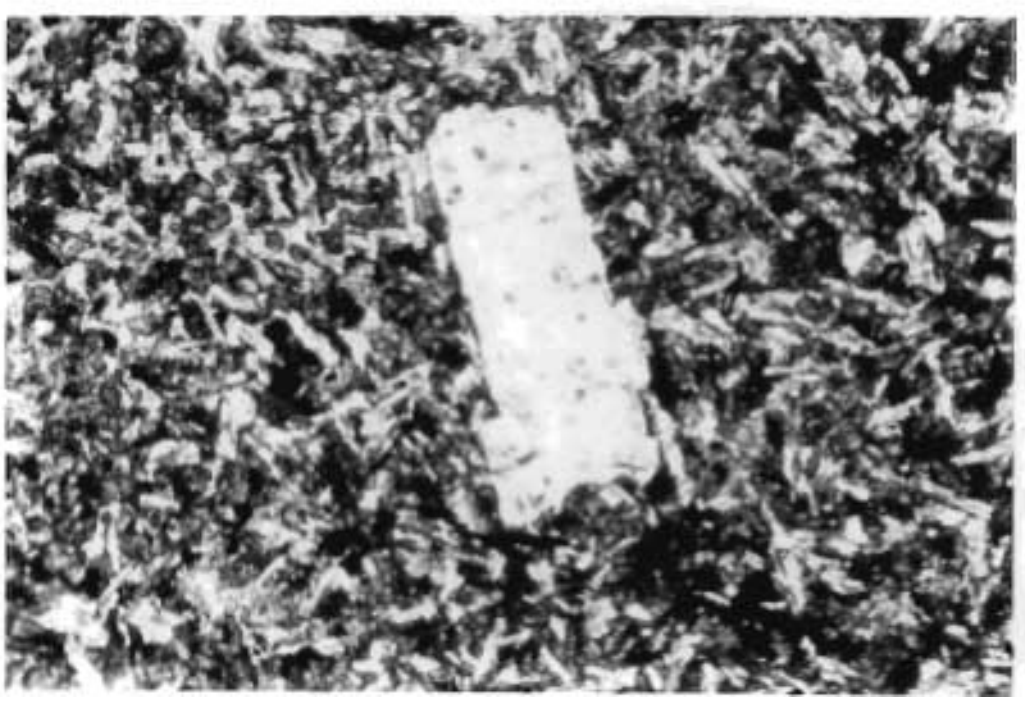

were noted in one olivine basalt specimen. These amygdales contained a fine grained chlorite, and occasionally subordinate quartz. Modal analyses of four samples of olivine basalt are shown in Table 3, p 14.

5.1.2 Mineralogy

Optically determined compositions and some of the properties of the major rock forming minerals present in the olivine basalt are listed in Table 4, p 15.

5.1.3 Geochemistry

Two specimens of olivine basalt were submitted to the National Institute for Metallurgy, for analysis, both of them fine grained, variolitic types. The results shown in Table 5, p 16 indicate they are olivine normative basalts, essentially tholeiitic in character. Further discussion of their geochemistry is given in the section on the geochemistry of the basic volcanics (see later).

5.2 Basalts

A thick sequence of tholeiitic, essentially olivine-free basalts lies directly and conformably upon the olivine basalts at the base of the volcanic succession. These are overlain in turn by a few lavas of intermediate composition, which form the transitional zone between the tholeiitic basalts and the acid volcanics. The basalts are present over a roughly rectangular area, which, in an east-west direction stretches from the base of the Lebombo Range to within a few tens of meters of the olivine basalt-Karroo sandstone contact, a distance of some 8 km. In a north-south direction they may be traced continuously through the entire area (13 km). A further small lens of basalts is exposed interbedded with the acid volcanics in the southern third of the Lebombo Range.

Strikes are generally within 8° east or west of north and dips are variable, increasing from 5° to 10° east near the eastern contact of the basalts to 25° to 30° east at the foot of the Lebombo Range. Estimates

TABLE 3

Modal analyses of Olivine Basalts from the Komatipoort Area

(vol/%)

Sample no.	Olivine	Clinopyroxene	Plagioclase	Glass	Ore	Alteration Products
CL45	22.0	26.3	-	44.4	4.7	2.6
CL46	20.6	28.7	24.3	14.2	5.8	6.4
CL47	14.9	34.4	36.8	4.7	3.5	5.7
CL48	11.3	36.2	34.9	8.5	6.1	3.0

TABLE 4

Properties of Rock-forming minerals present in the Olivine Basalts

Rock Type	Mineral	Twinning	Zoning	Composition*	Refractive Indices	2V	Alteration
Olivine Basalt	Groundmass Plagioclase	Present	Slight normal	Core - An_{58} Margin- An_{32}	-	-	Not observed
	Phenocryst Plagioclase	Present	Core-oscillatory zoned mantle-rim	Core - An_{75} Rim - An_{50}	-	-	not observed
	Clinopyroxene (Diopsidic Augite)	Not observed	Occasional oscillatory zoning. Rare oscillatory zoned mantle - rim - structure		x y z	$(+)2V_z$	
				Core: $Mg_{40}Ca_{38}Fe_{22}$	1,720 1,698 1,695	49°	
				Rim : $Mg_{26}Ca_{32}Fe_{32}$	1,728 1,705 1,700	42°	not observed
	Olivine	Not observed	Not observed		x y z	$2V_x$	Partly altered to chlorite, magnetite and antigorite
				Range: Fa_{20} to Fa_{35}	1,716 1,705 1,680	88°	
					1,745 1,722 1,695	82°	

x Compositions given represent an average for at least 5 grains, determined by optical methods, (see Appendix 1).

TABLE 5

Chemical analysis, CIPW Norm and Niggli Values of two specimens of olivine basalt from the Komatipoort area. (analyst NDM).

Sample CL20 Differentiation Index 53,2						Sample CL25 Differentiation Index 41,9					
Chemical analysis		CIPW Norm		Niggli values		Chemical analysis		CIPW Norm		Niggli values	
SiO_2	48.78	or	2.24	Si	103.438	SiO_2	48.68	or	6.38	Si	101.058
Al_2O_3	9.99	ab	12.68	Al	12.485	Al_2O_3	8.06	ab	10.314	Al	9.861
Fe_2O_3	2.64	an	19.39	Fm	65.809	Fe_2O_3	1.36	an	13.32	Fm	68.681
FeO	11.83	di	15.32	C	18.109	FeO	10.02	di	19.35	C	17.573
MgO	12.75	hy	39.42	Alk	3.598	MgO	15.77	hy	32.63	Alk	3.886
CaO	7.97	ol	1.03	mg	0.612	CaO	7.90	ol	7.353	mg	0.710
Na_2O	1.50	mt	3.84	c/fm	0.275	Na_2O	1.22	mt	1.98	c/fm	0.256
K_2O	0.30	il	4.12	k	0.143	K_2O	1.08	il	5.74	k	0.368
H_2O^-	0.14	ap	0.46	ti	3.237	H_2O^-	0.47	ap	0.63	ti	4.418
H_2O^+	2.24	H_2O	2.38	p	0.189	H_2O^+	1.20	H_2O	1.67	p	0.255
CO_2	0.39					CO_2	0.09				
TiO_2	2.03					TiO_2	2.83				
P_2O_5	0.21					P_2O_5	0.29				
MnO	0.18					MnO	0.21				
						Cr_2O_3	0.16				
						CuO	0.01				
Total :-	100.95		100.88				99.34		99.36		

of the thickness of the basalt succession are complicated both by the variation in dips from west to east and by the possible presence of strike faults (mentioned in the section on dolerites) of indeterminate throw. Downthrow to the west on these strike faults as suggested by du Toit (1929), would tend to exaggerate the thickness of the basalts. Urie and Hunter (1963) suggested a thickness of 2 300 m for the Stormberg age basalts of the Lebombo in Swaziland, some 50 km south of Komatipoort, but du Toit (1929) has proposed a figure of 1 600 m for the Karroo basalts in the Komatipoort area. On the basis of the present work, the latter figure appears acceptable as a maximum, and 1 000 m as an estimated minimum.

Individual basalt flows as defined by auto-brecciated upper surfaces range from ten to twenty meters in thickness, but their lateral extent is impossible to gauge as outcrops are usually present in stream beds only. In the field, the basalts show little variation, normally consisting of a dark blue microcrystalline rock, which frequently contains phenocrysts of feldspar, or less commonly, ferromagnesians. The basalts are greenish coloured in places and towards the top of individual flows may assume a reddish colour, due to oxidation. Vesicles are abundant, particularly in the upper parts of flows, where they commonly vary between 1 and 3 cm in diameter, although exceptionally, larger vesicles 10 to 15 cm in diameter may occur. Often these are infilled with agate, quartz, calcite, epidote, chlorite or zeolites. Pipe amygdales, usually infilled with agate, occur at the base of some flows, particularly in the upper part of the basalt succession. Basalt sub-types recognised in handspecimen by Hunter in Swaziland (Urie and Hunter, 1963) were named according to the locality in which they occurred, however, these sub-types have not been recognised in the Komatipoort area.

Classification of the Komatipoort basalts for the purpose of petrographic description has been based on the relative abundance of major constituent minerals, including both those in the groundmass and those occurring in the form of phenocrysts. This classification is similar in some respects to that used by Cox et al. (1965) for the description of the basalts of Nuanetsi

area. The same system is used in describing the petrography of the dolerites (see later), which are considered the intrusive equivalents of, and feeders to, the basalts. Thus the basalts may be subdivided into:

(i) Non-porphyritic basalts
(ii) Quartz basalts
(iii) Feldsparphyric basalts
(iv) Pyroxenephyric basalts
(v) Olivine-bearing basalts

Four of the five basalt types recognised, namely the non-porphyritic basalts, the feldsparphyric basalts, the pyroxenephyric basalts and the olivine-bearing basalts differ essentially in the amounts of the three phenocryst phases (olivine, pyroxene and plagioclase) they contain. The quartz basalts however, show evidence of contamination by the underlying sedimentary rocks.

5.2.1 Petrography

Non-porphyritic Basalts

Microcrystalline to cryptocrystalline phenocryst-poor basalts are fairly common, usually displaying an intergranular texture. They consist essentially of tiny granules of clinopyroxene and plagioclase with variable amounts of opaque ore minerals, (Plate 1, p 12), and the dark cryptocrystalline glassy intetstitial material in which minute needlelike crystals of apatite may be set. The clinopyroxene is commonly altered in part to chlorite, and plagioclase is clouded by abundant cryptocrystalline alteration products. Amygdales containing a variety of minerals are common in the upper parts of flows. Modal analysis of typical non-porphyritic basalts are shown in Table 6, p 19.

Quartz Basalts

Near the base of the basalt sequence, close to the basalt-olivine basalt contact, a few flows occur which have a distinctive greyish colour.

TABLE 6

Modal analyses of basalts from the Komatipoort area

Sample number	CL38	CL39	CL40	CL41	CL42	CL43	CL44
Basalt type	Feldsparphyric Basalt	Feldsparphyric Basalt	Non-porphyritic Basalt	Non-porphyritic Basalt	Non-porphyritic Basalt	Pyroxenephyric Basalt	Quartz Basalt
Plagioclase	59.1	64.7	49.5	44.5	45.6	36.1	60.0
Clinopyroxene	33.0	18.9	44.3	43.8	41.3	43.7	26.8
Altered Olivine	1.1	3.5	-	-	-	3.9	-
Ore	3.9	8.9	5.9	11.7	9.6	9.3	6.3
Fine-grained interstitial material	1.5	1.3	0.3	-	3.5	2.9	3.3
Quartz	-	-	-	-	-	-	2.3
Alteration products	1.4	-	-	-	-	1.7	1.3
Amygdaloidal material	-	2.7	-	-	-	2.4	-

These basalts are distinguished from the non-porphyritic basalts by the presence of free quartz, which forms discrete patches surrounded by a dark cryptocrystalline mantle as in the quartz dolerites (see later). Quartz may also be present as small, irregular grains occurring interstitially to the pyroxene and plagioclase. Rarely, recognisable xenolithic fragments of sedimentary rocks were noted. As may be seen from the modal analysis of a quartz basalt shown in Table 6, p 19 the rock contains a somewhat higher proportion of plagioclase than is usual for the basalts of this area and it is this abundance of plagioclase rather than the quartz content that gives the rock its distinctive greyish colour.

Feldsparphyric and Pyroxenephyric Basalts

Abundant subhedral phenocrysts of plagioclase varying between 2 mm and 50 mm in length characterise the relatively uncommon feldsparphyric basalts. The phenocrysts occur singly, but more usually they comprise glomeroporphyritic aggregates, to which solitary highly altered (former) olivine crystals may be attached. The modes of several feldsparphyric basalts are shown in Table 6, from which it may be seen that these rocks differ from the quartz basalts in quartz content rather than in feldspar content, although they are distinctly richer in plagioclase than the other basalt types.

The pyroxene- rich basalts are similar to the feldsparphyric basalts but for the fact that the phenocrysts present are composed predominantly of clinopyroxene. The relatively few examples of these rocks encountered in the Komatipoort area contain subhedral clinopyroxene phenocrysts up to 10 mm in length, set in finer grained groundmass similar in all respects to that of the previously described basalts. Occasional plagioclase phenocrysts may be present in addition to those of clinopyroxene, commonly occurring as glomeroporphyritic aggregates together with the pyroxenes, and infrequently with altered olivine crystals. The mode of a pyroxenephyric basalt is shown in Table 6, p 19.

Olivine-bearing Basalts

Minor amounts (up to 5 % by volume) of highly altered olivine occur in certain examples of all of the four preceding sub-types. The former olivine crystals display rounded and embayed outlines for the most part, although in places euhedral faces may be preserved along contacts with phenocrysts of plagioclase or pyroxene. The olivine may occur as isolated phenocrysts or, in porphyritic rocks, it may be associated with glomero-porphyritic aggregates of plagioclase and pyroxene.

5.2.2 Mineralogy

Compositions and some properties of the major rock forming minerals are listed in Table 7 . Ore minerals and minerals present in amygdales are briefly described below.

Ore Minerals

Magnetite, pyrite, chalcopyrite and less commonly ilmenite are the main ore minerals present in the basalts. The magnetite normally occurs as irregular granules, partially martitised to hematite, and rarely ilmenite is found in crystals of similar form. Pyrite is by far the most abundant of the two sulphide minerals, usually occurring as irregular interstitial grains. Chalcopyrite is occasionally noted as minute, irregular grains, frequently associated with the altered olivine crystals.

Native copper was noted in one basalt flow near the middle of the basalt succession. The copper usually occurs as small discrete grains (0.01 to 0.05 mm in diameter), included in altered olivine crystals, in plagioclase and pyroxene phenocrysts, in the groundmass silicates, and in amygdales. In some plagioclase crystals the native copper is present as a cloud of minute disseminated specks, in others however, it occurs as discrete grains, often located along cracks, twin planes or cleavage planes. The larger grains of native copper frequently show the development of a narrow border of digenite and in addition digenite may occur as discrete grains, usually in the vicinity of larger grains of native copper. Where

TABLE 7

Compositions and Properties of Rock-Forming minerals present in the Basalts

Rock Type	Mineral	Twinning	Zoning	Composition	Alteration	Grain Size
Basalt	Groundmass Plagioclase	Present	Normal	Core :- An_{56} Margin :- An_{32}	Not observed	0,1 mm - 0,5 mm
	Phenocryst Plagioclase	Present	Some Normalzoning.Also coreoscillatory zoned mantle-rim	Core :- An_{65} Mantle :- An_{55}-An_{60} Rim :- An_{55}-An_{35}	Not observed	2 mm - 15 mm
	Clinopyroxene	Not observed	Not observed	Range :- Ca Fe Mg 34 20 46 to 36 24 40	Not observed	0,1 mm - 1,0 mm
	Olivine Pseudomorph	-	-	-	Altered to Chlorite, magnetite, antigorite and calcite	0,5 mm

the copper is included in plagioclase or pyroxene grains, a narrow rim composed of a fine grained white alteration product may be present along the copper-silicate boundary. This proved too narrow for adequate identification.

Other ore minerals identified in this rock include hematite (altered magnetite) containing exsolution lamellae of ilmenite, and traces of chalcopyrite.

Amygdale Minerals

Aside from quartz, chlorite, and calcite, several zeolites may be present in amygdales found in the basalts, including natrolite, thomsonite, stilbite, and chabazite. These minerals are commonly zonally arranged within the amygdales, with calcite and quartz usually occupying a central position. No attempt was made to establish the presence of a zonal distribution of the zeolites within the lava sequence. In the samples collected, however, a tendency for the quantity of zeolitic minerals to increase in the upper part of the basalt sequence was noted. Calcite, chlorite, and silica minerals only, were observed in the overlying rhyolites.

5.2.3 Geochemistry

The results of the chemical analysis of two non-porphyritic basalts are listed in Table 8, p 24 . CIPW norms and Niggli values are also shown. The analyses will be discussed in the section on geochemistry, (see later).

5.3 Metamorphism of the Basalts

As may be seen from the geological map, a large number of dolerite dykes have intruded the basalts, producing widespread low-grade thermal metamorphism. The resulting metamorphic effects are usually restricted to the development of turbid feldspars and the alteration of pyroxene to chlorite.

TABLE 8

Chemical analyses, CIPW Norms, and Niggli Values for two specimens of basalt and one specimen of andesite(icelandite) from the Komatipoort Area.

Analyst: National Institute for Metallurgy

CL19						CL31						CL33					
Chemical analysis		CIPW Norm		Niggli Values		Chemical analysis		CIPW Norm		Niggli Values		Chemical analysis		CIPW Norm		Niggli Values	
SiO_2	61.11	q	20.46	Si	229.43	SiO_2	50.83	q	1.67	Si	122.72	SiO_2	53.62	q	11.24	Si	150.39
Al_2O_3	13.14	or	18.24	Al	29.07	Al_2O_3	13.06	or	3.54	Al	18.58	Al_2O_3	12.91	or	8.03	Al	21.34
Fe_2O_3	3.70	ab	25.53	Fm	39.70	Fe_2O_3	2.30	ab	23.59	Fm	47.39	Fe_2O_3	4.31	ab	22.23	Fm	46.51
FeO	6.12	an	13.16	C	12.83	FeO	10.96	an	21.33	C	26.57	FeO	8.94	an	19.39	C	22.57
MgO	1.73	di	0.65	Alk	18.39	MgO	5.74	di	23.36	Alk	7.46	MgO	3.83	di	13.54	Alk	9.59
CaO	3.19	hy	10.11	Mg	0.24	CaO	10.27	hy	17.56	Mg	0.44	CaO	7.51	hy	12.13	Mg	0.34
Na_2O	3.02	mt	5.38	c/Fm	0.32	Na_2O	2.79	mt	3.34	c/Fm	0.56	Na_2O	2.63	mt	6.26	c/Fm	0.49
K_2O	3.09	il	2.78	k	0.40	K_2O	0.60	il	4.58	k	0.12	K_2O	1.36	il	4.77	k	0.25
H_2O^-	0.33	ap	0.70	ti	3.87	H_2O^-	0.27	ap	0.52	ti	4.10	H_2O^-	0.22	ap	0.55	ti	4.96
H_2O^+	1.92	H_2O	2.25	p	0.51	H_2O^+	0.44	H_2O	0.71	p	0.25	H_2O^+	1.90	H_2O	2.12	p	0.30
CO_2	0.28			H_2O	24.04	CO_2	0.15			H_2O	3.54	CO_2	0.10			H_2O	17.77
TiO_2	1.37					TiO_2	2.26					TiO_2	2.35				
P_2O_5	0.32					P_2O_5	0.24					P_2O_5	0.25				
MnO	0.11					MnO	0.21					MnO	0.18				
						Cr_2O_3	0.034					Cr_2O_3	0.017				
						CuO	0.02					CuO	0.01				
Total	99.43		99.26				100.174		100.20				100.14		100.26		

Occasionally, however, the pyroxene is altered to actinolite, and the plagioclases are saussuritised. Close to the larger dykes, the hornblende-hornfels or higher grades of contact metamorphism may be reached. The metamorphic rocks here are usually fine-grained hornfelses,consisting of plagioclase,diopside, and sometimes hornblende and biotite in small, roughly equidimensional crystals (Plate 2, p 26).Further metamorphic products include small patches of epidosite that are developed locally and are not associated with intrusives; in these the basalt is reduced to a mass of clinozoisite and epidote.

The best examples of metamorphosed basalts in the Komatipoort area, however, are found in the metamorphic aureole of the Komatipoort Intrusion, described later (see section on Komatipoort Intrusion).

5.4 The Transitional Zone

Although lenses of acid lavas occur interbedded in the upper part of the basaltic sequence, the transition from predominantly basaltic lavas to acid extrusives proper, takes place over a vertical distance of some 60 m. In this zone, here termed the transitional zone, are extrusive rocks in part apparently of intermediate composition.

The poorly exposed upper contact of the basalts with this transitional zone lies close to the base of the Lebombo range. The few weathered specimens available from this zone suggest the rocks may be classified as andesine basalts. In places these were found to display a variolitic texture.

An analysis of a sample of one of these rock types is presented in Table 8 , p 24 . This sample consists of a groundmass of andesine, clinopyroxene, opaque iron oxides and interstitial glass enclosing sparsely distributed labradorite phenocrysts. In view of the relatively low Al_2O_3 content and the high total Fe content, this rock type is

PLATE 2

1 Hornblende Hornfels. Idioblastic crystal of hornblende (showing amphibole cleavage) in matrix of plagioclase (white) ore minerals (black) and diopside. A large biotite crystal is observable at the far right (dark grey). (Transmitted light X96.)

2 Pyroxene Hornfels. Relict clinopyroxene grain, crowded with granules of iron ore (centre) set in a crystalloblastic groundmass of plagioclase clinopyroxene and iron ore. (Transmitted light, X60.)

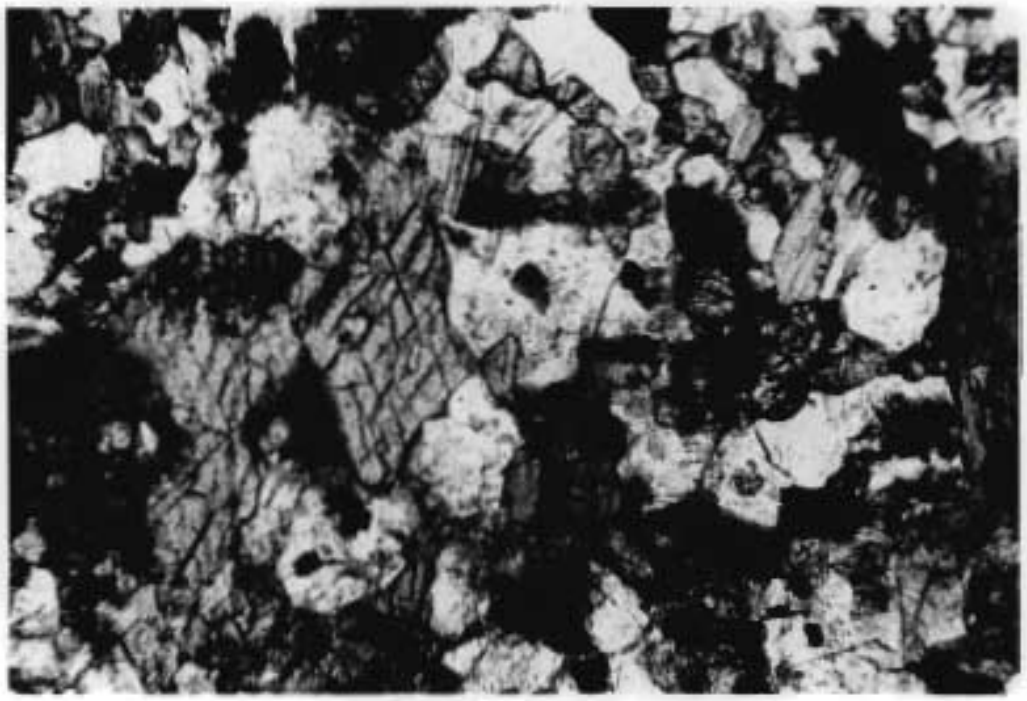

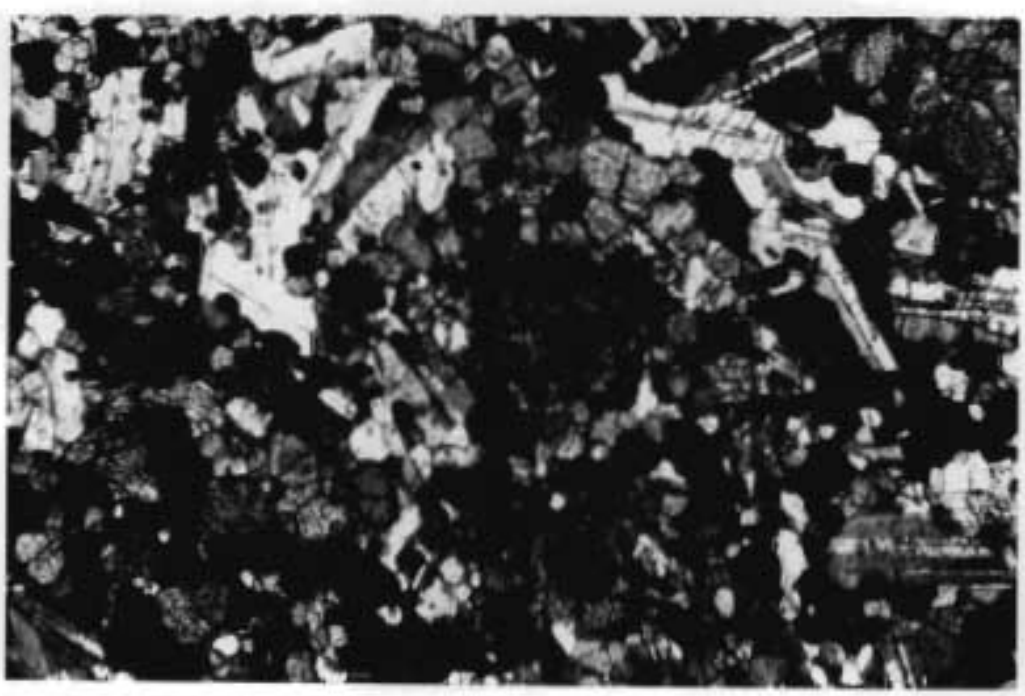

probably better described as an icelandite, (cf Carmichael,1964, p 442).

In contrast to the transitional zone found in the Komatipoort area, Lombaard (1952), has described rocks with limburgitic rather than andesitic affinities from a borehole which intersected the transitional rocks near the Makonkolweni River in the Kruger National Park. This rock he describes as being greyish-pink in colour, composed of plagioclase, augite, chlorite and much ore; the chemical analysis he quotes indicates the basic nature of the rock. Stratten (1965) has described a transitional zone from the Natal Lebombo which resembles that found at Komatipoort, consisting of what he has termed, andesites, interbedded with a tuff horizon and dacites.

5.5 The Acid Volcanics

J.J. Frankel (1960) estimated the thickness of the Lebombo acid volcanic rocks as approximately 5 000 m but the full succession is not seen in the Komatipoort area. Most of the lavas lie across the border in the neighbouring territory of Mozambique, with only an estimated 500 m of these acid rocks, comprising the lower-most part of the acid volcanic succession, occurring within the Komatipoort area. Even if the volcanics in Mozambique are included in the estimate, it seems unlikely however, that a thickness of 5 000 m is present in this part of the Lebombo.

The rhyo-dacitic effusives are confined almost entirely to the Lebombo Range proper, forming a narrow strip along the eastern margin of the area. Basalts occur interbedded with the acid extrusives and conversely minor amounts of acid lavas also occur in the upper-most part of the underlying basalt succession. Interbedded acid lavas are best developed just north of the Crocodile-Komati River junction, from where a 30 m thick lens of rhyolitic lavas, interbedded with the upper basalts, extends northwards for about 5 km, reaching its maximum development a few hundred meters north-east of Komatipoort itself.

Dips on the acid lavas usually lie between 25° and 35° east, increasing eastwards, and strikes locally vary within 15° east or west of north.

5.5.1 Petrography

(A) Acid lavas

Acid lavas occur interbedded with the upper part of the basalt sequence, and also form several of the lower units and part of the highest portions of the main acid volcanic succession.

The flows are usually of the order of 10 to 15 m thick (although occasionally 100 m thick sequences were noted) and extend for a distance of a few hundred meters along strike, grading from a compact fine-grained to glassy base into a highly vesicular, auto-brecciated upper surface, and varying in colour from deep maroon to pale pink and buff on weathered surfaces. Where fresh, they may have a greyish-green colour, but fresh specimens are obtainable only from recent excavations. In outcrops these rocks, as with the other acid volcanics, invariably show a prominently developed colour banding consisting of an alternation of buff, pink and brownish red streaks, which range from a few mm to a few cm in width.

In thin section the texture of these volcanics varies from cryptocrystalline to felsitic, or less commonly intergranular, and the rocks are almost always porphyritic, commonly consisting of various phenocrysts set in a groundmass composed of an aggregate of quartz, feldspar, and minor amounts of iron ore. The groundmass feldspar is usually a sodic plagioclase, but clouded potassium feldspar crystals are also present in places,

and iron ore usually occurs as irregular grains ranging in size from 0.1 mm to 0.5 mm. Phenocrysts are usually composed of similar minerals, namely quartz, (occasionally euhedral), feldspar and ore minerals, although less commonly a pale green clinopyroxene may be present. The feldspar phenocrysts again consist of sodic plagioclase or alkali feldspar, both forming subhedral to euhedral crystals which may show signs of cracking and corrosion. Occasional phenocrysts of what appears to be anorthoclase were observed, but all minerals in the acid lavas are much clouded and altered, and identification rests on dubious determinations of the optic signs and optic axial angles.

Glassy rocks both in the form of true glasses and pitchstones are not common, but in places, form small lenses three to five meters thick extending along strike for a distance of approximately 100 m. The volcanic glasses are green to grey rocks where fresh, consisting of a dark, glassy, partially devitrified groundmass, containing a few phenocrysts of feldspar, and occasionally clinopyroxene and iron ore. In some samples, weathering has produced colour banding, and flow structures, including widespread flow-folding, are conspicuous. These glassy rocks show a sharp contact with both overlying and underlying flows. Much thinner, but very similar glassy layers form the base of some of the flows. The pitchstones form outcrops of similar dimensions to the volcanic glasses, but are commonly a deep reddish brown in colour. Under the microscope they show a dark coloured devitrified groundmass, crowded with microlites and displaying a well developed flow structure.

Phenocrysts, usually consist of single crystals of sodic plagioclase, and pale green clinopyroxene, and glomeroporphyritic aggregates of plagioclase and pyroxene. Quartz may also form phenocrysts, as well as ore minerals, which build somewhat smaller irregular grains (see Plate 3 , p 30).

The acid lavas are frequently amygdaloidal, particularly in the upper parts of flows and these amygdales may show signs of elongation by flow. The amygdales usually contain calcite, agate, quartz crystals, and less

PLATE 3

1 Tuffaceous Sandstone. Quartz grains set in a semi-opaque matrix. (Transmitted light, X60.)

2 Pitchstone. Phenocryst of clinopyroxene (grey) ore minerals (black) plagioclase and quartz (white) set in a partially devitrified groundmass. (Transmitted light, X60.)

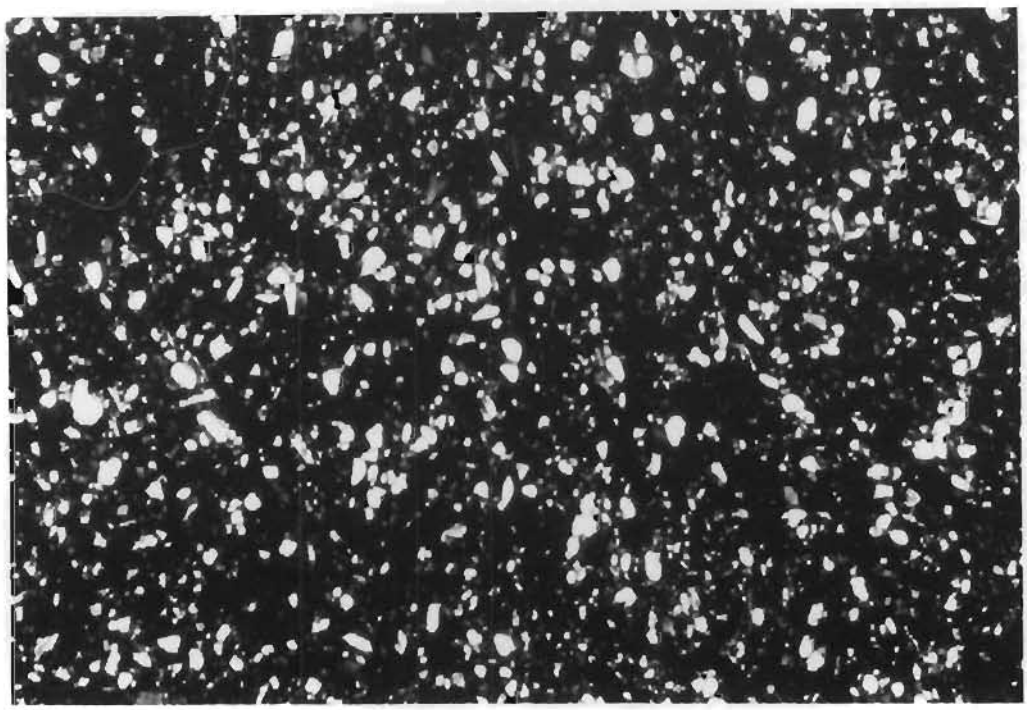

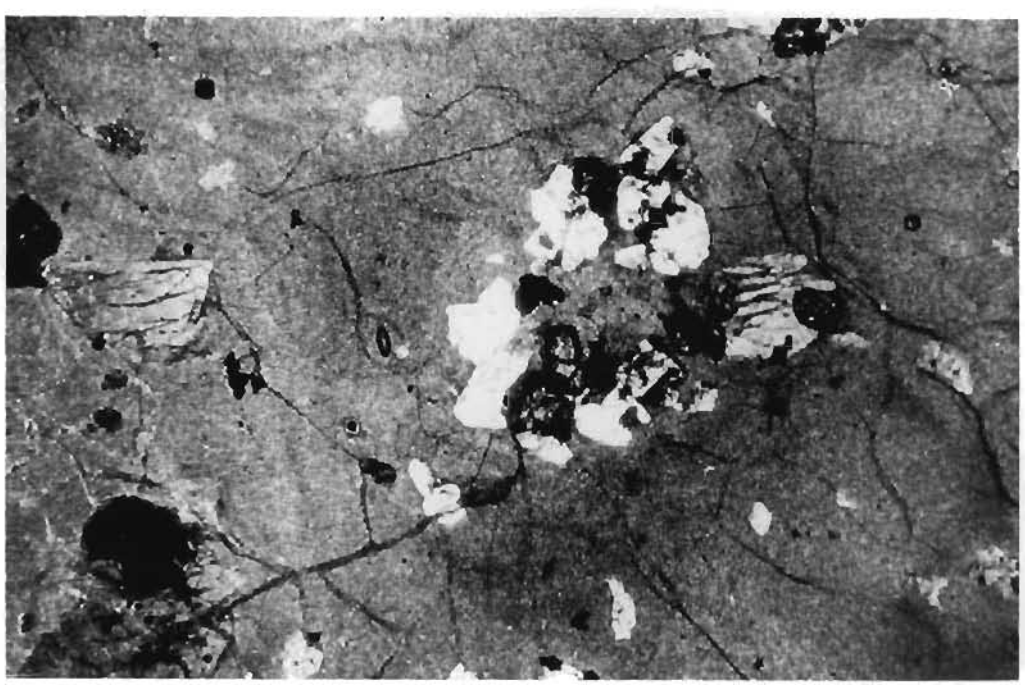

commonly, chlorite. These lavas are predominantly dacitic in composition, although subordinate rhyolites do occur. This assessment is, however, based on modal compositions and this may produce misleading results, particularly as in many of the rock types the groundmass minerals are too fine-grained to be readily identified, and classification must then be based on phenocryst composition alone.

Autobrecciated zones, consisting of angular fragments and blocks of acid lava set in a fine-grained matrix of similar material, mark the upper surface of the lavas. The autobreccias vary between two and six meters in thickness, and may frequently be traced along strike for several kms. Mineralogically and texturally they are indistinguishable from the more abundant breccia dykes described in a later section. The matrix material is composed of a fine-grained felsitic textured aggregate of quartz and feldspar in which are set the usual phenocrysts, (quartz, feldspar, and lesser amounts of pyroxene). In a few of these rocks ore minerals may be relatively abundant as small irregular grains present in the groundmass. The material composing the lithic fragments in the autobreccia consists of normal acid lava. Glassy zones are sometimes present along the edges of the lithic fragments, suggesting partial melting of these fragments may have taken place.

(B) Sandstones and Tuffs

Interbedded with the acid volcanics are occasional lenses of sandstone which vary in colour from brown to deep red. They are invariably fine-grained, compact rocks, consisting of minute (0.1 mm to 0.2 mm) angular grains of quartz, and less commonly plagioclase set in a sparse groundmass, (see Plate 3, p 29). The tuffs also form thin lenses and some types are deep red to brown in colour. These rocks may consist of glass shards or of lapilli, (in places showing concentric zoning), set in a fine-grained felsitic groundmass. Possible soil horizons separating successive dacitic units have been noted in the gorge of the Komati River by R. W. Cleverly, (personal communication).

5.5.2 Mineralogy

Data concerning the minerals occurring in the acid lavas are listed in Table 9 p 33.

5.5.3 Geochemistry

Samples of the two freshest available specimens of acid volcanics were submitted for analysis, and the results of these analyses are shown in Table 10, p 34, together with CIPW norms, niggli values and magma type. Lombaard (1952) has also presented an analysis of a rhyolite from the Komatipoort area and this is shown in the same table with two rhyolites from the adjacent area in Mozambique (de Assunção, et al. 1961).

5.5.4 Mode of Eruption

Previous workers in the Lebombo have found it difficult to reconcile the apparent constant thickness and extensive areas covered by what appear to be individual extrusive rhyolitic and dacitic units, with the commonly assumed extreme viscosity of acid lava flows, particularly since vents in the Lebombo Range may be widely spaced, (Urie and Hunter, 1963).In more recent years, several authors have suggested that the majority of the acid effusives consist of tuffs and welded tuffs emitted from fissures (Stratten, 1965 , Cox, et al., 1965, Urie and Hunter 1963).

The most convincing evidence for the presence of welded tuffs in the Lebombo has been provided by Cox, et al. (1965) who described rocks of this type from the Mateke area, in Rhodesia. They claim, however, that the type of evidence produced by P.Marshall, (1935), to confirm the nature of the New Zealand ignimbrites would not be expected to be available in the much older Lebombo volcanics, due to the natural devitrification of glass, but advance several indirect lines of evidence. Within each welded tuff sheet in the Mateke area, they have recognised a definite structure, beginning with a non-welded basal zone

TABLE 9

Mineralogical Data for Minerals present in the Acid Lavas

	Mineral	Zoning	Composition	Refractive Indices	2V	Alteration	Grain Size
A	Plagioclase i) Phenocrysts	Slight normal zoning, oscillatory zoning rare.	$An_8 - An_{34}$	-	-	usually turbid, cracked and corroded	1 - 5 mm
	ii) Groundmass	Slight normal zoning	$An_7 - An_{16}$			turbid	0,01 - 0,15 mm
B	Clinopyroxene	Not observed	Mg Ca Fe Range(28 42 30 26 41 33	N_B 1,700 N_B 1,714	$2V_B$ 54^o 52^o	cracked, corroded, altered to chlorite or hornblende in places	1 - 3 mm
C	Quartz i) Phenocrysts					cracked, rounded and embayed	2 - 3 mm
D	Ore Minerals i) Magnetite					altering to hematite with ilmenite exsolution lamellae	0,2 - 4 mm
	ii) Hematite						0,3 - 3,5 mm
	iii) Pyrite						0,05 mm
E	Accessory Minerals i) Zircon ii) Rutile iii) Sphene iv) Apatite						((0,2 mm (

TABLE 10

Chemical analyses, CIPW Norms, and Niggli Values for three samples of acid volcanics from the Komatipoort Area.(Analyst: NIM) Analyses from adjacant Mozambique (from de Assunacão et al.) are also shown.

Chemical analysis						CIPW Norms						Niggli Values			
Sample no.	CL21	CL22	*29-C	* 44A	**746		CL21	CL22	*29-C	* 44A	**746		CL21	CL22	**746
SiO_2	68.99	65.62	63.90	67.37	68.93	Q	30.04	35.99	11.40	19.46	30.25	si	352.71	330.21	334.70
Al_2O_3	12.14	11.81	10.74	11.51	12.56	or	29.93	6.49	40.59	26.57	26.71	al	36.58	35.02	35.90
Fe_2O_3	4.44	1.80	5.45	5.92	4.76	ab	27.05	20.29	36.77	34.06	28.68	fm	29.44	24.72	25.30
FeO	2.45	3.60	2.49	1.61	1.51	an	0.97	18.19	-	-	3.12	c	1.59	25.02	8.80
MgO	0.19	0.31	1.15	0.48	0.22	di	-	3.84	10.44	4.70	-	alk	32.40	15.24	29.90
CaO	0.29	4.64	2.40	1.71	1.70	hy	0.88	3.44	-	-	0.55	mg	0.05	0.09	0.06
Na_2O	3.20	2.40	4.94	5.29	3.39	mt	6.45	2.62	-	2.97	3.80	c/fm	0.05	1.01	0.35
K_2O	5.07	1.10	6.86	4.49	4.52	il	0.75	0.79	2.13	1.29	0.80	k	0.51	0.23	0.47
H_2O^-	0.26	1.02	1.50	0.22	0.98	ap	0.18	0.15	0.34	0.26	trace	ti	1.42	1.48	1.50
H_2O^+	0.73	5.64	-	0.03	0.05	H_2O	1.01	6.66	-	-	1.03	p	0.17	0.15	trace
CO_2	0.58	0.17	n.d.	n.d.	0.84	hm	-	-	-	0.67	2.14	H_2O	12.45	94.64	-
TiO_2	0.37	0.39	1.08	0.68	0.42	cc	-	-	-	-	1.91				
P_2O_5	0.08	0.07	0.24	0.12	trace	c	1.03	-	-	-	0.95				
MnO	0.10	0.10	0.09	0.06	0.05	ac	-	-	-	9.24	-				
Total	98.91	98.67	100.84	100.31	99.93		98.29	98.46	101.67	99.22	99.94				

* From de Assunção et al., (1961)
(Analyst: A. Lopes Vieira).

** From Lombaard, (1952).
(Analyst: W.R. Herdsman)

of vitric tuffs and breccias, which is immediately overlain by a welded, glassy, eutaxitic zone. These two basal units comprise less than 1/10th of the total thickness of the deposit, the upper 9/10ths being composed of massive, well-jointed, even, fine-grained rocks, with a felsitic texture. The latter texture may, in places, be partially masked by the development of a fine granophyric texture throughout. The evidence they have for considering these rocks as welded tuffs consists mainly of observations which offer some indication of a high temperature for the vitric tuff when it was deposited, a feature which distinguishes these tuffs from other non-welded tuffs.

Urie and Hunter (1963) have not found similar structures in the Swaziland Lebombo, but nevertheless describe the acid volcanics from this area as ignimbrites, largely on account of the extensive nature of these volcanic units.
Again in the Komatipoort area no structural units resembling those found by Cox et al. were encountered, nor were any of the criteria suggested by Cook (1955) recognisable, although it must be borne in mind that only a proportion of the volcanic succession falls within the Komatipoort area.

In the Komatipoort area, the rhyolites show considerable persistance in a north-south direction, parallel to the strike of the feeder dykes, but there is no evidence of great lateral extent in an east-west direction. Thus appropriate spacing of the feeder dykes could possibly account for the observed sequence of rhyolitic flows here.

More recently, Wachendorf (1971), indicated the presence of dome structures in the Lebombo succession of the adjoining territory of Mozambique. These dome structures are elongated in a north-south direction but are apparently of little lateral extent in an east-west direction. However, close-spacing of these structures, might, Wachendorf considers, give the impression of laterally extensive sheets of rhyolitic volcanics. The dome structures are reported to show a distinct variation

in texture from the base upwards viz. a rapidly chilled glassy-textured zone close to the contact between the base of the unit and the surface onto which it was extruded, followed upwards by microgranophyric and felsitic textured rocks in the interior of the dome, and a flow folded outer zone near the upper surface.

Some of the flows in the Komatipoort area, do show this upward sequence of textural changes, although no domical structures could be recognised. Instead a lens-shaped cross-section, rather, is displayed, for example by the rhyolitic lavas interbedded with the uppermost basalts in the Komatipoort area, (see geological map).

The rhyolites of the Komatipoort area, may simply represent the effusion of less viscous lava unconnected to the dome structures described by Wachendorf (1971). They could, however, represent an earlier, volatile-rich (and therefore less viscous) fraction extruded from the same vent as the rhyolite domes, either as a separate event, preceding the extrusion of the dome, or as less viscous, wider spreading extremities of the dome structure. No field evidence is available in support of this possibility.

The acid extrusives at Komatipoort appear to have been emplaced as extensive flows, presumably of lower viscosity than is usually assumed for acid lavas. Hydrous minerals are absent from these acid lavas and this low viscosity is therefore more likely to result from unusually high temperatures than a high volatile content.

In summary, evidence is available for the presence of viscous rhyolitic domes in Mozambique, (Wachendorf , 1971) and of welded tuffs in the Nuanetsi area, (Cox et al. 1965), although neither have been recognised in the Komatipoort area. Instead the bulk of the rhyolites show evidence of at least final emplacement as flows, ($\pm$100 m thick), as evidenced by several features including a chilled, glassy basal zone, flow-folding occasionally present in their upper middle portions and autobrecciated upper surfaces. Where vesicles are present, and these may exceptionally reach 30 cms in diameter, they frequently show signs of elongation by flow. Tuffs and sediments form a subordinate proportion of the sequence.

5.6 Minor Intrusives

5.6.1 Minor Mafic and Ultramafic Intrusives

Basic dykes in the Komatipoort area form a dense meridionally trending swarm cutting across both acid and basic lavas. The swarm extends some 5 km to the west of the area mapped (du Toit, 1929), traversing the underlying Karroo Sediments and metamorphic Precambrian basement rocks with little regard for pre-existing structures. The dykes range from olivine-free dolerites, to quartz dolerites, and in addition, near the olivine basalt-sandstone contact, two dykes occur which may have alkali basalt affinities. Both, however, are somewhat weathered.

(A) Alkali Basalt Dykes

In general, nephelinitic rocks of the type found at the base of the volcanic succession in the northern Lebombo, do not occur at Komatipoort. Only two dykes with possible alkali basalt affinities were found during the present investigation, both occurring within the lower part of the Karroo basalt succession, a few hundred feet from the basalt-sandstone contact. They are subvertical, north-south striking dykes, about 2 meters in width, composed of a dark, greenish black, microcrystalline material.

The first of these may be a marginal type, intermediate between the olivine basalts and true alkali basalts. It consists of large phenocrysts of biotite, now largely replaced by chlorite, which in turn, is altered to a brown mineraloid. Other mineral constituents are a few corroded crystals of altered plagioclase and, in the groundmass, altered olivine crystals, tiny plagioclase crystals, irregular patches of chlorite, and combs and needles of ore of the types common in the olivine basalts. The small euhedral to anhedral olivine crystals are almost completely replaced by calcite, chlorite, antigorite and ore.

The other dyke shows somewhat less alteration and contains altered possibly hexagonal phenocrysts (1 mm diameter), now composed of calcite and zeolites, that may once have consisted of a feldspathoid. The groundmass consists of a brown crypto-crystalline material, in which a few small crystals of diopsidic augite and labradorite occur.

(B) Olivine-Rich Dyke Rocks

Near the base of the volcanic succession a few poorly exposed olivine-rich rocks occur. Where fresh, they are dense, black, medium-grained rocks, easily distinguishable in the field from the average dolerite, however, as a result of their free-weathering characteristics, exposures are commonly limited to man-made excavations.

(i) Petrography

In thin section many of these rocks bear a strong resemblance to some of the coarser-grained olivine basalts, consisting of subhedral olivine and clinopyroxene crystals set in a dark brown to black crypto-crystalline or glassy groundmass that is often crowded with minute specks of an opaque ore mineral. The olivine and clinopyroxene crystals are both of roughly the same size (average diameter 2.5 mm) although in some of these rocks, finer grained pyroxene crystals are also present in some abundance, (Plate 4, p 39). In more completely crystallised examples, plagioclase makes its appearance in the groundmass in the form of elongated laths which may reach 1.5 mm in length.

(ii) Mineralogy

Mineral Data are listed in Table 11, and modal analyses of three typical dyke rocks are shown in Table 12. Variations present consist principally of an increase in plagioclase content at the expense of the other three main constituents, pyroxene, olivine, and interstitial glass.

PLATE 4

1 Olivine-rich Dyke Rock. Phenocrysts of olivine (lower centre, showing alteration cracks) and clinopyroxene (other large crystals) with smaller clinopyroxene crystals, set in semi-opaque glassy groundmass. (Transmitted light, X96.)

2 Porphyritic Hyaline Dolerite. Large phenocryst of plagioclase (white), fringed with iron ore needle, set in glassy matrix, rich in iron ore needles. (Transmitted light, X96.)

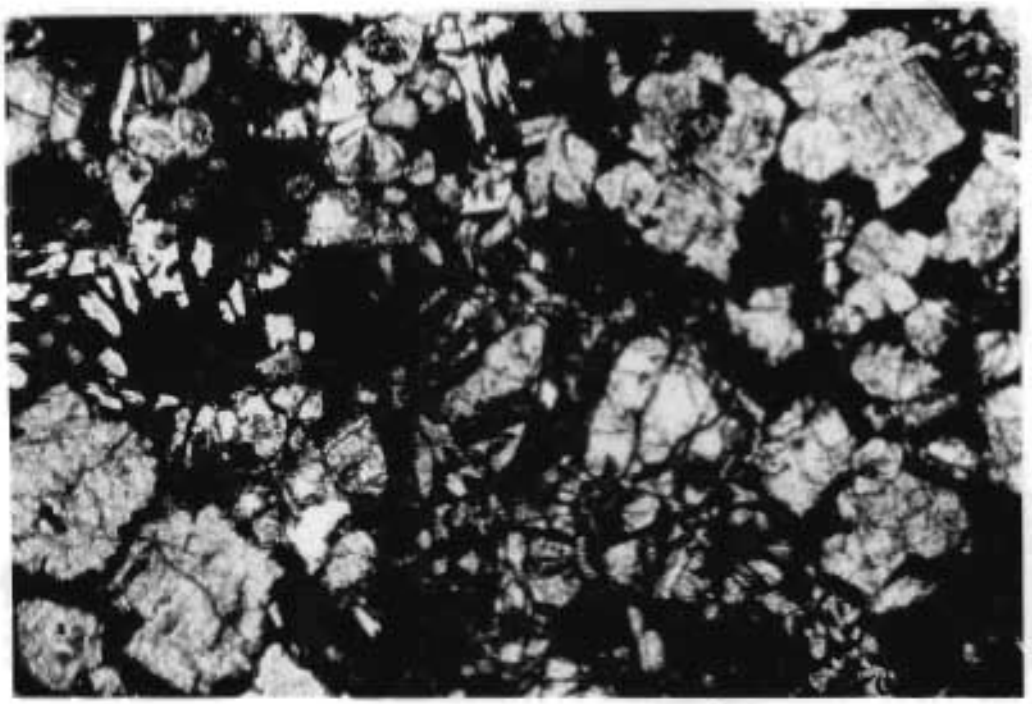

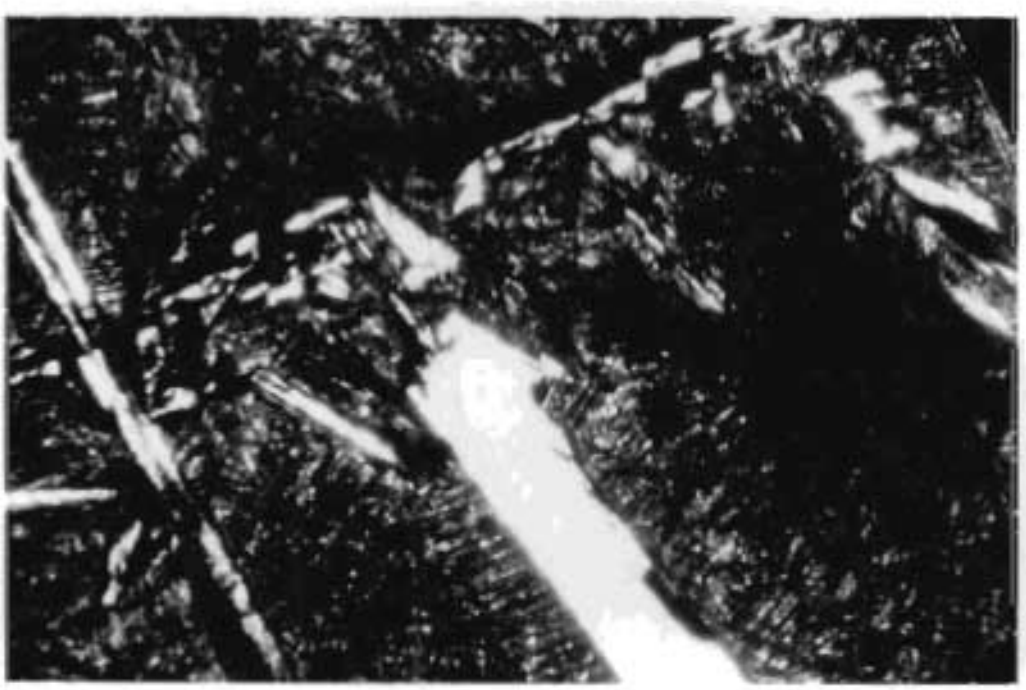

TABLE 11
Mineral Data for Minerals present in the Olivine-Rich Dyke Rocks

	Mineral	Zoning	Composition	Refractive Indices	Colour	2V	Alteration	Grain Size	Shape or Form
A	Olivine	not observed	Mg Fe Range (80 20 72 28	Ny 1,692 1,713	colourless	$2V_x$ 87° 82°	Partly altered to chlorite and antigorite	0,5mm - 3,0mm	Euhedral to subhedral- more rarely corroded and rounded
B	Pyroxene								
	(i) Clinopyroxene	oscillatory zoning may be present	x Mg Fe Ca Range (38 38 24 33 35 32	Ny 1,698 1,750	colourless to pale brownish pink	$2V_z$ 46° 45°	not observed	0,05 - 3,0mm	subhedral
	(ii) Orthopyroxene	not observed	En_{88}	Nz 1,675	colourless	$2V_z$ 87°	not observed	±1,0mm	corroded cores mantled by augite
C	Plagioclase	slight normal zoning	Rim Core Range An_{55}-An_{60}	not determined	colourless	-	-	0,1mm	Needles or laths
D	Ore Minerals								
	(i) Ilmenite							0,3mm	Needles & Comb-structures with exsolved magnetite
	(ii) Magnetite							0,5mm	Irregular interstitial patches rarely euhedral octahedra
	(iii) Pyrite and Chalcopyrite							0,05 - 0,5mm	Irregular interstitial patches

x This optically determined composition is likely to be unreliable due to the probable high Ti - content of the pyroxene suggested both by the colour of the pyroxene and the high Ti-content of the analysed olivine-rich dyke-rock (see Table 13).

TABLE 12

Modal proportions of three specimens of olivine-rich dyke rocks (vol./%)

Sample no.	Olivine %	Augite %	Plagioclase %	Ore minerals %	Interstitial glass %
CL49	22.5	35.0	0.0	0.5	42.0
C128	18.5	33.0	12.0	1.0	35.5
C150	10.0	34.5	29.0	0.5	26.0

(iii) Geochemistry

A single fresh specimen of an olivine rich dyke rock was analysed and the results of this analysis is shown in Table 13, p 42, together with the norm and Niggli values of the rock. As may be seen from the modal analysis (Table 12) the rock is an olivine gabbro. Discussion of this analysis and comparison with analyses of other rocks from the area will be dealt with in a later section.

(C) Dolerites

Karroo dolerites are the most widely distributed of the basic intrusives present, forming the major part of the north-south trending basic dyke swarm. Although vertical dolerite dykes do occur throughout the area, non-vertical dykes are more common. High dips (80° to 90° west) were recorded near the western boundary of the area, where the dip of the country basalts is low, and lower dips (70° to 80° west) were noted eastwards towards the base of the rhyolitic succession. In the rhyolites themselves, few dykes are present and those observed were all found to be vertical. Strike is usually constant within 10° east or west of north, but there is a tendency for younger dykes (i.e. those intruding the

TABLE 13

Chemical analysis, CIPW norms and Niggli Values for a specimen of an olivine-rich dyke rock,(olivine gabbro).

Analyst: National Institute for Metallurgy

Sample No. CL28

Chemical analysis Differentiation Index 60,8		CIPW Norm		Niggli Values	
SiO_2	51.62	Qz	7.93	si	130.965
Al_2O_3	11.42	Or	10.27	al	17.076
Fe_2O_3	2.62	Ab	12.26	fm	49.737
FeO	8.33	An	19.50	c	26.805
MgO	7.06	Di	21.82	alk	6.383
CaO	9.89	Hy	15.38	mg	0.537
Na_2O	1.45	Mt	3.80	c/fm	0.539
K_2O	1.74	Il	6.20	k	0.441
H_2O^-	0.17	Ap	0.90	ti	5.839
H_2O^+	1.68	H_2O	1.85	p	0.440
CO_2	0.46				
TiO_2	3.06				
P_2O_5	0.41				
MnO	0.17				
Cr_2O_3	0.045				
CuO	0.01				
Total	100.1		99.91		

rhyolites proper or the granophyre body at Komatipoort) to have a strike east of this general trend. Other small dykes within the Komatipoort granophyre follow a rectilinear pattern while still maintaining a generally north-south trend, and adjacent to these the country rock forming the eastern margin of the dyke has suffered displacement southward, relative to the western margin.

Field characteristics of the dykes have been described by Kynaston (1907) and less fully by du Toit (1929). They vary in width from a few cm to about 50 m , common widths being of the order of 5 to 10 m. Slickensided contacts and occasionally observable displacement of country rocks suggests strike faulting is associated with the dykes, with downthrow to the west, although conceivably the slickensiding may be the result of forceful intrusion of viscous magma. Closely spaced jointing at right angles to the contacts of the dykes, or platy jointing parallel to the contacts is common. Composite and intersecting dykes were frequently observed with the composite types composed of up to three separate intrusions. Du Toit (1929) considered sills to be rare in this area, but contacts are seldom exposed and a fine-grained dolerite sill would be virtually indistinguishable from the coarser basalts. However, no undoubted small sills were observed.

In hand specimen the rocks are fine to medium grained dark blue occasionally green varieties which are frequently porphyritic. Walker and Poldervaart (1949) have provided a complex classification of South African Karroo dolerites, recognising some thirty-two varieties which are distinguished by textural and compositional characteristics. The classification is descriptive rather than genetic and for this reason the dolerites are here grouped, as were the basalts (see Section 5.2), according to their phenocryst composition. Like basalts, the dolerites may be divided into the following sub-types:

(a) Non-porphyritic
(b) Feldsparphyric
(c) Pyroxenephyric
(d) Quartz dolerites

(i) Petrography

(a) Non-Porphyritic Dolerites

Textures vary from intersertal through interstitial to sub-ophitic, with the mineralogy qualitatively remaining essentially the same. The groundmass consists of small crystals of diopsidic augite and plagioclase that usually have an interstitial or sub-ophitic relationship to each other, and variable amounts of fine-grained interstitial micropegmatite or a brownish coloured glass. Pigeonite is apparently absent from many of the dolerites, but does occur both as mantles and as cores to augite crystals, as well as in the form of individual pigeonite grains in some dolerites. Opaque ore minerals are also present as irregular interstitial patches and apatite may be a conspicuous accessory in micropegmatite-rich types.

(b) Feldsparphyric Dolerites

The essential feature of these rocks is the presence of relatively abundant feldspar in the form of phenocrysts of plagioclase up to 3 cm in length, which may occur as single crystals of various sizes, but more often, form glomeroporphyritic aggregates. No difference was found between the groundmass of most of these rocks and that of the non-porphyritic dolerites and the description will therefore not be repeated. Other textural variations of the feldsparphyric dolerites do occur. Smaller dykes are characterised by a hyalophyric texture. Typical of these are small dykes crosscutting the Komatipoort granophyre, which are composed of elongated, somewhat corroded plagioclase phenocrysts reaching up to 5.0 mm in length, set in a glassy groundmass. The groundmass shows signs of devitrification and is crowded with needle-like microlites of iron ore. Similar crystals are arranged at right angles to the margin of the plagioclase crystals in the form of a fringe (see Plate 4, p 39).

(c) Pyroxenephyric Dolerites

Clinopyroxene phenocrysts occur alone or less commonly as glomeroporphyritic aggregates of smaller crystals. Occasionally the pyroxene may occur together with plagioclase in glomeroporphyritic aggregates, although these are not common. Augite is the most abundant pyroxene present, but pigeonite was occasionally noted. For the rest these rocks are identical with the non-porphyritic dolerites.

(d) Olivine-bearing Dolerites

The olivine occurs as euhedral to rounded phenocrysts which either form discrete crystals in the groundmass, or in places, occur associated with glomeroporphyritic aggregates in plagioclase. The latter mode of occurrence is, however, rare. Olivine may constitute up to 5 per cent of the rock but it is seldom fresh, usually being completely replaced by an aggregate of secondary minerals.

(e) Quartz-bearing Dolerites

Quartz-bearing dolerites are relatively common near the basalt-sandstone contact, both in the sediments themselves, and cross cutting the lower basalt flows. In these dolerites, remnants of sandstone and basement rock xenoliths are usually noticeable, frequently only on a microscopic scale. Digestion of these xenoliths is commonly more or less complete, but residual cores up to 5 mm across consisting of aggregated quartz and muscovite grains are present in many of the dykes. These cores are surrounded by a finer grained rim of more basic material which grades into the normal non-porphyritic type groundmass, previously described. With progressive assimilation of the xenoliths a quartz rich patch of otherwise normal dolerite results. Pyroxene is usually absent from the rim material surrounding the xenoliths, which consists of a glassy groundmass containing small clouded plagioclase laths of indeterminate composition and granules of an opaque ore mineral.

(ii) Mineralogy

Data for the major minerals present in the dolerites are listed in Table 14. In addition, however, it was noted that there is a slight tendency for the more basic plagioclase to occur in the dolerites low in micropegmatite, with the most basic plagioclase composition, An_{60}, being found in the dolerites with less than 10 per cent micropegmatite plus iron ore. Most micropegmatite-rich dolerites on the other hand, contain plagioclase with an average composition of about An_{50}. This is illustrated in Figure 2 where the micropegmatite content of twenty dolerites is plotted against the anorthite content of their constituent plagioclase cores, (p 48).

(iii) Modal Composition

Modal analyses of seventeen dolerites collected along an east-west section across the entire Komatipoort area are shown in Table 15, p 49, and the variation in volume percentage of the three main mineral phases are shown in the triangular diagram in Figure 3, p 50 . This diagram suggests a steady increase in the micropegmatite content of the dolerites at the expense of pyroxene and olivine, with the plagioclase content remaining constant. A roughly similar trend was found by Gunn (1962) in the Ferrar dolerite of Antarctic (see fig 4, p 50) and the differentiation of the Red Hill dolerites in Tasmania, likewise produced a similar trend (Mac Dougall, 1962).

(iv) Geochemistry

On the basis of their modal analyses (described in the previous section) four dolerites were selected covering the whole range of variation shown in the triangular diagram shown in Figure 3, p 50 , and submitted for chemical analysis, (Table 16, p 51). As may be seen from the analyses shown in Table 16, three of the rocks are of very similar composition in spite of wide apparent variation in modal composition, (samples CL16,

TABLE 14

Mineral Data for Dolerites of the Komatipoort Area

	Mineral	Zoning	Composition	Alteration	Grain Size	Shape or Form
A	Plagioclase					
	(i) Groundmass	Normal Zoning	Range(Core An_{60} Rim An_{35}	Not observed	0,1 - 1,0 mm	laths
	(ii) Phenocrysts	Normal zoning, occasional oscillitary zoning	Range(Core An_{60}-An_{70} Rim An_{35}	Not observed	1,0 - 5,0 mm	Sub-hedral laths and plates
B	Pyroxene		Mg Fe Ca			
	(i) Augite	Not observed	Range(44 20 36 / 38 27 35	May alter to chlorite	0,1 - 1,0 mm	Irregular ophitic to subhedral grains or subhedral phenocrysts
	(ii) Pigeonite	Not observed	Range(53 38 9 / 48 43 9	Not observed		As for augite. May also form cores to augite crystals
C	Olivine			Completely altered to antigorite, magnetite and chlorite	1,0 - 3,0 mm	Euhedral to rounded
D	Ore Minerals					
	(i) Magnetite			Often altered to hematite	Up to 1,5 mm	Irregular interstitial grains
	(ii) Ilmenite			Not observed	Up to 1,5 mm	Irregular interstitial grains
	(iii) Pyrite			Not observed	Up to 0,5 mm	Irregular interstitial grains

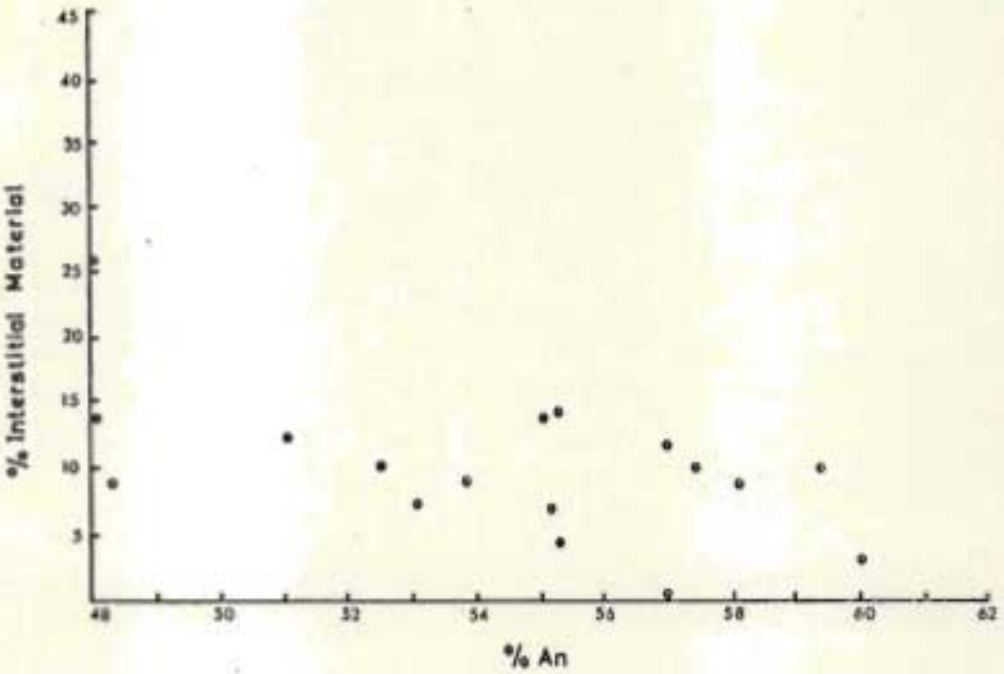

Figure 2. Variation of An Content of Plagioclase with Interstitial Micropegmatite Content in seventeen Dolerite Specimens from the Komatipoort Area, (for modes see Table 15, p. 49).

TABLE 15

Modal analyses of seventeen dolerite specimens from the Komatipoort Area

Sample no.	CL 55	CL 56	CL 57	CL 58	CL 59	CL 60	CL 61	CL 62	CL 63	CL 64	CL 65	CL 66	CL 67	CL 15	CL 16	CL 17	CL 18
Plagioclase	46.2	49.8	45.8	44.7	47.1	48.7	51.6	44.3	47.5	44.7	43.0	43.4	46.6	48.5	47.6	46.9	50.1
Clinopyroxene	38.3	35.3	36.7	35.3	32.8	46.7	41.3	36.9	39.9	33.6	36.8	34.2	38.3	36.2	38.7	24.1	34.0
Ore Minerals	6.4	7.7	6.9	8.7	7.4	3.1	3.0	6.6	4.3	7.4	6.3	7.6	7.3	4.9	9.4	4.2	6.1
Interstitial Material	8.3	7.0	10.3	10.4	12.7	0.7	3.2	12.2	8.3	14.3	13.9	14.6	7.2	10.4	4.0	26.8	9.1
Altered Olivine	0.8	0.2	0.3	0.9	-	0.8	0.9	-	-	trace	-	0.2	0.4	-	0.3	-	0.7

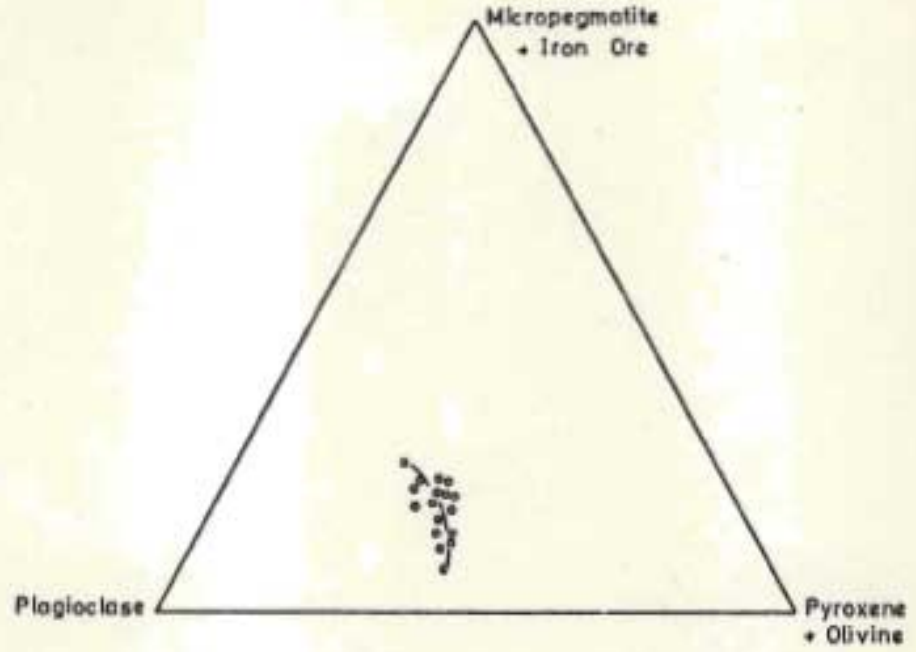

Figure 3. Triangular Variation Diagram showing the Variation in Major Modal Minerals of seventeen Dolerite Samples from the Komatipoort Area, (see Table 15, p. 49 for modes).

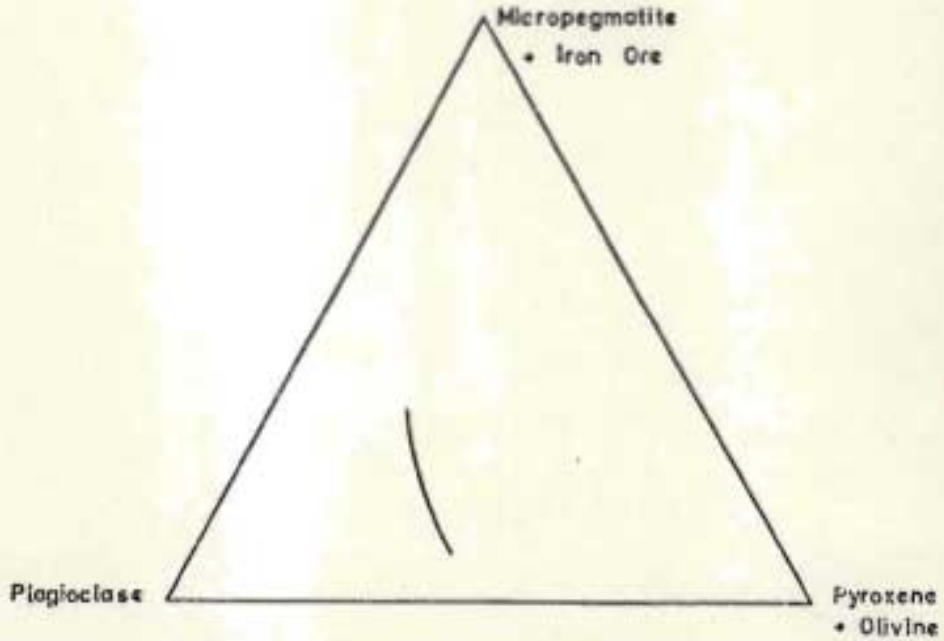

Figure 4. Triangular Variation Diagram showing the Variation Trend of Major Minerals for the Ferrar Dolerites of Antarctica, (after Gunn, 1962).

TABLE 16

Chemical analyses, CIPW Norms, and Niggli Values for four specimens of dolerite from the Konatipoort Area (Analyst: NIM).

Chemical analyses					CIPW Norms					Niggli Values				
Sample no.	CL 15	CL 16	CL 17	CL 18		CL 15	CL 16	CL 17	CL 18		CL 15	CL 16	CL 17	CL 18
SiO_2	52.64	50.10	49.50	49.98	Si	144.93	116.39	116.08	120.05	q	11.88	1.53	2.99	4.60
Al_2O3	12.71	13.59	12.76	12.75	Al	20.62	18.61	17.64	18.18	or	9.98	2.18	3.54	4.49
Fe_2O_3	5.06	3.14	3.23	3.37	Fm	47.93	48.53	50.84	50.56	ab	18.35	20.97	17.67	17.67
FeO	9.00	10.94	11.42	11.40	C	22.69	26.74	25.88	25.18	an	19.93	24.84	23.65	23.15
MgO	3.95	6.16	6.37	5.79	Alk	8.76	6.13	5.65	6.08	di	11.53	22.54	21.15	19.10
CaO	7.69	10.74	10.30	9.71	Mg	0.34	0.44	0.44	0.41	hy	13.22	19.38	20.36	19.65
Na_2O	2.17	2.48	2.09	2.09	c/Fm	0.47	0.55	0.51	0.50	mt	7.35	4.56	4.69	4.90
K_2O	1.69	0.37	0.60	0.76	k	0.34	0.09	0.16	0.19	il	4.52	3.35	4.66	4.77
H_2O^-	0.51	0.25	0.33	0.38	Ti	4.62	2.88	4.01	4.28	ap	1.57	0.44	0.68	0.72
H_2O^+	1.53	1.09	1.26	1.28	P	0.84	0.20	0.31	0.34	H_2O	2.04	1.34	1.59	1.66
CO_2	0.30	0.18	0.23	0.26	H_2O	14.05	8.44	9.85	10.33					
TiO_2	2.23	1.65	2.30	2.35										
P_2O_5	0.72	0.20	0.31	0.33										
MnO	0.22	0.23	0.24	0.23										
Total	100.42	101.12	100.94	100.68						Total	100.37	101.13	100.98	100.71

17 and 18). The explanation for this is probably to be sought in the composition of interstitial glass in the three relevant specimens. If this is the case, the glass must have a basic composition, in no way comparable to the composition of interstitial micropegmatite so abundant in sample CL15. Further discussion of the geochemistry of the dolerites, including a comparison with Karroo dolerites from elsewhere in South Africa, will be given in the section of the geochemistry of the basic volcanics.

(v) Rheomorphic Veins produced by the Action of Dolerites

Metamorphism of basalts by dolerites has been described in the relevant section (see before), however, the dolerites do have another metamorphic effect, in that rheomorphic veins of siltstone have been produced near the base of the volcanic succession.

5.6.2 Minor Acid Intrusives

The minor acid intrusives consist for the most part of sub-vertical, approximately north-south trending dykes, together with a few thin sheets, although the latter are not common. These intrusives show a tendency to occur in the upper part of the basalt sequence and within the rhyolitic lava succession (see geological map), strikes of the acid dyke rocks appear to follow two distinct trends, one close to north-south , as exemplified by the Causeway Dyke exposed in the Komati River (see geological map), and the other some 10° to 20° east of north, a strike followed by the majority of the acid dykes cross-cutting the basalts. The possibility that the latter strike is characteristic of a younger series of acid dykes is suggested by the fact that the north-south striking Causeway Dyke is cut by the granophyre of the Komatipoort intrusion, which in turn is intruded by a felsite dyke striking some 20° east of north within the Kruger National Park. A prominent dyke in the southern part of the Komatipoort area, however, may be seen to swing from a north-south strike to one some 10° east of north (on the geological map), and the

probability exists that the relationship between the two strike directions is more complex.

Width of the dykes varies from about 3 m to about 30 m, while along strike they may extend for considerable distances; for example, the Causeway dyke may be traced over a distance of more than 16 km, (see geological map). The finer grained acid rocks are resistant to weathering and where they crosscut the free-weathering basalt, they form low, continuous, north-south striking ridges. In the field the dykes are for the most part indistinguishable form the acid lavas. Most of these acid dykes appear to be single intrusions; composite dykes were not observed.

(A) Petrography

The rock types composing these dykes show textural rather than mineralogical differences. They include rhyolite breccias, porphyritic microgranites, granophyric microgranites and also coarser grained granophyres, and aphyric microgranites. Rock types intermediate between these varieties may also be found and a general impression is gained, in places, of a gradation from one rock type to another. In the field, some of these rocks may be difficult to distinguish from others. Rhyolite breccias, porphyritic microgranites and coarser grained granophyres may easily be identified, but the finer grained aphyric types all appear as pink to buff, or brown weathering, microcrystalline, felsitic rocks. Where fresh the minor acid intrusives are usually grey or greyish-green in colour and in the porphyritic types, phenocrysts of plagioclase and sometimes ferro-magnesian minerals are conspicuous. All types may contain xenoliths or microxenoliths, usually of a fine grained basalt or dolerite, but in the vicinity of the gabbro intrusions, this rock type may also be present. With a marked increase in the amount of included material, these rocks grade into the hybrid types described in another section.

(i) Aphyric and Porphyritic Microgranite Dykes

Porphyritic dykes contain phenocrysts of feldspar and occasionally pyroxenes,

set in a groundmass similar to that of the aphyric microgranite dykes. The feldspar phenocrysts, where identifiable, consist of plagioclase crystals up to 5 mm in length often showing signs of corrosion. Slight normal zoning is usually developed. Another mineral forming phenocrysts is pyroxene, partly altered to chlorite. Iron ore may also form large irregular grains, which are macroscopically conspicuous in some rocks. The groundmass of the non-aphyric rock types consist of clouded feldspar crystals and quartz, with occasional minute grains of hematite and shreds of altered ferromagnesian minerals, now consisting predominantly of chlorite. Determination of the composition of the groundmass minerals is difficult due both to the fine grained nature of the groundmass and to persistent clouding of the feldspar crystals occurring in the groundmass. Fairly low optic axial angles measured in some of the feldspars suggest that anorthoclase may be present.

(ii) Granophyres

Granophyres proper consist of a coarse intergrowth of orthoclase and quartz, often optically continuous in small patches centered around plagioclase crystals. Scattered corroded phenocrysts of pale green clinopyroxene and irregular grains of iron ore constitute the rest of the rock. The phenocrysts typically show reaction and resorbtion effects, the plagioclase commonly being embayed and rimmed with orthoclase, while the pyroxene crystals are usually irregular corroded remnants, marginally altered to hornblende and magnetite.

(iii) Rhyolite Breccias

Rhyolite breccia dykes are confined to the rhyolitic lava sequence and are particularly well exposed in the gorge the Komati River has cut through the Lebombo range. The larger dykes (1 to 10 m in width) have a roughly north-south strike, but the smaller intrusives tend to be highly irregular. These range from a centimeter to a meter in width.

The dykes consist of subangular blocks of rhyolite ranging from less than

1 cm up to 1 m in diameter, set in a fine grained, pale pink to buff coloured rhyolitic matrix. They are normally crowded with angular fragments of rhyolite, but in some cases relatively few blocks are present, and the dykes become difficult to distinguish from the surrounding rhyolitic lavas. In thin section the rhyolitic matrix material closely resembles the fine grained groundmass present in the microgranite dykes. Phenocrysts are common, consisting of feldspar and quartz typically, although the pale-green clinopyroxene phenocrysts noticed in the microgranite may also be present. Ore minerals occur in minor amounts as irregular grains.

(B) Mineralogy

Mineral data for the major rock forming minerals of the minor acid intrusives are listed in Table 17

(C) Modal Compositions

Most of the dyke rocks are too fine grained for satisfactory micrometric determination of modal compositions. The relative proportions of phenocrysts and groundmass material in three samples of acid dyke rocks are shown in Table 18 together with the modal analysis of a coarser grained granophyre.

(D) Geochemistry

No new chemical analyses of the acid dyke rocks were made during the present investigation. Lombaard (1952) has analysed a specimen of the Causeway dyke, a granophyric microgranite and the results of this analysis together with the CIPW Norm, Niggli Values and magma type as calculated by Lombaard are shown in Table 19.

TABLE 17

Mineral Data for the Minor Acid Intrusives from the Komatipoort Area

Mineral	Zoning	Composition	Refractive Indices	2V	Alteration	Grain Size	Colour
A Plagioclase							
(i) Phenocrysts	Slight normal-common Oscillatory -rare	$An_{10} - An_{35}$	Not determined	-	Often turbid	1-5 mm	
(ii) Groundmass	Slight normal-common	$An_{8} - An_{14}$			Often turbid	0,01-0,2 mm	
Note: Anorthoclase and orthoclase possibly also present in some specimens							
B Clinopyroxene		Mg Fe Ca		2V			
(i) Phenocrysts	Not observed	Range(30 25 45 / 24 32 44	Ny Range(1,705 / 1,715	$42\frac{1}{2}^{o}$ / 44^{o}	Altered to chlorite in places	1-3 mm	Pale Green
C Quartz							
(i) Phenocrysts						2,0 mm	
(ii) Groundmass						0,01 - 0,2 mm	
D Ore Minerals							
(i) Magnetite						0,2 -2,0mm	
(ii) Hematite						0,2 mm	
(iii) Pyrite						0,2 mm	
D Accessory Minerals							
Zircon							
Chlorite							

TABLE 18

Modal composition of acid dyke rocks (volume/percentage)

Mineral	Sample CL51 %	Sample CL52 %	Sample CL53 %	Sample CL54 %
Groundmass Plagioclase	0	15	22	13
Porphyritic Plagioclase	5	7	0	0
Interstitial Material	93	64	47	80
Pyroxene	1	9	15	1
Ore	1	3	13	5
Quartz	0	2	3	1

CL51 : Causeway dyke, granophyric

CL52 : Porphyritic microgranite

CL53 : Granophyre

CL54 : Aphyric microgranite

TABLE 19

Analysis of an acid dyke rock from the Komatipoort area
(after Lombaard, 1952)

		CIPW Norm		Niggli Values	
SiO_2	68.89				
Al_2O_3	13.46	Q	27.57	si	299.50
Fe_2O_3	3.10	Or	25.04	si	34.50
FeO	3.51	Ab	26.22	fm	27.40
MgO	0.63	Wo	0.58	alk	24.80
CaO	2.83	Di En	0.20	k	0.47
Na_2O	3.08	Fs	0.40	mg	0.15
K_2O	4.27	Hy En	1.41	c/fm	0.49
H_2O^+	1.12	Fs	2.64	ti	1.80
H_2O_-	0.45	Mt	4.40	p	0.26
MnO	0.15	An	10.29	c	13.30
TiO_2	0.54	Il	1.05		
P_2O_5	0.15	Ap	0.34		
CO_2	0.24	CC	0.60		
		H_2O	1.57		

Causeway dyke Komatipoort, porphyritic granophyric microgranite.

Magma type: normal granitic.

Analyst : W.H. Herdsman.

5.7 Major Intrusives

Three relatively major intrusive masses occur in the Komatipoort area:

(i) The Crocodile River Intrusion - a basic plutonic intrusion which has invaded the Precambrian basement rocks and is in turn overlain by the Karroo sediments.
(ii) The Basal Intrusion - a composite intrusive mass occurring at the base of the volcanic succession just above the Karroo sediments.
(iii) The Komatipoort Intrusion - a large composite intrusive mass emplaced in the upper part of the basalt succession.

5.7.1 The Crocodile River Intrusion

The Crocodile River Intrusion forms the southern extension of a line of basic intrusive masses, frequently showing well developed layering, that stretch southwards from the Letaba and Olifants Rivers which lie some 140 km to the north of Komatipoort. These may be traced along a roughly north-south trending line from the Letaba River as far south as Pretoriuskop in the Kruger National Park (see fig 5, p 60), from where they swing eastwards and pass beneath the Karroo Sediments on the north bank of the Crocodile River in the Komatipoort area, (Saggerson and Logan, 1970).

A Form of the Intrusion

Near Komatipoort the intrusion forms a discontinuous outcrop which was examined over a distance of about 2½ km. The dyke-like intrusion varies in width from a maximum of almost a kilometer to a minimum of 300 m, just before disappearing beneath the Karroo Sediments. The vertical, dyke-like nature of the intrusion is suggested by the lack of variation in its strike with changes in relief, and its independence of structural control by the enclosing Precambrian rocks, until the Komatipoort area is reached. Contacts are not well exposed, however, and no further evidence of the form of the intrusion is available.

B Age of the Intrusion

The age of the intrusion could not be determined with any certainty. Clearly two possibilities exist:

Figure 5. Distribution of possible Karroo Age Basic Intrusive Masses within the Pre-cambrian Rocks between the Lebombo River and Komatipoort, (after Saggerson and Logan, 1970).

(a) The intrusion may be of Karroo or post-Karroo age intruded into the Precambrian basement rocks beneath a pre-existing Karroo cover.
(b) The intrusion may be pre-Karroo in age with a period of erosion intervening prior to the deposition of the Karroo age rocks.

The question could be resolved easily if the nature of the contact between the gabbro and the Karroo Sediments was known, but the contact was not found in the Komatipoort area. Saggerson and Logan (1970) encountered similar difficulties in the Olifants River area to the north, where the Karroo sediment-gabbro contact is again obscured. Between these two points, the line of intrusives lies some distance to the west of the position of the present Karroo sediment outcrop (see fig 5, p 60), and it was not found possible to determine relative ages by this means. The roughly north-south strike of the line of intrusives between the Letaba River and Pretoriuskop suggests that the intrusion may be related to the Lebombo tectonic zone. For this reason Saggerson and Logan (1970) have suggested an early Stormberg Age, however, it may be significant that the Lebombo belt is located parellel to the Mozambique mobile belt and volcanic activity may have been spread over a considerable period of geological time; in this case the rough parallelism between the Lebombo and line of basic intrusions may be of little importance as an indicator of age.

Detailed mapping of that part of the line of mafic intrusions lying to the south of the Crocodile River shows the presence of north-south trending dolerite dykes of apparent Karroo age both cross-cutting and terminating against the approximately east-west trending mafic intrusive, (see fig 6). The mafic intrusive is, therefore, not younger than Stormberg, and the termination of some of the dykes against the major intrusive suggests they may have been transected, supporting the possibility of an early Stormberg age.

Exposures providing supporting evidence such as the metamorphism of the dolerite dykes by the Crocodile River Intrusion are, however, lacking and

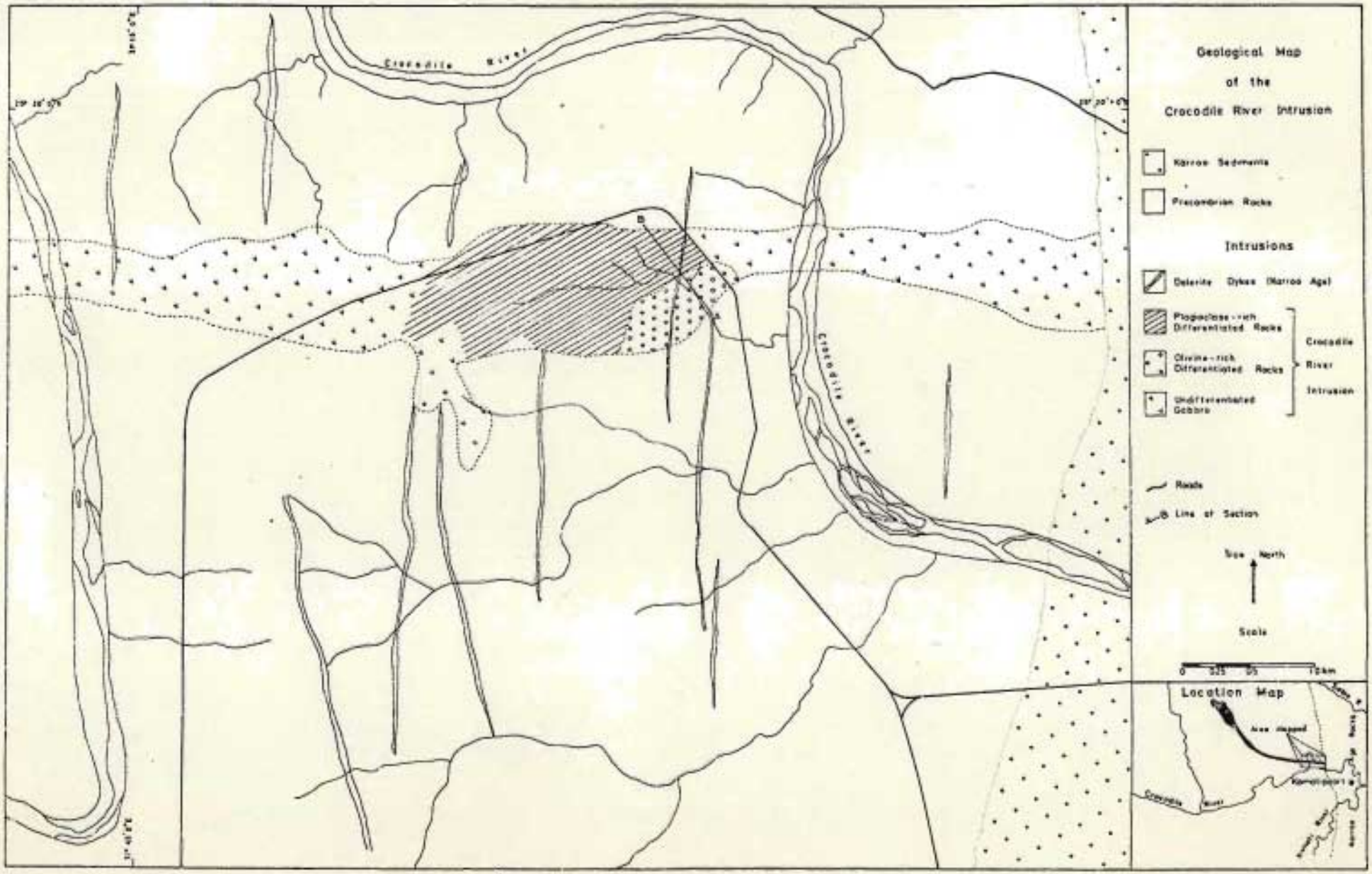

Figure 6. Geological map of the Crocodile River Intrusion

the age of this intrusion cannot be regarded as proven.

In summary available evidence indicates that the line of intrusives could possibly be of early to middle Stormberg age and a description of this intrusive has therefore been included in the present work.

C Petrography

At Komatipoort the bulk of the intrusion consists of a relatively homogeneous medium grained gabbro, composed of clinopyroxene, plagioclase, ore minerals and minor amounts of interstitial micropegmatite. Occasionally small quantities of hypersthene or biotite may be present. Approaching the contact between the gabbro and the granitic country rock, the amount of interstitial micropegmatite present increases in abundance and this is accompanied by a marked decrease in the grain size of the constituent minerals. Plagioclase and pyroxene crystals decrease in length from 2 to 3 mm near the centre of the intrusion to less than one millimeter within a meter of the contact.

More highly differentiated rock types are present along the southern contact of the dyke on the south side of the Crocodile River (see fig 6, p 62). Here rock types ranging from olivine norite (olivine-orthopyroxene-clinopyroxene cumulate) to normal gabbro (plagioclase-clinopyroxene cumulate) occur.

(i) Petrography of the Differentiated Series

The most basic rock occurring in the Crocodile River Intrusion, is an olivine-orthopyroxene-clinopyroxene cumulate, that consists of cumulus olivine, hypersthene and lesser amounts of augite set in large intercumulus poikilitic plates of plagioclase, or less commonly, augite. Occasionally, smaller olivine crystals are enclosed by the hypersthene or augite crystals which in turn are set in the plagioclase plates, although this textural relationship is not common.

The olivine crystals in general vary in size from 2 to 3 mm and the poikilitic plagioclase and pyroxene plates are of the order of 10 mm in diameter. The cumulate subhedral augite crystals that are also found enclosed in the poikilitic plagioclases are about 2 mm in diameter. Accessories include opaque ore minerals and a brown pleochroic biotite, and these two minerals frequently appear in close association, with the biotite forming patches occassionally reaching 2 mm in diameter, surrounding a core of the ore minerals.

Examination of further specimens shows that within a vertical distance of 15 m, plagioclase appears as a cumulus phase, initially together with and enclosed by the large intercumulus plagioclase crystals, however, 6 m above this point the intercumulus plagioclase and augite plates disappear and the rock becomes equigranular, consisting of euhedral to subhedral plagioclase,orthopyroxene and to a lesser extent clinopyroxene crystals. The grain size of all of these minerals is between 2 and 3 mm. Accessory minerals are again, brown pleochroic boitite, which is present in reduced amounts, and smaller quantities of opaque ore minerals.

Over a vertical interval of a further twenty meters the orthopyroxene content decreases markedly, and the rock, although texturally unchanged is composed largely of augite, pigeonite and plagioclase crystals that are usually subhedral and 2 to 3 mm in length. Green pleochroic biotite occurs in yet smaller quantities, and there is a slight increase in the iron ore content. Interstitial micropegmatite content increases sharply and there is some evidence of reaction between the micropegmatite and the pyroxene in the form of embayments in the pyroxene crystals.

To summarise, passing upwards through the intrusion there is a gradual change in the relative abundance of the major mineral phases with an increase, initially, in the ortho and clinopyroxene content of the rock at the expense of olivine and to a lesser extent, biotite (see fig7, p65). Subsequently, plagioclase and clinopyroxene content increases relative to the percentage of orthopyroxene, which in turn decreases to vanishing point. Textural evidence suggests that the order of crystallisation of the

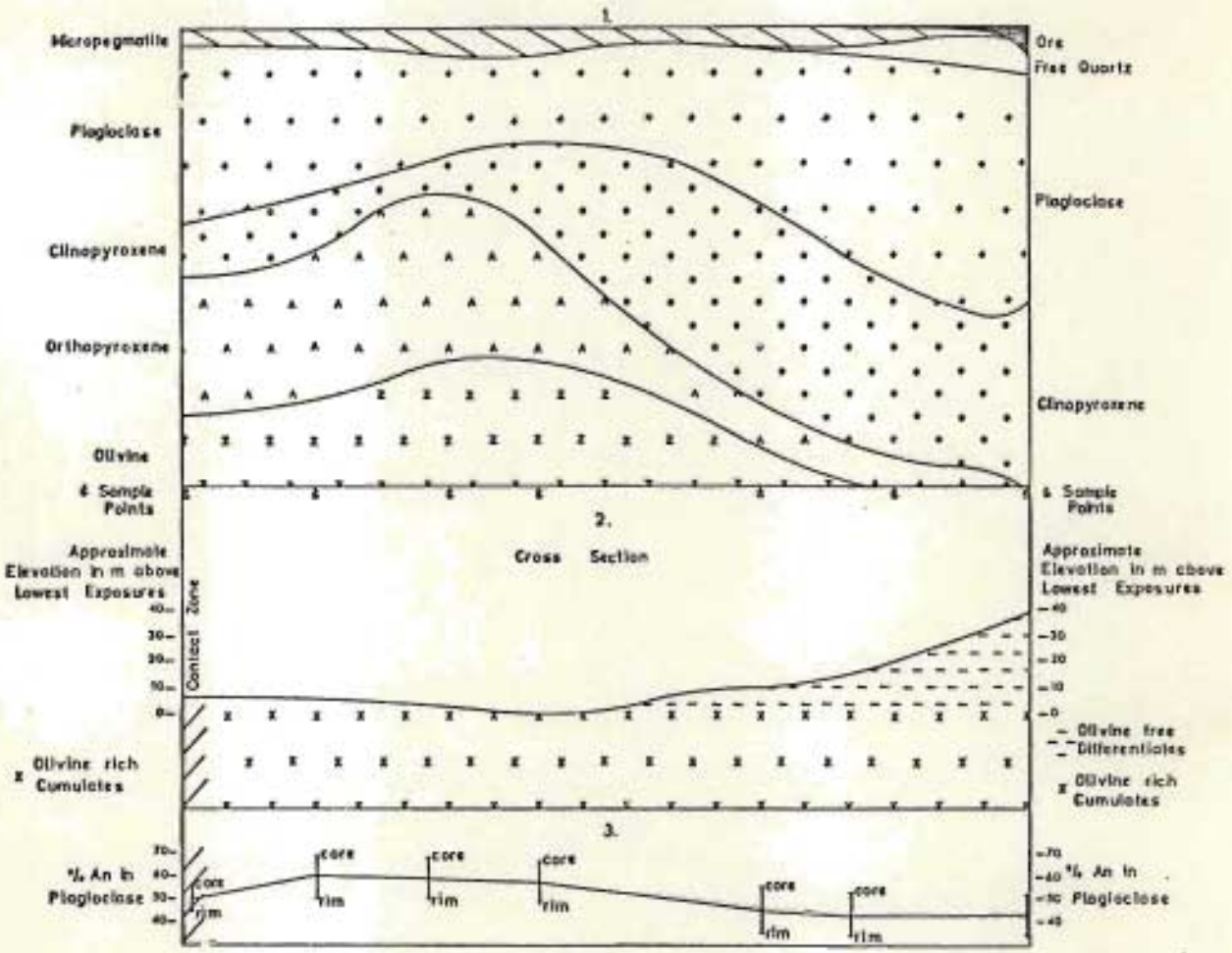

Figure 7. Diagrams showing:

1. Variations in modal proportions along a N-S cross-section of the Crocodile River Intrusion.
2. Diagrammatic cross-section of the Intrusion.
3. Variations in plagioclase composition along the cross-section of the Intrusion.

major rock forming minerals was olivine, hypersthene, augite, plagioclase.

(ii) Petrography of the Contact Zone

As shown on the map in fig 6, p 62 , the most basic rocks in the intrusion are exposed near the southern margin of this dyke-like body, a distribution that is probably the result of local relief (see section in fig 7, p 65), i.e. produced by erosion of a series of differentiated rock types developed in approximately horizontal layers. The most basic rock in the intrusion, the olivine-orthopyroxene-clinopyroxene cumulate, (described above) first occurs at a distance of some 14 m from the southern contact and in this intervening 14 m wide contact zone the rocks show a rapid variation in both the texture and abundance of the major mineral phases, even in samples collected in the same horizontal plane. In addition these contact zone rocks display unusual textural relationships, which suggest reversals in the order of crystallisation deduced from textures present in other parts of the intrusion, (see page 64) For example orthopyroxene, encloses crystals of intermediate plagioclase, a lower temperature phase.

Samples collected between the olivine-orthopyroxene-clinopyroxene cumulate and the contact of the intrusion show the following series of changes. In a specimen located some 6 m from the contact, plagioclase appears in two forms, firstly as the large plates noted in the olivine-orthopyroxene-clinopyroxene cumulate and secondly as small (? to 3 mm in length) subhedral crystals, which are frequently embayed and corroded. These smaller crystals are included in any of the other minerals present, except olivine, although in places they are associated with olivine in glomeroporphyritic aggregates. Hypersthene occurs as large irregular crystals 4 to 6 mm in diameter which enclose not only the smaller embayed plagioclase crystals, but similar clinopyroxene crystals and euhedral to subhedral olivine crystals. Clinopyroxene in the form of augite is present in subordinate amounts as the small crystals mentioned above but for the most part forms extensive plates enclosing olivine or

occasionally the small embayed plagioclases. Olivine is present in subhedral and euhedral crystals of reduced size (1 to 2 mm in diameter), and these crystals are included in all of the other mineral phases. Accessory minerals, as before, are biotite and opaque ore minerals, although here the biotite in places grades from a core of the brown pleochroic variety into a rim of the green pleochroic type.

At a distance of 9 m from the contact the large platy plagioclase crystals have disappeared, and plagioclase occurs only in the form of small subhedral to anhedral crystals, 1 to 3 mm in length. They are usually included in orthopyroxene crystals, which, in addition to forming large irregular plates (3 to 6 mm in diameter), enclosing the plagioclase and augite, also occur both as smaller (1 to 2 mm in length) subhedral grains and as cores to the augite crystals included in all the major mineral phases. From this point there is a sharp increase in olivine and hypersthene content and the rock grades rapidly into the olivine-orthopyroxene-clinopyroxene cumulate described at the beginning of this section (p 63).

D Mineralogy

Plagioclase

Within the differentiated part of the intrusion the plagioclase occurs in two forms, firstly as the extensive intercumulus plates found in the more basic rocks and secondly as the smaller subhedral cumulus crystals present in the upper parts of this intrusion.

The intercumulus plates average about 10 mm in diameter , and commonly show slight normal zoning, with the range in composition of the zoning being dependent on the vertical position of the plagioclase in the intrusion. In the lowest and most basic rocks, the plagioclase composition ranges from An_{68} to An_{50} whereas in the highest parts of the intrusion in which the platy crystals occur, the range is from An_{62} to An_{45}.

Stronger zoning of the type: core - oscillatory zoned mantle - rim is usually shown by smaller cumulus crystals, with typical plagioclase crystals from the base of the plagioclase-hypersthene-augite cumulate having cores with a composition of An_{60}, mantles oscillating between An_{55} and An_{50}, and rims which grade rapidly from An_{45} to An_{35}. Higher in the intrusion the plagioclase is slightly more sodic with the following average composition: core An_{52}, oscillatory zoned mantle, between An_{42} and An_{50}, rim An_{32}. The variation in the anorthite content of these feldspars, together with a cross-section of the differentiated portion of the intrusion is shown in fig 7 , p 65.

In the contact zone there is a marked difference in the composition of the two textural modifications of plagioclase that are present. The large platy crystals have a composition of about An_{60}, that is similar to the composition of those occurring in the adjacent hypersthene-olivine-augite cumulate and the smaller corroded plagioclases have a composition in the range An_{50} to An_{55}, that is almost identical to those occurring in the plagioclase-hypersthene-augite cumulate.

The medium grained gabbro that forms the undifferentiated portion of the intrusion contains subhedral, normally zoned crystals of plagioclase, zoned from An_{50} in the cores of these crystals to An_{32} at the margins. No oscillatory zoned plagioclases were noted in these rocks.

Pyroxene

In the differentiated portion of the intrusion, both orthopyroxene and clinopyroxene are present in almost all rocks, the augite-plagioclase cumulate being the only exception. This rock forms the uppermost part of the intrusion and in places apparently contains clinopyroxene only.

(i) Orthopyroxene

The orthopyroxene, hypersthene, initially shows a steady decrease in quantity upwards through the differentiated rocks. It normally appears

as a cumulus phase crystallising before the clinpyroxene in which it is frequently included. The composition of the hypersthene shows a steady change upwards through the intrusion as may be seen from the diagram in fig 8 , p 70 , with extreme variations ranging from En_{74} to En_{64} . Exsolution of clinopyroxene was not observed in hypersthene from any level of the intrusion.

(ii) Clinopyroxene

Augite is present in all rocks, rapidly increasing in quantity from a minimum value in the olivine-orthopyroxene-clinopyroxene cumulate to become the dominant ferromagnesian mineral in the uppermost rocks of the differentiated series. Its crystal form is variable ; in the differentiated rocks it occurs as subhedral cumulus chadocrysts, but in the marginal rocks, the augite may form ophitic or even poikilitic crystals. Exsolution of orthopyroxene is common, but the orthopyroxene usually takes the form of irregular, randomly arranged blebs rather than crystallographically orientated lamellae. Simple twinning on (100) is occasionally present. The composition of the augite shows a fairly regular variation upwards through the differentiated rocks with a gradual increase in iron content at the expense of magnesium. Extreme values were found to range from $Mg_{45}\ Ca_{35}\ Fe_{20}$ in the most basic rocks, to $Mg_{34}\ Ca_{34}\ Fe_{32}$ for augites from the upper parts of the intrusion. Variations in pyroxene composition are shown in the diagram in fig 8, p 70.

(iii) Biotite

Although biotite is present in variable amounts in all rocks of the intrusion, differences in the colour of the biotite present in various rock types suggest changes in composition may occur. Maximum absorption colour of the biotite varies from a deep reddish-brown in the most basic rocks, through a dark greyish-brown in the intermediate rocks, to green in the most leucocratic rocks present.

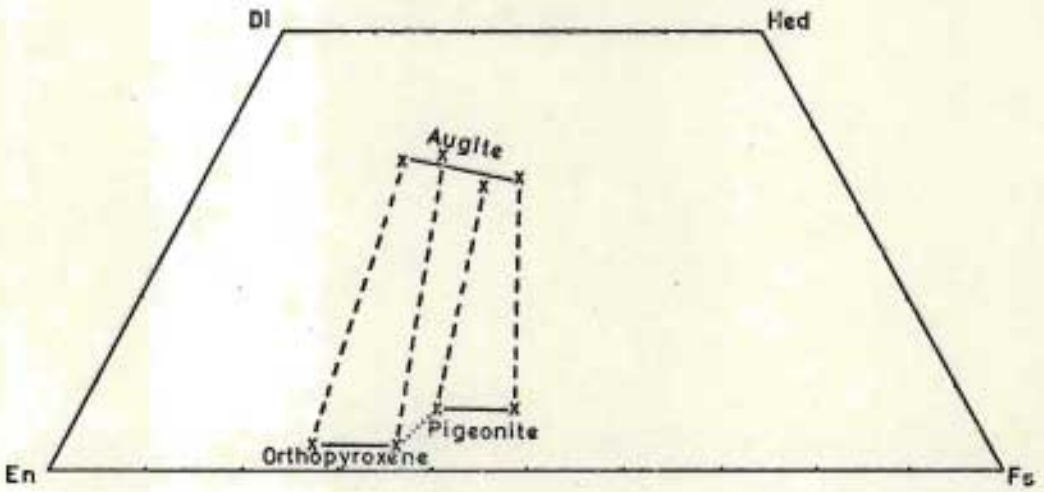

Figure 8. Variation in Pyroxene Composition in the Differentiated Rocks of the Crocodile River Intrusion.
(Tie lines join co-existing pairs).

Colour-zoned biotites were also noted in some of the more leucocratic rocks. Commonly the biotite shows partial alteration to iddingsite and chlorite, and although it is apparently a primary crystallisation product in the lowermost basic rocks of the intrusion, its occasional mode of occurrence as a corona around pyroxene crystals and ore mineral grains suggests the biotite is probably a subsolidus reaction product in the uppermost rocks, as suggested by Nash (1976) for biotite in the Skaergaard Intrusion.

(iv) Ore Minerals

Minor quantities of ore minerals consisting of one or more of the following, chalcopyrite, pyrite, ilmenite and magnetite, are always present.

Chalcopyrite

This mineral reaches its greatest abundance in the most basic rocks of the intrusion where it occurs as tiny irregular grains either interstitially, or concentrated along alteration cracks in olivine crystals. Chalcopyrite, however, is never present in more than accessory amounts.

Pyrite

Most rocks contain minor amounts of pyrite, although in general the mineral appears to increase in abundance upwards through the rocks of the differentiated series. It is also present in small quantities in the undifferentiated medium-grained gabbro which forms the bulk of the intrusion. Typically the pyrite forms interstitial irregular grains which may reach 2 mm in diameter and less commonly it occurs as cores to biotite crytstals.

Ilmenite

Variable quantites of ilmenite are present in the differentiated rocks, particularly towards the base of the series. The mineral is less common

in the undifferentiated medium grained gabbro. Although ilmenite may occur as tiny needles (length 0.3 mm), irregular interstitial grains are more common and , in these, orientated exsolution lamellae of magnetite are occasionally present.

Magnetite

Magnetite is the commonest of the ore minerals present in all the rocks of this intrusion, and is usually present as irregular interstitial grains up to 1.5 m in diameter. In the more basic rocks of the differentiated series, a few euhedral octahedra were noted, but these are not widespread. Partial martitisation of the magnetite to hematite is common but exsolved ilmenite is not present.

E Modal Analyses

The variation in the proportions of the major constituent minerals along a cross-section of the intrusion is shown in fig 7, p 65. As may be seen from the diagram there is a regular variation in the mineral proportions related to elevation within the intrusion. From the southern margin of the mass to a point about one-tenth of the way across there is a steady increase in the olivine and orthopyroxene content and a corresponding decrease in the plagioclase and augite content. This variation is considered to be the results of rapid cooling due to the proximity of the contact and is not related to relief. This portion of the intrusion has been designated the contact zone and has been described as such in the relevant section. From this point onward, however, the rocks gradually become more leucocratic and the changes in mineral proportions in outcrops may be related directly to changes in elevation within the intrusion, as a consequence of variation in relief. The plagioclase and clinopyroxene content increases rapidly, their proportions varying inversely with those of olivine and orthopyroxene which show a corresponding decrease. Biotite content decreases gradually, while towards the northern contact, that is in the uppermost part of the

intrusion sampled along the section at present under discussion, the interstitial micropegmatite content and opaque ore minerals show a marked increase. The variations are probably best explained as a result of the development of sub-horizontal layers of various rock types, as shown in the cross-section in fig 7, p 65.

F Country Rock

The dyke is intruded into a medium grained granitic rock consisting for the most part of alkali feldspar (orthoclase) and quartz in grains up to 10 mm across, and minor amounts of mica and ore minerals.

G Contact Metamophism

Near the contact with the gabbro the granite shows both dynamic and thermal metamorphic effects, that at a distance of 3 m from the contact, consist of undulose extinction and partial recrystallisation developed in the quartz grains. Closer to the contact the quartz grains, in addition to showing these effects, are surrounded by mantles of graphically intergrown orthoclase and quartz. Within 1 m of the contact, much of the original granitic texture disappears, and the rock consists of a few irregular, clouded, relict fragment of orthoclase set in a fine grained recrystallised groundmass of orthoclase and quartz, which are in places granophyrically intergrown. Garnet in small rounded granules, is common.

H Rheomorphic Veins

Cross-cutting the gabbro itself are numerous light coloured veins of granitic material, varying from a few millimeters to about 10 cm in thickness. The larger veins appear to have had a metasomatic effect on the adjacent gabbro which is often paler in colour over a distance of 2 to 3 cm.

Close to the gabbro-country rock contact, the rock forming the veins consists of large turbid crystals of orthoclase and plagioclase and

smaller deformed quartz grains, all set in a fine grained groundmass. Irregular remnants of pyroxene crystals may also be present but these are extensively altered to hornblende or an aggregate of chlorite crystals. Smaller corroded basic plagioclases (An_{50}) are also present in minor amounts. The narrower veins tend to be finer grained, although they are composed of the same minerals. Minerals present in these narrower veins include radiating aggregates of prehnite and less commonly euhedral crystals of sphene, but the remnants of unaltered pyroxene found in the larger veins are rare.

Adjacent to the veins the gabbro shows extensive alteration of pyroxene to hornblende and chlorite, the plagioclase is clouded and in part altered to prehnite. Quartz may also occur in small fine grained patches.

I Comparison with Similar Intrusions from Other Parts of the Lebombo.

Saggerson and Logan (1970) have presented modal and chemical analyses of the northern-most representatives of the line of layered basic intrusives, of which the Crocodile River Intrusion forms part. Modal variations for the layered intrusion they sampled in the Olifants River area are shown in fig 9, p 75 , which indicates that the major difference between the two intrusions appears to lie in their ferromagnesian mineral contents. Although total ferromagnesian content in each intrusion is similar at approximately the same elevations in the two intrusions, there is a marked difference in the relative proportions of the main ferromagnesian minerals, olivine, clinopyroxene, orthopyroxene. The olivine content of rocks of the Crocodile River Intrusion reaches a maximum value of 28 per cent, whereas the Olifants River body has a maximum olivine content of 48 per cent. For orthopyroxene the position is reversed with the Crocodile River Intrusion containing over 35 per cent in the most orthopyroxene-rich rock-type, and Olifants River Intrusion rocks having a maximum content of some 12 per cent. Maximum clinopyroxene content of the Crocodile River Intrusion rocks is also somewhat lower than that of the Olifants River mass. Whether this difference may be related to a change in

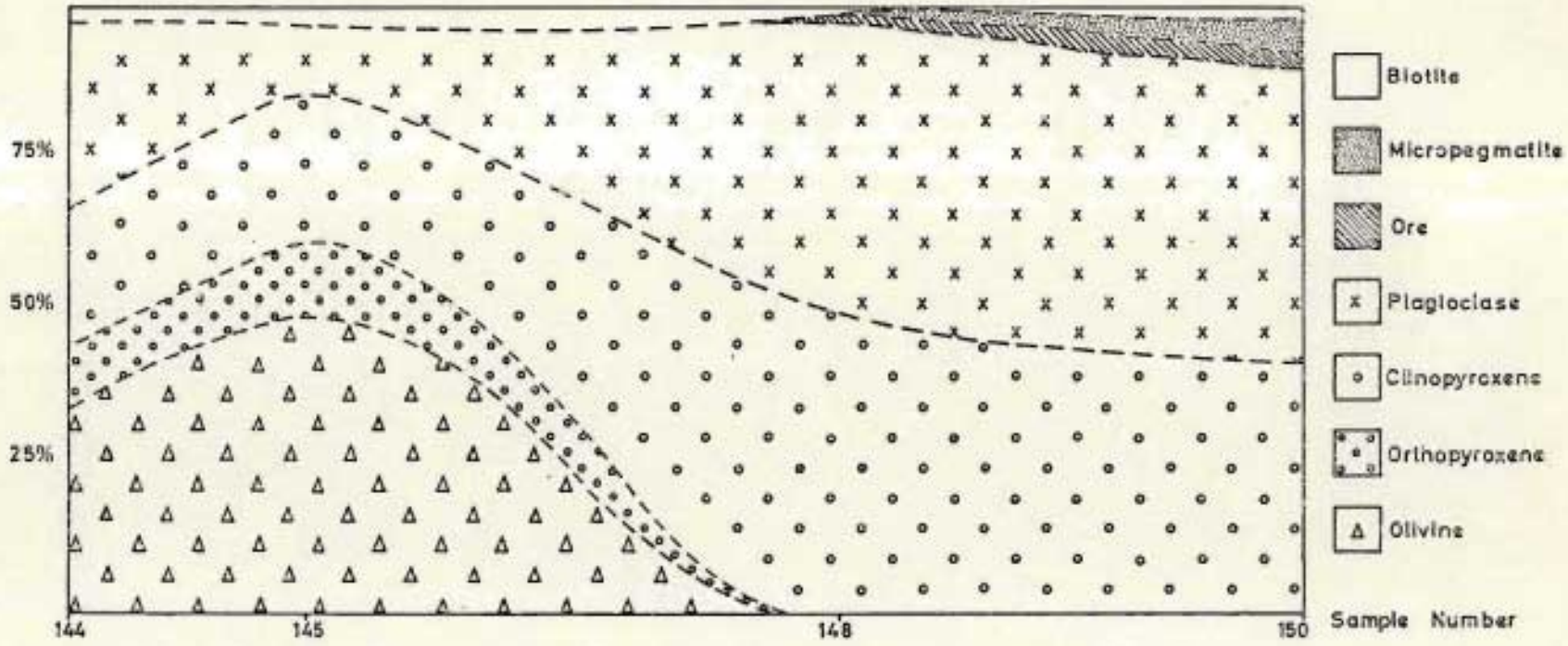

Figure 9. Variations in Modal Proportions in the Differentiated Rocks from a Layered Mafic Intrusion in the Olifants River area of the Lebombo. (After Saggerson and Logan 1970).

composition of the magma forming the intrusion or whether this represents a difference in the degree of differentiation of the two intrusions is not certain. Considering the relatively limited size of the differentiated portion of the Crocodile River Intrusion, the latter explanation should probably be regarded more favourably. Visser and Verwoerd (1960) have briefly described an intrusion from the same line of intrusives in the Pretoriuskop area and a subsequent examination of the intrusion in the same area by Saggerson and Logan showed the presence of a compositionally and texturally similar series of rocks, forming a layered mass.

J Petrogenesis

The nature of the textural and mineralogical variations occurring in the Crocodile River Intrusion suggests that simple crystal settling would be adequate to produce the observed rock series. This conclusion is supported by the strong resemblance between the Crocodile River Intrusion and the layered body occurring in the Olifants River area for which a similar origin was proposed by Saggerson and Logan, (1970). In the thickest portion of the intrusion cooling would appear to have been sufficiently slow for the crystallisation and initial settling out of olivine, but later joined by orthopyroxene. Subsequently clinopyroxene and then plagioclase crystallised from the melt as cumulus phases. This order of crystallisation is confirmed by the fact that plagioclase and augite tend to form intercumulus plates in the lower-most rocks of the intrusion, and are clearly lower temperature phases. The relative abundance of the hydrous mineral biotite, in several of the rock types present suggest that water may have been relatively freely available, which could have facilitated crystal settling by lowering the viscosity of the magma to some extent.

Although convection currents do not appear to have played a significant part in the development of the textures of any of the rock types, (since layered and oriented structures are not conspicuous), they may have been present, as the oscillatory zoning noted in plagioclases occurring in the upper part of the intrusion could have resulted from the circulation of

these crystals in convection currents (as suggested by Wager and Brown, 1939),which must then have operated at least subsequent to the middle stages of crystallisation of this intrusion.

The occurrence of lower temperature minerals included in the higher temperature phases in the contact zone of the intrusion, that is, an inverse textural relationship, is probably the result of lower temperature phases crystallising in cooler regions adjacent to the wall-like contact of the intrusion or possibly the roof and subsequently, during settling, drifting or being carried by convection currents into hotter regions. Here these minerals would no longer be stable and resorbtion and the observed corrosion would result. Some crystals would be completely resorbed, but others, although corroded, could be included in the higher temperature mineral phases as these began to crystallise. Thus protected, they would survive as the rock solidified completely.

5.7.2 The Basal Intrusion

A Introduction

An elongated intrusive mass composed of several rock types, which here has been termed the Basal Intrusion, occurs close to the base of the basaltic sequence near the southern end of the Komatipoort area, (see geological map). The intrusion is emplaced wholly within the basalts at an estimated vertical distance of some 15 m above the sandstone-basalt contact. As a result of weathering, which has produced a fairly deep soil cover, its presence is for the most part indicated only by the occurrence of small boulders of surface float, although a few exposures are available in man-made excavations such as drainage ditches. The intrusion appears to have a maximum width of 200 m and extends along the strike of the basalt for a distance of about 2 km. It is composed of three major rock types which form narrow north-south trending zones, the most westerly of which is composed of olivine gabbro. This zone, at its eastern margin is in contact with an olivine-bearing gabbro, which in turn is succeeded to the east again by the third rock type occurring in the

intrusion, a feldspar-rich, olivine-free gabbro. Due to the relatively poor exposures, neither the mutual relationships of the rock types, nor the attitude of the intrusion could be determined in the field. The rock types show a slight difference in distribution with the olivine gabbro confined to a relatively narrow strip extending 1 km north of Tributary 1, (see geological map).

The olivine-bearing and olivine-free gabbros, although present over a similar distance along strike both begin and end some distance further to the north.

The width of the zones formed by the different rock types varies; the olivine gabbro reaches a maximum width of 30 m whereas the olivine-bearing gabbro and the olivine-free gabbro have maximum widths of about 120 m and 50 m respectively. Samples representative of two cross-sections of the intrusion were collected, and these were supplemented where possible by specimens taken from elsewhere in the intrusion. The number of cross-sections available is limited by exposures, the two mentioned were collected along the only man-made excavations traversing the intrusion, namely a road in the southern part of the intrusion and a drainage ditch in the northern part.

B Petrography

(i) Olivine Gabbro

The olivine gabbro, is a dark, aphanitic , freely weathering rock that seldom forms outcrops. Where outcrops are available the weathered surfaces invariably present usually show the development of a reddish brown crust, as well as pitting due to the differential weathering of olivine. Both texture and modal proportions vary in successive samples collected along an east-west traverse, across the olivine gabbro, as described below.

At the western margin of the zone the rock is composed of euhedral to anhedral, altered olivine crystals (approximately 4 mm in diameter) and

elongated normally zoned plagioclase laths (around 8 mm long) consisting of pyroxene and ore minerals, (see Plate 5 , p 80). The plagioclase shows irregular boundaries with other mineral phases with which it is in contact and occasionally encloses tiny (about 0.1 mm) subhedral crystals of clinopyroxene. The clinopyroxene also occurs interstitially, in two forms, firstly as small subhedral grains similar to those enclosed in the plagioclase, and secondly as larger (2 to 3 mm in diameter) subhedral crystals. The smaller grains are more abundant than the larger crystals. Ore minerals are conspicuous as needle-like crystals, occasionally showing signs of developing the comb-type structure common in the olivine basalts, and usually occurring interstitially, although they may be partially enclosed by plagioclase. Ore minerals are also present as larger, irregular, interstitial patches, although these are less common.

In successive samples collected across the 30 m over which the olivine gabbro is exposed, the following changes in texture occur. Over the first 3 m the olivines increase in size, reaching 6 mm in diameter, and the tiny pyroxene crystals increase in abundance. Pyroxene phenocrysts also become more common simultaneously showing a small increase in size and displaying slight zoning. The olivine crystals, the larger pyroxene crystals and the needle-like ore minerals are all commonly completely enclosed in the plagioclase, which forms larger poikilitic plates, but smaller clinopyroxene crystals, although in places included in the plagioclase oikocrysts, sometimes tend to be concentrated interstitially, forming closely packed aggregates of tiny crystals between the boundaries of adjacent plagioclases. Irregular patches of iron ore are usually subophitically enclosed by the plagioclase in contrast to the mode of occurrence of the needle-like type. Small patches of crypto-crystalline interstitial material are also present and in these acicular crystals of apatite are usually present.

Eastwards from this point, plagioclase crystals tend to show a gradual decrease in size, although they retain their platey habit, and olivine,

in places displaying rounded outlines, decreases in abundance. The large subhedral clinopyroxene become more abundant, and the smaller pyroxenes increase in size to between 0.3 and 0.5 mm in diameter. Ore minerals are similar to those found in the rocks described above, but for the fact that the needle-like crystals are here somewhat scouter and the irregular grains larger. Cryptocrystalline interstitial material forms larger patches, in places becoming slightly coarser-grained and allowing a graphic intergrowth between feldspar and quartz to be recognisable.

A horizontal gap of some 10 m in which no exposures are found, intervenes between these rocks and the first outcrops of olivine-bearing gabbro.

(ii) Olivine-bearing Gabbro

The olivine-bearing gabbro is a greenish-grey, aphanitic and occasionally pophyritic rock, more resistant to weathering than the previously described olivine gabbro.

In thin section it consists of a deep brownish, glassy to cryptocrystalline groundmass in which are set abundant needle-like crystals of ore minerals, variable quantities of subhedral plagioclase and clinopyroxene crystals and a few rounded and completely altered former olivine phenocrysts. Clinopyroxene in the form of augite is the most abundant crystalline phase present, often occurring as discrete patches up to 6 mm across. These patches frequently consist of an aggregate of tiny (0.2 to 0.4 mm) clinopyroxene grains, however, larger clinopyroxene crystals form glomeroporphyritic aggregates of similar diameter, (see Plate 5 , p 80). The individual crystals have an average diameter of about 3 mm and may show signs of deformation, such as with the development of fractures and bending. The clinopyroxene occasionally shows alteration to aggregates of small chlorite crystals. Plagioclase is relatively common as subhedral laths 2 to 3 mm in length which occur evenly distributed throughout the fine grained groundmass. Clouding and alteration of the plagioclase is common, but where fresh, slight normal zoning may be detected. Ore minerals

frequently form relatively large skeletal or needle-like crystals (3 mm by 0.2 mm), although the comb structures noted in the olivine gabbro are not present in these rocks. The groundmass, although glassy in places, is more commonly cryptocrystalline, and intimately associated with this groundmass material are elongated, and frequently curved, crystals of apatite.Texturally, the olivine-bearing gabbro is relatively uniform, although slight variations do occur in the relative proportions of the constituent minerals as described in the section on modes.

(iii) Olivine-free Gabbro

The olivine-bearing gabbro is abruptly succeeded by a medium to coarse grained leucocratic gabbroic rock. A complete cross-section of the zone was not exposed, but available specimens give some idea of the petrographical variations which occur in this zone.In hand specimen, glomeroporphyritic aggregates of plagioclase crystals are conspicuous and larger specimens show a distinct layering, apparently resulting not from the preferred orientation of the plagioclase crystals, but from the concentration larger individual phenocrysts and glomeroporphyritic aggregates of these phenocrysts, in discontinuous layers, usually only a few centimeters, in horizontal extent. The dip on the layering, although somewhat variable, is apparently close to the dip of the enclosing basalts, that is about 10° east. The attitude suggested for the layering is difficult to verify, however, as outcrops are small and it is not certain whether many of them were actually in situ.

In thin section the rock is composed of subhedral crystals of clinopyroxene and plagioclase which display a subophitic to intergranular texture. The normally zoned plagioclase laths range in size form about 1.0 mm to 3.0 mm and the pyroxenes, although building somewhat less regular crystals, have a similar diameter. Irregular to subhedral patches of ore minerals and cryptocrystalline material, the latter invariably containing needles of apatite, occur interstitially to the pyroxene and plagioclase. Set in this groundmass are large porphyritic plagioclases which, in places, occur clustered together in glomeroporphyritic aggregates. Clinopyroxene and more

rarely altered olivine crystals also form phenocrysts and these may be attached to the glomeroporphyritic aggregates of plagioclase. Complex zoning is displayed by the porphyritic plagioclases, usually of the type core-oscillatory zoned mantle-rim, but partial resorbtion and duplication of any of these zones, except the outermost, may occur and many variations in structure were noted. In the outermost zone, smaller crystals of plagioclase with the composition of the normal groundmass crystals are occasionally included.

This rock again shows little systematic qualitative variation along the cross-section, although small fluctuations do occur in the amounts of the various minerals present.

(C) Mineralogy

(i) Olivine Gabbro

(a) Feldspar

The change in habit of the plagioclase eastwards through the olivine gabbro, noted in the section on petrography, is accompanied by a slight variation in plagioclase composition. Along the western margin of the olivine gabbro, the plagioclase has an average composition of approximately An_{50}, but the large platey crystals present in rocks a few meters from this contact have an average composition of approximately An_{58}, showing zoning from An_{62} to An_{50}. In rocks further from this contact the plagioclase becomes slightly more sodic, until near the estimated position of the eastern contact (with the olivine-bearing gabbro), the plagioclase has an average composition of An_{56}. These crystals are zoned from approximately An_{58} in the cores to An_{52} at the margins. Thus the plagioclase in the olivine gabbro, from west to east, initially becomes more basic and subsequently shows a possible slight enrichment in the albite molecule. All plagioclase in this rock type appears from optical measurements, to be in an intermediate structural state.

(b) Pyroxene

Augite, the only pyroxene occurring in the olivine gabbro forms colourless, euhedral to subhedral crystals ranging in size from 0.1 mm to nearly 3.0 mm. The mineral shows a slight variation in composition from west to east across the zone ranging from $Mg_{48}\ Ca_{39}\ Fe_{13}$ near the western margin of the olivine gabbro to $Mg_{45}\ Ca_{40}\ Fe_{15}$ in the most easterly outcrops, as determined by refractive index and optical axial angle measurements. There is apparently no corresponding compositional variation between crystals of different sizes.

(c) Olivine

Olivine occurs in varying amounts in all specimens collected from the olivine gabbro zone. It is usually completely altered to aggregates of chlorite and talc and contains sinuous trains of antigorite and iron ore preserved from the original olivine crystals, Many of these altered crystals have a perfect euhedral outline, although subhedral and even anhedral forms are present. A few unaltered olivine phenocrysts occur in rocks adjacent to the western contact of the olivine gabbro zone, and these have the following optical properties:
Optically negative, 2V 82°, Beta refractive index 1.75.
These properties indicate a composition of $Fo_{72}\ Fa_{28}$.

(ii) Olivine-bearing Gabbro

(a) Feldspar

Although there is a marked difference in habit, there is little difference between the composition of the plagioclase of the olivine-bearing gabbro and that of the olivine-free and olivine gabbros. The plagioclase crystals are lath shaped and much smaller, showing no tendency to enclose other mineral phases. They have an average composition of about An_{58}, display slight normal zoning, ranging from An_{60} in the cores to An_{54} at the margins

of the crystals, and are again in an intermediace structural state. No regular, measurable variation was found in the composition of the plagioclase in successive samples collected along the east-west cross-section of the olivine-bearing gabbro zone.

(b) Olivine

Former olivine crystals were too highly altered for the determination of original olivine composition. They now consist of antigorite, talc, and iron ore, predominantly.

(c) Pyroxene

An average composition of $Mg_{44}\ Ca_{40}\ Fe_{16}$ was recorded for augite, the only pyroxene present, from a series of optical determinations. No measurable variation in composition was found to exist between pyroxene crystals of different sizes, present in the same rock and similarly, no compositional variation was detected between pyroxenes from different samples along the cross-section. Delicate oscillatory zoning is present in several of the larger crystals, (Plate 6 ,p 86;, but differences in composition could not be determined by optical methods.

(d) Ore Minerals

The majority of the ore minerals present consist of ilmenite which forms needle-like crystals in the contact rocks. These gradually become larger eastwards across the zone. Magnetite occurs both as minute exsolved blebs in the ilmenite crystals or less commonly as separate somewhat irregular, elongated crystals. Chalcopyrite and pyrite are present as minute (0.1 mm) grains with slightly different modes of occurrence: the pyrite occurs interstitially but the chalcopyrite is confined for the most part to the interior of the large altered olivine crystals.

PLATE 6

1 Olivine-free Gabbro, (Basal Intrusion) - Pyroxene phenocryst composed of a core of orthopyroxene, (dark grey), surrounded by a mantle of clinopyroxene, (pale grey), set in a matrix of plagioclase and clinopyroxene. (Transmitted light, crossed nicols, X96).

2 Olivine-bearing Gabbro, (Basal Intrusion) - Delicate oscillatory zoning present in a clinopyroxene phenocryst. (Transmitted light, crossed nicols, X200).

(iii) Olivine-free Gabbro

(a) Feldspar

The groundmass plagioclase of the olivine-free gabbro zone occurs as abundant, small (1.0 to 3.0 mm), lath shaped crystals showing strong normal zoning ranging from An_{64} in the cores to An_{55} at the margins of the crystals, with an estimated average composition of An_{58}. No regular variation in the composition of the plagioclase across the zone was found, and the plagioclase is again in an intermediate structural state.

The plagioclase phenocrysts which are common in this zone differ widely from the groundmass crystals both in composition and in the type of zoning present. Zoning is usually complex, as described previously, with the cores of the large phenocrysts having an average composition of near An_{80}, the oscillatory zoned mantles lying in the range An_{74} to An_{70} and the rims grading rapidly from about An_{68} to An_{55}. Smaller plagioclase crystals which are frequently included in the rims of the phenocrysts have the same composition as the groundmass crystals.

In places microscopic inclusions are present often forming rows marking former crystal outlines or also they are randomly scattered through the plagioclase near the core of the crystal. The inclusions are usually around 0.05 mm. They may be spherical although in some there is a suggestion of crystal outlines developing. They frequently have an vermicular internal structure and in this, as in their other features they resemble the inclusions found in anorthite megacrysts from the Isle of Skye by Donaldson (1975). X-Ray diffraction patterns of a few of the larger inclusions showed that at least some of the inclusions in the plagioclase of the olivine-free gabbro now consist in part of pigeonite. The lack of homogeneity of these inclusions suggest they may originally have consisted of a glass, presumably representative of the magma from which the plagioclase was crystallising.

(b) Pyroxenes

Augite is the most abundant pyroxene in the olivine-free gabbro, occurring both as small irregular groundmass crystals (± 0.3 mm) and as large phenocrysts (± 4 mm), of two types. The most distinctive feature of the first type of augite phenocryst is the presence of a corroded core consisting of augite of a slightly more magnesium-rich composition than the surrounding mantle. These are termed Type 1 phenocrysts.

Occasionally, smaller phenocrysts with subhedral to euhedral outlines are preserved within glomeroporphyritic aggregates of plagioclase, and these euhedral phenocrysts have Mg-rich subhedral to euhedral cores, showing no signs of corrosion, which are surrounded by more Fe-rich mantles of the same mineral (Type 2 phenocrysts). The mantle augite of the Type 2 phenocrysts shows strong zoning, (in the form of increasing Fe-content), from adjacent to the core-mantle boundary, to the outer margin of the crystal.

Pigeonite was noted in the groundmass in minor amounts, occurring as crystals of a similar size and shape to the groundmass augite, but it was not observed as phenocrysts.

Rarely orthopyroxene in the form of hypersthene, occurs as irregular corroded phenocrysts, mantled by clinopyroxene overgrowths, (see Plate 6).

The compositions of the groundmass augite, both types of augite phenocryst, and a mantled phenocryst of hypersthene were determined by means of an electron microprobe. The results of these analyses are listed in Table 20 .

I Major Element Chemistry of the Ca-rich Clinopyroxenes

The analysis of the groundmass augite shown in Table 20 indicates that

TABLE 20

Results of Electron Microprobe Analyis of Five Pyroxenes from the Olivine-free Gabbro, Basal Intrusion

	Pyroxene 1		Pyroxene 2		Pyroxene 3		Pyroxene 4		Pyroxene 5	
SiO_2	50,63		50,96		51,61		51,13		52,58	
CaO	17,51		17,58		17,00		18,84		2,29	
MgO	15,48		15,89		17,19		18,25		23,09	
TiO_2	0,73		0,98		0,57		0,56		0,48	
FeO	12,40		13,82		11,10		7,25		20,81	
Al_2O_3	1,69		2,34		1,44		2,60		1,18	
Total	98,44		101,57		98,91		98,03		100,43	
Cations on the basis of 6 oxygens.										
Si_{4+}	1,928		1,892		1,939		1,904		1,945	
Al_{6+}	0,072	2,00	0,102	1,994	0,061	2,00	0,096	2,00	0,055	2,00
Al	0,004		0,000		0,002		0,018		0,000	
Ca	0,715		0,699		0,685		0,752		0,091	
Mg	0,879	2,013	0,879	2,034	0,962	2,014	0,013	2,015	1,273	2,021
Ti	0,021		0,027		0,016		0,016		0,013	
Fe	0,395		0,429		0,349		0,226		0,644	
	$Ca_{35,6}\ Mg_{43,74}\ Fe_{20.20}$		$Ca_{34,4}\ Mg_{43,2}\ Fe_{22,4}$		$Ca_{34,0}\ Mg_{47,9}\ Fe_{18,1}$		$Ca_{37,5}\ Mg_{50,5}\ Fe_{12,0}$		$Ca_{4,5}\ Mg_{63,0}\ Fe_{32,5}$	

Analyst:- National Institute for Metallurgy

Pyroxene 1 Augite - Groundmass
Pyroxene 2 Augite - Mantle of Type 2 pyroxene phenocryst.
Pyroxene 3 Augite - Intermediate Zone of a Type 1 clinopyroxene phenocryst.
Pyroxene 4 Augite - Core of Type 1 phenocryst.
Pyroxene 5 Orthopyroxene - Corroded Core.

the augite is of an intermediate composition, ($Ca_{35,6}Mg_{43,7}Fe_{20,7}$). In fig 10 this composition has been plotted in the pyroxene quadrilateral of a Ca, Mg, Fe diagram, on which the Ca-rich pyroxene fractionation trend of both the Skaergaard and the Komatipoort Intrusion (see later) are shown. The composition of the Ca-rich groundmass pyroxene from the olivine-free gabbro plots very close to the Ca-rich pyroxene compositional variation trend of the Komatipoort Intrusion which is likely to have crystallised at relatively high levels (see later).

The core and the mantle of the analysed Type 1 clinopyroxene phenocryst have compositions of $Ca_{37,5}Mg_{50,5}Fe_{12}$ and $Ca_{34}Mg_{47,9}Fe_{18,1}$, respectively. When these values are plotted in the pyroxene quadrilateral (fig 10), they are found to lie to the Mg-rich side of the Ca-rich fractionation trend of the Komatipoort Intrusion, possibly defining a parallel but more Mg-rich trend. More data would be needed to confirm this. From the limited available data it appears that the composition of both the augite phenocrysts and the groundmass augite, may record an evolution of the parental magma towards more iron-rich compositions, in a manner fairly typical of fractionated tholeiitic intrusions.

Optical properties suggest that the cores of the Type 2 Ca-rich pyroxene phenocrysts are similar in composition to the cores of the Type 1 phenocrysts, however the strongly zoned mantles of the Type 2 phenocrysts appear to differ in composition from the mantle of the Type 1 phenocrysts. This is confirmed by the electron microprobe analysis of the outer parts of the mantles of the two types of phenocryst, shown in Table 20 .

The nature of the compositional differences between the mantle augites of the two types of phenocryst are illustrated in fig 10 , where points representing the analyses have been plotted in the pyroxene quadrilateral. A strong similarity in the major element chemistry of the Type 2 mantle augite and the groundmass augite is apparent.

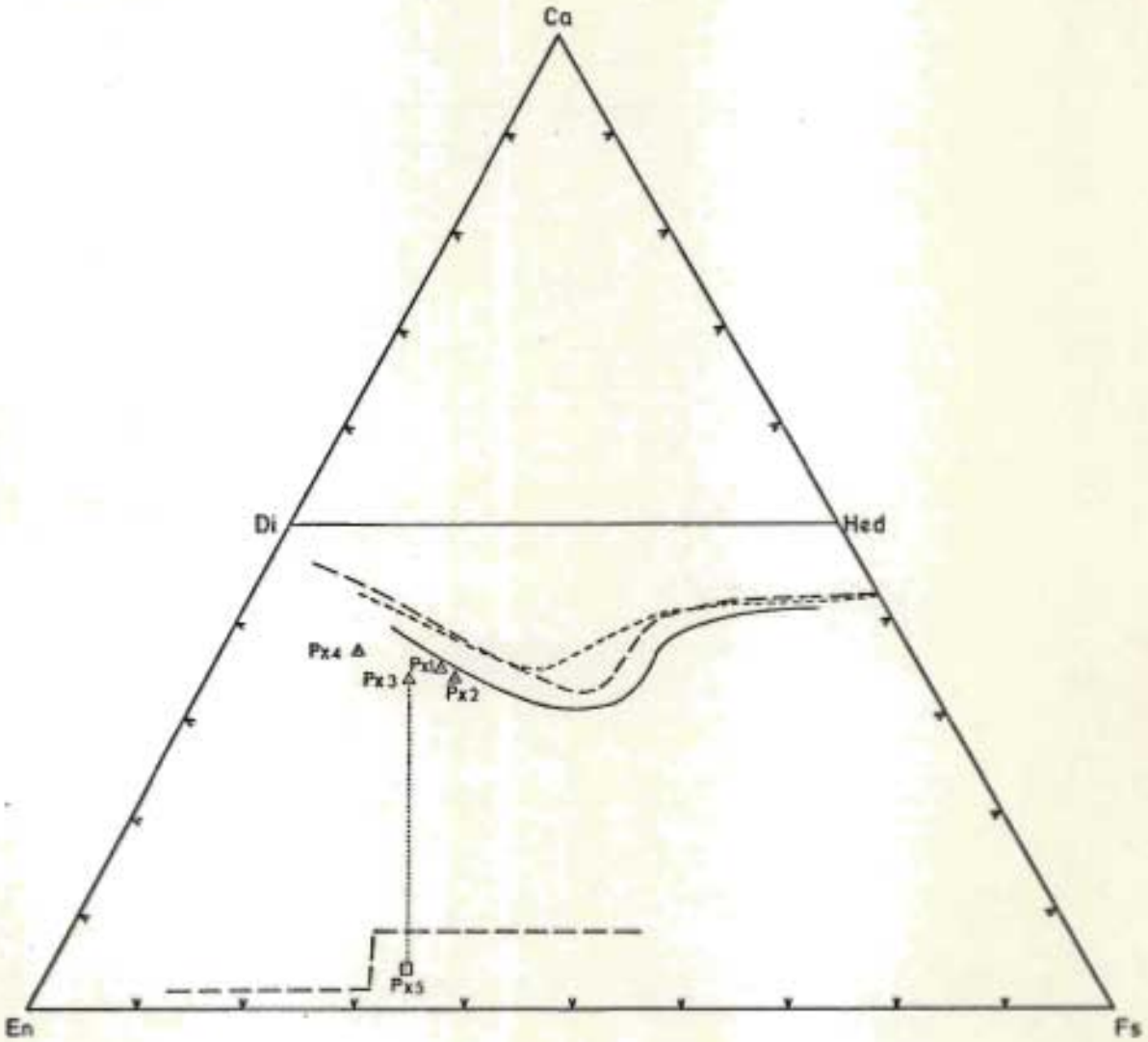

Figure 10 Analysed pyroxenes of the Basal Intrusion plotted in the pyroxene quadrilateral.

Px1 Groundmass clinopyroxene - core
Px2 Augite phenocryst - mantle material
Px3 Augite phenocryst - corroded core
Px4 Mantled orthopyroxene phenocryst - core
Px5 Augite mantle around orthopyroxene phenocryst
— Komatipoort Intrusion
– – Bushveld Intrusion
– – – Skaergaard Intrusion

II Minor Element Chemistry of the Ca-Rich Clinopyroxenes

Al and Ti are the only minor elements for which the Ca-rich clinopyroxenes of the olivine-free gabbro have been analysed, however the four analyses of clinopyroxenes presented in this section do show variations in the levels of these elements. Ti-Al and Si-Al relations are summarised in figs.11 and 12 , and if analysis Px2 is not considered it may be seen that Al decreases with fractionation whereas Ti shows only slight variation.

Type 1 Augite Phenocrysts

The Type 1 clinopyroxene phenocryst shows a higher Al_2O_3 content in the core of the crystal than in the mantle, although the TiO_2 content remains constant, suggesting a decrease in the Al_2O_3 content of the pyroxene with fractionation (see Table 20). This conforms with the observation of both Brown (1957) and Nwe (1976) who have noted constant TiO_2 values and decreasing Al_2O_3 content in the pyroxenes of the Skaergaard intrusion with increasing fractionation. In this respect the work of Kushiro (1960) and LeBas (1962) may have some relevance. They have demonstrated that the Al^{3+} content of natural Ca-rich pyroxenes varies inversely with the SiO_2 content of the magma from which they crystallised. Both Brown (1957) and Carmichael and others, (1970) have offered an explanation for this and a more general explanation has been given by Campbell and Borley (1974). In terms of the explanation Al^{3+} entering the pyroxene does so by substitution for Si^{4+}, thus the a_{SiO_2} is a dominant influence on the Al^{3+} content of the pyroxene. However the presence of Al^{3+} in the pyroxene creates a charge imbalance that requires the simultaneous entry of Cr^{3+}, Ti^{4+}, Fe^{3+} or Al^{3+} into octahedral sites. Since the a_{SiO_2} commonly increases with a rise in the concentration of SiO_2 during fractionation, the Al^{3+} content and the Ti^{4+} content may be expected to decrease.

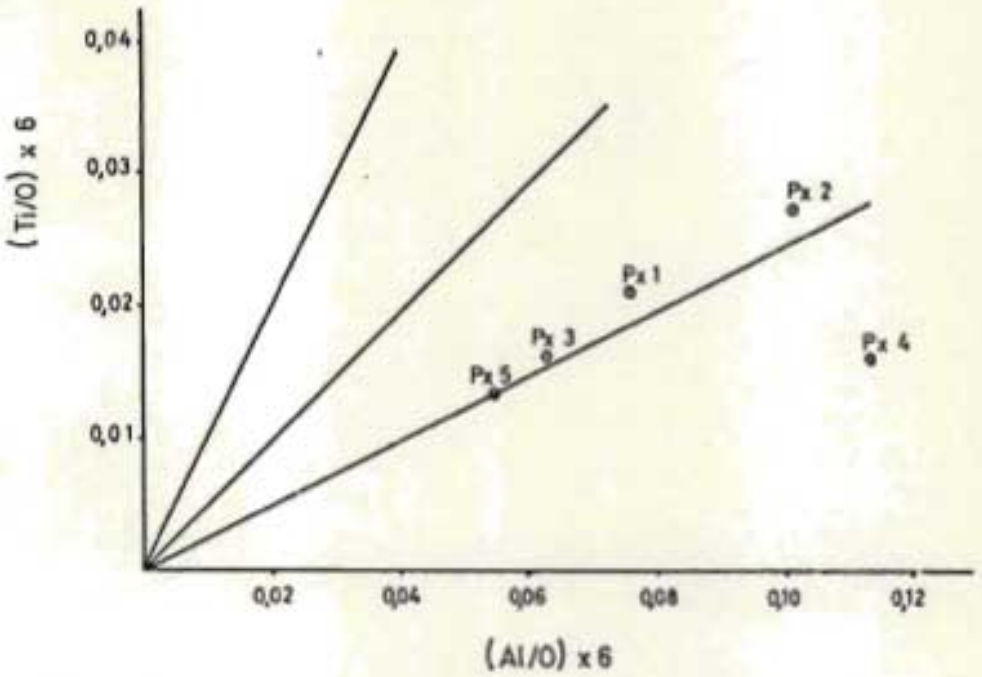

Figure 11. Ti-Al relations for pyroxenes of the olivine-free gabbro (Numbering as in Table 20)

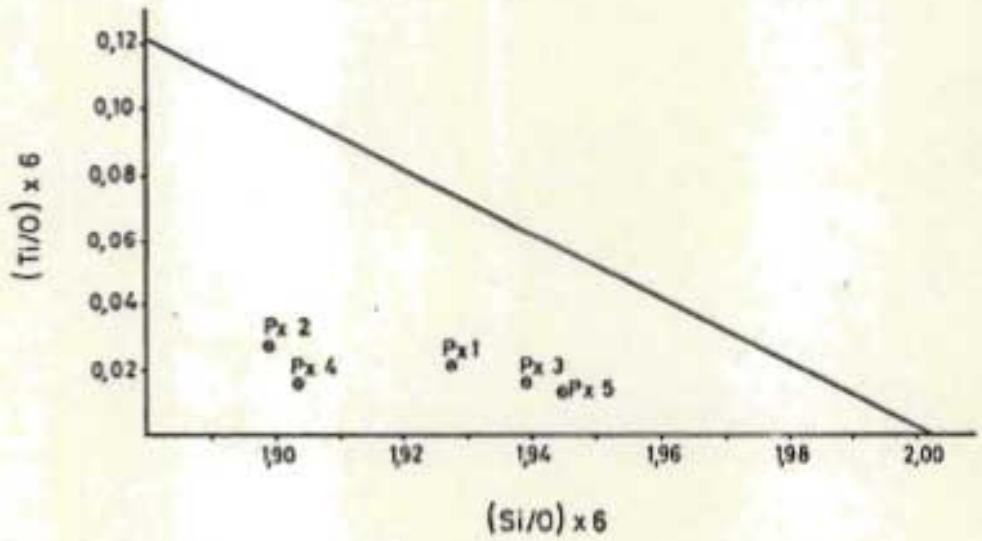

Figure 12. Ti-Si relations for pyroxenes of the olivine-free gabbro (Numbering as in Table 20)

The abrupt change in the Al_2O_3 content of the Type 1 Ca-rich pyroxene from the core to the mantle therefore may have resulted from an increase in the a_{SiO_2} of the magma in which the phenocryst was crystallising. The abruptness of the change and the presence of an irregular, corroded core-mantle boundary suggests that if so, this increase to a_{SiO_2} was sudden and not a gradual change due to simple fractionation of the magma. This change in the composition of the magma, would also explain the increase in the Fe content of the mantle pyroxene, relative to the core in the Type 1 phenocrysts (see table 20, fig 10).
The steady TiO_2 value is more difficult to explain, but may be the result of an increase in the TiO_2 content of the magma, although Brown (1957) was able to discount this explanation for the earlier Ca-rich pyroxenes of the Skaergaard Intrusion. It is apparent however from the work of Brown (1957) and Nwe (1976) on the pyroxenes of the Skaergaard that this steady TiO_2 content is not incompatible with a change in the magma from a less-evolved to a more-evolved composition. Campbell and Borley (1974), have noted however, that Ti^{4+} cannot compete with Cr^{3+} for octahedral sites in the pyroxene, as a consequence of the high crystal field stabilisation energy (CFSE), of Cr^{3+} and the zero CFSE of Ti^{4+}. In intrusions such as the Skaergaard, Cr concentration is known to decrease from the less fractionated to the more fractionated rocks (Wager and Brown 1968) and this decrease in Cr^{3+} concentration would allow increased substitution of Ti^{4+} in octahedral sites of the pyroxene. However Ti^{4+} can enter the pyroxene only if the charge balance is maintained by the substitution of two Al^{3+} ions in tetrahedral sites for every Ti^{4+} ion occupying an octahedral site. Since, in the Fe-rich mantle of the Type 1 phenocryst of the olivine gabbro there is a decrease in the Al_2O_3 content, a balance may have been achieved between factors tending to produce an increase and a decrease respectively in Ti^{4+} content, resulting in the observed approximately stable Ti^{4+} content of the pyroxene. Unfortunately Cr analyses of the pyroxene were not available to confirm this suggestion. However the Ti:Al ratio (see fig 11), of less than 1:4 obtained for the core of the Type 1 phenocrysts could imply extra components such as R^{2+} Cr^{3+} $SiAlO_6$, (Boyd 1971).

Type 2 Augite Phenocryst and groundmass Augite

It is convenient to discuss the minor element content of the mantle of the Type 2 augite phenocryst and that of the groundmass augite together as they show some compositional similarities, (see Table 20). In fig 10, there is some suggestion that the groundmass augite and the Type 2 phenocryst mantle compositions could together define a late-stage compositional variation trend for the clinopyroxene of the olivine-free gabbro, i.e. the compositional variation trend of the clinopyroxene of the olivine-free gabbro after the emplacement of this unit in its present position. Despite the similarity in major-element composition however, the Al_2O_3 content of the Type 2 clinopyroxene mantles does not resemble that of the Mg-rich Type 1 phenocryst cores, (see Table 20). Differences in Al_2O_3 and TiO_2 contents between the groundmass augite and the Type 2 phenocryst margins indicate that, if these two pyroxenes compositions do define a late stage compositional variation trend, crystallisation of the pyroxene was accompanied by a marked increase in the Al_2O_3 content of the augite and a less noticeable increase in TiO_2, (compare analyses 1 & 2, Table 20). This is in direct contrast to the variation of Al_2O_3 and TiO_2 expected in augite on fractionation of a basic magma, (see earlier discussions).

It is possible therefore that the Type 2 augite mantle composition is not directly related to the groundmass composition, but instead is an original outermost zone of the phenocryst formed prior to the onset of crystallisation of the groundmass pyroxene. As mentioned earlier however, optical data suggest a similarity in major element composition at least, exists between the cores of the Type 2 phenocrysts and the corroded cores of the Type 1 phenocrysts. If this observation is taken into consideration the possibility arises that the Type 1 and 2 Ca-rich phenocrysts are essentially the same, the Type 2 having been protected against corrosion and deposition of a further pyroxene mantle by virtue of surrounding phenocryst phases such as plagioclase. This would suggest that the Al_2O_3 content of the phenocryst pyroxene decreased slightly as crystallisation proceeded, and simultaneously the TiO_2 content showed a fairly marked

increase, (compare minor element analyses of Pyroxene 2 and Pyroxene 4, Table 20).Pyroxene phenocrysts not protected by surrounding phenocryst phases could then, following an abrupt change in conditions of crystallisation, have suffered corrosion and resorbtion followed by the deposition of the Type 1 mantles.

Textural evidence tends to favour the proposal that the Type 2 phenocrysts have been protected from corrosion by adjacent phenocryst phases, as many of the phenocrysts of this type that have been observed, are surrounded by plagioclase or other pyroxene phenocrysts. However in view of the fact that the thin sections provide a two dimensional view of the three dimensional textural relationships,further pyroxene analyses, particularly of the outermost zones of the groundmass pyroxenes, will be required to confirm this conclusion.

III Orthopyroxene

Hypersthene was observed in the form of corroded phenocrysts surrounded by augite mantles. In some cases corrosion appears to have reduced the hypersthene to a few small irregular remnants near the centre of a clinopyroxene phenocryst. In other cases (see Plate 6) the hypersthene constitutes the major proportion of the phenocryst. The hypersthene crystals form a very small proportion of the rock, (less than one per cent). They may occur alone or as part of a glomeroporphyritic aggregate with plagioclase, olivine and clinopyroxene phenocrysts.

In Table 20 the results of an electron microprobe analysis of a hypersthene phenocryst are shown. This analysis indicates a composition of $Mg_{63}Fe_{32,5}Ca_{4,5}$. The Al_2O_3 content of the hypersthene is slightly lower than that of mantled orthopyroxene phenocrysts from the Nuanetsi area, (Cox and Jamieson, 1974),but the TiO_2 content is of the same order or higher than that of some of the mantled orthopyroxene from Nuanetsi.

(c) Olivine

Olivine occurs as rounded to subhedral crystals almost invariably forming part of a glomeroporphyritic aggregate with one or more of the other phenocryst phases, usually plagioclase. These olivines are usually partially or completely altered to chlorite antigorite and magnetite. A partial analysis by electron microprobe of an unaltered portion of an olivine phenocryst is shown in Table 21 and indicates the olivine to be of an intermediate composition ($Mg_{80,4}$). The olivine phenocrysts are usually around 1,5 mm in diameter.

TABLE 21

Results of a Partial Analysis of an Olivine Phenocryst (by Electron-Microprobe).

CaO	0,43
MgO	44,43
TiO_2	0,01
FeO	19,32
Al_2O_3	0,00
Mole % Fo	80,4

Analyst :- National Institute for Metallurgy.

(d) Ore Minerals

The predominant ore mineral in the olivine-free gabbro is magnetite, usually martitised to hematite and containing crystallographically orientated lamellae of ilmenite. Ilmenite was not observed as a separate mineral phase. The magnetite grains, which are often irregular, occur interstitially to the silicate minerals and average between 2,0 and 3,0 mm

in diameter. Pyrite in grains of a similar size and shape to the magnetite is relatively abundant, for the most part occurring interstitially, although in one instance it was observed as an irregular mass enclosed by a groundmass plagioclase lath. Very minor amounts of chalcopyrite are also present in minute (0,1 mm) interstitial grains.

(D) Modal Analysis

The variations in modal proportions and mineral compositions in samples collected along cross-sections of each of the three zones are shown in Figure 13 ,p99 . All three zones show minor variations in the relative proportions of the major mineral phases, and variations within one zone do not appear to be related to variations in other zones. The olivine gabbro displays a fairly rapid increase in pyroxene content at the expense of interstitial material close to the contact, but over the rest of the zone, changes are slight. Amongst these are a variation of olivine and plagioclase content, which show a steady, but very small increase, as the pyroxene content decreases across the zone. Interstitial material increases gradually and ore minerals display a slight decrease.

The olivine bearing gabbro also shows small variations, the most prominent of these being an increase in the pyroxene and olivine content at the expense of plagioclase. It is doubtful, however, whether these variations are greater than the limits of accuracy of the method used for the modal determinations. The most marked variation is shown by the olivine-free gabbro which suffers a decrease in pyroxene content and a corresponding increase in plagioclase and interstitial micropegmatite content, from west to east across the zone.

(E) Geochemistry

No fresh specimens of olivine gabbro were available for chemical analyses but samples of both the olivine-bearing gabbro and the olivine-free gabbro

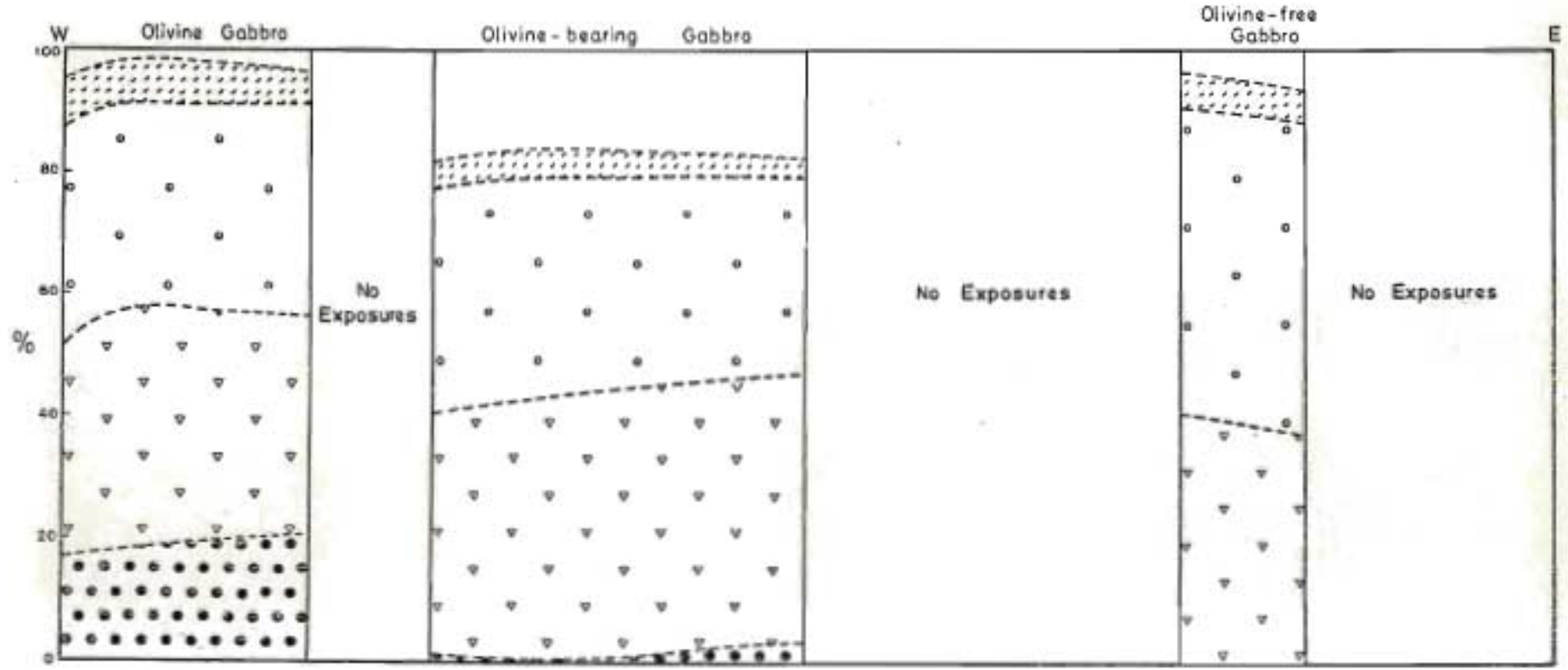

Figure 13. Variations in modal proportions in the Basal Intrusion along a W-E cross-section.
Ore | Plagioclase | Olivine | Pyroxenes | Interstitial Micropegmatite

were collected and submitted for chemical analyses. The results of these analyses are shown in Table 22 , p 101, together with the corresponding modes, CIPW norms, and niggli values. As may be seen from a comparison of the analyses, the two rock types have a somewhat similar composition with the olivine bearing gabbro possessing a slightly higher silica and a significantly higher total alkali content, and in particular higher K_2O, P_2O_5 and TiO_2 contents than the olivine free gabbro.

The higher concentrations of Al_2O_3 and CaO present in the olivine free gabbro would be expected from its higher plagioclase content.

(F) Petrogenesis of the Basal Intrusion

(i) Possible relationships between the three rock types

Although the eastward succession of rock types present in the Basal Intrusion (olivine-gabbro, olivine-bearing gabbro, olivine-free gabbro), is suggestive of an eastward dipping sheet differentiated in situ, the distribution of these rock types, their compositions, and the textures described earlier, leave little doubt that the intrusion is composite, and consists of three seperate intrusive phases. For example the limited distribution of the olivine gabbro indicates it is unlikely to be a product of in situ differentiation, and the porphyritic texture of the olivine-bearing gabbro is suggestive of a small hypabyssal composition between the olivine-bearing gabbro and the olivine-rich dyke rock (olivine clinopyroxenite) described in a previous section (compare analysis of sample C128, Table 13 , p 42 , with that of sample C130, Table 22 , p101), i.e. intrusives of this composition are present in the area.

Further evidence against an in situ differentiation origin for these rocks, may be found in the fact that although the differentiation index $\frac{FeO + Fe_2O_3}{FeO + Fe_2O_3 + MgO} \times 100$, of the olivine-bearing gabbro (60,6) is lower

TABLE 22

Chemical analyses, CIPW norms and Niggli values for two samples from the Basal Intrusion (CL29: Olivine-free Gabbro; CL30: Olivine-bearing Gabbro) ; (Analyst : NDH)

Chemical Analyses			CIPW Norms			Niggli Values		
Sample no.	CL29	CL30		CL29	CL30		CL29	CL30
SiO_2	50.01	52.56	Q	1.91	1.93	si	116.89	134.95
Al_2O_3	14.31	11.25	Or	2.01	12.69	al	19.71	17.02
Fe_2O_3	2.58	1.49	Ab	19.11	24.60	fm	45.83	49.05
FeO	9.43	9.08	An	27.88	11.26	c	28.83	23.16
MgO	6.45	6.88	Di	23.22	22.83	alk	5.63	10.76
CaO	11.51	8.42	Hy	17.56	16.62	mg	0.49	0.54
Na_2O	2.26	2.91	Mt	3.75	2.17	c/fm	0.63	0.47
K_2O	0.34	0.15	Il	3.20	6.25	k	0.09	0.33
H_2O^-	0.29	0.26	Ap	0.35	0.92	ti	2.78	5.95
H_2O^+	0.90	1.29	H_2O	1.19	1.55	p	0.16	0.46
CO_2	0.16	0.08				H_2O	7.02	11.04
TiO_2	1.58	3.08						
P_2O_5	0.16	0.42						
MnO	0.20	0.16						
CuO	0.01	0.01						
Cr_2O_3	0.038	0.047						
Total	100.23	100.08						

than that of the olivine-free gabbro (65,0), the olivine-bearing gabbro contains more SiO_2, K_2O, TiO_2 and P_2O_5 than the overlying olivine-free gabbro.

Another possibility is that the three rock types may be the result of the withdrawal of magma during successive stages of differentiation of a deep-seated basic mass. The differences in chemistry between the olivine-bearing and olivine-free gabbro mentioned in the previous paragraph imply that the former rock type could be derived from the latter by crystal fractionation but not vice-versa. The K_2O content of the olivine-free gabbro, however, would require to be increased by a factor of approximately seven, to reach the level present in the olivine-bearing gabbro.

It is not, therefore, considered reasonable to attempt to derive the one rock type from the other by means of crystal fractionation of the observed mineral phases. Comparison of the analysis of the olivine-bearing gabbro with an olivine-basalt analysis (sample CL25, Table 5 , p 16), reveals marked similarities and suggests that fractionation of olivine and orthopyroxene could produce magma with the composition of the olivine-bearing gabbro from a parental magma similar in composition, (although probably slightly poorer in K_2O), to the olivine basalt (CL25). Sample CL30, on the other hand, does not differ greatly from the normal tholeiitic basalts (compare with analyses in Table 8 , p 24), nor the tholeiitic dolerites from this area (compare with analysis of sample CI 16, Table 16, p 51).

As will be described later, (see section on geochemistry of the Karroo volcanics), the basalts themselves can be subdivided into two series, a high Mg series and a low Mg series which are unlikely to be related by low pressure crystal fractionation. It is considered that the olivine-bearing gabbro belongs to the high Mg series and the olivine-free gabbro to the low Mg series and therefore it may be concluded that there is no direct genetic relation, in terms of low pressure crystal fractionation between the two rock types.

In the absence of an analysis of the olivine gabbro, its relation to the other two rock types is difficult to define. The presence of ilmenite needles in this rock type suggest it may be related to the high Mg series, representatives of which commonly have high TiO_2 contents, however, no firm conclusion could be reached, as the rock could equally well be considered to be enriched in cumulus olivine; and thus derived by fractionation of low-Mg tholeiitic magma. The olivine gabbro, therefore could conceivably be genetically related to either of the other two rock types.

(ii) The nature and origin of the phenocrysts present in the olivine-free gabbro

The presence of mantled orthopyroxene phenocrysts in the olivine-free gabbro of the basal intrusion together with glomeroporphyritic aggregates of olivine, plagioclase and clinopyroxene suggest comparison of the olivine-free gabbro with rocks described from the Nuanetsi area by Cox and Jamieson(1975), which also contain jacketed orthopyroxenes. As noted earlier, the analysis of the olivine-free gabbro (see Table 22), shows that this rock belongs to the Mg-poor series, and not the Mg-rich series, to which the rocks described from Nuanetsi belong and the presence of jacketed orthopyroxenes in rocks representative of the Mg-poor series also suggests the possibility of a genetic relationship between the two series. Initial inspection of the compositions of the mantled orthopyroxene and clinopyroxene phenocrysts indicate these minerals could have been in equilibrium with each other, however, examination of fig. 10, in which the pyroxene compositions have been plotted in the pyroxene quadrilateral, suggests that the core of the Ca-rich clinopyroxene phenocryst may, in fact, be too Mg-rich to be in equilibrium with the hypersthene. Following Cox (1975), the distribution coefficient of Fe and Mg between the orthopyroxene and the Ca-rich clinopyroxenes was used to test for equilibrium between the pyroxenes.

According to Kretz (1961),(1963)

$$K_{D(Mg:Fe)} = \frac{X_{opx}\ (1 - X_{cpx})}{X_{cpx}\ (1 - X_{opx})}$$

where X_{opx} and X_{cpx} are the mole fractions of Mg in each pyroxene phase. Results obtained for the distribution coefficient between the Type 1 Ca-rich clinopyroxene phenocryst core and mantle and the Type 2 clinopyroxene mantle on the one hand and the core of the orthopyroxene phenocryst on the other are listed in Table 23. Kretz (1963) obtained values in the range of 0,65 - 0,86 from igneous environments and the values obtained here confirm that while the mantles of both Type 1 and Type 2 phenocrysts could possibly be in equilibrium with the orthopyroxene the Ca-rich clinopyroxene phenocryst core appears to be too Mg-rich to be in equilibrium with the orthopyroxene phenocryst core.

Considering the limited amount of analytical data available on the pyroxene at present, several explanations are possible. Olivine and clinopyroxene and perhaps plagioclase may have crystallised fairly extensively prior to the formation of the first orthopyroxene , a fairly uncommon order of crystallisation, another possibility is that the analysed orthopyroxene does not represent the most Mg-rich orthopyroxene present in the rock, i.e. the orthopyroxene may be zoned.

Cox and Jamieson(1974) quote Bowen and Schairer (1935), Ramberg and De Vore (1951) and O'Hara (1963), and show that some olivine phenocrysts in the Nuanetsi olivine-rich lavas, are in equilibrium with the mantled orthopyroxene phenocrysts. The work of those authors indicates that orthopyroxene and olivine, in equilibrium in magnesian igneous assemblages, have similar Mg:Fe ratios, or that olivine is more magnesian than the orthopyroxene. Applying the same criteria to the phenocrysts in the olivine-free gabbro shows that the olivine ($Mg:Fe_{80,4}$) is more magnesian than the orthopyroxene ($Mg:Fe_{63}$) suggesting possible equilibrium, however the difference in composition may be too great for the minerals to be regarded as co-precipitates from the same magma. The olivine

TABLE 23

Pyroxene Distribution Coefficient. Calculated for Mg and Fe between the analysed orthopyroxene and three different clinopyroxenes present in the Olivine-free Gabbro.

Pyroxene Analysis No.	X^{*}_{cpx}	X^{*}_{opx}	$K_{D(Mg:Fe)}$
2	67,2	63,0	0,83
3	73,4	63,0	0,62
4	81,8	63,0	0,38

*Mole fraction of Mg in pyroxene, where molecular proportion Mg + molecular proportion Fe = 1

Pyroxene 2	Augite - mantle of Type 2 phenocryst.
Pyroxene 3	Augite - intermediate zone of Type1 phenocryst.
Pyroxene 4	Augite - core of Type 1 phenocryst.

composition is, in fact, in the same range as the high pressure olivine phenocrysts analysed by Cox and Jamieson (1974), from Nuanetsi, which they show were in equilibrium with orthopyroxene with an Mg:Fe ratio of 82 to 92, far more magnesian than the orthopyroxene analysis presented here. There is some evidence therefore that the orthopyroxene and the olivine are also unlikely to have been in equilibrium with each other.

Comparison of the olivine composition with the analysis of the olivine-free gabbro suggest that the olivine may in fact be too Mg-rich to have crystallised from a liquid of this composition. However, olivine-liquid equilibrium has been studied experimentally by Roeder and Emslie (1970) and Roeder (1974), and this work has suggested that the distribution coefficient

$$K_D = \frac{(X^{Ol}_{FeO})}{(X^{Liq}_{FeO})} \cdot \frac{(X^{Liq}_{MgO})}{(X^{Ol}_{MgO})}$$

that relates the partitioning of magnesium and iron between olivine and liquid is equal to 0.30 and is independent of temperature and possibly pressure. Roeder (1974) has shown that the composition of the olivine reflects only the divalent metal cations in the melt, (Ni, Mg, Ca, Fe, Mn) and is little affected by other elements in the melt. Mysen (1974) has produced data which conflicts with this conclusion, however Cawthorn and O'Hara (1976) have suggested that Mysen's (1974) data may be quantitatively invalid. Further support for the conclusions of Roeder and Emslie (1970) and Roeder (1974) has been given by experimental work on lunar basalts by Longhi and others (1975), who have produced results which give similar K_D values to Roeder and Emslie (1970) over a wide range of temperatures and pressures up to 12 kb.

This distribution coefficient was therefore used to test for possible equilibrium between the olivine and the olivine-free gabbro, using the assumption that the whole rock analysis of the olivine-free gabbro approximated the liquid composition from which the olivine crystallised. Although phenocryst phases are present in the rock the majority of those

consist of plagioclase. Since this is an Mg and Fe-free phase the absolute amounts of MgO and FeO present will be affected but not the MgO:FeO ratio. Using the relationship

$$K_D = \left(\frac{FeO}{MgO}\right)^{ol} \cdot \left(\frac{MgO}{FeO}\right)^{liq} = 0.3 \text{ (Roeder 1974)}$$

and substituting the mole percentages of FeO and MgO from the whole rock analysis in Table 22 it was estimated that an olivine with FeO/MgO = 0.246 would be in equilibrium with a liquid of this composition. The analysed olivine has FeO/MgO = 0.243 (using mole percentages again, with SiO_2 content estimated by subtraction), indicating probable equilibrium between the olivine and the olivine-free gabbro.

The work of Roeder and Emslie (1970) and Roeder (1974) also provides data on the relationship between olivine compositions, the MgO and FeO content of the magma, and the temperature of the magma. Using this data and the MgO and FeO content of the analysed sample of olivine-free gabbro, recalculated to allow for the presence of an estimated 10 per cent plagioclase phenocrysts, a crystallisation temperature of 1175°C may be inferred for the olivine.

This temperature may be used in an effort to determine the relationship of the plagioclase phenocrysts to the other phenocryst phases. Drake (1976), using experimental data has shown that the composition of plagioclase crystallising at known temperature from a dry melt of known composition may be predicted from:

$$\left(X_{Ab(p)} = X_{NaAlO_{2(liq)}} \cdot X^3_{SiO_{2(liq)}} \cdot \exp\,(6100/T-2.29) \right)$$

where $X_{Ab(p)}$ is the mole fraction of albite in plagioclase.

$X_{NaAlO_{2(liq)}}$ is the mole fraction of $NaAlO_2$ in the magma.

$X^3_{SiO_{2\ (liq)}}$ is the mole fraction of SiO_2 in the magma.

T is temperature in degrees K.

and where $XNaO_{0,5\ (liq)} + X\ AlO_{1,5\ (liq)} + X\ SiO_{2(liq)} + X\ CaO_{(liq)} = 1$

If possible effects of volatile pressure can be ignored, it may be predicted by this method that plagioclase with a composition of about An_{63} would be expected to have crystallised from the olivine-free gabbro magma at the temperature at which the olivine is estimated to have crystallised (1175°C). That is, the olivine would have crystallised from the olivine-free gabbro magma in equilibrium with plagioclase with a composition similar to that of the middle and outer parts of the mantles of the zoned plagioclase phenocrysts present in the olivine-free gabbro. If the plagioclase phenocryst cores had crystallised from a liquid, similar in terms of plagioclase components to the olivine-free gabbro, crystallisation may be estimated by the same method, to have commenced at around 1425°C, a somewhat high temperature.

The available data thus, suggest that the cores of the clinopyroxene phenocrysts and the olivine phenocryst are both too magnesian to have crystallised in equilibrium with the analysed orthopyroxene phenocryst. The plagioclase, however could have crystallised in part at least, simultaneously with the olivine from the olivine-free gabbro. In view of the intimate textural relationship between the olivine, clinopyroxene and plagioclase phenocrysts, it is possible that these minerals represent a co-precipitated phenocryst assemblage. The analysed orthopyroxene could be considered a xenocryst, or the analysis could be considered to represent a more Fe-rich portion of a zoned orthopyroxene crystal. The orthopyroxene could also represent a later phase to crystallise from the magma, after reduction of the Fe:Mg ratio of the magma to a suitable value, by some process such as crystal fractionation.

A further complication is provided by the Fe-rich mantles present around the Type 2 Ca-rich clinopyroxene phenocrysts, which on the basis of the major element chemistry, would presumably be expected to crystallise in the later stages of crystallisation of the magma.

To summarise, certain Ca-rich pyroxene phenocrysts often apparently surrounded and protected by other phenocryst phases appear to have euhedral, relatively Mg-rich cores surrounded by Fe-rich mantles, whereas similar phenocrysts in unprotected positions apparently have corroded relatively Mg-rich cores and Fe-rich mantles that contain slightly less Fe than the previously mentioned Ca-rich pyroxene phenocrysts. The minor element chemistry of the Ca-rich pyroxenes indicates that the zoning present in the clinopyroxene phenocrysts may have resulted from a change, (increase), in the a_{SiO_2} of the magma from which it was crystallising.

Distribution coefficients and other evidence suggests that:-

(a) The olivine crystallised from a magma with an Mg:Fe ratio similar to that of the olivine-free gabbro.

(b) The orthopyroxene is unlikely to be in equilibrium with either the olivine or a magma with the composition of the olivine-free gabbro.

(c) The orthopyroxene does not appear to be in equilibrium with the Ca-rich pyroxene phenocryst cores, but may be in equilibrium with the Ca-rich pyroxene mantles, (both type 1 and type 2).

(d) The middle and outer portions of the plagioclase phenocrysts could have crystallised in equilibrium with the analysed olivine at a temperature of 1175°C.

Textural evidence suggests that the olivine, the Ca-rich pyroxene phenocrysts and the plagioclase phenocrysts in general terms constitute a co-precipitated three-phase phenocryst assemblage.

On the basis of this evidence it is suggested that the crystallisation history of these phenocrysts involved:-

(a) Precipitation of Ca-rich pyroxene, plagioclase and olivine phenocrysts and the formation of glomeroporphyritic aggregates.

(b) Crystallisation of the outer zone of Type 2 clinopyroxene phenocrysts and possibly crystallisation of the orthopyroxene in a more Fe-rich magmatic environment, probably with a higher a_{SiO_2}.

(c) Corrosion of unprotected Ca-rich pyroxene phenocrysts (and possibly the orthopyroxene phenocrysts), followed by crystallisation of the mantles of the type 1 clinopyroxene phenocrysts, (and possibly the clinopyroxene mantles around the corroded orthopyroxenes), in a slightly more Mg-rich magmatic environment, such as the olivine-free gabbro magma.

(d) Solidification of the olivine free gabbro in its present position and formation of the outermost rims (with compositions corresponding to the groundmass clinopyroxene) around all pyroxene phenocrysts, and corresponding feldspar rims around the plagioclase phenocrysts.

In order to explain this suggested crystallisation history it is suggested that the phenocrysts may represent pre-existing cumulate crystals, (with Fe-rich adcumulus zones present around the Ca-rich pyroxenes), which became caught up in the olivine-free gabbro magma. Prior to the emplacement of the olivine-free gabbro in its present position corrosion, and subsequent mantling of the unprotected pyroxene phenocrysts could have occurred. The magnetite (mentioned in the section on ore minerals) found included in the groundmass plagioclase could then be interpreted as part of the same xenocryst assemblage. This model suffers from several difficulties, namely the equilibrium between the olivine and the olivine-free gabbro must be regarded as coincidental and secondly the position of the orthopyroxene in the crystallisation sequence is not certain, unless it is regarded as an intercumulus phase. In the absence of more adequate analytical data further speculation on the nature of the phenocrysts does not however , seem justifiable.

The motive for the examination of the possible origins of these phenocrysts lies in their potential to determine if the magma is primary or a derivative of a more basic magma. In this case it appears likely that the phenocrysts are relict crystals from the fractional crystallisation of an initially more Mg-rich liquid. This initial liquid may have had a composition potentially parental to the olivine-free gabbro since the analysed olivine and part of the plagioclase crystals which are considered to have crystallised from this earlier liquid were also found to be in equilibrium with the olivine-free gabbro.

(G) The Form and Crystallisation History of the Intrusion

Textures and mineralogical variations present in both the olivine and the olivine-bearing gabbro provide no convincing evidence of the form of these two intrusive bodies. Both could equally well be interpreted as subvertical dyke-like bodies. as concordant sheets, or as some form intermediate between the two. The olivine-free gabbro, however, has a crude layering, each layer being defined by several discontinuous elongated patches of large feldspar phenocrysts (described in a previous section), and this lamination appears to be parallel to the local dip of the basalts. Although individual crystals do not show any marked preferred orientation, the layering is considered to be most probably the result of crystal settling, with the settling units possibly consisting of small glomeroporphyritic aggregates. Other evidence of crystal fractionation may be provided by the eastward decrease in pyroxene content, coupled with an increase in the proportions of plagioclase and micropegmatite. Much of the groundmass of these rocks however does not appear to be composed of cumulus phases, and instead tends to resemble textures observed in adjacent dolerite dykes. The layering may therefore be the result of crystallisation predominantly from the base of the sheet upwards combined with the settling of the glomeroporphyritic plagioclases. According to Wager and Brown (1968) crystallisation in thin sills takes place mainly from the floor of the intrusion upwards, at a relatively rapid rate. If phenocrysts were in suspension in the olivine-free gabbro magma at the time of intrusion, and settling rates of these crystals were slow relative to the rate at which bottom crystallisation was causing the floor of the intrusion to rise, small clusters of plagioclase phenocrysts could be incorporated in the rising floor before the accumulation of a sufficient numbers of crystals to form a well defined layer.
No other process seems adequate to explain the observed textures and discontinuous layering. Flowage differentiation for example, as described by Battacharji and Smith (1964) and Battacharji (1967), could have orientated the crystals but it also produces a concentration of phenocrysts in the centre of dykes, and a similar effect would be expected in sills.

The observed layering and textural and modal variations are therefore considered likely to be the result of the crystallisation of thin eastward dipping sheet from the bottom upwards accompanied by the slow settling of glomeroporphyritic aggregates of plagioclase and other phenocryst phases. If this interpretation of the intrusion as a sub-concordant sill with a dip approximately that of the surrounding basalts is correct, then its thickness maybe estimated to be of the order of 10m to 20m.

Petrographic data suggests that phenocryst phases were also present in the other two units of the Basal Intrusion. In the olivine-bearing gabbro both olivine and the larger Ca-rich clinopyroxenes are considered to represent phenocryst phases. The presence of oscillatory zoning in the clinopyroxenes suggest that this magma also may have had a complex crystallisation history prior to emplacement in its present position. The necessary analytical data to attempt to interpret this history is lacking however. Olivine appears to have been the only phenocryst phase present in the olivine gabbro but the widespread alteration of the olivine crystals has obscured their composition and the possibility of relating them to phenocryst olivines in either the olivine-bearing or the olivine-free gabbro.

The interpretation of the olivine-free gabbro as a thin sill suggests the possibility that all three intrusive phases may have had a sheet-like form, however no indications of crystal settling were noted either in the olivine gabbro, or the olivine-free gabbro. Crystal settling may have been expected to occur in particular, in the olivine-bearing gabbro, that contained fairly abundant, large phenocrysts of pyroxene and olivine on intrusion, however fairly rapid cooling is indicated by the fine-grained groundmass of this rock type, and may account for the absence of crystal fractionation. The olivine gabbro, if of a sheet-like form, would possibly have been thin enough for rapid cooling again to have prevented crystal settling. Textures described in the section of petrology are not in accord with sudden cooling, however, and as this

intrusion cannot be related to either of the other two intrusive phases, it may have an intermediate or dyke-like form.

Thus, no really compelling evidence has been produced to indicate the attitude of any of these intrusive bodies within the exception of the olivine-free gabbro, and this, it is suggested, is probably a sub-concordant sheet.

(H) Order of Intrusion

The olivine-free gabbro shows least sign of metamorphism and may therefore, be the youngest of the three magma pulses. No further evidence is available as to the relative ages of the other two intrusions.

5.7.3 The Komatipoort Intrusion

(A) Introduction

The Komatipoort Intrusion forms a large elongated mass of divergent rock types, representatives of which have been found as far as 10 km north and 13 km south of the village of Komatipoort. At its widest point, just south of Komatipoort itself, the intrusion outcrops over a width of almost 2 km, (see geological map).

The intrusion consists of five major rock units, apparently in the form of roughly concordant sheets, superimposed one upon the other to give an estimated seven hundred and seventy meter thick layered structure at the point of maximum development. These sheets appear to dip, with the surrounding basalt, at about 25^{o} to the east. Exposures of the complex as a whole are poor, however, and the precise limits of distribution of the lower units are difficult to define. In general, the rock units appear to form an overlapping series from the bottom upwards with each successive sheet having a greater lateral extent than its predecessor, (see geological map).

Evidence presented here suggests that the intrusion is multiple, and several possible separate intrusive pulses, have been postulated. Crystal settling was a significant process during the cooling of some of these pulses and has played an important part in the formation of the layered structure that comprises the Komatipoort Intrusion, in that some of the rocks present are considered to be cumulates.

The major features of the five rock units comprising the intrusion are summarised in Table 24, p 115.

Table 24

Major features of the Komatipoort Intrusion

	Unit	Rock Type	Maximum Vertical thickness
	Country Rock	Metamorphosed Basalt	
		——— Intrusive Contact ———	
Top	5	Feldspathic Gabbro	± 100 m
		——— Inferred Intrusive Contact ———	
	4	Granophyre	± 175 m
		——— Inferred Intrusive Contact ———	
	3	Granophyric Gabbro	± 225 m
	2	Clinopyroxene - Plagioclase Cumulate	± 250 m
		——— Inferred Intrusive Contact ———	
Bottom	1	Olivine Gabbro	± 20 m
		——— Inferred Intrusive Contact ———	
		Hornfelsed Basalt	
	Estimated Maximum Total Vertical Thickness		± 770 m

(B) Unit 1 - The olivine gabbro

(i) Distribution and Lithology

The olivine gabbro has been mapped as a narrow north-south trending belt extending down the western margin of the intrusion. This unit is considered to form a roughly concordant sheet approximately 20 m thick, dipping at around 25° to the east together with the other rock units comprising the intrusion.

The presence of olivine in these rocks has made them more susceptible to weathering than the adjacent olivine-free country basalts and the unit is normally covered by deep soil. Definition of the exact extent of the unit is therefore difficult, but it continues for at least 5 km north of the Ngweti River and 3 km south of it, although float distribution suggests possible thinning of the zone in both directions. Reasonably good exposures do occur in the Townlands running along the north bank of the Ngweti River, and somewhat better exposures are present just south of the Sihlangula Stream, (see geological map).

In general these rocks have a fairly uniform appearance in hand specimen. They are dark greenish black, phanero-crystalline and coarse grained, containing conspicuous plates of dark pyroxene. Samples collected close to the estimated position of the basal contact near the Sihlangula Stream, (see geological map), do show significant textural differences. Close to the contact the rock is a melanocratic aphanitic variety, strongly resembling the adjacent hornfelsed basalt. A fine lineation is apparent at the contact, and this lineation becomes less distinct in samples collected away from the contact towards the interior of the intrusion. In samples collected near the Ngweti River no lineation was observed.

(ii) Petrography

Because of the textural differences noted between samples collected adjacent to the Ngweti River, the petrography of samples from both locations are described.

In the Ngweti River section textures are reasonably uniform, however, the textures of samples collected from the Sihlangula Stream section suggest a continuous gradation from a plagioclase-olivine-magnetite hornfels at the lower contact to an olivine gabbro near the upper contact of unit 1.

(a) Sihlangula Stream Section

The finely lineated rock found at the lower contact of unit 1, near the Sihlangula Stream is a microcrystalline plagioclase-olivine-magnetite hornfels. This rock, as described in the section on petrogenesis is considered to represent a thermally metamorphosed portion of the olivine gabbro unit . The average modal composition of the finely lineated rock is :- plagioclase 54%, olivine 32%, pyroxene 10% and iron ore 6 %. Over the few centimeters for which this rock is exposed, however, the modal composition varies slightly. Thus there is a noticeable sympathetic variation in the amounts of olivine and plagioclase and a corresponding antipathetic variation in the amount of pyroxene present.

The plagioclase occurs in two generations, firstly in the form of tiny tabular laths, about 0,1 mm in length, which make up most of the groundmass of the rock, and secondly, as large apparently relict crystals 1 - 5 mm in length. These large crystals occur either alone or as small aggregates.

The groundmass plagioclase crystals may show a fairly marked preferred orientation in a direction parallel to the estimated dip of the rock units in the intrusion, (i.e. the lineation dips at around 25^{o} to the east). Where the large plagioclase are present

as single crystals, rather than aggregates, a similar orientation of these crystals is apparent.

Olivine forms discrete, subhedral to anhedral crystals varying in size from 0.5 mm to 1.0 mm, that occur interstitially to the plagioclase. The olivines occasionally form aggregates, or chains of up to three or four crystals, and these chains tend to lie parallel to the preferred direction of the plagioclase, as do the long axes of the occasional larger, elongated olivine crystals which occur in this rock. The olivine crystals locally disturb the preferred orientation of the long axes of the groundmass plagioclase crystals described earlier, and these groundmass plagioclases tend to curve around both above and below the olivines.

Magnetite usually occurs as single, euhedral, intergranular crystals, (octrahedrons and cubes), that occasionally protrude slightly into the margins of olivine crystals, but may also form small clusters or be linked together in short chains of five or six units; in the latter case the chains lie parallel to the direction of preferred orientation of the other minerals in the rock.

The pyroxene is present interstitially as tiny grains of hypersthene and augite, (neither showing ex-solution phenomena), which range in size from 0.03 mm to 0.05 mm.

Within a few centimeters the finely lineated rock gives way to a coarser variety, a change produced by a variation in both the modal proportions and the mode of occurrence of the constituent minerals.

The changes include the following. The olivines show poikiloblastic 'extensions' which usually enclose plagioclase crystals only. These plagioclases resemble the normal groundmass crystals but for the absence of an outer mantle and rim invariably present around the groundmass crystals. These olivine extensions bear some

resemblance (on a much smaller scale) to the crescumulus type growth occurring in the olivines of the Isle of Rhum (Wadsworth 1961, Brown 1956), and in some of the rocks of the Skaergaard Intrusion (Wager and Brown 1968), in that addition of crystalline material has taken place preferentially in the (010) direction, and the ' extension ' has a dendritic form. Although this ' extension ' in the Komatipoort rocks has usually occurred in one direction only, it differs from those described from igneous rocks in that it is not always upwards. On the contrary the ' extensions ' may extend downwards as well as parallel to the general lineation in the rock, or less commonly in some intermediate direction, (see Plate 7 , p 120).

Also present at this level are narrow lenses free of interstitial pyroxene, containing olivine in two forms, firstly as tiny interstitial grains, roughly equal in size to the groundmass plagioclase, and secondly in the form of large crystals attached to aggregates of large augite and hypersthene crystals. Both the olivine and the marginal pyroxene crystals of the aggregates may show poikiloblastic ' extensions ', although those around the pyroxene form rims of fairly constant width and do not have the dendritic form typical of the olivines. These large aggregates also disturb the general orientation of the plagioclase crystals as noted in the case of the olivine crystals described previously, although not to the same extent. Neither plagioclase nor magnetite show any change in their mode of occurrence.

Within a few centimeters the texture of the rock again changes, inclusions of plagioclase are no longer present in the olivine outgrowths only. Instead the entire olivine crystals contain inclusions and these olivines are often bordered by rims of pyroxene, (see Plate 7 , p 120). The habit of the groundmass pyroxene changes and this mineral occurs as poikolitic plates, although the aggregates of large augite and hypersthene crystals, described above , are present in addition in increasing abundance. Plagioclase is not closely

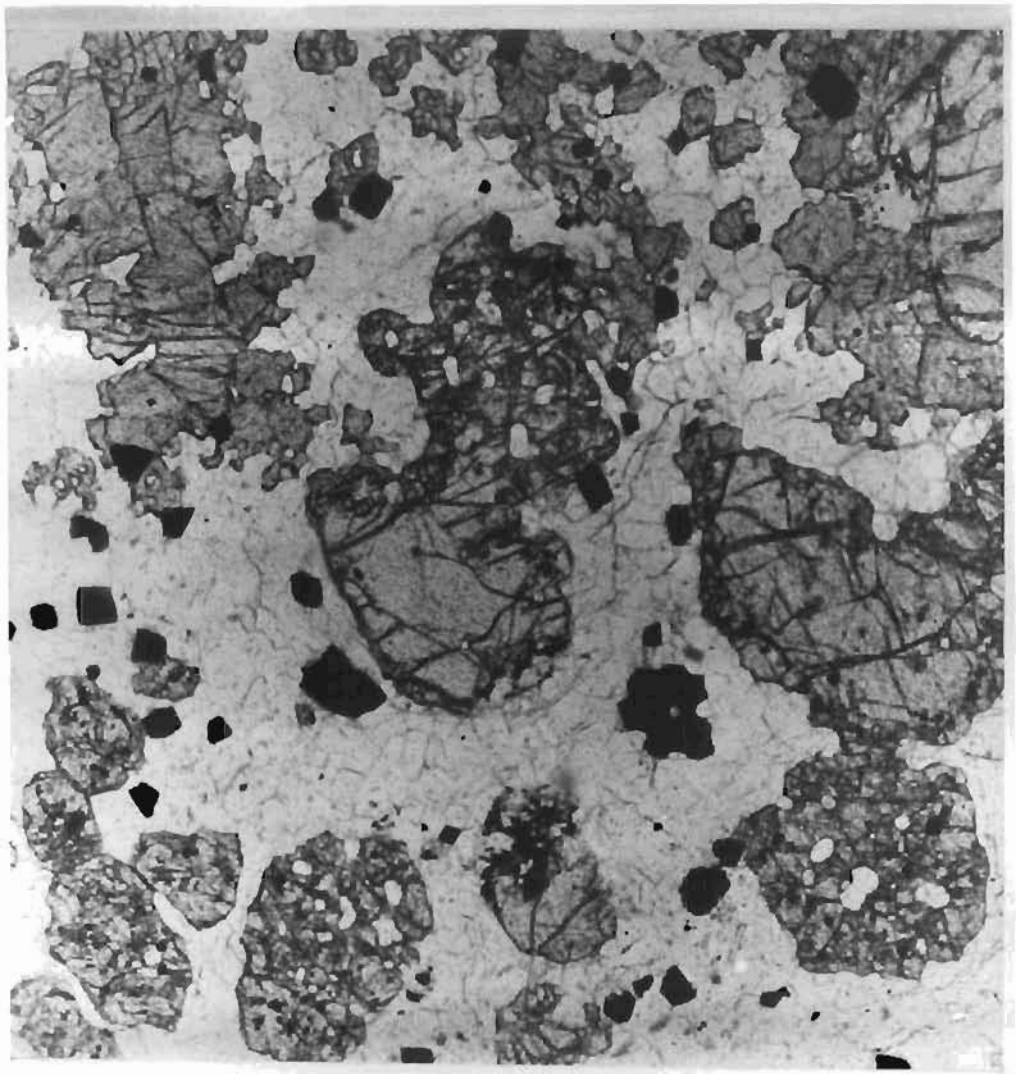

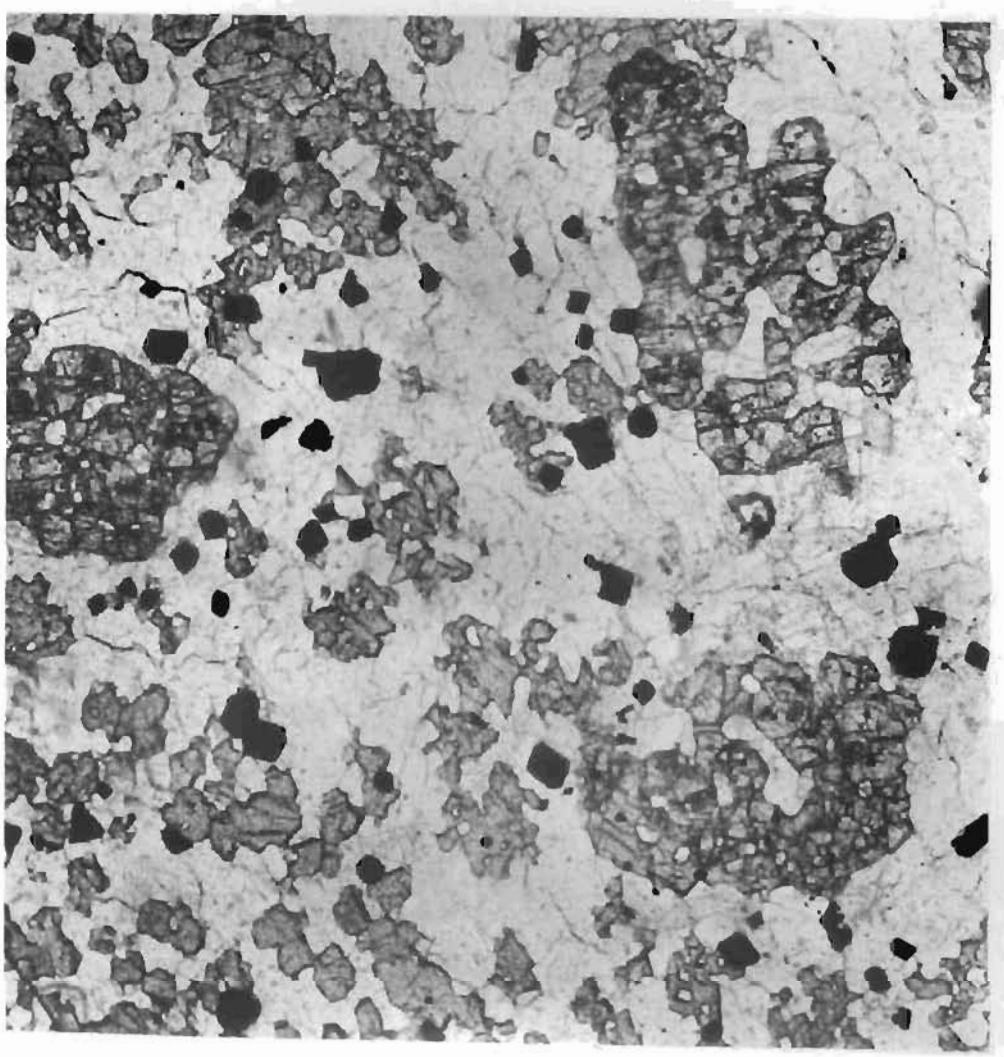

packed in the poikilitic pyroxene plates, and the pyroxene may be plagioclase-free over relatively large areas. The large plagioclase crystals, still, however, show signs of partial recrystallisation.

The rock becomes coarser-grained a few metres away from the lineated zone just described and here consists of olivine, plagioclase and magnetite, set in extensive plates of pyroxene (often up to 2 cm in diameter). The olivine forms crystals (1.5 mm diameter) with an elongated and frequently a dendritic form (see Plate 8 , p 122, fig 1). These invariably enclose tiny crystals of plagioclase, around 0.2 mm in length. Occasionally larger plagioclase crystals are enclosed marginally. The large poikilitic plates of pyroxene usually consist of hypersthene (inverted pigeonite) containing abundant exsolved clinopyroxene, both in the form of orientated blebs and lamellae and as blebs in a graphic-type intergrowth. Uninverted pigeonite, together with augite, forms similar plates enclosing the olivine, plagioclase and magnetite. Plagioclase not included in the olivine grains has a seriate texture, grading from tiny crystals less than 0.1 mm in length to laths 2.5 mm long, (see Plate 8, 122). Commonly, the smaller plagioclase crystals consist of a euhedral core, (basic) surrounded by a mantle and rim of a different composition, but the larger crystals ranging from about 1 mm upwards differ. They typically show severely corroded cores, which in places are reduced to a series of discontinuous patches, similar to those described by Vance (1965). In addition the mantle itself shows a zonal structure, consisting of up to five oscillatory zones followed by the usual relatively acid rim (An_{35} at the outer edge). Outlines of the plagioclase crystals, even where enclosed by olivine, tend to be irregular and embayed. Smaller crystals may occur as single units, but the larger plagioclases have a tendency to form aggregates. Ore minerals appear in two forms, firstly as small euhedral crystals, and secondly as irregular grains, filling the interstices between the other mineral phases.

Plate 8

(1) Olivine Gabbro, Komatipoort Intrusion - poikiloblastic olivine crystal, crowded with tiny plagioclase grains (upper left quadrant), large relict plagioclase phenocryst (lower right quadrant) and abundant smaller, often embayed plagioclase crystals, set in an extensive clinopyroxene plate, (upper right quadrant). A relatively clear, inclusion free recrystallised rim surrounding the relict plagioclase phenocryst is just visible at the right end of the phenocryst. Lower limit of olivine gabbro. (X48). Sihlangula Stream Section.

(2) Olivine Gabbro, Komatipoort Intrusion -Plagioclase crystals, many rounded or embayed, set in an extensive crystal of olivine. Slightly higher in the olivine gabbro than (1) above. (X 96). Sihlangula Stream Section.

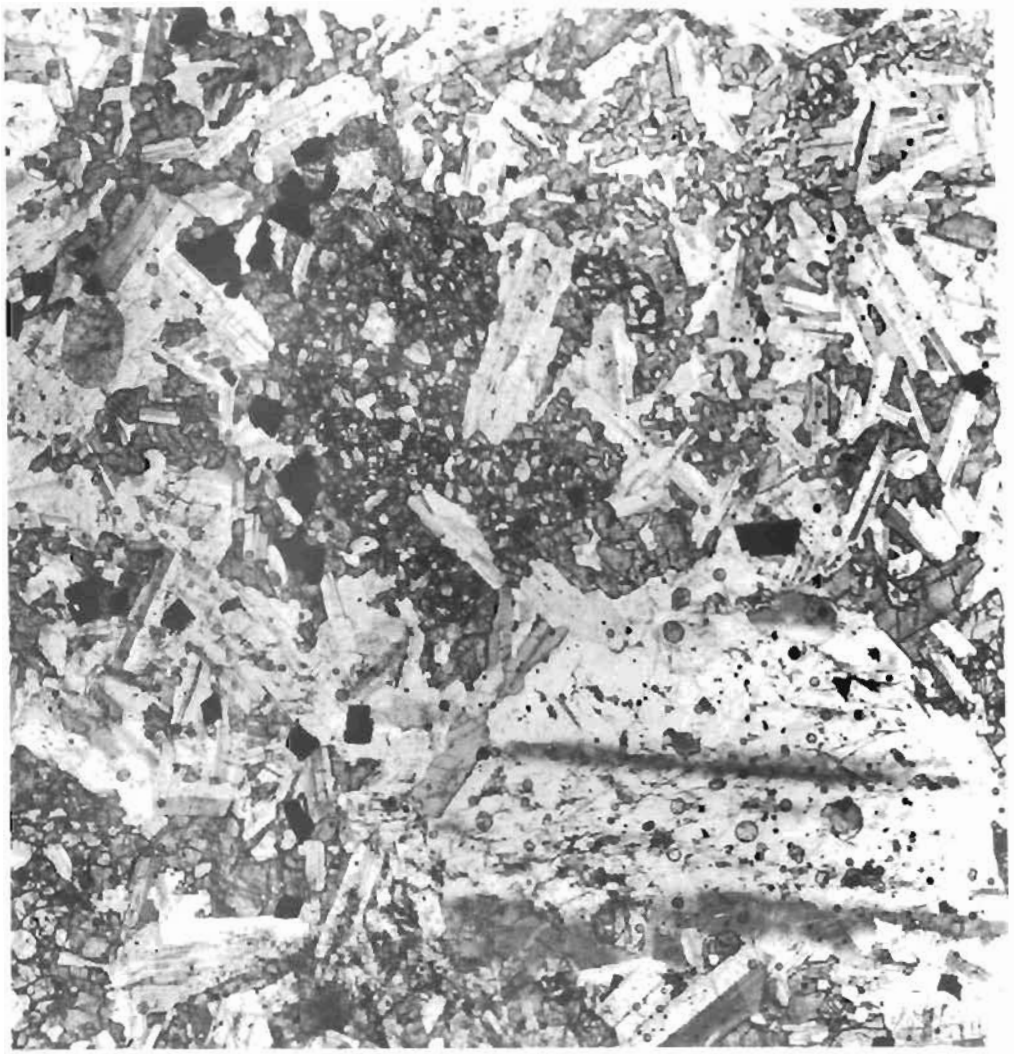

The texture of the rock gradually coarsens to the east and samples are composed of larger crystals of plagioclase, (with corroded cores and complex mantle structure), and dendritic olivines that occasionally reach 2 cm in length, both set in oikocrysts of augite and pigeonite about 3 cm across, (see Plates 8 and 9). Magnetite and sulphide minerals form irregular patches filling the interstices. Slightly further east the olivine shows a chain texture,(see Plate 9). Near the contact between unit 1 and unit 2, the plagioclase shows a tendency to form clusters, (in places up to 1 cm across), interstitial to the large pyroxene plates (pigeonite and augite) with olivine, now forming rounded and embayed, rather than dendritic crystals, (see Plate 9, p 124 , usually associated with the plagioclase rather than the pyroxene. This gives, in hand specimen, the macroscopic mottled appearance noted in the previous section on lithology. The range of textural variations from the base to the top of the Basic Unit are illustrated in Plates 7 to 9.

(b) Ngweti River Section

Olivine Gabbro

No fine-grained lineated rocks were found in the Ngweti River Section and the lower part of the unit consists of a rock composed essentially of plagioclase and clinopyroxene in the proportions 2:1 together with about 10% olivine. In the central part of the unit , the olivine content increases to 25% at the expense of the pyroxene, which constitutes only 10% to 15% of the rock. Plagioclase still constitutes some 60% of the rock. Locally however, specimens with a troctolitic composition were encountered, (olivine 34%, pyroxene 4%, plagioclase 62%, by volume). In general there is a tendency for the plagioclase and the olivine content to decrease upwards through the zone until the rocks representing the contact with unit 2 are reached. A little orthopyroxene is developed, forming patches associated with the olivine or clinopyroxene and this almost always contains lamellae and blebs of exsolved clinopyroxene which may show a preferred

Plate 9

(1) Olivine Gabbro, Komatipoort Intrusion. Extensive dendritic olivine, composed of several sub-units surrounded by large cumulate plagioclase crystals. Upper part of olivine gabbro. (X 96)

(2) Olivine Gabbro, Komatipoort Intrusion. Olivine grains and cumulate plagioclase crystals showing complex zoning set in an extensive plate of clinopyroxene. Near upper boundary of the olivine gabbro. (X 96).

orientation. Small interstitial patches,(up to 2 mm across), of medium grained micropegmatite were occasionally noted and evidence of corrosive reaction between the micropegmatite and both clinopyroxene and plagioclase is apparent. The olivine gabbro in the Ngweti River section, has a fairly uniform ophitic texture with plates of clinopyroxene up to 3 cms across, enveloping both the plagioclase and olivine.

(c) The southern extremity of the olivine gabbro zone

Boulders of olivine gabbro are present at the southern extremity of this zone and some of these consist of rocks very similar to those encountered in the Ngweti River section, described above. Some, however, are composed of a finer grained variety of olivine gabbro. These finer grained rocks consist of euhedral to rounded olivine crystals 0.8 mm to 3.2 mm in diameter, clinopyroxene crystals 1 to 2 mm in diameter, which may include a few small grains of plagioclase, and what appear to be two generations of plagioclase crystals. The majority of the plagioclases range in size from 0.1 to 0.8 mm, and many of the larger crystals in this size range show oscillatory zoning. The outer normally zoned rims present in plagioclases from other parts of the olivine gabbro zone are, however, absent. In addition to these plagioclases there are also other, larger crystals, 1.5 mm to 3 mm in length, which are further distinguished by the presence of patchy, irregular zoning.

(iii) Mineralogy

(a) Olivine

Near the lower contact the olivine may constitute as much as 32% of the rock, but the concentration fluctuates widely in samples collected over the rest of the unit. The olivine near the base of the unit has a composition of around Fo_{66} Fa_{34} as determined by an X-ray diffraction method, (see section on methods) and there appears to be little variation in composition of the olivine vertically. through unit 1. Several electron microprobe analyses of olivines from the olivine gabbro unit are shown in Table 25.

The changes in the habit of olivines present in a a series of olivine gabbro samples collected along the Sihlangula Stream cross-section are illustrated in Plate 7 to Plate 9. Close to the contact the texture of olivine changes rapidly over a distance of some 10 cms, from small (0.5 mm) rounded inclusion-free grains set in a groundmass of plagioclase and pyroxene to grains of a similar size showing small, dendritic poikiloblastic extensions, containing inclusions of plagioclase. These are rapidly succeeded by irregular poikiloblastic olivine grains of similar size, (see plate 7, fig 1 and fig 2). In samples collected away from the contact the olivine successively forms larger grains crowded with minute plagioclase inclusions and set in a groundmass of coarser plagioclase, (see Plate 8, fig 1 , note change in enlargement), then more extensive grains containing larger plagioclase inclusions, which show signs of resorbtion, (see Plate 8, fig 2). These are succeeded by extensive dendritic olivines which are largely interstitial to the plagioclase, and in places may consist of several olivine crystals linked to form a sinuous chain-like unit, (see Plate 9 ,fig 1, and Plate 9, fig 2). Finally close to the base of the overlying clinopyroxene plagioclase cumulate the olivines are rounded and embayed grains containing no inclusions, (see Plate 9, fig 2).

Electron microprobe analyses were made of a series of olivine grains from the finely lineated rocks present at the western contact of the olivine gabbro. These olivines occur in a variety of forms, (described earlier, see Plate 7), including small rounded olivine grains , large rounded olivine grains, olivine grains showing poikiloblastic extensions and large poikiloblastic olivine grains. Examples of each of these forms were marked and submitted for analysis by electron microprobe. The results of these analyses are listed in Table 25, p 128. An examination of this Table shows that there is no significant difference in the composition of the olivines showing different crystal forms. All have a composotion of the order of $Fo_{65,4}$, and contain similar amounts of Ni and Mn.

A few olivines from the interior of the olivine gabbro unit have been analysed by J. Bristow of the University of Cape Town, (personal communication), and these results show the presence of olivines with a composition of the order of Fo_{52}-Fo_{66}, near the western contact of the unit, while olivines from the interior of the unit have compositions in the range Fo_{65}-Fo_{66}. Bristow has suggested that this is contrary to what would be expected in a simple model involving crystal settling of pre- existing olivine crystals, and in fact could be more satisfactorily explained by inward crystallisation from the walls of a sheet or dyke-like body. In view of the fact that the extent of zoning in the olivines is unknown at this juncture, and that the effects of recrystallisation, which appear to have had an important influence on the textures of at least some of the rocks in the olivine gabbro unit, are not completely understood, this interpretation is not adopted here.

An interpretation of the petrogenesis of the olivine gabbro unit is given in the relevent section, (see p 265 and p 274),in which crystal settling of pre-existing phenocryst phases is considered to have played a significant role.

TABLE 25

Electron Microprobe Analyses of 5 Olivines from the Olivine Gabbro and Analyses of Olivines from the Clinopyroxene Plagioclase Concentrate

	Olivine 1	Olivine 2	Olivine 3	Olivine 4	Olivine 5	Olivine 6	Olivine 7	Olivine 8	Olivine 9	Olivine 10
MnO	0,44	0,43	0,46	0,48	0,44	0,77	0,77	0,77	0,74	1,10
NiO	0,17	0,13	0,18	0,18	0,18	0,00	0,00	0,00	0,10	0,00
MgO	33,59	34,21	33,94	34,07	34,19	16,18	15,44	16,78	17,38	10,99
FeO	32,3	32,34	31,82	32,05	32,16	53,74	53,89	52,62	51,68	56,54
SiO_2	36,33	37,01	37,10	36,59	36,91	33,53	32,95	33,14	33,85	33,25
CaO	0,00	0,00	0,00	0,00	0,00	0,00	0,04	0,00	0,00	0,10
TOTAL	102,83	104,12	103,5	103,36	103,88	104,22	103,09	103,31	103,74	101,98
Fo	65,3	65,3	65,5	65,5	65,4	34,9	33,8	36,2	37,47	25,73
Fa	34,7	34,7	34,5	34,5	34,6	65,1	66,2	63,8	62,53	74,27
Cations per 4 oxygens										
Si	0,9670	0,9706	0,9766	0,9671	0,9699	0,9804	0,9785	0,9749	0,9844	1,0135
Fe^{2+}	0,7192	0,7093	0,7005	0,7085	0,7069	1,3142	1,3385	1,2946	1,2570	1,4415
Mn	0,0099	0,0095	0,0104	0,0107	0,0098	0,0192	0,0195	0,0193	0,0181	0,0283
Mg	1,3329	1,3370	1,3318	1,3426	1,3394	0,7054	0,6833	0,7538	0,7533	0,4995
Ca	-	-	-	-	-	-	0,0013	-	-	0,0032
Ni	0,0035	0,0027	0,0038	0,0038	0,0038	-	-	-	0,0024	-
SUM	3,0326	3,0291	3,0230	3,0326	3,0297	3,0192	3,0211	3,0247	3,0152	2,9861

Olivine Gabbro

Olivine 1 - large non-poikiloblastic olivine - olivine gabbro - lineated zone - lower contact.
Olivine 2 - small non-poikiloblastic olivine - olivine gabbro - lineated zone - lower contact.
Olivine 3 - non-poikiloblastic portion of a compound olivine crystal - same location as 1 and 2.
Olivine 4 - poikiloblastic portion of same crystal as olivine 3.
Olivine 5 - large poikiloblastic olivine crystal - same location as olivines 1 to 4.

Clinopyroxene-plagioclase cumulate

Olivine 6 - small subhedral grain - lower contact of the clinopyroxene-plagioclase cumulate.
Olivine 7 - small subhedral grain - lower contact of the clinopyroxene-plagioclase cumulate.
Olivine 8 - larger subhedral grain - lower contact of the clinopyroxene-plagioclase cumulate.
Olivine 9 - larger subhedral grain - lower contact of the clinopyroxene-plagioclase cumulate.
Olivine 10 - large irregular grain - from the upper portion of the clinopyroxene-plagioclase cumulate.

Plagioclase

In the uppermost parts of the olivine gabbro in the Sihlangula Stream section and in most of the samples collected from elsewhere in unit 1, two generations of plagioclase are present.

First Generation Plagioclase

First generation plagioclase is distinguished by its large size, more basic composition, the complexity of the zoning present and by a tendency to enclose smaller, normally zoned plagioclases marginally. The large first generation crystals consist of three structural units, a basic unzoned core, an oscillatory zoned mantle around the core, and a normally zoned rim surrounding the mantle. Either of the first two units may be repeated, one or more times, in any one crystal, as may be seen in fig 14, p 130 , in which the compositional variations in a selection of first generation plagioclases are shown. As shown in fig 14, where a unit is repeated, the second unit is separated from the first by an irregular, corroded boundary. Cores of crystals, whether single or multiple, usually have a composition in the range An_{72} to An_{82} , i.e. bytownite. The composition of the oscillatory zoned mantles, ranges between An_{70} and An_{58} , generally being closer to the more sodic extreme, and plagioclase forming the rims of the crystals commonly grades rapidly from near An_{58} where in contact with the oscillatory zoned mantles to around An_{50} at the margin of the crystal.

Second Generation Plagioclase

These smaller plagioclase crystals display none of the complex zoning found in the first generation crystals and usually consist of a core with a composition in the range An_{65} - An_{56} which grades progressively to a margin with a composition of An_{54} to An_{50}.

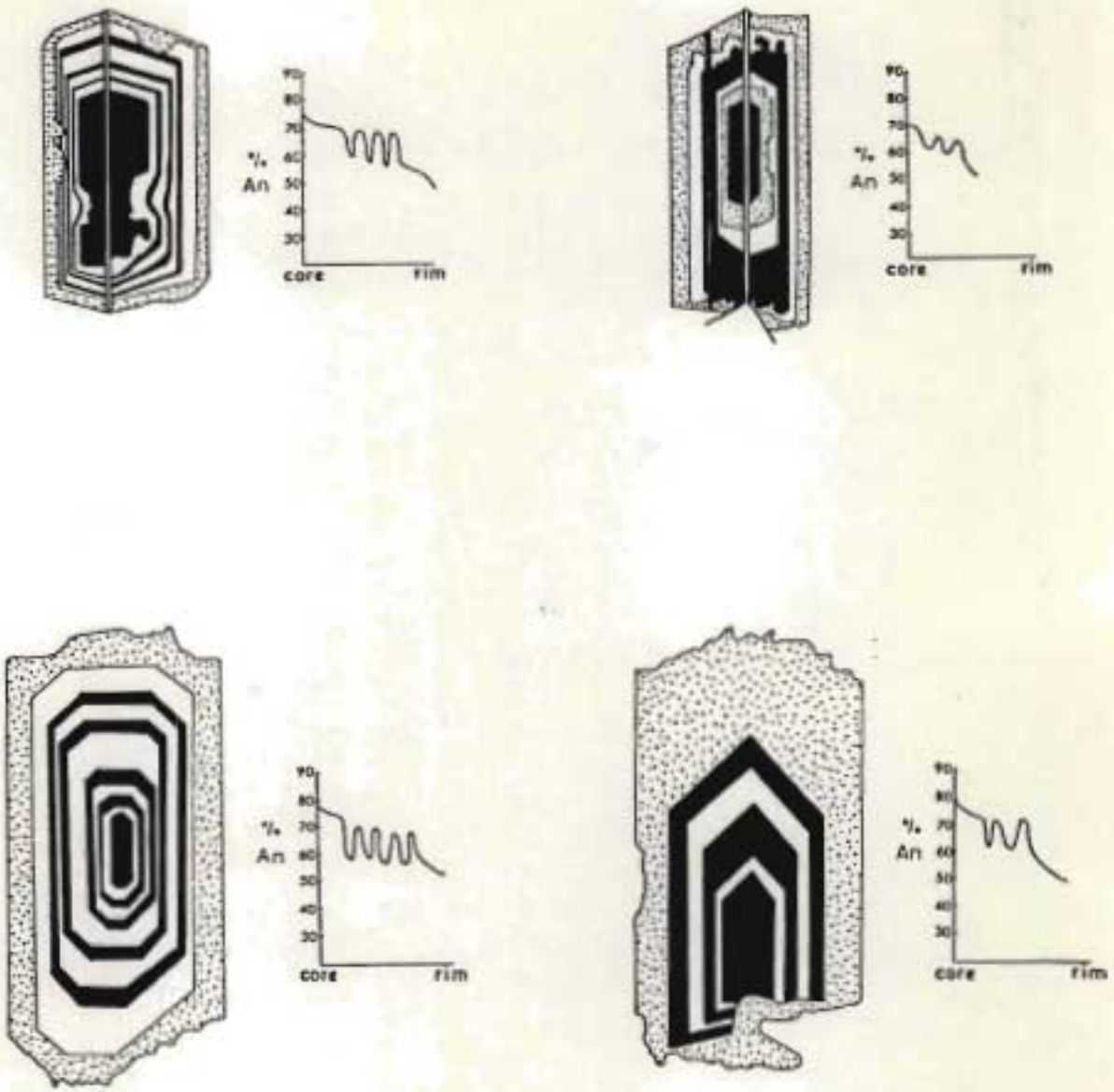

Figure 14. Compositional zoning present in first-generation plagioclase crystals of the olivine gabbro

In samples collected along the Ngweti River Section textural relationships of the plagioclase do not vary, however in the Sihlangula Stream Section (see geological map) considerable variations in texture occur, although in the upper parts of the unit textures resemble those just described. Passing downwards through unit 1 in the Sihlangula Stream section the habit of the olivine changes (see section on the mineralogy of olivine), and some plagioclase of both generations may be included in the more extensive, often dendritic olivine crystals. These included plagioclases tend to have an embayed outline, (see Plate 8, fig 2 and Plate 9, fig 1), with the embayments cross-cutting the pre-existing zoning present in the plagioclase. The composition of the included plagioclase is, however unchanged. Closer to the base of the olivine gabbro unit many of the plagioclases included in the olivine are reduced to small embayed and rounded remnants, although adjacent plagioclase crystals which may be either included in pyroxene plates or occur interstitially are identical to those described from the top of the unit. In the lowermost rocks of the olivine gabbro unit, the plagioclase included in the olivine consists of small (0.1 mm) embayed grains. These grains tend to be clouded and compositions could not be determined by optical means. Some of the plagioclase included in the adjacent pyroxene is also embayed at this point and resembles the plagioclase observed included in olivines at higher levels in unit 3. A seriate texture results with the plagioclase varying in size from small embayed grains to large first generation phenocrysts, (see Plate 8).

Close to the contact in the fine-grained lineated rocks the plagioclase occurs for the most part as tiny tabular laths, (usually showing a preferred orientation), about 0.1 mm in length. These small laths which comprise much of the groundmass of the rock are usually zoned. They are composed of a core with a composition of about An_{55} surrounded by a more Ca-rich mantle (composition An_{65}) which grades into a rim with a composition of An_{50}. The mantle thus forms a reversed zone. In the largest of the groundmass crystals oscillatory zoning may be present in the core.

Large apparently relict plagioclase crystals also occur in this rock either singly or as small aggregates. They are distinguished not only by their size but also by the presence of deformational effects such as bending, glide twinning and cracking, and in places by partial recrystallisation to smaller grains. The average composition of these large plagioclase crystals is around An_{62}.

(b) Pyroxene

Augite, pigeonite and hypersthene are all present in the lowermost parts of the olivine gabbro whereas in the uppermost parts only augite and pigeonite are found. At all levels within the unit the amount of pyroxene varies antipathetically with that of the olivine and is always less abundant than the plagioclase.

Pyroxene in the olivine gabbro usually forms extensive plates, up to 30 mm in diameter enclosing large olivine grains and plagioclase crystals. Near the basal contact of the unit in the Sihlangula Stream Section other textures were noted. The pyroxene here initially forms somewhat less extensive plates crowded with small plagioclase inclusions, and then closer to the lower contact forms tiny grains of a similar size to the small plagioclase grains. In addition to these modes of occurrence the pyroxene also occurs as large porphyroblasts which may show poikiloblastic extensions.

Orthopyroxene

Hypersthene is the only orthopyroxene identified and is confined to the lower parts of the olivine gabbro including

the finely lineated rocks at the basal contact in the Sihlangula Stream section. In the olivine gabbro, hypersthene usually occurs as rims around irregular embayed olivine crystals, or less commonly forms large (3 cm diameter) plates enclosing plagioclase and olivine grains. Exsolved blebs of clinopyroxene are common. At slightly higher levels in the zone, the extensive plates of hypersthene have cores of pigeonite suggesting that the hypersthene was not a primary crystallisation product but represents inverted pigeonite.

In the fine-grained hornfels-textured rocks of the contact zone primary hypersthene occurs (primary in the sense that it does not represent inverted pigeonite) as small (0.1 mm) groundmass crystals and/or larger porphyroblasts. The porphyroblasts appear to have an intermediate composition (Mg_{66}) as may be seen from the results of microprobe analyses of several grains listed in Table 26. The groundmass hypersthenes proved too small for satisfactory compositional determination.

The analyses listed in Table 26 suggest that the Mg content of the orthopyroxene may increase upwards through the fine-grained, lineated contact rocks, however the range of compositional variation is small, (Mg_{65} to Mg_{68}). The analysis also shows that strong compositional similarities are present between the analysed hypersthene from the top of the olivine gabbro and that from the contact zone, (see Table 26).

Augite

Augite is present in variable amounts in all specimens of the olivine gabbro. In the lowermost parts of the contact zone it occurs both as tiny, (0.1 mm), groundmass crystals and as larger porphyroblasts. Higher in the contact zone it tends to form poikiloblastic plates and in the average olivine-plagioclase-cumulate these increase in size up to about 30 mm in diameter.

Exsolution is present in the form of thin crystallographically orientated lamellae of pigeonite or, less commonly, as discontinuous platelets of orthopyroxene. Abundant randomly distributed blebs of orthopyroxene are present in some augites and in places these form narrow trails meandering across the host augite.

TABLE 26

Electron Microprobe Analyses of 4 Orthopyroxenes from the Olivine Gabbro

Orthopyroxene Analysis No.		(1)	(2)	(3)	(4)
SiO_2		53,08	52,10	53,33	53,16
CaO^2		2,11	2,13	1,95	2,10
MgO		25,66	23,82	24,96	24,46
TiO_2		0,65	0,76	0,53	0,67
FeO^2		20,70	18,80	17,49	19,17
Al_2O_3		0,89	1,29	0,88	0,93
TOTAL		103,09	98,90	99,14	100,49
(1)		Large orthopyroxene grain from lower part of the contact zone.			
(2)		Large orthopyroxene grain from middle of the contact zone.			
(3)		Large orthopyroxene grain from upper part of contact zone.			
(4)		Orthopyroxene 'plate' (inverted pigeonite) from upper part of olivine gabbro.			
Cations per 6 oxygens	Si	1,913 + 0,038 = 1,951	1,94 + 0,057 = 1,997	1,996 + 0,034 = 2,000	1,948 + 0,040 = 1,988
	Al	0,000	0,000	0,000	0,000
	Ca	0,082	0,085	0,077	0,083
	Mg	1,378	1,322	1,371	1,336
	Ti	0,018	0,022	0,015	0,019
	Fe	0,624 = 2,102	0,586 = 2,015	0,539 = 2,002	0,588 = 2,026
	O	6	6	6	6
	Fe	30,53	30,17	27,66	29,93
	Mg	65,59	65,61	68,49	66,00
	Ca	3,88	4,22	3,85	4,07

Electron microprobe bulk analyses of seven representative augites from the contact zone and the overlying olivine gabbro are listed in Table 27. These analyses are shown plotted in the pyroxene quadrilateral in fig 15. From these results it is apparent that the pyroxenes show little variation in composition. The two analysed pyroxenes from the lower and middle levels of the olivine gabbro in the Sihlangula Stream section, are however noticeably more diopsidic and Si-rich and poorer in Fe and Ti, than the clinopyroxenes of the fine-grained lineated rocks at the basal contact in the Sihlangula Stream section, and the analysed augite from the top of the olivine gabbro. Ti-Al and Si-Al relationships are illustrated in figs 16 and 17. The Ca-rich pyroxenes from the contact zone appear to plot as a distinct group containing more Ti and to a lesser extent Al than the pyroxenes from the olivine gabbro. The Ca-rich pyroxene from the uppermost part of the olivine gabbro however plots closer to the clinopyroxenes of the contact zone than the augites from the lower-middle parts of the olivine gabbro unit.

Pigeonite

Pigeonite occurs in a form identical to that of augite in the olivine gabbro although it was not noted in the contact zone. Exsolution in the pigeonite consists of narrow augite lamellae orientated parallel to the basal cleavage of the pigeonite itself.

(c) Ore Minerals

Several ore minerals occur in the olivine gabbro including magnetite, ilmenite, pyrite, chalcopyrite, bornite, neodigenite and covellite.

Samples collected from the lowermost part of the zone contain chalcopyrite as tiny granules less than 1 mm in diameter and irregular patches of pyrite and magnetite up to 3 mm across. For the most part these minerals

TABLE 27

Electron Microprobe Analyses of Clinopyroxene from the Olivine Gabbro

CLinopyroxene Analysis no.		(1)	(2)	(3)	(4)	(5)	(6)	(7)
SiO_2		50,55	51,35	50,78	50,77	51,67	52,77	51,16
CaO^2		18,87	18,70	19,05	18,81	19,62	19,54	18,90
MgO		15,75	16,16	15,91	15,49	16,29	16,64	15,69
TiO_2		1,19	1,05	1,26	1,25	0,67	0,72	0,93
FeO^2		11,44	11,16	11,04	10,71	8,41	8,60	10,33
Al_2O_3		2,48	1,98	2,55	2,64	2,18	2,26	2,11
SUM		100,28	100,40	100,59	99,67	98,84	100,53	99,12
Fs		19,32	18,66	18,25	18,62	14,27	14,46	17,63
En		43,35	44,40	43,67	43,45	45,96	46,38	44,15
Ca		37,33	36,94	37,59	37,93	39,78	39,15	38,23
Cations per 6 oxygens	Si	1,889 } 1,998	1,911 } 1,998	1,889 } 2,000	1,900 } 2,000	1,931 } 2,000	1,936 } 2,000	1,922 } 2,000
	Al	0,109	0,087	0,111	0,100	0,069	0,064	0,078
	Al	0,000	0,000	0,001	0,017	0,027	0,034	0,015
	Ca	0,756	0,746	0,759	0,755	0,786	0,768	0,761
	Mg	0,878 } 2,026	0,896 } 2,019	0,882 } 2,021	0,864 } 2,006	0,907 } 2,002	0,910 } 1,996	0,879
	Ti	0,034	0,030	0,035	0,035	0,019	0,020	0,026
	Fe	0,358	0,347	0,344	0,335	0,263	0,264	0,325
	O	6	6	6	6	6	6	6

Pyroxenes (1) and (2) Lower part of fine-grained lineated contact rocks.

Pyroxenes (3) and (4) Middle part of fine-grained lineated contact rocks.

Pyroxene (5) Lower part of olivine gabbro

Pyroxene (6) Lower-middle olivine gabbro

Pyroxene (7) Upper olivine gabbro

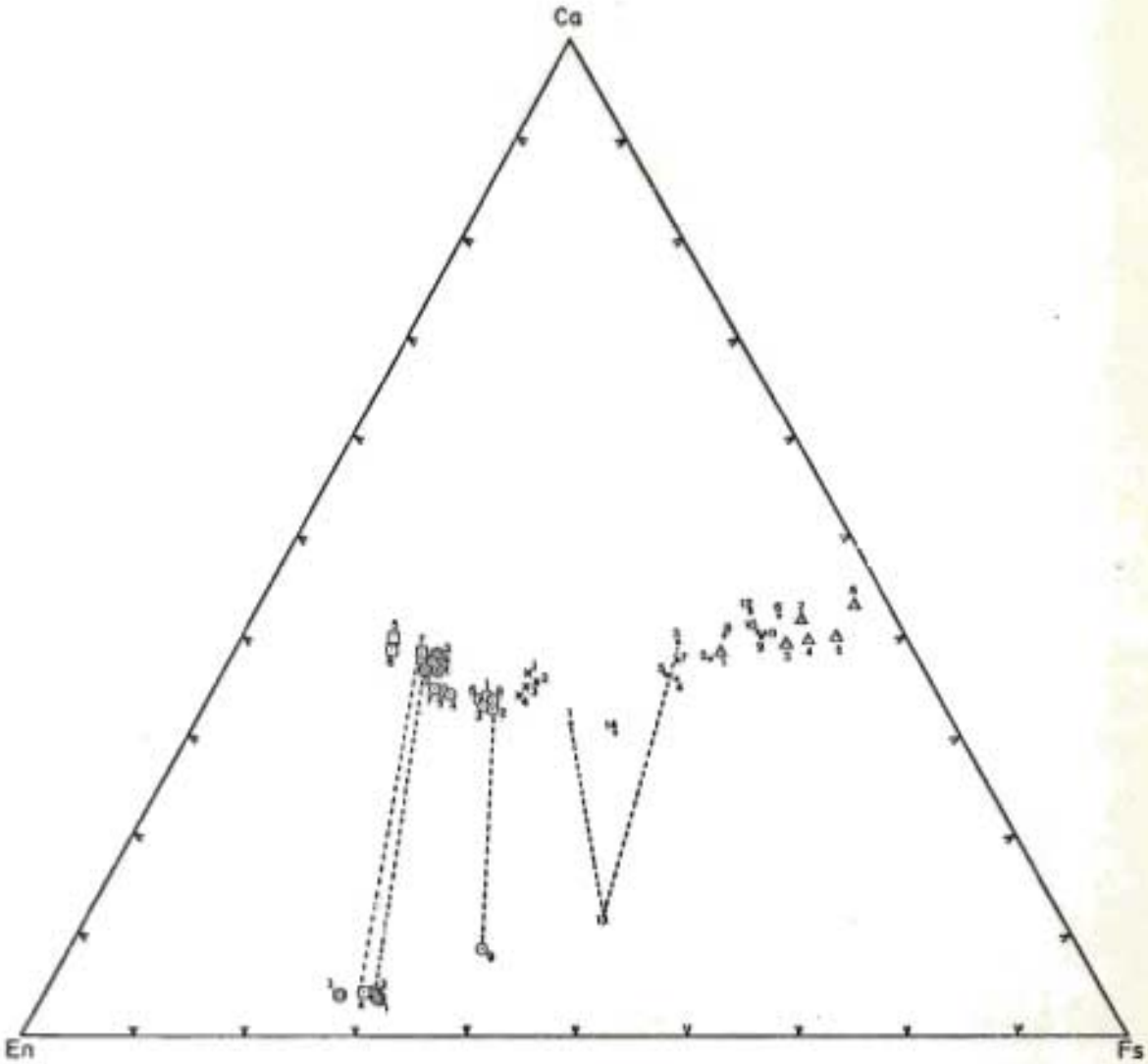

Figure 15. Analyses of pyroxenes from the Komatipoort Intrusion plotted in the pyroxene quadrilateral.

- ⊕ 1-4 Contact zone - olivine gabbro
- □ 5-7 Olivine gabbro
- ○ 1-9 Clinopyroxene-plagioclase cumulate
- • 1-14 Granophyric gabbro
- △ 1-6 Granophyre
- • 1-4 Feldspathic gabbro

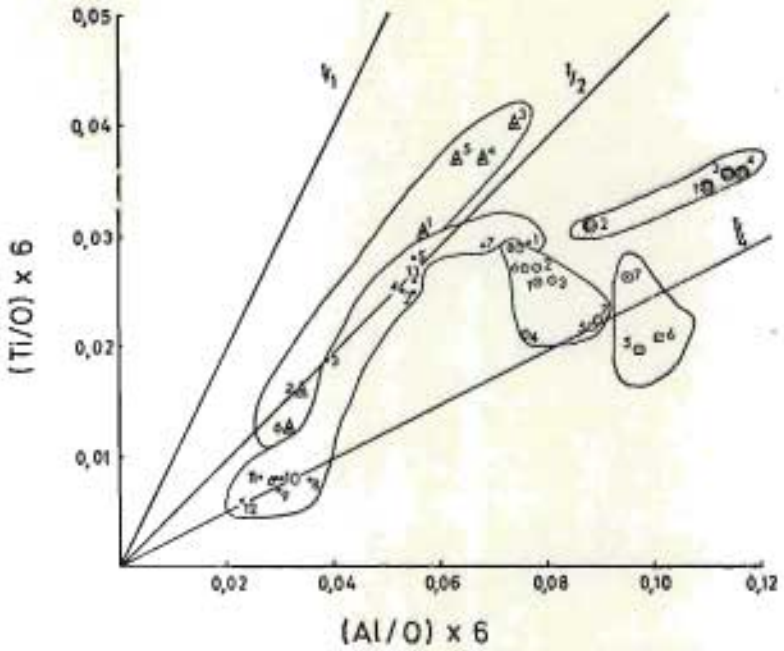

Figure 16. Ti-Al Relations for the Ca-rich Clinopyroxenes of the Komatipoort Intrusion

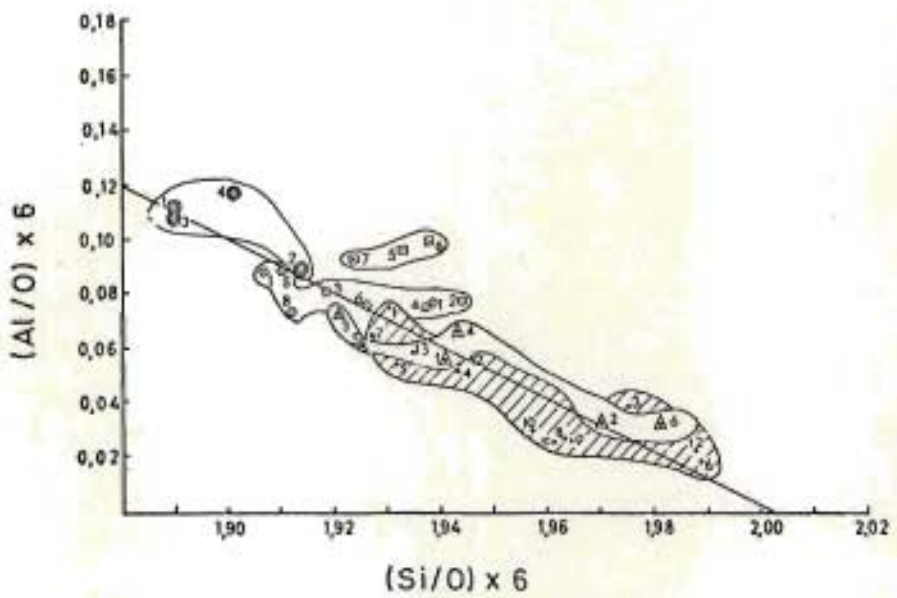

Figure 17 Si-Al Relations for the Ca-rich Clinopyroxenes of the Komatipoort Intrusion

- ▫ Olivine Gabbro
- O Olivine Gabbro
- ◦ Clinopyroxene-plagioclase cumulate
- · Granophyric Gabbro
- ▲ Granophyre

Numbering as in Tables 27, 30, 31, 32

occur interstitially although in places small amounts of chalcopyrite occur together with magnetite along alteration cracks in olivine.

Slightly higher in the zone, composite grains of bornite, digenite, covellite and chalcopyrite are present. These composite copper sulphide granules are generally of the order of 0.2 mm in diameter, but may reach 1 cm exceptionally. In addition to the copper sulphides, magnetite and pyrite are also present in minor amounts; magnetite in the form of both euhedral crystals and irregular interstitial patches, and pyrite, as irregular patches only. The magnetite is usually martitised to hematite to a variable extent and exsolution lamellae of ilmenite are occasionally present. Near the upper boundary of the unit, ilmenite makes its appearance as small, elongated, subhedral crystals.

(C) Unit 2 - The clinopyroxene-plagioclase-cumulate (Igneously Laminated Gabbro)

(i) Distribution and Lithology

Overlying unit 1,(the olivine gabbro), is the much thicker clinopyroxene-plagioclase-cumulate, a dark grey, holocrystalline, medium to fine-grained, phaneric, gabbroic rock. In plan the unit has a fairly constant east-west width of around 500 m and crops out over a north-south distance of 11,5 km (see geological map). The upper part of the unit is deeply weathered, but the lower part is apparently more resistant to weathering and fresh specimens are available from outcrops which occur at several points along the western margin of the unit. Along the northern bank of the Ngweti River, the lower part of the unit is particularly well exposed. A few specimens of the upper part of the unit are also obtainable here, since the weathering products of this rock have been found suitable for use as road ballast and a shallow quarry

has been established. Near the middle of unit 2 a weakly outcropping zone of leucocratic gabbroic rock occurs. This rock resembles the feldspathic gabbro forming unit 5, the uppermost part of the Komatipoort Intrusion, and was initially considered to be a xenolith. A finer-grained marginal phase of this weakly outcropping zone, was noted in recent excavations by Dr. A. Duncan of the University of Cape Town, (personal communication), and it thus appears possible that this rock type is a later intrusive phase.

The clinoyroxene-plagioclase-cumulate shows a fairly distinct igneous lamination which results from the preferred orientation of small platy feldspar and pyroxene crystals. In addition weak rhythmic layering, is present in a few specimens from this unit, and may be visible in the form of faint bands on the weathered surfaces of some outcrops. Prominent rhythmic layering was observed in some boulders present in the bed of the Komati River, apparently derived from the upper part of the clinopyroxene-plagioclase-cumulate unit,(see Plate 10, p 141). The layers in these boulders usually have a thickness of from 10 to 25 cm and in most, a gravity stratification (Buddington, 1936), is developed with a gradation from a lower, melanocratic, ferromagnesian-rich layer to an upper, leucocratic, plagioclase-rich layer.

Estimates of the thickness of this unit were made using the assumption that the dip of the unit as a whole corresponds to that of the igneous lamination. These estimates are complicated by the fact that the transition from the pyroxene-plagioclase-cumulate to the overlying granophyric gabbro, is not exposed. If this transitional zone, which represents an estimated vertical distance of 50 m, is included with the freely weathering intermediate zone, the thickness of the whole zone is estimated to be of the order of 250 m.

PLATE 10

1. Clinopyroxene-plagioclase cumulate, Komatipoort Intrusion, -rhythmic layering developed in a boulder of clinopyroxene-plagioclase cumulate, (diameter of coin approximately 27,5 mm).

2. Granophyric Gabbro, Komatipoort Intrusion, (Granophyric Gabbro). Typical pitted appearance of weathered outcrop of Granophyric Gabbro, cut by fine-grained vein of Granophyre.

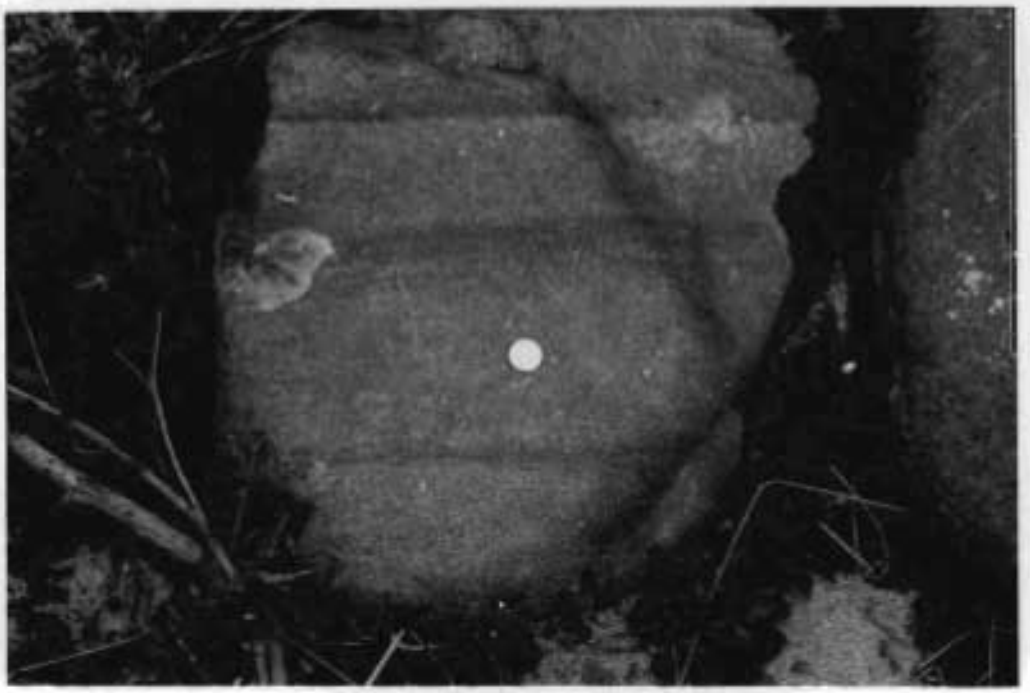

(ii) Petrography

The contact between Unit 1 and Unit 2

Samples collected from the sparse outcrops of the contact between the olivine gabbro and the clinopyroxene-plagioclase-cumulate in the Ngweti River cross-section, have a texture in many ways intermediate between that of these two rock types, and their petrography provides significant evidence of the relationship between the two units. Close to the estimated position of the contact, the rock is relatively fine grained, although a detailed examination shows a seriate variation in the grain size of the most abundant minerals present, i.e. plagioclase, augite and pigeonite. Plagioclase ranges in length from around 0,04 mm to about 4 mm, with some of the largest crystals showing complex zoning similar to that noted in the plagioclase of the olivine gabbro. Pigeonite and augite range in size from small rounded grains (diameter 0,2 mm) through prismatic crystals 2-3 mm in length, to large platey crystals around 5 mm in diameter, reminiscent of the platey augites present in the olivine gabbro. Textural relationships vary widely. Smaller plagioclase crystals, show strong normal zoning and may have as inclusions irregular embayed remnants of plagioclase crystals or less commonly small rounded grains of clinopyroxene. Conversely the clinopyroxene, frequently ophitically or sub-ophitically encloses plagioclase crystals. The extensive pyroxene plates usually enclose both large and small plagioclase crystals, but in addition contain widely scattered corroded remnants of what appear to have been former extensive plates of clinopyroxene. These pyroxene remnants are now in optical, although not in physical continuity with each other.

The prismatic clinopyroxene crystals mentioned above show strong similarities to these occurring in the main body of the clinopyroxene-plagioclase-cumulate (described later). Similarities include size, shape and the presence of a core-mantle structure. Small rounded cores of a slightly more Mg-rich clinopyroxene are often present

within these prismatic crystals. Less commonly the core is composed of pigeonite and the mantle of augite or vice versa. In addition to the cores however, randomly orientated, irregular grains of clinopyroxene may also be included in the outer mantle of the prismatic crystals.

Minor mineral constituents include olivine, quartz, ore minerals, amphibole and biotite. The olivine occurs either as small rounded to euhedral grains 0,3 to 0,5 mm in diameter or as extensive grains several millimeters in diameter. Patches of magnetite and ilmenite up to 2 mm in diameter constitute the bulk of the ore minerals, although minor pyrite, chalcopyrite and pyrrhotite do occur. The ore minerals replace plagioclase and pyroxene to some extent. Quartz, graphically intergrown with feldspar or associated with needle-like quartz paramorphs after tridymite occurs interstitially in patches of a similar size to the ore minerals. Fairly extensive reaction appears to have occurred between this interstitial material and the feldspars and pyroxenes.

Specimens further away from the olivine gabbro-igneously laminated gabbro contact are coarser grained. With a decrease in the amount of platey pyroxene, oscillatory zoned plagioclase crystals, large olivine grains, and subophitic clinopyroxenes and a corresponding increase in the quantity of prismatic to tabular pyroxene and plagioclase crystals without oscillatory zoning, these rocks grade into the typical clinopyroxene-plagioclase-cumulate.

The clinopyroxene-plagioclase-cumulate

The clinopyroxene-plagioclase-cumulate consists predominantly of tabular to prismatic plagioclase and clinopyroxene crystals with variable amounts of olivine and lesser quantities of ore minerals and interstitial material. Orthopyroxene is almost completely absent. In general, plagioclase and clinopyroxene contents show little systematic variation in the lower half of the unit, however the olivine content decreases steadily from around 5% at the base

of the unit, to zero near the middle. At this point fayalitic olivine appears abruptly in significant amounts, (around 20%), as large irregular crystals partly enclosing the other silicates. Subsequently the olivine content again decreases, and the drop in olivine content is accompanied by an antipathetic increase in the amount of interstitial micropegmatite present, (see Plate 11, fig 2).

Excluding the rhythmic units, (discussed later) overall variations in mineral proportions are as follows:-

Plagioclase varies from 55% to 65%, clinopyroxene from 22% to 30% and olivine from 0% to 20%, although in the lower half of the unit the olivine content is usually less than 5%. In the uppermost part of unit 2 interstitial micropegmatite content reaches 8%.

Igneous Lamination

In both hand specimen and thin section a feature of the clinopyroxene-plagioclase-cumulate is the development of a weak igneous lamination, produced by the preferred orientation of the tabular plagioclase and clinopyroxene crystals which characterise these rocks. The feldspars appear to be orientated with their long axes approximately parallel to the plane of the layering. To investigate this, the orientations of the normals to the albite twin lamellae, (i.e. 010 face poles), which are invariably present, were measured in two hundred plagioclase crystals in a section cut normal to the "c" fabric axis. A petrofabric diagram (fig 18, p 146), was prepared after the method of Fairbain (1942) showing the frequency of distribution of the face poles. The marked axial symmetry indicates a preferred orientation of the plagioclases with their largest face (the 010 face) parallel to the igneous lamination.

PLATE 11

1. Olivine Gabbro, Komatipoort Intrusion, (Olivine) - Dendritic olivine and abundant second generation plagioclase crystals, set in an extensive plate of intercumulus clinopyroxene. (Transmitted light, crossed nicols, X96).

2. Clinopyroxene-plagioclase cumulate, Komatipoort Intrusion, - Subhedral crystals of plagioclase and clinopyroxene (mid-grey) showing distinct igneous lamination. Interstitial ore minerals (black), are relatively abundant. (Transmitted light, crossed nicols, X96).

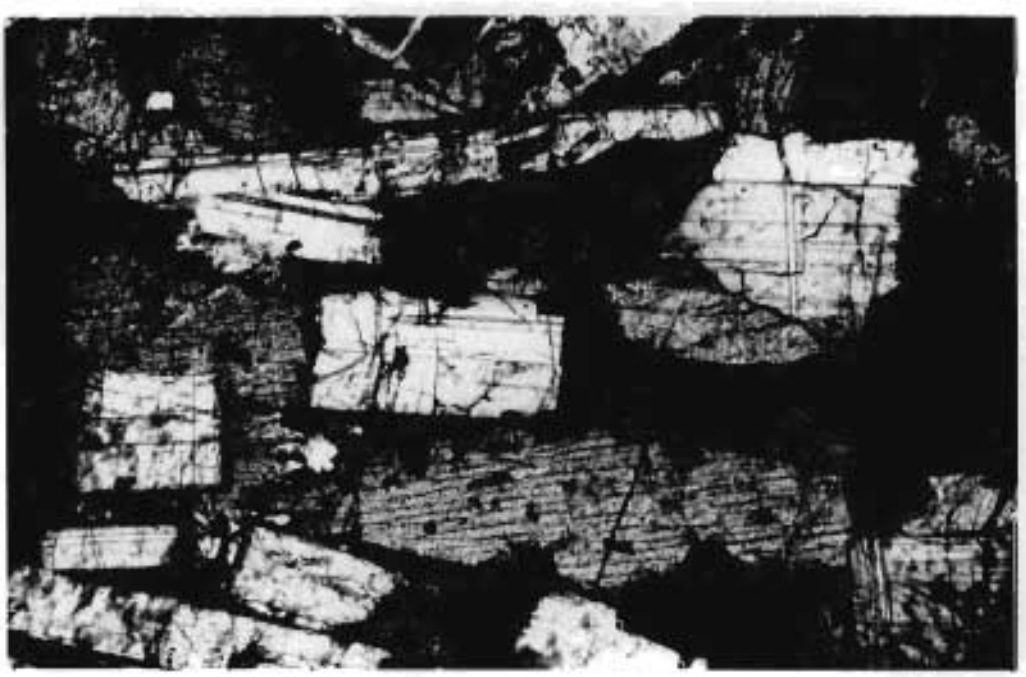

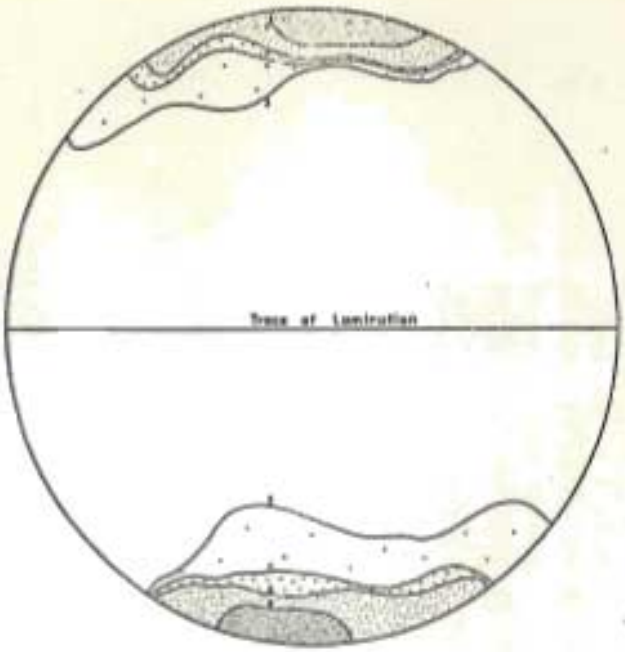

Figure 18. Petrofabric Diagram for Plagioclase in the Clinopyroxene-plagioclase Cumulate, showing the Distribution of Two Hundred (200) Face Normals in Sections cut at Right Angles to the Plane of Igneous Lamination. Distribution Contours are Shown in Percentages.

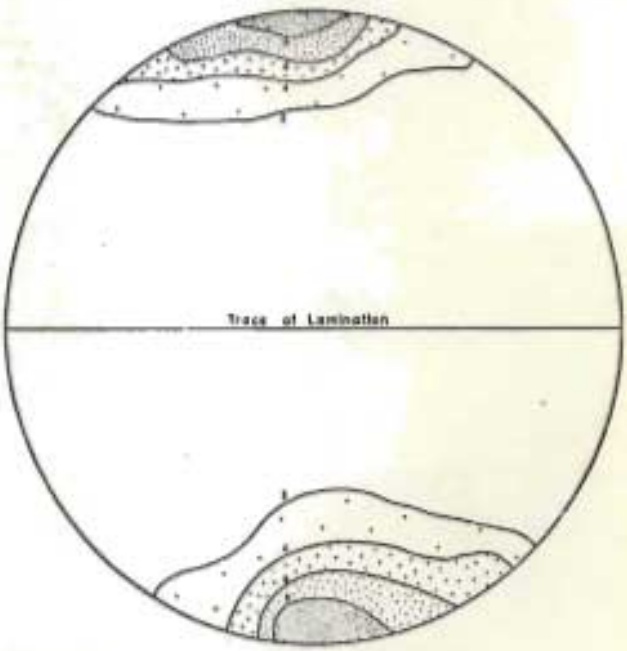

Figure 19. Petrofabric Diagram for Pyroxenes in the Clinopyroxene-plagioclase Cumulate, showing the Distribution of Two Hundred (100) Twin Plane Normals, in Sections cut at Right Angles to the Plane of Igneous Lamination. Distribution Contours are Shown in Percentages.

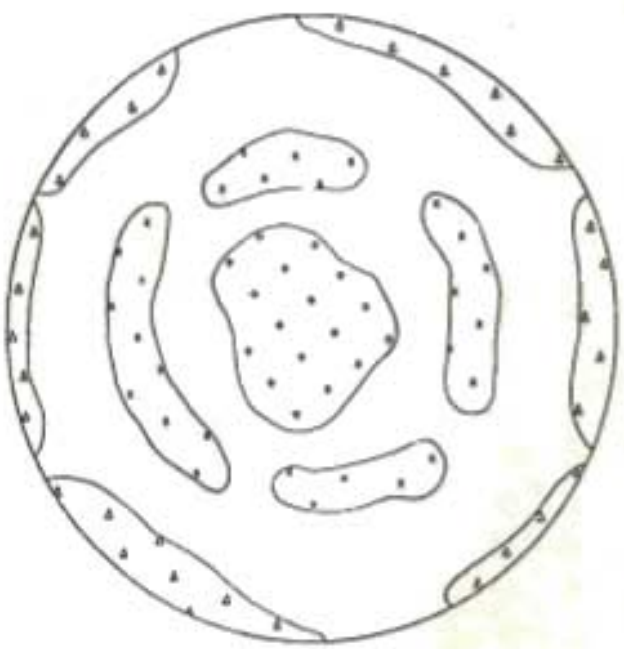

Figure 20. Stereographic Projection showing Qualitative Distribution of Two Hundred X, Y and Z Directions for Pyroxenes in Sections cut Parallel to the Plane of Igneous Lamination in the Clinopyroxene-plagioclase Cumulate.

[A] X, Y and Z directions. [B] X and Z directions. [C] Y directions.

As has been mentioned, the clinopyroxene also has a tabular form and a preferred orientation of these crystals is suggested in hand specimens. A variation of the elongation ratio of the pyroxene from almost 1,5:1 in sections cut parallel to the plane of the lamination to about 3:1 in sections cut perpendicular to the plane of the lamination, makes this preferred orientation more obvious in thin section. A petrofabric diagram was prepared for the clinopyroxene (fig 19, p 146), and this shows the distribution of 200 normals to the (100) twin plane, (100 twins are common in these pyroxenes), in several sections cut in the plane of the "c" fabric axis. Again the axial symmetry typical of a crystal cumulate is present. It was noticed that, in sections cut parallel to the plane of the igneous lamination, in spite of the preferred orientation indicated by the petrofabric diagram, occasional large crystals showed what appeared to be (100) twins. As a check on this, the distribution of X,Y and Z directions from 200 pyroxene crystals were measured in a section cut parallel to the plane of the lamination and plotted on a petrofabric diagram (see fig 20, p 146). The Y directions show two areas of concentration, first along the perimeter of the diagram and again in the centre of the diagram. The X and Z directions likewise show two areas of concentration, the one along the perimeter of the diagram and the other at around 45° from the centre of the diagram. Identical results were obtained for 200 X,Y and Z directions in a section cut normal to the plane of the lamination.

Since most of the crystals measured display large faces in sections parallel to the plane of the lamination and narrow elongated faces in sections cut normal to the lamination, it would appear that the clinopyroxene has two crystal forms; in the one type a large face is developed parallel to (100) and in the other, parallel to (010); it is on these large faces that the crystals have settled. The forms are present in about equal proportions and are composed of both augite and pigeonite.

(a) Rhythmic Layering

Rhythmic layers present in the clinopyroxene-plagioclase cumulate commonly display more or less well-developed gravity stratification resulting from a concentration of pyroxene and ore minerals in the base of each unit. This melanocratic base grades rapidly upwards into a leucocratic upper portion that, in turn, is abruptly succeeded by the pyroxene-rich base of the following unit. The rhythmic layers are not thick, ranging from around 10 cm up to about 40 cm.

Mineralogical variations in a single 20 cm thick unit, showing strong gravity stratification, were studied in some detail in a series of thin sections, some orientated parallel, and the rest perpendicular to the plane of layering. The variations in modal proportions of the major mineral constituents across this layer are shown in Table 28, p 149, and again graphically in fig 21, p 150, together with the modes of the immediately adjacent layers formed by the overlying and underlying rhythmic units. As may be seen from Table 29, there is a clear antipathetic variation between plagioclase plus interstitial micropegmatite on the one hand, and pyroxene plus ore of the other. The ratio of plagioclase to pyroxene changes from around 1:2 at the base of the unit to 6:1 at the top. No systematic variation is shown by actinolite, the only other measurable constituent of the rock. This mineral occurs as a late stage marginal alteration product of the pyroxene and its abundance therefore, is probably related both to the abundance of pyroxene in the rock and the quantity of late interstitial fluids present in the final stages of crystallisation. Although no regular variation in the proportions of this mineral would be expected, it may be noted that if the percentage of actinolite is added to the value for pyroxene, the regular upward decrease in pyroxene content is not affected.

TABLE 28

Variations in Modal Proportions and Grain-size in a Gravity-Stratified Rhythmic Unit

Position of sample	Plagioclase		Pyroxene		Interstitial micropegmatite	Opaque ore	Actinolite
	*Radius mm	Volume %	*Radius mm	Volume %	Volume %	Volume %	Volume %
Base of overlying rhythmic unit		33.7		51.2	3.1	8.6	3.4
Top 20 cm	0.77	70.8	0.32	12.5	6.7	4.0	6.0
15 cm	0.82	60.8	0.40	21.5	5.9	4.5	7.3
10 cm	0.73	52.3	0.45	31.7	4.6	5.0	6.4
5 cm	0.79	40.5	0.50	42.2	3.9	7.1	6.3
0 cm Base	0.71	29.3	0.49	53.5	1.2	10.7	5.3
Top of underlying rhythmic unit		65.5		20.2	4.0	6.3	4.0

*Grain size expressed as radius of a sphere equal in volume to average for 300 crystals at each level.

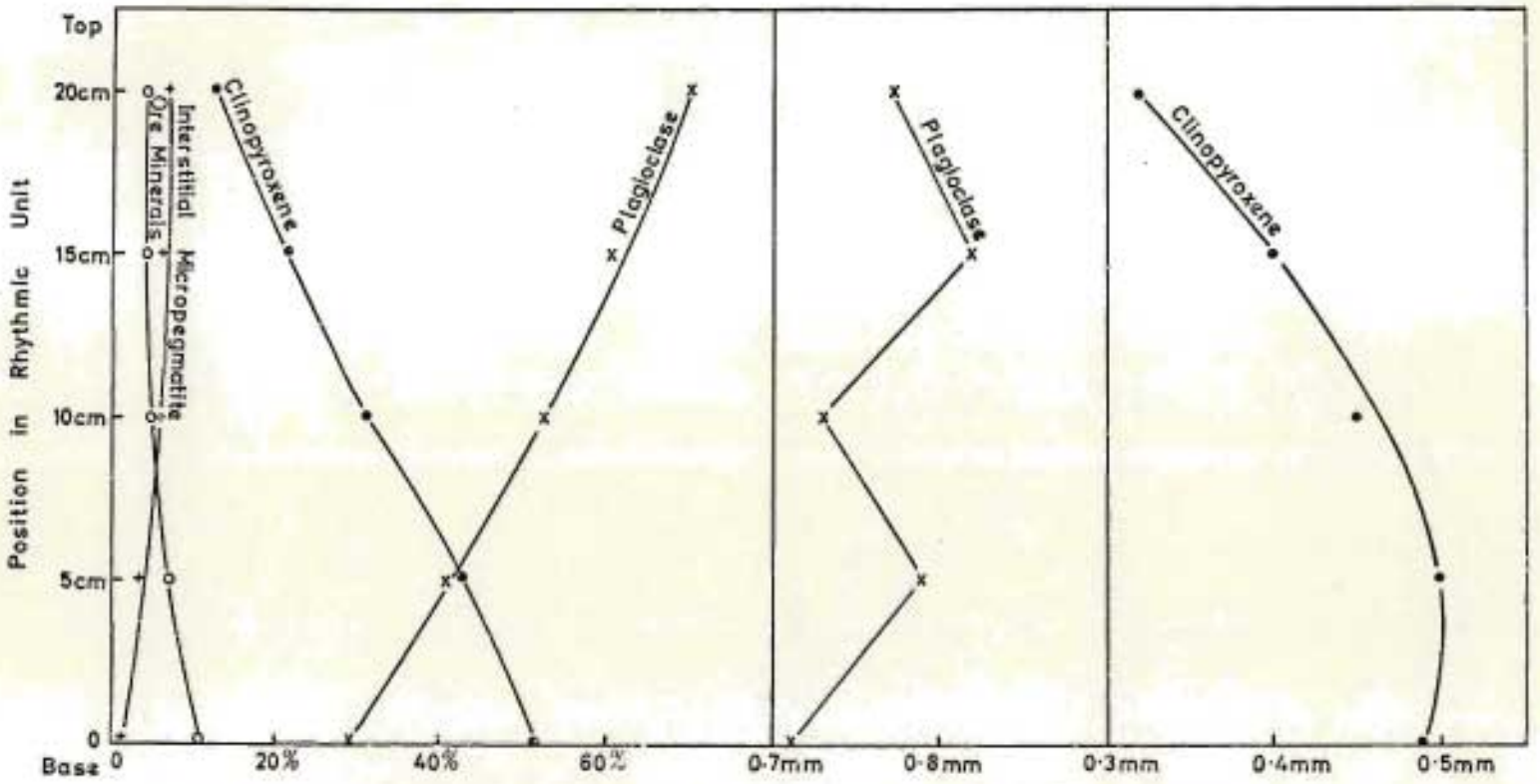

Variation in modal proportions (vol %) of major mineral phases in 20 cm. thick rhythmically layered unit.

Variation in grain size in pyroxene and plagioclase of 20 cm. thick rhythmically layered unit. (Grain size expressed as the radius of a sphere of equal volume to that of average measured crystals from each level).

Figure 21. Graphical Representation of Variation in Modal Proportions and Grain Size in a Rhythmic Unit. (Plotted from results shown in table 28 p. 149.).

In contrast to the pyroxene and plagioclase crystals of the igneously laminated rocks, those present in the rhythmically layered unit are orientated in two directions. Not only are these crystals orientated with their longest axes parallel to the plane of this rhythmic layering, but the long axes of the minerals have a preferred orientation, (particularly at the base of the unit), in one direction within the plane of the layering.

Grain size measurements were made on the plagioclase and pyroxene crystals at five different levels within the same rhythmic unit, 300 crystals at each level being measured. Measurements were made in planes perpendicular and at right angles to the plane of the layering, allowing the volume of both the average plagioclase and the average pyroxene crystal to be calculated for each selected level within the rhythmic unit. For comparative purposes these have been recalculated as radii of spheres of equal volume. Results are listed in Table 28, p 149 , and are shown graphically in fig 21, p 150.

As may be seen from these results the pyroxene shows the type of distribution that may be expected as a consequence of the settling of crystals of different sizes, with the largest crystals concentrated at the bottom of the layer, (see discussion later).

In contrast, the plagioclase in general shows a tendency to increase in size upwards through the rhythmic unit.

According to Wager (1968) some caution should be exercised before ascribing the development of rhythmic layering simply to differences in size or density between the settling crystals. Jackson (1961) has pointed out that in many cases crystals of different species at the same level in a rhythmic unit, do not have the same hydraulic equivalent, and many factors may play a part in the development of rhythmic layering. Campbell, (1978), discussed certain problems with cumulus theory and has suggested the possibility that rhythmic units could originate by a process of bottom crystallisation.

The size distribution of the plagioclase crystals was therefore examined in more detail, at least 1 000 crystals being measured at each of the selected levels within the rhythmically layered unit. In Table 29 results of the more detailed grain size analysis of the plagioclase crystals present in the rhythmic unit, are shown.

The results are here expressed in form of mean length of the plagioclase crystals at each level, as the previous measurements have shown no advantage in recalculation to the radius of sphere of equal volume.

TABLE 29

Mean length and dispersion calculated for a minimum of 500 plagioclase crystals per sample, for 5 samples taken at different levels within a rhythmically layered unit.

Sample Position	Sample no.	Mean Length (mm)	Measure of dispersion
Top	1	2,44	2,00
	2	2,21	2,54
	3	1,87	2,14
	4	1,73	1,65
Base	5	2,10	2,70

(Measure of dispersion = $\frac{(X_i - \bar{X})^2}{n} = \frac{x^2 i}{n} - (\bar{X})^2$

where $\bar{X}$ is the mean of Xi variables).

These results appear to confirm the previously described general tendency for the size of the plagioclase crystals to increase upwards

through the unit. A local maximum in size and dispersion is reached in the lowest part of the unit, but immediately above this point, mean length and the other parameter, (the measure of dispersion), drop to a minimum, and then increase upwards through the unit until just below the top. In the highest sample in the unit, mean length reaches a maximum, but dispersion decreases slightly to a value just below those of the sample occurring in the middle of the unit.

(b) Discussion

Roobol, (1972), has suggested that size grading in gravity stratified units is very rare, having been reported only from the Duke Island complex of Alaska (Irvine, 1963, 1965) and by Roobol himself from the Vesturhorn intrusion in Iceland. Roobol indicated however, that settling of crystals of different sizes from a magma layer will inevitably produce size grading in the resulting cumulate unless fairly special conditions prevail, namely, that the magma constitutes a thick layer moving by laminar flow, or a thinner layer moving by turbulent flow.

Wager and Brown (1968) have proposed that gravity stratified units are produced by crystal settling from relatively thin density currents. If this mode of origin is accepted, the pyroxene grain size distribution is in accord with the settling of a population of crystals with a range of grain sizes from a thin density current moving by laminar flow.

This proposal does not appear to be adequate to explain the plagioclase grain size distribution. Confirmation of this is provided by grain size analyses of water-laid sedimentary graded bedding produced both by a waning current and turbidity current. Deposition of sediments by a waning current tends to produce graded bedding in which grain size decreases upwards and dispersion remains relatively constant, on the other hand density currents produce graded bedding in which grain size and dispersion decrease upwards, (Pettijohn, 1957).

The plagioclase grain size data presented here (p 152) do not appear to match either of those patterns.

A mechanism for the modification of the texture of gravity stratified units has been advanced by Wager and Brown, (1968). This involves the addition of crystals to the density current from the overlying magma. An explanation could be proposed therefore, for the observed plagioclase grain-size distribution in terms of the steady addition of large plagioclase crystals only to the crystal population of the density current during formation of the gravity stratified unit. These plagioclases would have been expected to be accompanied by clinopyroxene crystals in view of the generally constant composition of the clinopyroxene-plagioclase-cumulate, and the pyroxene size distribution suggests that this has not occurred.

Adcumulus growth of the plagioclase crystals after settling may have effected the size of the crystals to some extent, but microscopic examination of the plagioclase crystals shows that the outermost zoned portion of the plagioclase crystals is not extensive enough to explain the observed size distribution. Further the presence of stagnant magma layers as suggested by Jackson (1961) does not seem likely in this case as noticeable movement of the magma is suggested by the marked orientation of the settled crystals in two planes.

An alternative explanation is that continued crystallisation of the more slowly settling plagioclase accompanied by a nucleation of new plagioclase crystals may have markedly affected grain size distribution in the following way. If the cumulate layer is assumed to have originated by crystal settling from crystal-charged magma, the major factors determining which plagioclase crystals reached the floor of the intrusion first are likely to be, settling velocity which may be equated with crystal size to a large extent (since we are dealing with plagioclase only) and the distance of any given plagioclase crystal from the floor of the intrusion when crystal settling commenced.

In the lowest part of the cumulate layer the largest, most rapidly settling plagioclases could therefore be expected to accumulate preferentially together with some small crystals which were close to the floor of the intrusion at the time settling was initiated, producing a population with large mean grain size and a large dispersion, as the range of grain sizes could approximate that of the crystal population suspended in the magma, if the crystals were randomly distributed throughout the magma. If the crystal-charged magma from which the crystals were settling out was a layer of limited thickness, and in addition, if crystal growth was either absent or slow in relation to the crystal settling, depletion of the magma in large rapidly settling crystals would eventually occur. Thus the upward decrease in the mean size of the plagioclase crystals present in the lowest part of the cumulate unit, may result simply from an impoverishment of the magma in large rapidly settling plagioclase crystals. To account for the subsequent gradual increase in the size of plagioclase crystals upwards through the cumulate layer it is suggested that, due either to the slower settling rate of the smaller plagioclase crystals still in suspension, or to an increase in the rate of crystallisation of the plagioclase as a result of perhaps a gradual decrease in the temperature of the magma, the rate of crystallisation of the plagioclase becomes significant in relation to the rate of settling of the plagioclase crystals. The increase in dispersion which accompanies the increase in grain size upwards shown in Table 30, p 152 , may be explained provided that either (a) the large plagioclase crystals grew more rapidly in size than the smaller crystals, or

(b) that plagioclase crystals were still nucleating, homogeneously or heterogeneously.

In the highest part of the unit grain size dispersion decreases and it is possible therefore that both crystal growth and nucleation continued until the final stages of formation of the cumulate was reached, resulting in the steady increase in both grain size and dispersion. In the final stages dispersion decreases, possibly due to the fact that with decrease in temperature nucleation ceased although crystal growth

continued, leading to the large grain size and smaller dispersion of the uppermost part of the cumulate layer.

Thus it is suggested that the gravity stratified layer may have originated by crystal settling of plagioclase and pyroxene (and magnetite) crystals out of a crystal-charged magma layer of limited thickness, possibly a magmatic density current. Conditions in this magma layer were such that grain size distribution of pyroxene crystals were influenced predominantly by settling rates. Plagioclase grain size distribution may on the other hand be explained, if both nucleation of new plagioclase crystals and growth of existing plagioclase crystals occurred during the formation of the gravity-stratified cumulate layer.

(iii) Mineralogy

(a) Plagioclase

The plagioclase present in the clinopyroxene-plagioclase cumulate is invariably approximately tabular in form and commonly displays a core-mantle-rim structure. In many of the crystals the core and the inner edge of the rim are of a similar intermediate composition (An_{55}), while the mantle is on average of a slightly more basic composition (An_{60}), i.e. it is a reversed zone. The cores show irregular corroded outlines, and they are unzoned. When considered by themselves it may be seen that both the mantles and the rims display normal zoning. Some of the crystals have a mantle that is not a reversed zone and the An content of the plagioclase then drops steadily from the core through the mantle and the rim to the outer margin of the crystal. In the upper third of the clinopyroxene-plagioclase cumulate, crystals showing oscillatory-zoned mantles make their appearance.

Near the base of the unit small plagioclase crystals may be included within the larger plagioclases and higher in the unit minute clinopyroxene crystals are also enclosed by the plagioclase. Towards the top of the unit these included crystals are less common. The large first

generation phenocrysts displaying several sequences of oscillatory zoning, which were noted in both the olivine gabbro and the contact zone of the clinopyroxene-plagioclase cumulate are rare, although similar crystals were occasionally observed near the lower contact of the unit.

The plagioclase crystals have in places suffered mild deformation, evidenced by the development of some cracks, less commonly more severely deformed crystals were noted.

(b) Pyroxene

Augite and pigeonite, the pyroxene commonly present in the clinopyroxene-plagioclase cumulate, occur as small tabular crystals in the lower part of the unit. These tabular crystals are not always homogeneous, and often consist of cores of the one pyroxene surrounded by mantles of the other. Particularly in the lower and middle parts of the zone, crystals composed of cores of augite with pigeonite mantles, and the reverse relationship, are present in the same specimen. In addition, augite crystals mantled by augite with a slightly different crystallographic orientation and pigeonite crystals (with a similar structure), composed of two pigeonite phases were also noted in these rocks.

More rarely the pigeonite is partly inverted to orthopyroxene. Occasional bent crystals were noted although other deformational effects were limited to a little irregular cracking in some crystals. In the upper parts of the unit, the pyroxene shows alteration along crystal margins to a fibrous, strongly pleochroic (green to yellow) hornblende or to deep yellowish brown iddingsite. In places in the upper part of the unit interstitial micropegmatite has reacted with the pyroxene reducing it to a few embayed remnants, frequently darkened to a brownish colour at the edges and bordered by a few granules of iron ore.

TABLE 30

Results of Electron Microprobe analysis of 8 Ca-rich pyroxenes and one Ca-poor pyroxene from the Clinopyroxene-Plagioclase Cumulate, Komatipoort Intrusion.

Clinopyroxene Analysis No.	D 44 (1) 1	D 45 (2)* 2	D 46 (1) 3	D 46 (2) 4	D 47 (1) 5	D 47 (2) 6	D 47 (3) 7	D 47 (4) 8	D 45 (1)* 9
SiO_2	51,01	51,09	51,19	52,25	51,54	51,16	51,16	50,72	52,02
CaO	16,61	15,91	16,80	17,20	18,30	16,70	17,69	16,93	4,46
MgO	14,17	14,08	14,83	15,75	16,14	14,85	16,34	14,73	19,33
TiO_2	0,87	0,95	0,91	0,75	0,79	0,94	0,77	0,97	0,60
FeO	15,10	15,52	15,63	13,40	12,46	15,08	12,65	15,82	23,56
Al_2O_3	1,73	1,72	1,84	1,73	2,03	1,70	2,02	1,67	1,03
Sum	99,49	99,27	101,20	101.08	101,26	100,43	100,63	100,84	101,00

* Analyses 2 & 9 represent coexisting pyroxenes

Cations per six O

Si	1,938	2,000	1,944	2,000	1,918	1,991	1,937	2,000	1,910	1,999	1,926	2,000	1,907	1,996	1,912	1,986	1,950	1,996
Al	0,062		0,056		0,081		0,063		0,089		0,074		0,089		0,076		0,046	
Al	0,015		0,022		0,000		0,013		0,000		0,002		0,000		0,000		0,000	
Ca	0,676		0,649		0,674		0,684		0,727		0,674		0,707		0,684		0,179	
Mg	0,803	1,999	0,799	1,991	0,828	2,018	0,871	2,005	0,891	2,026	0,832	2,010	0,908	2,032	0,828	2,039	0,080	2,015
Ti	0,025		0,027		0,026		0,021		0,022		0,027		0,022		0,028		0,017	
Fe	0,480		0,494		0,490		0,416		0,386		0,475		0,395		0,499		0,739	
O	6		6		6		6		6		6		6		6		6	
Fs	25,45		26,47		25,54		21,93		20,14		24,97		20,49		25,83		37,52	
En	40,46		40,57		41,04		43,74		44,00		41,49		44,72		40,62		53,60	
Ca	34,09		32,95		33,42		34,33		35,86		33,54		34,00		33,56		8,88	

Analysis 1 Augite mantle - lower part of the clinopyroxene-plagioclase cumulate.
Analysis 2 Augite mantle - lower part of the clinopyroxene-plagioclase cumulate.
Analysis 3 Augite mantle - middle part of the clinopyroxene-plagioclase cumulate.
Analysis 4 Augite core - middle part of the clinopyroxene-plagioclase cumulate.
Analysis 5 Augite core - upper-middle part of the clinopyroxene-plagioclase cumulate.
Analysis 6 Augite mantle - upper-middle part of the clinopyroxene-plagioclase cumulate.
Analysis 7 Augite core - upper-middle part of the clinopyroxene-plagioclase cumulate.
Analysis 8 Augite mantle - upper-middle part of the clinopyroxene-plagioclase cumulate.
Analysis 9 Pigeonite - lower part of the clinopyroxene-plagioclase cumulate - coexists with augite of Analysis 2.

Electron microprobe analyses of eight Ca-rich pyroxenes from various levels in the unit, together with a single pigeonite analysis are shown in Table 30. These compositions have been plotted in the pyroxene quadrilateral in fig 15. It is apparent that inter-grain compositional variation is of the same order as inter-grain variation and that the composition of the Ca-rich pyroxene does not appear to change vertically through the unit. Noticeable compositional differences are present between the cores and the margins of the Ca-rich pyroxene crystals, the cores being distinctly more En rich than the mantles of these crystals. Al - Ti and Al - Si relations are shown in figs16,17. In general it may be said that the mantle augite is enriched in Ti and Si and depleted in Al relative the augite forming the cores. Core augite represented by analysis 4 however, has a relatively high Si content and correspondingly low Al content compared with the other two core-augite analysis. The Ti content of this core augite is however of the same order as the other core augites, (see Table 30).

(c) Olivine

In the western contact rocks of unit 2, olivine occurs both as small rounded grains and as occasional large irregular crystals with included plagioclases. X-ray determinations, (see Appendix), show the large olivines have a composition of around Fo_{60}, and these are interpreted as xenocrysts from the olivine gabbro. Electron microprobe analyses indicate the small olivines, in contrast, are fayalitic in composition,(see Table 25, p128). Over much of unit 2 olivine is absent, but where it reappears in the upper part of the unit, as extensive crystals partially enclosing plagioclase and pyroxene, it is more fayalitic than the rounded grains in the contact rocks, (see Table 25, p 128).

(d) Ore Minerals

Magnetite and ilmenite are the most abundant ore minerals present in the clinopyroxene-plagioclase cumulate, although minor amounts of pyrite, chalcopyrite, pyrrhotite and pentlandite were also noted. Both magnetite and ilmenite occur as irregular interstitial grains up to 2 mm in length, although magnetite,in the upper part of the unit also occurs as euhedral grains.

(D) Unit 3 - The Granophyric Gabbro

(i) Distribution and Lithology

The only location at which good exposures of the granophyric gabbro are available is in the Komati River bed, where in the last westward looping meander before the junction with the Crocodile River, the Komati River twice cuts across the Komatipoort Intrusion, (see geological map). In the most northerly of the two river sections the exposures are better, but they are for the most part accessible only during the dry winter months when the river is flowing at its lowest level. Most of the specimens on which the description of this zone is based, were, therefore, collected from these sections.

The exact position of the contact between the granophyric gabbro and the clinopyroxene-plagioclase-cumulate is not certain because, as mentioned in the previous section, a gap equivalent to a vertical distance of 50 m separates the last outcrop of the clinopyroxene-plagioclase-cumulate from the lowermost exposures of the granophyric gabbro. The boundary between units 2 and 3 shown on the geological map, is defined in the field by the most easterly exposures of the rocks of unit 3, in a strongly outcropping band of granophyric gabbro.

When fresh, the Granophyric Gabbro is a medium to coarse grained rock, often lighter coloured than the rocks of unit 1 and unit 2, a property which is to some degree obscured by the fact that the colour of these rocks deepens on weathering. They appear phaneric in hand specimen, but the presence of abundant, aphanitic, interstitial material between aggregates of large crystals of feldspar and pyroxene give polished hand specimens of some specimens of these rocks a glomeroporphyritic appearance. Preferential weathering of the crystal aggregates gives outcrops a pitted appearance, (see Plate 10, p 141).

As the contact between the granophyric gabbro and the granophyre is approached the grain size of the granophyric gabbro decreases rapidly over a horizontal distance of about 15 m, and at the contact, the granophyric gabbro is dark, fine grained, and speckled with small patches of pink micropegmatite. It is extremely tough and compact, and is further distinguished by the presence of irregular patches of pyrite up to 2 cm in diameter. Large xenolithic blocks of feldspathic gabbro (5 to 6 m across) are also present in the granophyric gabbro within a few meters of the contact. In these, pyrite occurs concentrated along cracks, apparently having been introduced by veins of granophyric material which cross-cut the xenoliths.

Assuming a dip of 25° for this unit, (to correspond with that suggested for unit 2), these rocks probably reach a thickness of the order of 225 m in the Komati River Section. Elsewhere the thickness seems variable, although difficult to estimate.

(ii) Petrography

A sharp contrast in both texture and composition exists between the rocks of unit 3 and the igneously laminated rocks of unit 2. The change is due to an increase in the average size of the plagioclase crystals and in the amount of interstitial micropegmatite present, (about 25% at the base of the unit). This produces a more coarsely textured rock with an almost porphyritic appearance in places, but without trace of rhythmic layering or igneous lamination.

The principle constituents of the rock are plagioclase, clinopyroxene, (augite and pigeonite), and micropegmatite. Modal proportions of the major minerals fluctuate widely on a local scale, but in addition there appears to be an enrichment in interstitial micropegmatite upwards through the unit. The range of variations of the modal proportions on the scale of a thin section are as follows. Plagioclase content varies from 30% to 45%, pyroxene concentration ranges from 8% to 18% and the micropegmatite content, varying inversely with the

plagioclase and pyroxene content varies from 56% to 25%.

Other constituents include iron ore (up to 5%), slender needles of apatite that occur in minor amounts but are distinctly more abundant than in the underlying rock, and rarely, minute, interstitial, euhedral zircons. Altered mafics always constitute a considerable proportion of the rock, ranging from 3 % to 10%, (see Plate 12, p 163).

The upper 30 meters of the zone is deeply weathered, but thin sections of the few available specimens indicate that it is distinguished by the appearance of small euhedral to subhedral crystals of a brown pleochroic hornblende in minor amounts.

Although in hand specimen this rock type shows a fairly uniform appearance, on the scale of a thin section the texture varies, and may best be described as poikilophitic. Locally it is ophitic to sub-ophitic with large pale brown clinopyroxene plates partly enclosing plagioclase laths up to 15 mm in length. Less commonly the pyroxene forms smaller granules and the texture becomes sub-ophitic to interstitial although neither of these textures persists over more than a few cm, as large amounts of irregularly distributed, fine-grained micropegmatite containing large grains of free quartz in places occur in the rock. These textures are, however, well developed in places where a minimum of the micropegmatitic material is present, and the rock in thin section then resembles normal gabbro containing 5% to 10% interstitial micropegmatite.

Where the micropegmatite content of the rock increases, its texture is porphyritic to glomeroporphyritic, and here the plagioclases, usually bordered by ragged remnants of brown to greenish pyroxene crystals, or forming small aggregates sub-ophitically enclosed by associated pyroxenes, occur in a matrix of micropegmatite. The plagioclases are often clouded and may be partly replaced by the alkali-feldspar of the micropegmatite matrix. Pyroxenes of these

PLATE 12

1. Granophyric Gabbro, Komatipoort Intrusion. Elongated plagioclase lath and corroded clinopyroxene crystals (dark grey) in matrix of micropegmatite and ore minerals, (black). (Transmitted light, crossed nicols, X96)

2. Granophyre, Komatipoort Intrusion, dark, partly corroded plagioclase crystals set in a matrix of coarse-grained micropegmatite. (Transmitted light, crossed nicols, X96).

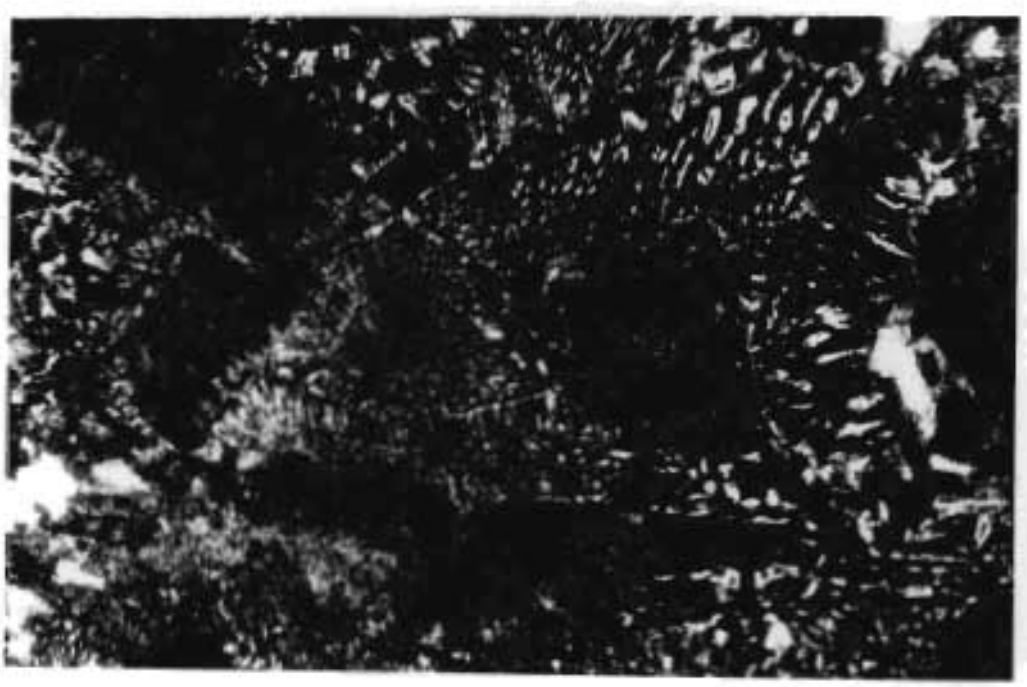

clusters that project into the micropegmatite show highly irregular, corroded boundaries. The micropegmatite patches, however, do not form regular lenses or schlieren as described from some differentiated tholeiite sheets.

A distinctive feature of the pyroxenes of unit 3, is that they are sometimes bent, as evidenced by the (110) cleavage traces, (see section on mineralogy).

(iii) Mineralogy

(a) Plagioclase

The plagioclase consists of lath-shaped crystals showing irregular outlines and varying in length from 2 mm to 15 mm. These plagioclase laths occasionally enclose small patches of pyroxene, but the reverse relationship is equally common. Where plagioclase is in contact with micropegmatite euhedral faces may occasionally be developed, but more frequently crystal margins are irregular and suggest reaction has taken place. Occasionally, small tongues of micropegmatite projecting into the plagioclase were noted and the margins of the crystals frequently show a brownish-pink clouding. Strong normal zoning from core ($\pm An_{60}$) to margin ($\pm An_{48}$) is common, although individuals displaying oscillatory zoned cores with normally zoned mantles are also present in this unit. A proportion of the plagioclase crystals show deformational effects such as cracking and more exceptionally bending. There is some suggestion that these deformed crystals increase in abundance towards the upper contact of the granophyric gabbro with the granophyre.

(b) Pyroxene

The pyroxene present in the granophyric gabbro has two distinct modes of occurrence.

(1) Pale brown crystals (up to 10 mm in diameter) occur associated with the plagioclase crystals in aggregates several cms across. Textures range from ophitic to intergranular and the pyroxene shows no sign resorbtion or alteration. The bulk of this pyroxene is a Ca-rich variety, however, pigeonite may form the cores to some of these crystals. Exceptionally more complex crystals showing four zones of alternating pigeonite and Ca-rich pyroxene were noted.

(2) In micropegmatite rich parts of the rock the Ca-rich pyroxene forms irregular grains several millimeters long and small corroded fragments scattered through the micropegmatite. In places it occurs graphically or dendritically intergrown with the margins of plagioclase crystals. Less commonly the pyroxene occurs in fan-shaped groups with a single augite crystal splitting into several curved radiating sub-units. These Ca-rich pyroxenes show strong compositional zoning from brown cores to green Fe-rich margins. The margins of these crystals are invariably irregular and may be rimmed by a variety of minerals including biotite, hornblende, "iddingsite" and opaque iron ore.

Occasionally rounded pale brown grains of pigeonite mantled by greenish brown Ca-rich pyroxene occur set in matrix of micropegmatite.

Electron microprobe analyses of 13 Ca-rich clinopyroxenes and one Ca-poor clinopyroxene are listed in Table 31 . The Ca-rich clinopyroxenes may, in general, be termed ferro-augite as their compositions range from approximately En_{34} to En_{10}. The most magnesian of these ferro-augites (analyses 1 and 13, Table 31) form part of 'gabbroic' textured clusters of plagioclase and pyroxene crystals, a few cms across, which contain little of the interstitial granophyric material so abundant in this unit. The composition of these two pyroxenes plots relatively close to the compositions of pyroxenes from the clinopyroxene-plagioclase cumulate in the pyroxene

INDEX TO TABLE 31

Sample 1-	1.	Core of large pale brown Ca-rich pyroxene crystal from 'gabbroic' textured plagioclase-pyroxene aggregate - (lower granophyric gabbro).
	2.	Core of large brown Ca-rich pyroxene crystal associated with interstitial micropegmatite - (same sample as analysis 1).
Sample 2-	3.	Brown Ca-rich pyroxene mantling pigeonite set in micropegmatite matrix - (lower granophyric gabbro) - the pigeonite composition is listed under analysis 13.
Sample 3-	4.	Brown Ca-rich pyroxene set in micropegamatite matrix -(middle granophyric gabbro).
	5.	Brown Ca-rich pyroxene set in micropegmatite matrix - (same sample as analysis 4).
	6.	Green Ca-rich pyroxene rimming brown pyroxene - set in micropegmatite matrix (same samples as 4 and 5).
Sample 4-	7.	Brown Ca-rich pyroxene - set in micropegmatite matrix - (upper part of granophyric gabbro).
	8.	Green Ca-rich pyroxene - set in micropegmatite matrix - (same sample as analysis 7).
	9.	Green Ca-rich pyroxene - set in micropegmatite matrix - (same sample as analyses 7 and 8).
	10.	Green Ca-rich pyroxene - set in micropegmatite matrix - (same sample as analyses 7 - 9).
	11.	Green Ca-rich pyroxene - set in micropegmatite matrix - (same sample as analyses 7 - 10).
	12.	Green Ca-rich pyroxene - set in micropegmatite matrix - (same sample as analyses 7 - 11).
Sample 4-	13.	Core of large brown Ca-rich pyroxene crystal from 'gabbroic' textured plagioclase-pyroxene aggregate (upper granophyric gabbro).
Sample 2-	14.	Pale brown Ca-poor pyroxene (pigeonite) - mantled by ferro-augite (composition of ferro-augite mantle listed under analysis 3).

TABLE 31

Results of the electron microprobe analyses of 14 pyroxenes from the granophyric gabbro, Komatipoort Intrusion.

Pyroxene Analysis No:	1	2	3	4	5	6	7
SiO_2	50,24	49,00	48,83	50,22	49,85	49,74	49,43
CaO	15,28	17,07	17,90	17,38	18,08	19,45	18,24
MgO	11,96	6,23	6,79	7,77	7,54	3,45	7,46
TiO_2	1,01	0,85	0,63	0,86	0,94	0,25	0,98
FeO	20,38	26,60	22,71	25,26	25,15	27,68	24,47
Al_2O_3	1,68	1,19	0,82	1,16	1,21	0,64	1,39
Sum	100,55	100,94	97,68	102,66	102,78	101,14	101,97
Fs	34,24	45,35	39,92	41,89	40,54	47,29	40,88
En	34,28	18,40	20,75	22,29	23,38	10,45	21,44
Ca	31,48	36,25	39,33	35,82	36,08	42,21	37,68
Cations per 6 oxygens:							
Si	1,930) 2,000	1,945) 2,000	1,925) 2,000	1,943) 1,995	1,931) 1,986	1,989) 2,000	1,927) 1,991
Al	0,070	0,055	0,025	0,053	0,055	0,011	0,064
Al	0,006)	0,000)	0,014)	0,000)	0,000)	0,019)	0,000)
Ca	0,629)	0,726)	0,776)	0,720)	0,750)	0,833)	0,762)
Mg	0,685)2,004	0,369)2,003	0,409)1,986	0,448)2,010	0,486)2,079	0,206)1,990	0,434)2,023
Ti	0,029)	0,025)	0,019)	0,025)	0,028)	0,008)	0,029)
Fe	0,655	0,883	0,768	0,817	0,815	0,924	0,798

TABLE 31 (continued)

Results of the electron microprobe analyses of 14 pyroxenes from the granophyric gabbro, Komatipoort Intrusion.

Pyroxene Analysis no:	8	9	10	11	12	13	14
SiO_2	48,59	49,35	48,21	49,00	49,19	48,87	50,40
CaO	18,73	19,26	19,09	19,14	19,30	5,83	15,10
MgO	5,40	4,45	4,39	4,33	4,26	13,92	10,73
TiO_2	0,27	0,24	0,26	0,26	0,19	0,46	0,91
FeO	26,01	28,14	27,51	28,23	26,19	28,07	23,55
Al_2O_3	0,59	0,52	0,62	0,55	0,49	0,49	1,28
Sum	99,59	101,98	100,08	101,51	99,62	97,64	101,97
Fs	43,85	46,51	46,22	46,89	44,92	46,88	38,78
En	16,07	13,01	13,03	12,71	12,94	40,83	30,43
Ca	40,08	40,48	40,74	40,40	42,14	12,29	30,79
Cations per 6 oxygens:							
Si	1,963) 1,991	1,964) 1,981	1,956) 1,986	1,961) 1,987	1,988) 2,000	1,958) 1,981	1,935) 1,993
Al	0,028	0,025	0,030	0,026	0,012	0,023	0,058
Al	0,000)	0,000)	0,000)	0,000)	0,011)	0,000)	0,000)
Ca	0,811)	0,821)	0,830)	0,821)	0,836)	0,250)	0,621)
Mg	0,325)2,023	0,264)2,029	0,266)2,037	0,258)2,032	0,257)1,995	0,831)1,986	0,614)2,017
Ti	0,008)	0,007)	0,008)	0,008)	0,006)	0,014)	0,026)
Fe	0,879	0,937	0,933	0,945	0,885	0,941	0,756

quadrilateral, (see fig 15). This is in contrast to the rest of the ferro-augite analyses which plot in a group near the Fs-Ca margin of the ferro-augite field, and are noticeably richer in Ca.

Ferro-augites occurring in association with interstitial micropegmatite also appear to be richer in Fe than those present in adjacent 'gabbroic' textured patches of granophyric gabbro. This results in large compositional differences between pyroxenes in the same sample and even the same section, (compare analyses 1 and 2, Table 31). In addition, the compositions of the ferro-augites associated with the micropegmatite commonly show a relatively large compositional range from brown-coloured cores to green margins, (compare analyses 5 and 6, Table 31).

Ti-Al and Al-Si relationships of the Ca-rich pyroxenes are shown in figs 16 and 17 . Again the pyroxene represented by analysis 1 plots adjacent to the pyroxenes of the clinopyroxene-plagioclase cumulate. The rest of the ferro-augites show a range of values with Ti and Al decreasing with increasing Si, over a wide range of Si values.

The Ca-poor pyroxene analysis has a relatively high Ca content. This may reflect the presence of undetected exsolved Ca-rich pyroxene lamellae. The calculation of Mg:Fe distribution coefficients suggests that the pigeonite is likely to be in equilibrium with the Ca-rich pyroxene represented by analysis 1 rather than that of analysis 3, the ferro-augite mantling the pigeonite. Values obtained were as follows:

Pyroxenes 3 and 13	$K_{D(Mg:Fe)}$	=	1,675
Pyroxenes 1 and 13	$K_{D(Mg:Fe)}$	=	0,87

Kretz (1963) has shown that for igneous pyroxenes this value lies between 0,65 and 0,86.

I Deformation of the Pyroxene

(i) Bending

Curved crystals of two distinct origins are present in the Granophyric Gabbro; one due to curvature developed during growth of the crystal, the other to mechanical deformation as a result of stress. The first type occurs as single, continuously curved units showing no sign of strain, and is usually found in the granophyric micropegmatite-rich patches present in the gabbro. The other variety, (often present in 'gabbroic' textured patches), although showing continuous (110) cleavage traces passing through the entire crystal, usually displays other deformation and recovery structures, as described below. The reasons for considering these bent crystals to be a deformational rather than a growth feature may be summarised as follows:

1 The bent crystals frequently show other deformational effects such as undulose extinction and cracking.

2 The pyroxene crystals show other deformational effect, such as undulose extinction, cracking or what is probably twin gliding.

3 Many of the bent crystals are composed of several sub-units and both the size and abundance of these sub-units varies with the degree of curvature of the individual crystal. In tightly bent crystals with small radius of bending, the size of the crystal sub-units often decreases towards the inside of the curve, this latter point corresponding to the area of greatest compression. The sub-units are considered to be the result of the stress-release mechanism, polygonization.

Although no previous detailed accounts of the field occurrence of bending in pyroxenes could be located, several laboratory studies have produced deformed pyroxene.

Experiments on the deformation of diopside were conducted by Muggë as long ago as 1898 and by Adams in 1910, both of whom reported the development of (001) twins during their experiments. More recently, Griggs, Turner and Heard (1960) found that at 500°C and at 5 kb diopside shows two methods of gliding.

(i) Translation with T = (100) and t = [001]

(ii) Twinning with T = (001) and t = [100]

Where T = glide or twin plane, and t = glide or twin direction.

In these experiments many large grains of diopside were conspicuously bent, with bending developed either continuously across the full width of the grain or sharply localised on either margin of kink bands.

More recently, Bidyut (1967), has confirmed these results, producing bent diopside crystals in laboratory experiments he conducted on the effects of stress on pyroxene-bearing silicate rocks at a hydrostatic pressure of 5 kb and temperatures ranging from 25° to 800° C. He used both dunite and pyroxenite and in the pyroxenite the diopside deformed by bending. The plastic deformation was associated with the development of glide twins on (001) parallel to [100] in the negative sense, and translation gliding on (100) along [001] as recorded by Griggs, Turner and Heard (1960).

The bent pyroxenes in the granophyric gabbro (and some of the other rocks in the Komatipoort area, described elsewhere in this work) differ from the experimentally deformed pyroxenes in the presence of block formation or polygonisation. These sub-units are not the result of cataclastic deformation, since the boundaries are seldom marked by cracks and are usually regular planes corresponding closely to (001).

Further, not only does the size of the sub-units vary with the degree of curvature of crystals, as may be seen by comparing figs. 22 , 23 , and 24 , (p 173), but the size of the sub-units decreases and their numbers increase towards the inside of the curve, where deformation is at its greatest. Since experimental work failed to produce the sub-units described here, these crystals are considered to have existed initially as single large bent crystals, which subsequent to their bending, have suffered sub-division into smaller units by the process of polygonisation (block formation) commonly observed in metals.

Polygonisation, according to Turner and Verhoogen (1960) is " ... a process wherby a single strained grain becomes divided into several, homogeneous, strain-free sub-grains of slightly different orientation. This is believed to involve migration of dislocations (developed during bending) from an initial random distribution in the strained grain into planar arrays at the sub-grain boundaries. These are approximately normal to the previously active glide planes of the crystal laths."

Polygonisation has been observed in several minerals e.g. it has been described previously by Grigor'ev (1965), in both galena and kyanite. In the latter, the sub-units are usually wedge-shaped, displaying regular boundaries, the blocks having an angular relationship to each other which may be expressed as:

$$r = 2 \text{ arc } \sin \frac{b}{2h}$$

where h = distance between dislocations and
r = angle between the blocks.

Where severe deformation has occurred, Grigor'ev reports this relationship does not hold, and a granular aggregate results. Severely bent pyroxenes are illustrated in Plate 13, p 174 and fig 24, p 173.

In fig 24 , the cleavage traces still form a fairly smooth

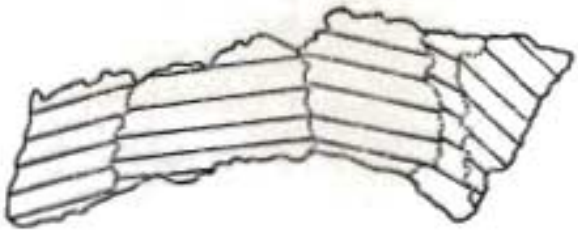

Figure 22 Mildly deformed pyroxene crystal . Relatively few sub-units are developed.

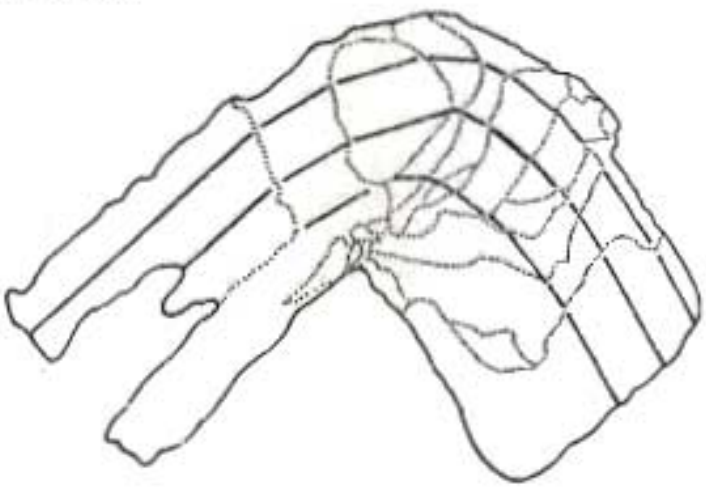

Figure 23 Moderately deformed pyroxene crystal

Figure 24 Strongly deformed pyroxene crystal. Over 60 sub-units are defined by dotted lines.

PLATE 13

1. Granophyric Gabbro, Komatipoort Intrusion, (Granophyric Gabbro) - bent clinopyroxene crystal. (Transmitted light, X200).

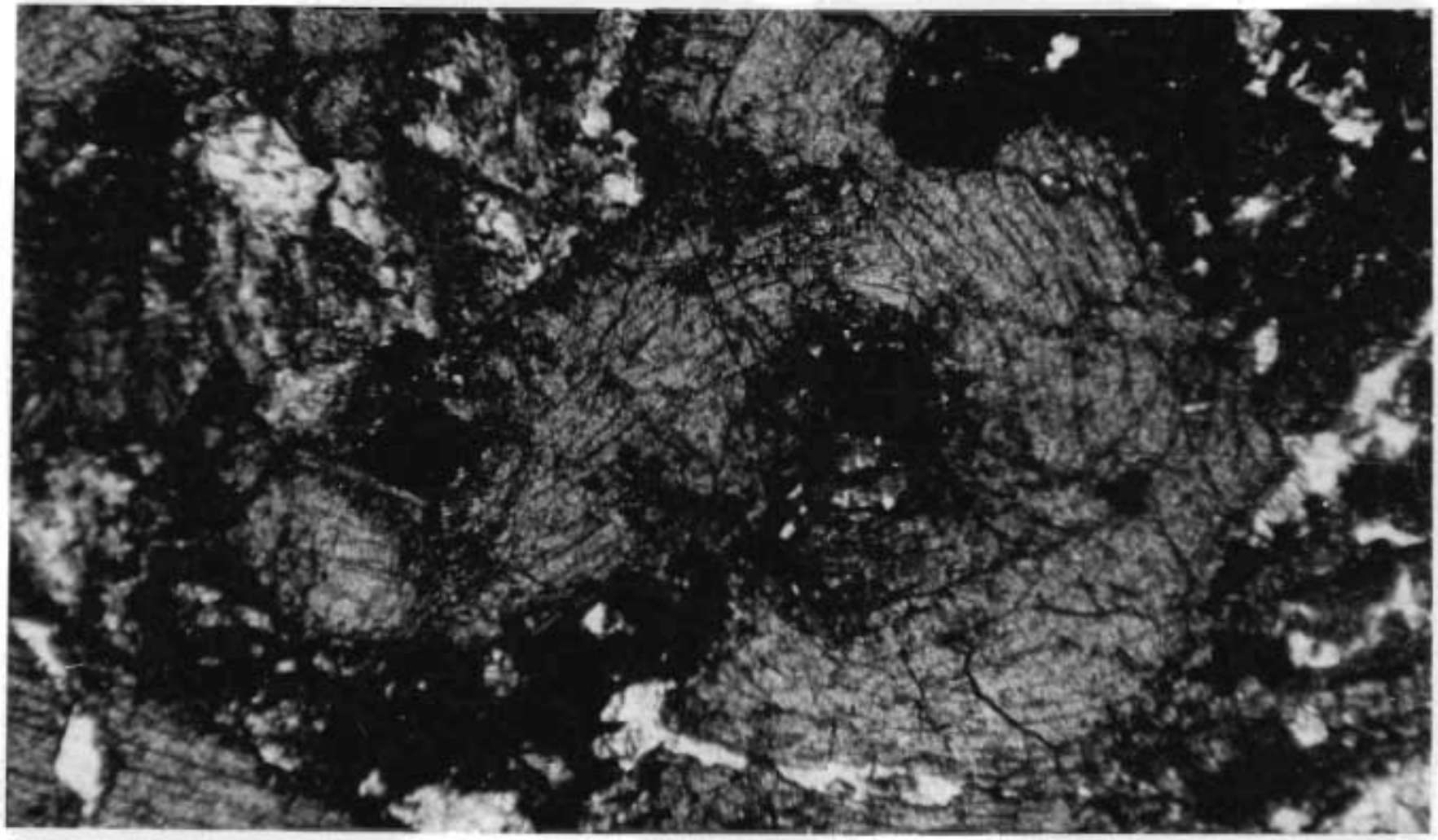

continuous curve, in spite of the fact that it is now sub-divided into more than 60 sub-units. In places however, small aggregates of disorientated pyroxene crystals do occur in addition to the large bent variety. The largest of the crystal fragments forming the aggregates occasionally show signs of strain, and these aggregates may represent the result of granulation of the type Grigor'ev mentions.

External rotation of the deformed pyroxenes in the granophyric gabbro is usually made obvious by their curved cleavage traces, but not all the bent crystals can be recognised in this way. Crystals bent in a plane at right angles to the plane of the thin section appear as a linear series of grains often showing a progressive variation in the interference colours of the sub-grains. For these, universal stage determinations of the orientation of the sub-grains reveals their relationship (see stereogram in fig 25, p 176). As noted at the beginning of this section, grain boundaries are frequently parallel to (010), that is normal to the experimentally determined glide system on (100). In some cases the sub-units have step-like boundaries in which (110) cleavage planes form the boundary in the horizontal part of the step, while a plane close to (001) forms the vertical part. (See fig 27, p 177). Comparing the latter diagram with the sketch of the deformed clay model produced by M.V. Gzovsky, (in Belousov, 1962) in experiments with models on tectonic uplift (see fig 26, p 177) it may be seen that in the clay models, cracking has taken place in two directions at both extremities of the deformed portion of the model, while in the crest of the curve, where tension is at a maximum, small triangular units tend to be developed, somewhat similar to those occurring at the left end of the crystal illustrated in fig 27 . The horizontal cracks occurring at either end of the clay model are directions of maximum stress and correspond to the (110) cleavage type boundaries in the deformed pyroxene. The step-like boundaries are thus possibly produced as a result of the migration of lattice defects to the planes corresponding most closely to directions of maximum stress.

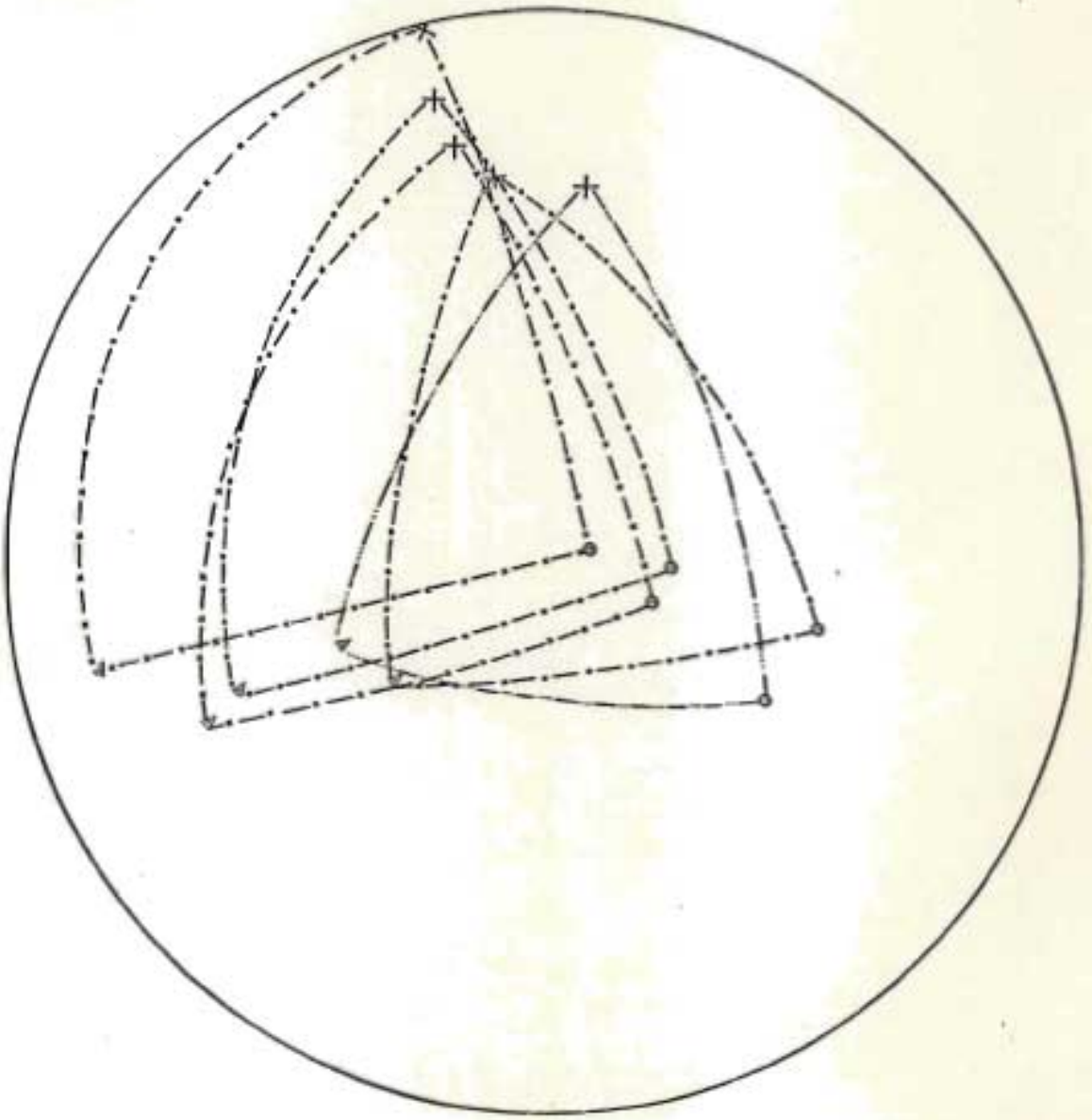

Figure 25 Stereographic projection of optic vectors of five sub-units present in a bent pyroxene of the Granophyric Gabbro, (⊙-x, ┼-y, Δ-z) showing relative orientation of sub-units.

Figure 26. Fractures developed in deformed clay model (after Gzovsky, in Belousov, 1962).

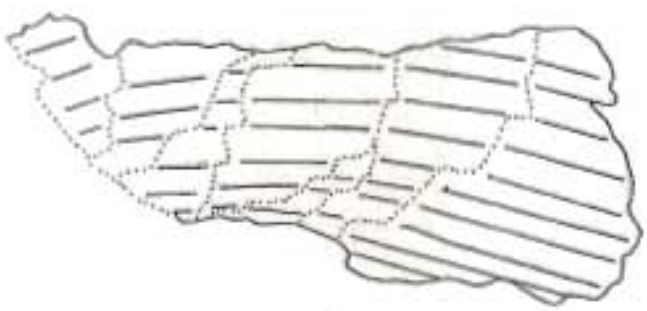

Figure 27. Detail of boundaries of sub-units in a bent pyroxene crystal from the Granophyric Gabbro.

By use of pre-existing (100) exsolution lamellae Griggs, Turner and Heard (1960), were able to show that in their bent diopside crystals, no internal rotation of this plane had occurred and hence derive the glide system T = (100) t = [001]. In many of the bent pyroxenes in the granophyric gabbro, (100) parting is developed which still shows a rational relationship to x, y and z (the optic vector) in the bent crystal in which it occurs. In the stereogram shown in fig 28 , p 179, crystal elements are plotted for part of a bent crystal, showing no polygonisation and it may be seen that the (100) plane still bears a rational relationship to x, y and z, despite an external rotation of 11° with y = (010), as the axis of external rotation. Bending in these cases would thus appear as in the experimentally deformed diopside, to have taken place by gliding on (100) in the direction [001].

The (010) plane is not the only plane forming a boundary to the sub-units. In fig 29, p 180 , four straight well-defined planar boundaries are present, (plus another which is fairly straight), one of these being a (100) twin plane. The other boundary planes are parallel to the (100) plane but the sub-units are not in a twinned relation to each other. Their cleavage traces are offset relative to their neighbours, by a fairly constant figure of approximately 8° suggesting that block formation has taken place. This may be the product of another glide system parallel to (001) but could also be due to strain hardening in the crystals leading to translation gliding of large units along the (100) plane now observable, with accumulated stress in these large units being relieved by migration of the lattice defects to the sub-units boundaries, defined by the (100) planes. In this respect it is probably significant that Bidyut (1962), in his experimental work on the deformation of dunite, found that in crushed grains of pyroxene, noted along with the development of a mylonitic structure, the clearest boundary between fragments appeared along the (100) plane.

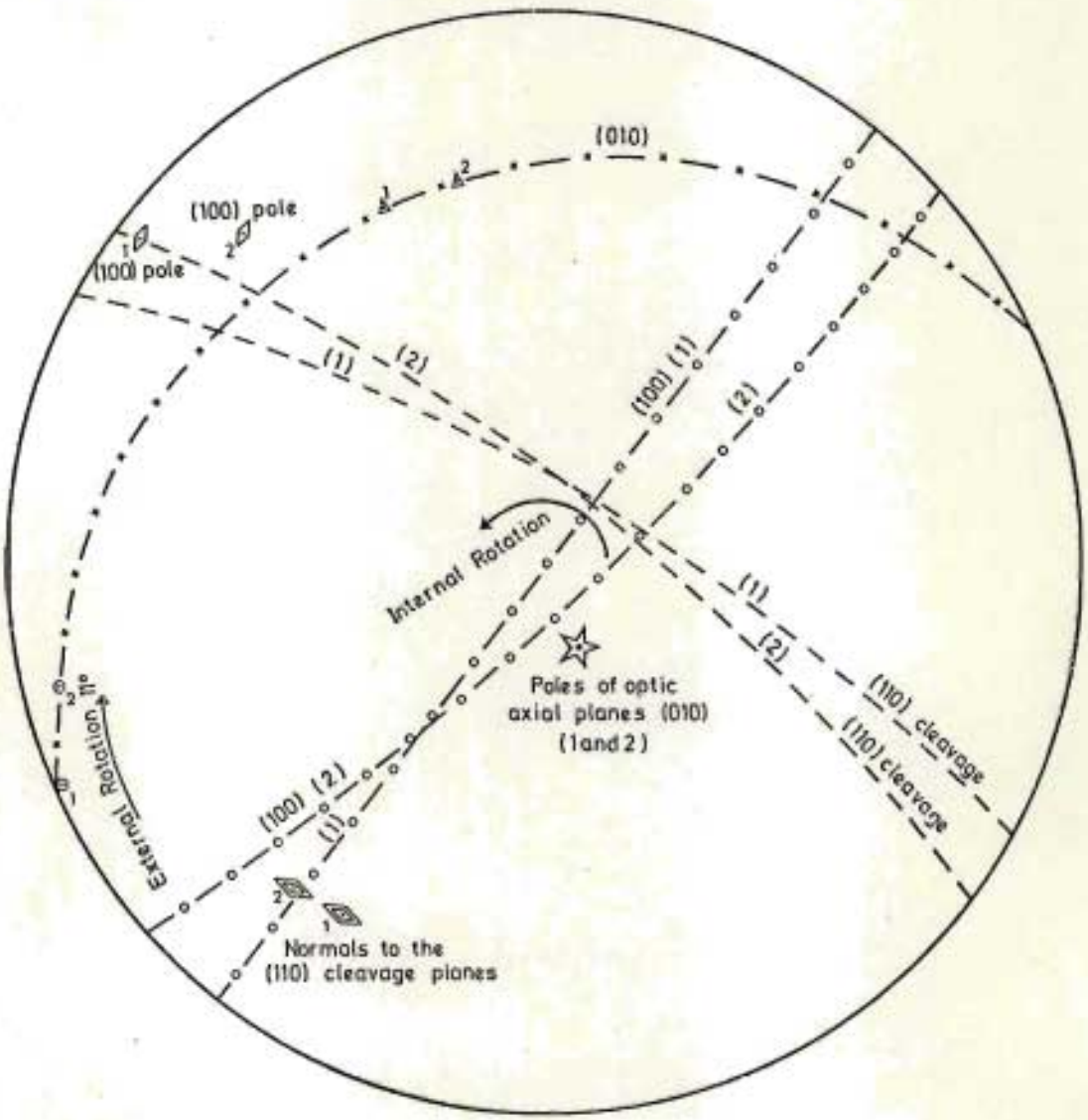

Figure 28. Stereogram showing relative orientation of crystal elements in two parts of a bent crystal which has not suffered polygonization

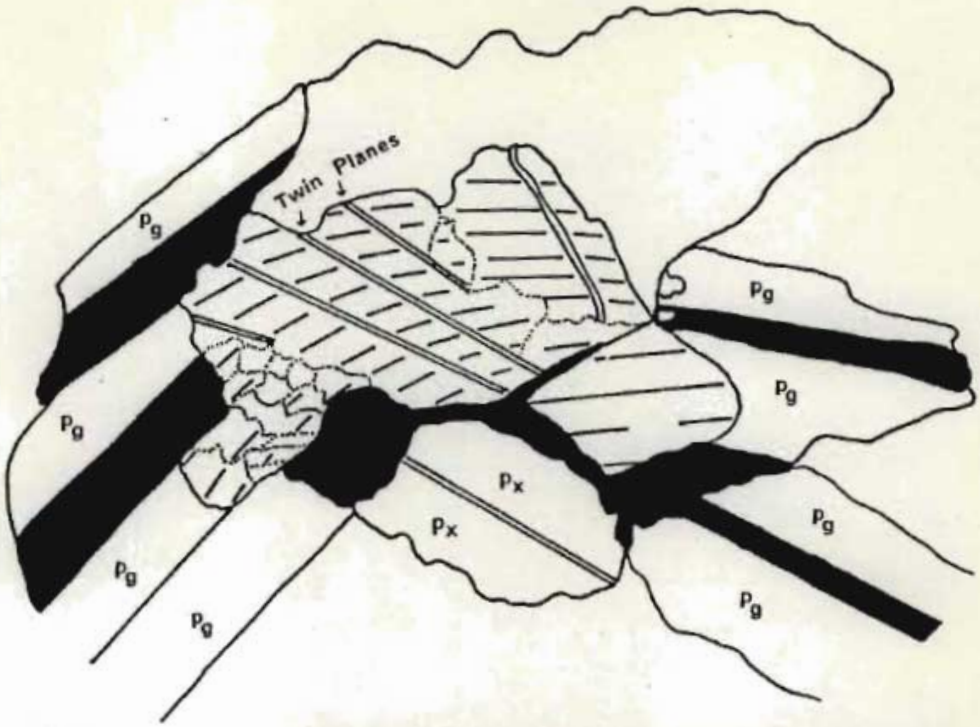

Figure 29 Four planar boundaries developed in a bent pyroxene crystal from the Granophyric Gabbro.

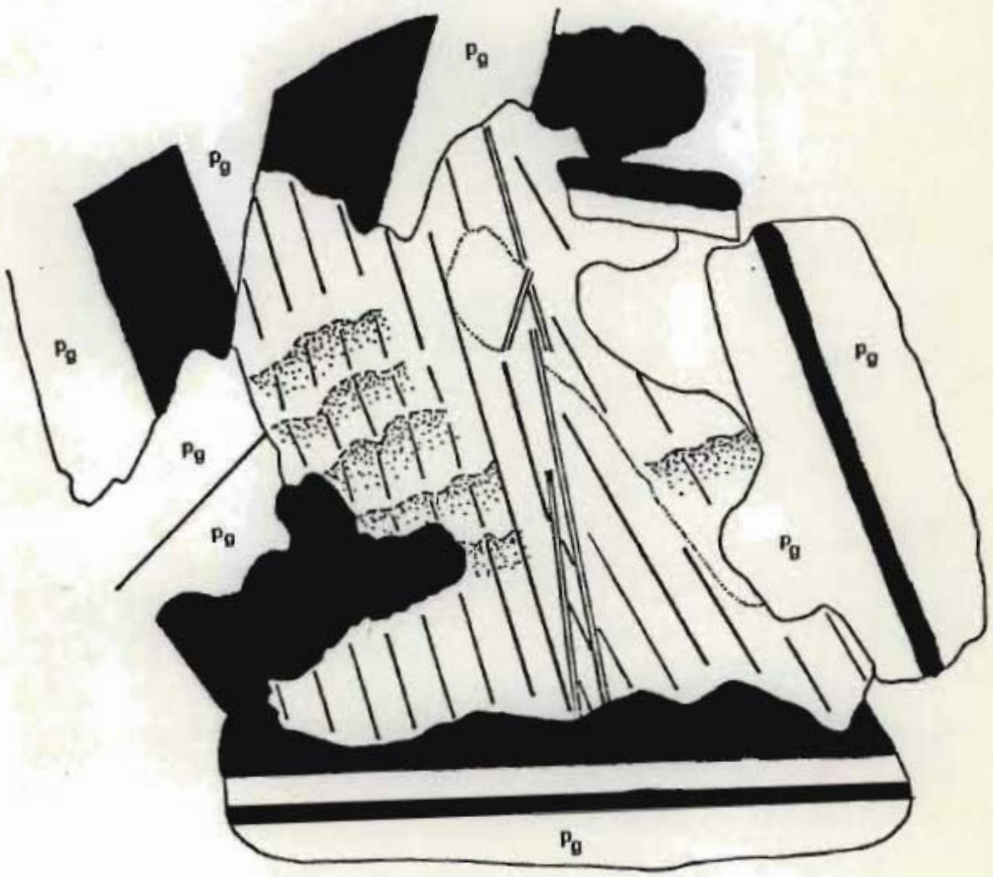

Figure 30 Undulatory extinction and deformational twinning developed in a deformed pyroxene crystal from the Granophyric Gabbro.

Block formation was observed in the pyroxene of several other minor porphyritic intrusives occurring in the Komatipoort area, covering a fairly wide range of composition in the diopside-hedenbergite series, but was not observed in Ca-poor pyroxenes. Compositions range from the Mg rich varieties present in the igneously laminated gabbro to the green hedenbergitic types typical of the granophyric microgranites, and bending followed by block formation may therefore be expected to be a common response to deformation of clinopyroxenes in rocks deformed under the correct temperature and pressure conditions. The exact limits of temperature and pressure conditions under which polygonisation will occur, have not been accurately defined, but it is known that at higher temperatures, about half way between absolute zero and the melting point, recrystallisation annealing occurs (annealing or Tasman temperature), with unstrained grains developing from new nuclei, completely replacing strained grains, (provided sufficient time is available). Some strained grains in the granophyric gabbro do appear to be partially replaced by unstrained grains, suggesting the deformation has occurred at elevated temperatures, or that subsequently the rock temperature has risen significantly.

II Other Deformational Effects

Undulose Extinction

The bending of the pyroxene is only one manifestation of the effects of deformation which it has suffered, other features being undulose extinction, twin gliding and mechanical twins. Undulose extinction, occurring either alone or in combination with the other deformational effects, is commonly observed as bands developed roughly parallel to the trace of the (001) plane, or, in places, to the b crystallographic axis of the pyroxene (see fig 30, p 180). The bands vary slightly in width, even within a single crystal, and when the orientations of optic vectors are measured in different parts of the same crystal, a maximum relative displacement of 8° in a direction normal to the (001) plane is usually recorded between the parts of adjacent bands showing the greatest difference in extinction

angle. Bands of undulose extinction are apparently only developed in certain crystals, possibly those in which the direction of stress was approximately parallel to the c crystallographic axis. In other crystals any undulose extinction that is present is of a patchy variety.

Mechanical Twins

According to Grigor'ev (1965), mechanical twins may be formed by twin gliding as a result of rotation of particles comprising the crystals through 180° around a twin axis or normal to a twin plane, a process that does not immediately involve the entire part of a crystal passing into a new position. Instead, a crystallite appears at one of the structural points, and dislocations are formed through the transition of the atoms into the new position. Thus the twin gradually spreads over the crystal.

Spry (1969) however, has pointed out that mechanical twinning by simple shear displacements parallel to a slip plane can only be achieved on body centered cubic lattices, and that twinning in lattices of lower symmetry involves additional displacements. Mechanical twinning in lower symmetry minerals such as diopside may be a semi-reconstructive or reconstructive process, (Raleigh and Talbot, 1967), and could not be produced by twin gliding.

Nucleation of mechanical twins in a mineral such as a pyroxene may take place at positions of strain such as dislocation concentrations or grain boundaries, and the size, shape and number of twins then depends upon the ease of propagation, which in a twin is influenced by a number of factors including temperature and strain rate (Spry 1969).

Spry (1969), states that after nucleating the twins tend to grow along a twin plane, to form a thin continuous twinned layer. Subsequently other twins may nucleate to give a series of thin

polysynthetic twins, or the twin plane may move laterally to thicken the twin.

A variety of twins considered to have a mechanical origin are observable in the pyroxenes of the granophyric gabbro. Twin planes with tapered ends extending over only part of a crystal, twins involving only a small part of the interior of a crystal and closely spaced polysynthetic twins (up to 6 per mm) are common. These are normally parallel to the (001) plane but occasional (100) twins were noted. Both the twin systems have been produced by experimental deformation of diopside (Raleigh and Talbot, 1967).

According to Turner and Verhoogen (1960), " ... great caution should be exercised in assessing the tectonic significance of microscopically obvious lamellae structure, such as 'deformation lamellae' in olivine, which have very generally been interpreted as manifestations of active glide systems responsible for the orientation of the grains in which they occur. There is no foundation in this belief.".

It is also noted by the same authors that although translation gliding in calcite is the most effective mechanism of strain relief it leaves no microscopical trace.

Visible lamellae along which translation appears to have taken place are occasionally observed in the deformed pyroxene crystals present in the granophyric gabbro. Plotting the crystallographic elements and optic vectors of the crystals stereographically, together with the orientation of these planes, (along which translation appears to have occurred), indicates the orientation of the latter planes to correspond with the (001) plane, and they are therefore probably due to a late stage incipient fragmentation of the crystal, following strain hardening. Similar planes, having a radial disposition are occasionally observed in the arch of crystals bent in the plane of a thin section and these are considered to have the same origin.

III Summary

It was noted that the pyroxenes in the granophyric gabbro, under stress , and probably at somewhat elevated temperatures and possibly pressures, have shown a tendency to deform by bending, a process which is apparently accommodated in the crystal lattice by gliding on (100). As deformation proceeds, it is probable that strain hardening occurred and various lattice defects accumulated. In some case this was followed by translation on the (001) plane. In other instances the accumulated strain (in the form of the lattice defects) was subsequently relieved by polygonisation, resulting in extreme cases in a granular aggregate. Where the pyroxenes were suitably orientated, glide twinning developed parallel to both (001) and (100), in other cases, parallel bands showing undulose extinction developed. Where orientation of the crystal was not quite optimal, irregular patches of undulose extinction were formed.

(c) Ore Minerals

Magnetite, pyrite, ilvaite, ilmenite and chalcopyrite all occur in the granophyric gabbro. Of these magnetite is the most abundant, forming large irregular patches up to 5 mm across, or occasional smaller (0.15 mm) subhedral crystals. Much of the magnetite has been martitised to hematite and rarely, exsolution lamellae of ilmenite were observed. Pyrite forms patches similar in size and shape to those of magnetite and is also relatively abundant. Euhedral and subhedral crystals are fairly common.

Although ilvaite is not, strictly speaking, an ore mineral it is most easily recognised in polished sections and has therefore, been included with the ore minerals. It occurs as aggregates of small subhedral crystals (0.5 mm) and occasional large irregular patches (5 to 6 mm) and is often associated with altered pyroxene.

Ilmenite and to a greater extent chalcopyrite, are uncommon. Ilmenite forms small irregular patches (0.5 mm) set in the granophyric groundmass and chalcopyrite is present as minute irregular grains.

(E) Unit 4 - The Granophyre

(i) Distribution and Lithology

The granophyre forming Unit 4 is a distinctive pink rock, which outcrops intermittently over a distance of about 18 km. It is divided into a southern and northern mass by a younger, roughly north-south trending, microgranite dyke, which cross-cuts the granophyre approximately 1 km north of Komatipoort (see Geological Map). From this intersection, the southern mass stretches southward for some 10 km, reaching a maximum horizontal width of 0.6 km near its southern extremity, although over much of the rest of the sheet, outcrop width does not exceed 200 m. At the southern end of the intrusion, the granophyre builds a discontinuous ridge consisting of two low masses offset progressively to the east from the general trend of the sheet. Slickensided granophyre float here present, suggests that possibility that the granophyre may have been displaced by faulting, but the slickensiding may equally well be an intrusive phenomenom. No further evidence could be found and mainly on the basis of float distribution, the granophyre near the southern extremity of the intrusion has been mapped as a single undisturbed mass. Throughout its length, this southern portion of the granophyre is apparently bracketed between the granophyric gabbro to the west and the feldspathic gabbro to the east. A possible further representative of the unit 4 granophyre, is a small roughly north-south elongated mass outcropping in the Sikwawa River a few kms east of the main granophyre body, (see Geological Map).

Outcrops are poor for approximately 1 km north of Komatipoort until

the cross-cutting microgranite dyke is encountered. Beyond this minor intrusion, small outcrops of the granophyre of the northern mass occur, here over an east-west width of 500 m, and these may be followed northwards across the Crocodile River into the Kruger National Park for a further 5 km.

Along its eastern margin the northern mass is everywhere in contact with the feldspathic gabbro and this rock type also forms lenses along the western contact. Where these are absent the granophyre along its western boundary appears to be in direct contact with either the basalt itself or in the southern portion of the northern mass, with the microgranite dykes.

At the contact with the granophyric gabbro, the granophyre of the southern mass is finer grained and slightly lighter coloured than normal, as a consequence of more abundant interstitial granophyric material. Further, pyrite, although present, is not as conspicuous as in the adjacent granophyric gabbro. This fine-grained rock grades into typical granophyre over a distance of 1 m to 2 m. The granophyre of the southern mass commonly consists of elongated patches of iron ore, often with a skeletal form, and greenish black pyroxene blades, frequently several centimeters in length, set in a fine-grained pink groundmass. Plagioclase laths, usually rimmed by a granophyric intergrowth of alkali feldspar and quartz are commonly visible only in polished slabs of hand specimens or in thin sections. Textural variations do occur and, in places, with an increase in feldspar content, the rock in handspecimen has a medium grained, equigranular texture. Variations in colour from pink to greyish brown or grey were also noted and towards the eastern contact in the Komati River section, a distinct zone some 10 m wide, consisting of a fine-grained pale grey granophyre, occurs.

In hand specimen the elongated patches of iron ore are the most striking feature of the rock (see Plate 14, p 187). These may occur as single lath-shaped structures ranging in length from 1 cm to 10 cm,

PLATE 14

1. Granophyre, Komatipoort Intrusion, typical Granophyre outcrop showing the development of abundant small "comb-structure".

2. Granophyre, Komatipoort Intrusion, "Comb-structures" displayed in three dimensions in freshly-broken boulder of Granophyre. Length of "comb-structures" approximately 10 cm.

which frequently possess a flow-type texture produced by the roughly parallel orientation of the iron ore patches. The common direction of orientation changes gradually, laterally through the rock. Alternatively the patches of iron ore occur associated in small groups usually forming one of three types of structures. They may form patches composed of up to 30 units of similar but variable size closely packed parallel to each other, or they may form 'comb' structures, (see Plate 14).

These comb structures vary in size, commonly ranging from 1 cm to 15 cm but exceptionally reaching 30 cm in length. Less commonly they form a rough gridiron pattern with angles between the two directions of orientation of the units ranging from 70° to 90°.

The northern mass of granophyre has cross-cut rhyolites flows inter-bedded with the basalts and as a result of differential weathering relatively strong relief is developed. The granophyre here closely resembles that just described, but variations, particularly in grain size are more frequent. Finer-grained, elongated, north-south trending zones,(with gradational contacts), that are usually only a few meters wide appear common in the relatively good exposures which occur just south of the Crocodile River.Although the Granophyre, even in handspecimen, shows a tendency to become more feldspathic close to the contacts, the common textural variations suggest that the Granophyre may be a composite intrusion at this point at least.

Within the Kruger National Park, a relatively good cross-section is exposed within the bed of a small tributary of the Crocodile River, (see Geological Map). Here, along its western contact, the grano-phyre is highly feldspathic, resembling a weathered gabbro in hand-specimen, although in thin section its granophyric affinities are clear. Eastwards this rock type grades into more typical pink granophyre containing a few large visible feldspars, and towards the centre of the section feldspar phenocrysts are almost entirely absent.

Near the eastern margin a pink fine-grained variety is again present. Thus while textural variations do occur these are not as common as in the exposures just south of the Crocodile River.

Within the northern mass the rock locally darkens in colour to become almost black, although this is not accompanied by a variation in texture.

If, as appears probable from its position between the Feldspathic Gabbro and the Granophyric Gabbro, the Granophyre has the form of a roughly concordant sheet, its thickness may be estimated as around 175 m.

(ii) Petrography of the Southern Granophyre Mass

The granophyre consists of partially resorbed, turbid plagioclase crystals (exceptionally reaching a length of 1 cm), and irregular corroded pyroxene crystals, set in a groundmass of fine to medium-grained micropegmatite. The pyroxene has several forms, but commonly occur either as prominent corroded blades, or as irregular roughly equidimensional crystals which may subophitically enclose plagioclase laths, thus forming small glomeroporphyritic aggregates similar to those forming the 'gabbroic' textured patches in the granophyric gabbro. Severe corrosion of the pyroxene blades, has in places reduced them to a series of narrow, discontinuous patches in optical continuity with each other, but it is clear that in places, the pyroxene blades, prior to resorbtion, averaged several centimeters in length. Some of the plagioclase laths are intimately associated with the pyroxene which occurs as thin stringers along twin planes or as granophyric or dendritic intergrowths with the plagioclase. Corrosion of the plagioclase crystals has occurred and these feldspar crystals are invariably rimmed by alkali feldspar.

Other conspicuous constituents of the granophyre are opaque ore minerals which occur both as elongated patches in various textural

modifications, as described in the section on lithology, and as formless patches up to 1.2 cm in diameter set in the granophyric groundmass. Apatite is also present in tiny acicular crystals both in the groundmass and included in the feldspar crystals. The grain size of the granophyric groundmass varies widely, ranging from a fine-grained micropegmatitic intergrowth to coarser-grained lobate textured intergrowths,although the latter are not common. Frequently the granophyre occurs as a mosaic of small units centered around plagioclase crystals producing a rhopalophyric texture. The grey granophyre (mentioned in the previous section) which forms a narrow zone outcropping in the Komati River, possesses a slightly different texture. Although rarely interstitial granophyric material may be coarse grained, it is more commonly very fine grained, often showing a plumose structure. Most of the pyroxene present is altered to chlorite or in part replaced by ore minerals. The plagioclase is clouded and much replacement by micropegmatite renders it barely distinguishable from the groundmass (see Plate 12, p 163).

The granophyre close to the contacts has a normal pink colour but contains variable quantities of obvious plagioclase xenocrysts. In addition, pyroxenes with a blade-like form may be absent, the irregular equidimensional crystals being more common. The plagioclase xenocrysts are distinguishable from the normal granophyric plagioclases not only by their composition (they are more An-rich) but by the lack of turbidity in the central portions of the crystals and the frequent presence of cataclastic deformational effects in the form of cracking. This in extreme cases results in fragmentation of the plagioclases. Granophyre samples collected adjacent to the feldspathic gabbro in the Komati River section, contain in addition to the feldspar xenocrysts needle-like quartz paramorphs after tridymite reaching 1.5 cm in length, scattered through the groundmass (see Plate 15, p 191).

PLATE 6

1. Granophyre-Gabbro Hybrid. Small quartz paramorphs after tridymite, developed in interstitial material adjacent to a fractured crystal of plagioclase. Specimen from adjacent to the Feldspathic Gabbro-Granophyre contact of the Komatipoort Intrusion. (Transmitted light, X96,)

2. Felsite-Gabbro Hybrid. Acicular quartz paramorphs after tridymite, (white), associated with a clouded, roughly rectangular feldspar crystal, set in a semi-opaque microcrystalline groundmass. Specimen from the upper contact of the feldspathic gabbro, in the Komatipoort Intrusion. (Transmitted light, X200.)

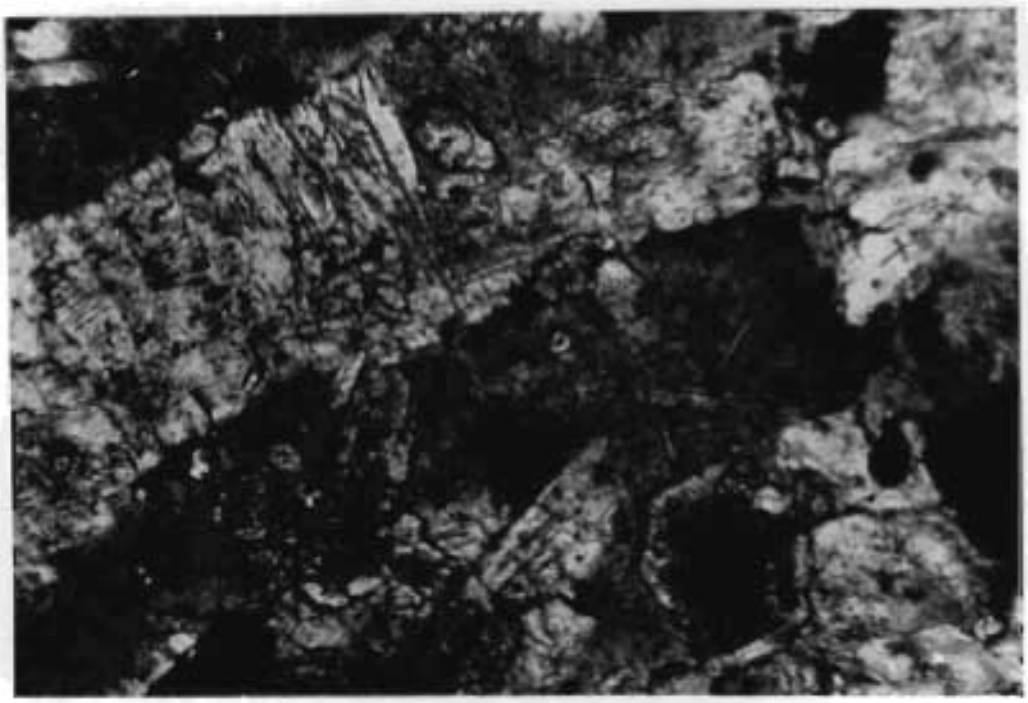

(iii) Petrography of the Northern Granophyre Mass

Differences in the petrography of the two granophyre masses are restricted to the rapid textural variations which characterise the granophyre just south of the Crocodile River, and the presence of highly feldspathic, obviously hybrid rock types, along the western margin of the northern mass. For the rest, the actual textures of the granophyre in both masses are very similar.

The contact rocks along the western margin of the intrusion north of the Crocodile River, are exceptionally rich in xenocrysts and partially digested fragments of feldspathic gabbro, which give the rock a gabbroic appearance in handspecimen. In thin section, however, these rocks may be seen to be composed of abundant clouded and partially corroded, feldspar xenocrysts set in a granophyric matrix.

(iv) Mineralogy

(a) Plagioclase

The plagioclase occurring in the granophyre typically forms irregular, elongated crystals (length:breadth ratio of the order of 5:1) varying in length from 0.1 to 1 cm, which are usually too turbid for reliable optical determination of composition. Average compositions estimated from optical measurements on the least altered available crystals range between An_{18} and An_{34}, although these results are based on relatively few crystals. Normal zoning is usually present and in the crystals measured was found to grade from around An_{40} in cores to between An_{14} and An_{24} at the boundaries. For the most part, however, it is only by staining of thin sections and polished slabs that the plagioclase could be differentiated from the alkali feldspar.

The plagioclase crystals commonly show a distinctive brownish-pink turbidity and are frequently partly replaced by micropegmatite. The replacement is often extensive with the original plagioclase crystals reduced to a few remnants that are surrounded by micropegmatite. The K-feldspar component of this micropegmatite may preserve the initial orientational differences present in the plagioclase as a result of twinning. Selective replacement of the more basic plagioclase cores is not unusual.

Relatively unaltered xenocrysts of plagioclase derived from adjacent rock types, invariably either the feldspathic gabbro or the granophyric gabbro, are easily distinguished by compositional and textural features as described in the section on petrography.

The xenocrysts along the western margin of the southern granophyre mass are similar to those present in the adjacent granophyric gabbro in that core composition averages around An_{55}. Zonal variation in composition is also similar, although in places reaction with the granophyre appears to have removed part of the outer zones, and the xenocrysts become progressively more altered away from the contact, making recognition difficult.

Near the upper contact, compositional differences between the xenocrysts and the primary granophyric plagioclase are not easily established, as the plagioclases in the feldspathic gabbro itself are normally turbid. They possess, however, a distinctive white turbidity, rather than the pinkish-brown colouration shown by the typical granophyric plagioclases, and in addition display the effects of cataclastic deformation.

(b) Alkali Feldspar

Orthoclase, the only alkali feldspar present, occurs in two forms, first graphically intergrown with quartz in the groundmass and secondly forming narrow rims around the corroded plagioclase crystals,

and in places apparently replacing them. Although it is usually turbid and somewhat reddened, it was found possible to measure the optic axial angles in places, (from 67^{o} to 74^{o}).

(c) Pyroxene

As mentioned in the section on petrography the only pyroxene present in the granophyre, is a Ca-rich variety. It occurs in two forms; as irregular, roughly equidimensional grains, that resemble the Ca-rich pyroxene which occurs associated with micropegmatite-rich areas in the granophyric gabbro, and as elongated prismatic crystals with irregular corroded-looking margins. Both forms of the pyroxene have brownish interiors which grade into green coloured rims at the irregular margins of the crystals.

Chemistry

The compositions of six Ca-rich pyroxenes from the granophyre, which were analysed by electron microprobe, are listed in Table 33 . Analyses 1 and 2 in this table represent the composition of the brown core and green margin of an irregular equidimensional grain from near the western margin of the granophyre. The remainder (analyses 3 - 6) are the results of the analyses of both the interior (analyses 3) and the green margins (analyses 4 - 6) of blade-like pyroxene crystals, in a sample collected from near the centre of the granophyre. As may be seen from fig 15, in which the pyroxene compositions have been plotted in the pyroxene quadrilateral, these Ca-rich pyroxenes range from ferroaugites to ferrohedenbergites, (En_{17} - $En_{3,5}$). Large differences exist between the major element contents of the equidimensional crystals and the blade-like crystals. In addition analyses 1 and 2 have a major element composition that lies within the compositional range of similar pyroxenes from the granophyric gabbro. In contrast the composition of the core of the analysed blade-like crystal (analysis 3) corresponds to the extreme Fe-rich limit of the granophyric gabbro Ca-rich pyroxenes. The rest

TABLE 32

Electron microprobe analysis of 6 Ca-rich pyroxenes from the Granophyre, Komatipoort Intrusion.

Pyroxene Analysis No.	1	2	3	4	5	6
SiO_2	48,63	48,43	47,37	46,57	46,92	47,40
CaO	18,24	19,05	18,28	17,58	18,42	19,18
MgO	5,78	2,92	3,71	2,92	2,15	1,14
TiO_2	1,00	0,52	1,32	1,19	1,19	0,40
FeO	25,49	28,86	27,97	27,83	30,23	29,98
Al_2O_3	1,21	0,72	1,54	1,39	1,29	0,64
Sum	100,35	100,50	100,19	97,48	100,20	99,04
Fs	43,94	49,76	49,26	51,04	53,29	53,28
En	17,15	8,83	11,17	9,19	6,52	3,57
Ca	39,91	41,41	39,57	39,77	40,18	43,15
Cations per 6 oxygens						
Si	1,941	1,966	1,921	1,943	1,927	1,981
Al	0,057 } 1,998	0,034 } 2,000	0,074 } 1,995	0,057 } 2,000	0,063 } 1,990	0,019 } 2,000
Al	0,000	0,000	0,000	0,011	0,000	0,013
Ca	0,780	0,829	0,794	0,786	0,810	0,854
Mg	0,344 } 2,005	0,177 } 2,002	0,224 } 2,007	0,182 } 1,987	0,132 } 2,017	0,071 } 1,993
Ti	0,030	0,016	0,040	0,037	0,037	0,013
Fe	0,851	0,980	0,949	0,971	1,038	1,042
O	6	6	6	6	6	6

Analysis 1 Brown core of irregular, equidimensional crystal, near W margin of granophyre.

Analysis 2 Green margin of irregular equidimensional crystal, near W margin of granophyre.

Analysis 3 Interior of bladed pyroxene crystal, near centre of granophyre.

Analysis 4)
Analysis 5) Margins of bladed pyroxene crystals, near centre of granophyre.
Analysis 6)

of the analyses of the blade-like crystals are distinctly more iron rich and correspondingly Mg-poor than the pyroxenes of the granophyric gabbro, grading to $En_{3,5}$ in the most extreme example.

Ti-Al and Si-Al relationships are shown in figs 16 and 17, p 138. Both Ti and Al contents of the pyroxenes from the granophyre appear to decrease steadily with increasing Si. In terms of the minor elements there is again a similarity between the irregular equidimensional pyroxenes from the granophyric gabbro and the pyroxenes from the granophyre represented by analyses 1 and 2. The bladed pyroxenes on the other hand, while apparently similar in Al content are noticeably higher in Ti.

(d) Ore Minerals

Pyrite, magnetite (including martite) and ilvaite together with minor amounts of ilmenite and chalcopyrite, are the most abundant minerals observed in polished section. The mode of occurrence of these minerals is almost identical to that of the granophyric gabbro (see previous section) and the description will not be repeated here. One major difference is the tendency for the magnetite to occur in the form of elongated patches. Occasionally ilvaite associated with what appears to be altered pyroxene, occurs in the same form.

(F) Unit 5 - The Feldspathic Gabbro

(i) Distribution

The feldspathic gabbro forms a continuous band 200 to 250 m wide, stretching from a point 11km north of the Komatipoort Township's Bantu Location to the confluence between the Sikwawa and Komati Rivers 12½ km south of the location (see geological map). At the southern-most extremity of the Komatipoort Intrusion proper, the band

is still some 200 m wide.

A further small exposure of the feldspathic gabbro occurs in the Sikwawa River a few kms east of the most southerly exposure in the Komatipoort intrusion, (see geological map). This isolated outcrop is fairly closely associated spatially with the minor elongated mass of granophyre exposed in the bed of the same stream. A fault could be inferred to explain the apparent easterly displacement of what appear to be the two uppermost units of the Komatipoort intrusion . No direct field evidence of a fault was found, however, and the possibility that these outcrops represent separate intrusions cannot be discounted at this stage.

The western boundary of the unit is not exposed, but rocks occurring along the eastern margin may be seen in three places.

(i) In the Crocodile River towards the northern end of the unit.

(ii) In a cross-section of the unit exposed in the bed of the Komati River just upstream from the railway bridge, (hereafter termed the railway bridge section).

(iii) In a more limited cross-section of the unit exposed in the Komati River at the confluence between the Komati and Sikwawa Rivers, (hereafter termed the Sikwawa River section).

The contact itself is observable only at the second of the sites listed above.

Samples representing a cross-section of the unit were collected at both localities in the Komati River (ii & iii above), but in the Crocodile River unweathered outcrops are rare and few usable specimens were obtained.

The contact exposed in the Komati River just upstream from the railway

bridge appears transgressive, and Du Toit (1929), has suggested the body to be in the form of a steeply inclined dyke, rather than a sheet. Petrographical and mineralogical variations, however, point rather to a subconcordant sheet, inclined roughly parallel to the lower rock units in the intrusion, (i.e. dipping to the east at 25° to 30°) as the most probable form. Generally, in hand specimen , the feldspathic gabbro has a distinctive and rather uniform appearance. It is a fine to medium grained, phaneric, holocrystalline rock distinguished by the presence of abundant altered chalky-white plagioclase laths, which make the rock look more feldspathic than modal analysis reveal. Variations in mineral proportions do occur across the band but no distinct layers of markedly different rock-types are developed. The mineralogy and petrography of the rocks collected along the two cross-sectional traverses are similar, but modal analyses indicate a difference in proportions of minerals present.

(ii) Lithology

Railway Bridge Cross-section

In the Komati River, upstream from the Railway Bridge rocks representative of at least the upper two thirds of the sheet are exposed. The rock occurring in the centre of the sheet is a medium-grained leucocratic, phaneric gabbro containing moderate amounts of a pink interstitial material, which although not conspicuous, is occasionally visible in hand specimen. This gabbro often has a mottled appearance, due either to the presence of black patches of finely disseminated iron ore 2 cm to 5 cm across or to the fact that the plagioclase is unaltered in small patches and loses its chalky-white appearance.

Towards the eastern margin of the sheet there is a decrease in grain size and the gabbro grades into a variety with anorthositic affinities. In these marginal types the pink interstitial material is more obvious, particularly on weathered surfaces where it forms small, pale, resistant

nodules and patches a few millimeters across. Also fairly common are small patches of zeolites.

A slight decrease in grain size is noted in the few exposures near the western margin of the sheet.

The upper contact between the feldspathic gabbro and the basalt is exposed in the Komati River bed at the site of the railway bridge just outside of Komatipoort. Over about 3 m adjacent to the basalt, the feldspathic gabbro shows a rapid decrease in grain size and small patches of pinkish material (about 0.5 cm across) become increasingly abundant as the contact is approached. Small xenolithic blocks, up to about 0.5 m across, consisting of basalts in various stages of digestion, are also common within one or two meters of the contact (see Plate 16, p 200).

Thin veins and sheets of feldspathic gabbro (0.5 to 1.5 cm thick), intruded the basalt, along joint planes, often down the dip of basalt, for distances up to 9 m away from the contact, and in places they follow a rectangular fracture pattern developed in the basalt, (see Plate 16, p 200).

The presence of the pink spots in the feldspathic gabbro near the upper margin give a misleading impression that the rock becomes more acid towards the upper contact. In the Sihlangula River, which flows into the Komati River just downstream from the railway bridge, the feldspathic gabbro, at the contact actually grades into a pinkish felsitic zone 1 m to 2 m wide, however detailed examination of specimens of this zone reveals that the felsitic zone is a result of hybridisation by an intrusive felsite sheet, (see section on the upper margin, p 205).

Variations shown in the Sikwawa River section are essentially similar although the sheet is somewhat narrower at this point.

PLATE 16

1. Feldspathic Gabbro, Komatipoort Intrusion, upper contact of the feldspathic gabbro with basalts.

2. Feldspathic Gabbro, Komatipoort Intrusion, partly recrystallised xenolith of basalt adjacent to upper contact. Dark mineral concentrated along xenolith contact is magnetite. Relict amygdales are conspicuous in the xenolith.

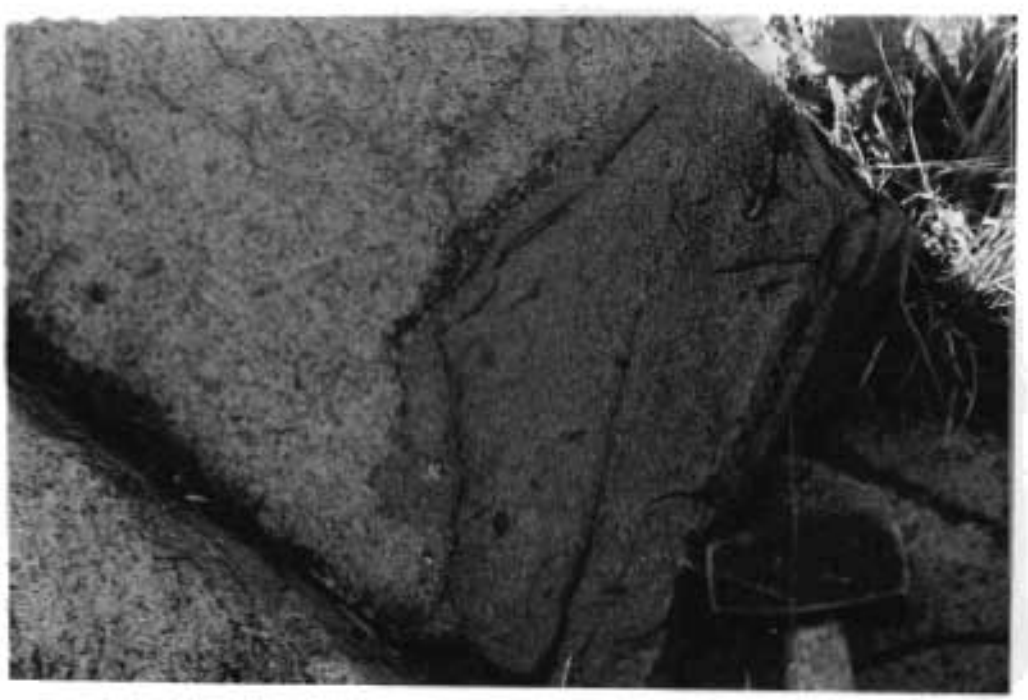

(iii) Petrography

In thin section, samples taken at 10 meter intervals along a cross-section of this unit in the Komati River show the following changes. The most westerly rock in the section, cropping out some 10 meters east of the main granophyre, has a poikilophitic texture with large euhedral plagioclase crystals set in either large irregular augite plates or a matrix of a brownish pink, glassy to cryptocrystalline material. This matrix contains tiny crystallites of iron ore often arranged in small 'comb' structure. Other interstitial constituents include small irregular patches of iron ore, zeolites, chlorite associated with small free quartz granules, as well as apatite needles, (see Plate 17, p 202).

The plagioclase forms euhedral laths, which have suffered extensive fracturing and alteration by sericitisation. The large plates of pyroxene too, show fracturing although in their case, it is both less extensive and less obvious. Two pyroxenes occur in this rock, the clinopyroxene pigeonite, and augite, with the pigeonite occurring as rounded and embayed granules enclosed by the augite. The pyroxenes are usually altered and commonly have a brownish turbid appearance. In places patches of green non-pleochroic serpentine associated with magnetite occur and here the included plagioclase, though fractured, is clear, showing no signs of sericitisation.

The pyroxene plates have an average diameter of 10 mm, but larger grains do occur. The pyroxene contacts with the interstitial material are irregular, with corroded boundaries and reaction rims similar to those occurring in the Granophyric Gabbro.

Radiating aggregates of zeolites are present in small patches interstitially, occasionally replacing pyroxene.

In a specimen taken 10 meters to the east, the pyroxene plates are far smaller and the plagioclase laths measurably larger. The pyroxene has two forms. It frequently occurs as small aggregates of two or

PLATE 17

1. Feldspathic Gabbro, Komatipoort Intrusion, altered plagioclase laths partly enclosed by pyroxene (black) near the base of the feldspathic gabbro. Quartz and Zeolites are present at upper right,(X96).

2. Feldspathic Gabbro, Komatipoort Intrusion, altered plagioclase showing signs of cataclasis, (see large white plagioclase crystal at lower right). Pyroxene, (grey), and ore minerals, (black), occur interstitially to the plagioclase, (X96).

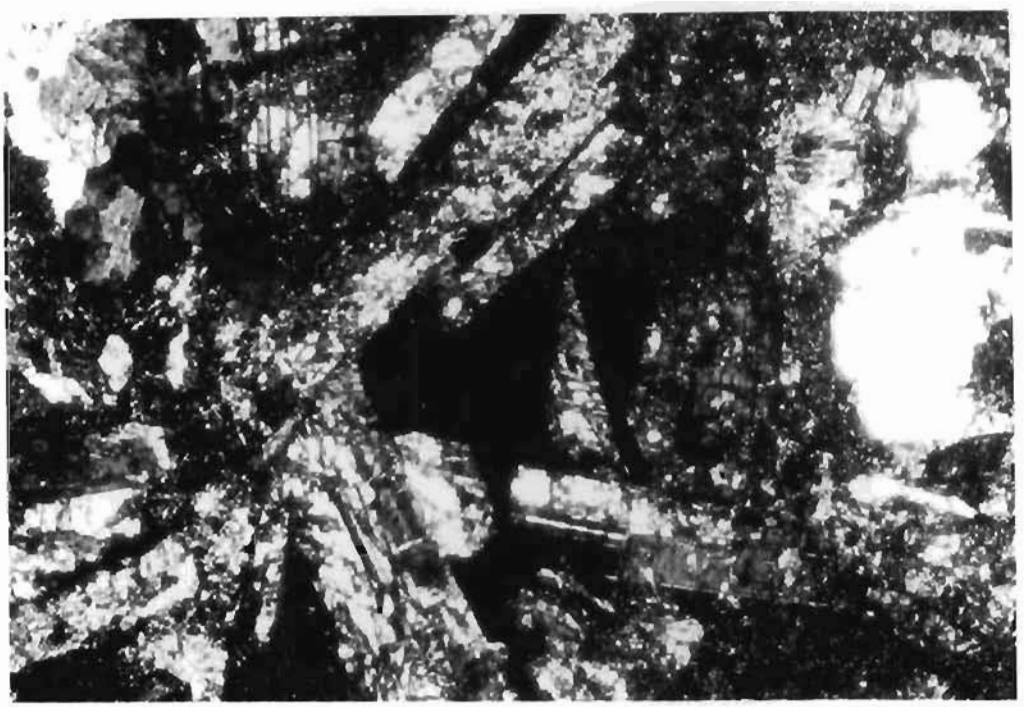

three crystals, with an average diameter of 0.7 mm , or as larger single crystals. The smaller grains have an intergranular relationship with the plagioclase, although larger crystals present may sub-ophitically enclose the plagioclase, (see Plate 17, p 202). Both pyroxenes show the usual reaction rims where in contact with the reduced amount of interstitial material present, and in places are partially or completely altered to chlorite or chlorite + zeolite.

The plagioclase here shows some suggestion of a preferred orientation. Two generations of plagioclase crystals are present, small corroded chadocrysts of the first generation occurring poikilitically enclosed in the margins of larger crystals of the second generation. All plagioclase crystals show cracking, and are again usually altered to some degree.

The small amounts of pink crypto-crystalline interstitial material present is crowded with aggregates of chlorite and patches of zeolite. Needles of apatite are also common. Iron ore occurs interstitially, partly surrounding plagioclase crystals, and replacing pyroxene.

Ten meters to the east of this sample, the rock again has a poikilitic texture with the pyroxene frequently forming large (0.8 cm across) plates enclosing the plagioclase, although in places it has a corroded columnar habit. Both augite and pigeonite are again present, the pigeonite sometimes forming small rounded inclusions in the augite. The plagioclase is frequently set in a glassy to crypto-crystalline matrix, and in this rock a narrow brown rim deeper in colour than the rest of the mesostasis often surrounds the plagioclase laths. The pyroxene is frequently surrounded by rims of green pyroxene iddingsite or intersitial material. In other places turbid pyroxenes are surrounded by narrow rims of clear, colourless pyroxene.

Apatite now appears in much larger hexagonal crystals, reaching a length of 2.5 cm, that occur set in the interstitial material together

with crystallites of iron ore and small clusters of granules of free quartz, which are usually associated with patches of chlorite or zeolite, and in places calcite. Small patches of interstitial material showing a fine grained granophyric texture are also present.

The succeeding sample in the cross-section differs from the previous rock in that it shows a slight increase in the amount of interstitial material present and in that hornblende, replacing pyroxene marginally, now begins to make its appearance in measurable quantities. A marked decrease in grain size characterises specimens collected eastward from here, although the texture remains poikilitic. The pyroxene plates are smaller and turbid, and marginally they are extensively altered to hornblende. Interstitial material diminishes in quantity and for the most part is greyish-brown in colour, although in places it is brownish-pink and composed of acicular crystallites arranged in subradiating to spherulitic groups, rather than crypto-crystalline material. The usual crystallites of iron ore are present in the groundmass and quartz paramorphs after tridymite are also present in the form of long needle-like crystals. Free quartz occurs as granules, often in small aggregates and in places, locally associated with zeolites. Towards the contact these zeolites are more abundant. The texture of the rock at the contact changes once more and becomes intergranular to subophitic.

Textural and mineralogical changes occurring in the Sikwawa River section are essentially similar, with textures ranging from intersertal near the base of the sheet to ophitic in the upper parts. Hornblende, however, is not a major consituent in the upper part of the sheet in this section. Specimens collected from the northern part of the intrusion and again specimens from the small isolated most southerly mass in the Sikwawa River both contain former olivine crystals completely altered to serpentine. Occasionally large irregular fresh crystals were found in the northern portion of the feldspathic gabbro.

(iv) The upper margin of the feldspathic gabbro unit

At the upper margin of the feldspathic gabbro unit of the Komati-poort Intrusion (see section on major intrusives for description), where it is exposed in the bed of the Sihlangula River (see Geological Map), a thin felsite sheet has been intruded between the feldspathic gabbro and the country basalts, producing some striking changes. In the field the feldspathic gabbro appears to grade continuously into a fine-grained pink hybrid rock, which macroscopically resembles a normal granophyric microgranite. The hybrid rock in turn, has a sharp but irregular contact with the adjacent basalt, penetrating the basalt in thin stringers along joint planes and occasionally forming angular patches within the basalt up to a meter from the contact.

In these patches, elongated or tear-drop shaped nodules of quartz occur, usually showing a dark, clearly-defined rim against the enclosing "felsite". In shape and size these nodules resemble amygdales present in the original basalt. At the contact between the basalt and the hybrid rock the basalt, in places, has a pinkish clour over a distance of 1 to 3 cm, although the contact may still be distinguished as a sharp line on the surface of the outcrop.

The pink felsitic hybrid is microcrystalline immediately adjacent to the basalt but becomes coarser in texture and darker in colour as it grades into the feldspathic gabbro.

Petrography

At a distance of 15 m from the contact the feldspathic gabbro appears to be unaffected by the felsite, and as elsewhere in the intrusion, consists of cracked partially sericitised plagioclase laths (68%), which are ophitically to sub-ophitically enclosed in pyroxene plates (13%), with interstitial patches of a brown crypto-crystalline material in which are set apatite needles and crystallites of iron ore, (19%). The pyroxene is extensively altered to a brownish material or to a

light yellow fibrous amphibole, and in places is replaced by patches of iron ore.

In successive samples collected closer to the basalt-hybrid contact, the plagioclase becomes heavily clouded with opaque iron-ore particles that tend to be concentrated along twin and cleavage planes, and simultaneously the margins of the plagioclase crystals are corroded and mantled with a narrow rim of potassium feldspar.

Hybridisation does not appear to have affected the composition of the plagioclase however, and this remains unchanged at around An_{50} right up to the basalt-hybrid contact.

In specimens collected about 15 m from the basalt contact the pyroxene is partly altered to green antigorite but closer to the contact it shows corroded boundaries and is extensively replaced by a green hedenbergitic pyroxene which forms a narrow rim around a core of altered pyroxene or occasionally replaces the original pyroxene in vein-like manner. At the basalt-hybrid contact, none of the original pyroxene remains, and the hedenbergitic pyroxene forms small aggregates of crystals with a mosaic texture. This pyroxene itself is slightly altered to iddingsite, antigorite or fan shaped aggregates of pro-chlorite.

Simultaneously, as the basalt contact is approached fine-grained interstitial material present in the feldspathic gabbro is progressively altered to a network of acicular quartz paramorphs after tridymite, set in a minimal amount of cloudy, brown, fine-grained interstitial material that staining techniques (see section methods), suggest consists predominantly of potassium felspar. The quartz paramorphs frequently form clusters radiating outwards from a central crystal, (see Plate 15, p 191).

(v) Modes

For the railway bridge cross-section, variations in the modal proportions of the three mineral groups (plagioclase, pyroxene and interstitial micropegmatite or glass plus iron ore) are shown in the diagram in fig 31, A, p 208. Fluctuations in mineral proportions along the Sikwawa River section, have been plotted in fig 31, B, p 208. Figure 31,A, clearly shows an increase in interstitial micropegmatite towards the central part of the zone. One of the most striking features of fig31A is the asymmetrical plagioclase concentration curve, showing a high plagioclase concentration near the west of the zone, a low value in the central portion and an intermediate value in the contact rocks in the east. Interstitial micropegmatite varies antipathetically with the plagioclase in the western and central portions of the zone, but like the plagioclase also has a median value in the fine grained eastern contact rocks, while the pyroxene content remains fairly constant throughout.

This is in contrast to the Sikwawa River section, (see fig 31B, p 208), where the plagioclase shows only slightly asymmetrical distribution, although here the pyroxene content varies strongly, ranging from a maximum near the western margin to a minimum at the centre of the sheet and then rising to another peak near the eastern margin before dropping to an intermediate value in the contact rock. The micropegmatite content shows a similar distribution curve to that recorded in the railway bridge section, reaching a maximum at the centre of the zone.

(vi) Mineralogy

(a) Plagioclase

Mineral compositions in the feldspathic gabbro could not be determined in the same detail as in the rest of the Komatipoort Intrusion due to the extensive alteration of the bulk of the rock-forming minerals. In a few specimens the plagioclase is relatively unaltered and in these the

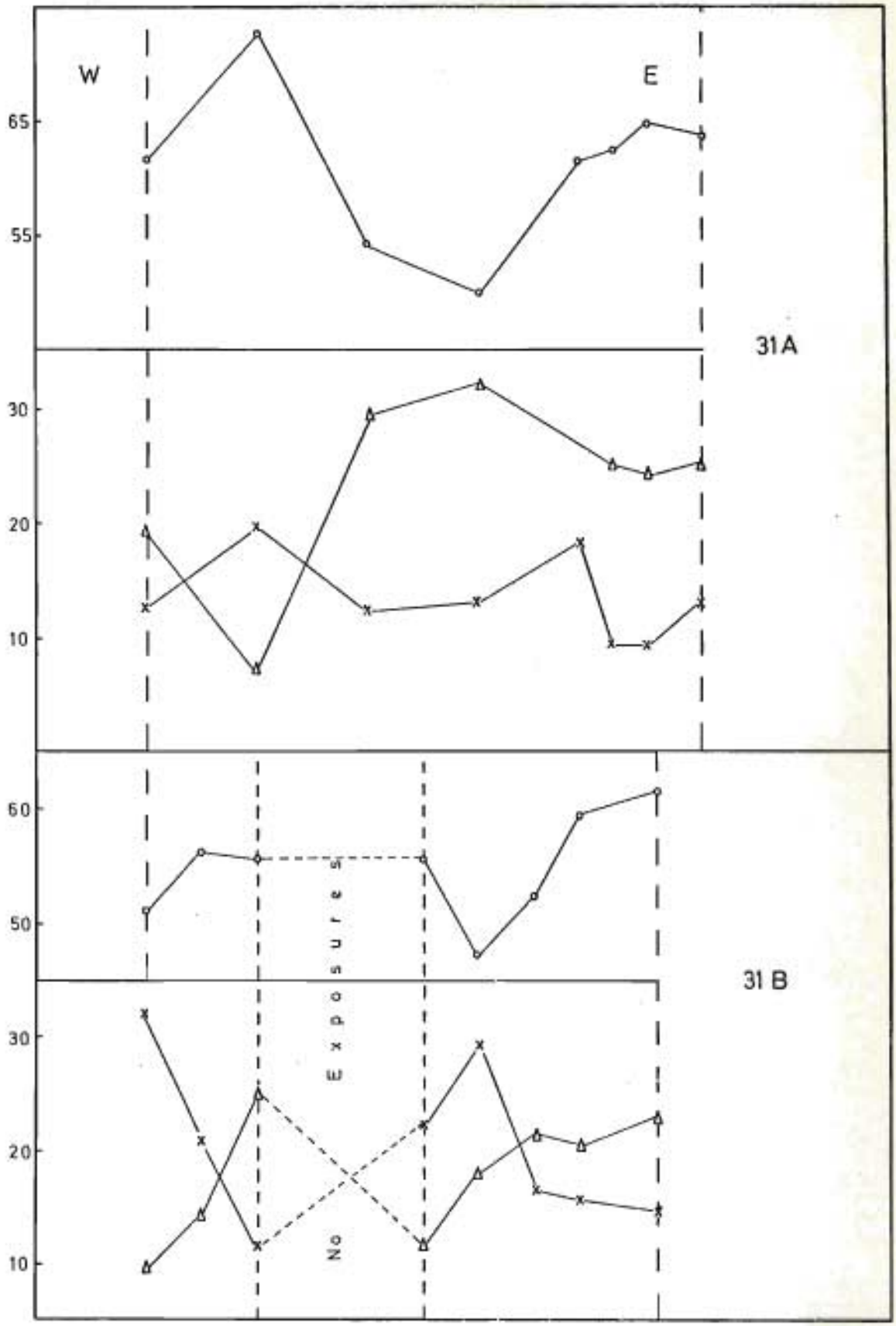

Figure 31. Variation of Modal Proportions in two cross sections of the Feldspathic Gabbro, Komatipoort Intrusion.

o Plagioclase Δ Micropegmatite x Pyroxene

plagioclase commonly has two forms. It occurs as large (2 mm) complexly zoned crystals and as smaller grains showing less complex zoning, that are usually included in the margins of the larger crystals.

The large crystals resemble the first generation plagioclase in the olivine gabbro in that they show a core-oscillatory zoned mantle-rim structure in many cases. The cores which may be embayed to some extent, have a composition around An_{70} in specimens collected from the 'Railway Bridge' section but in samples from the Sikwawa river section occasional crystals with cores as Ca-rich as An_{80} were recorded. Oscillatory zoned mantles usually have a composition of the order of An_{60-70} and the outer margins of the mantles have a composition around An_{65}.

The smaller normally zoned crystals included in the margins of the larger crystals show compositions ranging from near An_{50} in the cores of crystals to around An_{43} at the margins. Complexly zoned phenocrysts with cores of a composition of An_{20} also occur in the fine-grained contact rock in the railway bridge section. The smaller groundmass plagioclases have an intermediate composition around An_{50}.

(b) Pyroxene

The Ca-rich pyroxene shows several changes in texture from West to East across the feldspathic gabbro unit. In the most westerly rocks it forms fairly extensive plates enclosing the plagioclase crystals ophitically to sub-ophitically, in a texture resembling that of the olivine gabbro. Further to the east it occurs as smaller intergranular crystals and near the eastern contact it is present again as more extensive subophitic plates. In the fine grained contact rocks it occurs again as smaller intergranular crystals.

Electron microprobe analyses were made of several pyroxenes from the feldspathic gabbro and these are listed in Table 33,and have also been plotted in the pyroxene quadrilateral in fig.15,p.137.Much of the pyroxene in the feldspathic gabbro is altered and a representative

TABLE 33

Electron microprobe analyses of pyroxenes from the Feldspathic Gabbro, Komatipoort Intrusion

	Pyroxene 1	Pyroxene 2	Pyroxene 3	Pyroxene 4
SiO_2	49,25	50,09	51,22	50,64
CaO	17,24	17,42	17,08	16,90
MgO	12,10	12,05	11,31	11,42
FeO	18,99	18,29	18,89	18,96
Al_2O_3	1,15	1,11	1,25	1,17
MnO	0,50	0,45	0,56	0,48
Na_2O	0,35	0,34	0,27	0,23
TiO_2	0,28	0,33	0,35	0,47
TOTAL	99,86	100,08	100,92	100,28
Fe	30,31	29,46	31,62	31,64
Mg	34,43	34,60	32,78	33,12
Ca	35,25	35,94	35,59	35,23
Cations per 6 oxygens				
Si	1,9171	1,9350	1,9590	1,9513
Al	0,0529	1,97	0,0508	1,9858	0,0562	2,0152	0,0532	2,0137
Ca	0,7190	0,7211	0,7001	0,6979
Mg	0,7023	0,6942	0,6447	0,6562
Fe	0,6128	0,5911	0,6041	0,6112
Ti	0,0083	1,9855	0,0097	2,0561	0,0101	1,9970	0,0135	2,0115
Mn	0,0166	0,0148	0,0180	0,0156
Na	0,0265	0,0252	0,0200	0,0171

All the analysed pyroxenes presented here are from the central portion of the Feldspathic gabbro unit.

set of analyses were not completed. Pyroxenes from near the middle of the unit are zoned from about $Mg_{36}Ca_{35}Fe_{29}$ in the cores of crystals to $Mg_{27}Ca_{36}Fe_{37}$ at the margins.

(c) Minerals present in the 'Vesicles'

Quartz, chlorite, prehnite, calcite and a variety of zeolitic minerals were noted in what appear to be vesicles that are found particularly near the eastern margin of the feldspathic gabbro. Amongst the zeolites identified were thomsonite, natrolite and chabazite.

(d) Ore Minerals

The usual ore minerals found in the volcanic rocks of the Komatipoort area occur in the feldspathic gabbro. These are magnetite, ilmenite, pyrite, and chalcopyrite, in decreasing order of abundance, all of which occur for the most part as irregular interstitial patches. Magnetite is largely martitised to hematite, which in places, contains relict orientated lamellae of ilmenite.

(G) Minor Intrusives

A number of minor intrusives, ranging from dolerites to gabbros, occur associated with Komatipoort Intrusion.

(i) Dolerites

Several small north-east south-west striking dolerite dykes crosscut the Komatipoort Intrusion and are particularly conspicuous where they intrude the Granophyre Zone. They range between ,15 m and 1 m in width and as mentioned in the section on dolerites, appear to occupy a rectangular fracture pattern induced by tension from the south-east. At least two generations of dolerite dykes are present. The older

generation frequently contains feldspar phenocrysts that may be concentrated along the centre of the dyke as a result of flowage differentiation (Bhattacharji 1967). The petrography of the porphyritic aphyric variety has been described in the section on dolerites. For the rest these dolerites resemble the non-porphyritic types previously described.

(ii) Granophyres

Several small granophyre dykes crosscut the granophyric gabbro and the feldspathic gabbro on either of the main granophyre, and are possibly offshoots from it.

(iii) Granophyric Microgranites

Near the southern end of the Komatipoort Intrusion two granophyric microgranite dykes crosscut the lower three units of the Komatipoort Intrusion forming two large masses of contaminated felsite rocks (see Geological Map). These contain large quantities of xenocrysts and xenoliths set in a felsite groundmass. Textures are, in part, similar to those present in the margins of the granophyre unit of the Komatipoort Intrusion.

(iv) Composite Intrusions

An intrusive dyke-like body forms a prominent rockbar crossing the Komati River 1.5 km upstream from its confluence with the Ngweti River. The dyke trends approximately N-S (although both extremities curve slightly towards the west), and can be traced over a distance of almost a kilometer, at an average width of 30 to 50 meters. In spite of the apparent topographical uniformity of the body, it is composite, consisting in part of an initial intrusion of dolerite and, for the rest, of a later mass felsitic material. On the south bank of the Komati River the dyke consists for the most part of felsite with a thin wedge of dolerite along its western margin, but on the

northern bank dolerite is the dominant rock type. This produces a difference in the mode of outcrop on the two banks; on the south bank the resistant felsite forms a low ridge for about 200 to 300 meters, while on the north bank, no marked feature is present.

The dolerite forming the western part of the composite dyke is a hard, black, fine to medium-grained rock crowded with xenolithic blocks of gabbro and large detatched xenocrysts of plagioclase. Its contact with the granophyric gabbro to the west is sharp and clearly defined, but the contact with the felsite to the east is gradational.

Close to the contact with the dolerite the felsite is crowded with partly resorbed and altered phenocryst which become less abundant with increasing distance from the contact. The rock grades into a normal granophyric microgranite which has a sharp contact with the granophyre at its eastern limit, (see Geological Map).

(H) The Metamorphic Aureole of the Komatipoort Intrusion

(i) Metamorphism Adjacent to the Upper Contact

The basalts adjacent to the upper contact of the Komatipoort Intrusion are metamorphosed to a relatively mild degree. Meta-basalts showing the highest grade of metamorphism are present in a narrow zone approximately 15 m wide adjacent to the upper contact, in which rocks of the hornblende hornfels facies are erratically developed, In these, plagioclases are clouded with minute inclusions and show partial, marginal recrystallization, and tiny original pyroxene granules are partially altered to hornblende. The remaining pyroxene is crowded with minute granules of iron ore. Amygdales in the same rocks contain hornblende and recrystallized quartz, in contrast to the amygdales of the adjacent unmetamorphosed basalts in which chlorite and quartz are commonly present. Basalts showing only slight metamorphic effects in the form of a splintery fracture, due to baking, and the presence of small glassy nodules 2 to 3 mm across, are more common.

(ii) Metamorphism Adjacent to the Lower Contact

A band of hornfelsed basalts, is sporadically exposed along the western margin of the olivine gabbro. The hornfelsed basalts are best developed in a low ridge extending south from the banks of the Ngweti River at a point 200 m above its confluence with the Komati River (see Geological Map). A somewhat incomplete cross-section was collected along the banks of the Ngweti, and this was supplemented by samples obtained from sporadic outcrops along the length of the belt.

The hornfelsed basalts are hard, black, fine-grained rocks frequently containing small brownish patches and streaks, often slightly elongated, which in thin section are recognisable as palimpsest amygdales.

Even in thin section, the extremely fine grain of many of the basalts to some extent obscures details of the mineralogical variations across this metamorphosed zone, however somewhat similar changes have occurred in the associated coarser grained dolerites, facilitating the recognition of metamorphic grade. At a distance of some 100 m from the contact, the meta-basalt differs little from the normal unaltered basalts. Plagioclase phenocrysts are cracked and, as is usual in the unaltered basalts in this area, both phenocrysts and groundmass plagioclase are slightly clouded by the development of sericite; in addition the pyroxene in the groundmass is partially replaced by chlorite. Also common are somewhat irregular patches consisting solely of chlorite, (which appear to be altered mafic phenocrysts), and amygdales containing quartz, chlorite and a little zeolitic material.

Samples collected 50 m from the contact contain clear plagioclase phenocrysts that are severely cracked and bent, and enclose much larger inclusions along twin and cleavage planes, the largest inclusions consisting of clinopyroxene occurring together with minor amounts of iron ore in smaller granules. The pyroxene is heavily clouded with iron ore and in some cases, the pyroxene crystals are barely recognisable as such. The iron ore appears to be concentrated towards the centre of

some pyroxenes, particularly along cleavage or other crystallographic planes.

In contrast, a specimen collected from a dolerite dyke intruding the basalt at a similar distance from the contact about 4 km north of this point, consists essentially of biotite, augite, plagioclase and iron ore set in a groundmass of radiating needles of alkali feldspar and quartz. The biotite frequently forms cores to pyroxene crystals which appear to be developing at its expense. These pyroxene crystals are pale green in colour and heavily charged with dusty iron ore. The plagioclase shows signs of severe crushing, often being partly fragmented, and in addition it is clouded with minute inclusions of what appear to be iron ore.

A few meters closer to the contact hypersthene makes its appearance in patches occurring interstitially to the plagioclase. Within these patches of hypersthene, which are frequently finer grained than the surrounding groundmass clinopyroxene, little or no iron ore and magnetite occurs, although plagioclase may be present. Plagioclase crystals in contact with these aggregates of hypersthene granules show a narrow, clear, recrystallised rim. On the inside of this rim a zone crowded with tiny pyroxene and iron ore inclusions is developed. Immediately adjacent to the contact, the basalt display evidence of strong thermal metamorphism. The groundmass of plagioclase and pyroxene is completely recrystallised and has a crystalloblastic or in places a slightly schistose texture.
This groundmass is composed of a mosaic of small clear plagioclase laths with highly irregular boundaries, between which small recrystallised granules of pyroxene and euhedral octahedra of magnetite occur. The pyroxene is usually augite, but in places hypersthene also, may be present. Larger structures such as amygdales and porphyritic plagioclase are preserved but show complete recrystallisation.

The amygdales which are usually present in the basalts show a series of changes corresponding to those occurringin the rock-forming basalt

minerals, as the contact with the Komatipoort intrusion is approached. Rocks containing amygdales were collected only within a distance of a few tens of meters of the lower contact and no specimens showing intermediate or lower grades of metamorphism were found. In the metamorphosed basalts these amygdales commonly contain quarts, agate, epidote, chlorite and zeolite, but adjacent to the contact with the olivine gabbro, a variety of higher temperature minerals are present (Plate 18, p 217). In the most highly metamorphosed rocks the palimpsest amygdales consist, in their simplest form, of a coarse aggregate of augite grains, either alone or together with hypersthene crystals of approximately the same size. In places a small amount of plagioclase of indeterminable composition may occur in addition. More complex amygdales retain their original concentrically zoned structure, typically consisting from the outer layer inwards, of a surrounding zone enriched in small granules or iron ore, followed by a layer composed of an aggregate of coarse pyroxene crystals. This is succeeded by a zone composed of mosaic of recrystallised quarts, which in turn surrounds a core of coarse pyroxene, (augite and hypersthene). The structure and mineralogy of these amygdales is variable, however, and is clearly dependent on the structure and composition of the original amygdales. Less commonly other mineral assemblages may be found in relict amygdales close to the contact, including some showing cores of quartz and orthoclase and more rarely, the assemblage cordierite, orthoclase and garnet.

(I) Modal variations in the Komatipoort Intrusion.

Features of interest in the modal variation diagram, (folder 2, in map pocket), include the presence of olivine at two levels within the clinopyroxene-plagioclase cumulate, and a gradual increase in intersitial micropegmatite in the upper parts of this unit. The granophyre shows a marginal concentration of iron ore, plagioclase and pyroxene and a central high in granophyric matrix material. In the divine gabbro, modes tend to flu-tuate, but in the granophyric gabbro compositions seem reasonably constant. Modal variations in the feldspathic gabbro are discussed in the section on modes,(see p207).

PLATE 18

1. Zoned Palimpsest Amygdale. Rim of iron ore granules, inner zone of clinopyroxene and core of quartz paramorphs after tridymite. (Transmitted light, X60).

2. Unzoned Palimpsest Amygdale. Aggregate of clinopyroxene, orthopyroxene, minor plagioclase and ore, becoming coarser towards the centre. (Several air bubbles are present in the photomicrograph). (Transmitted light, X60).

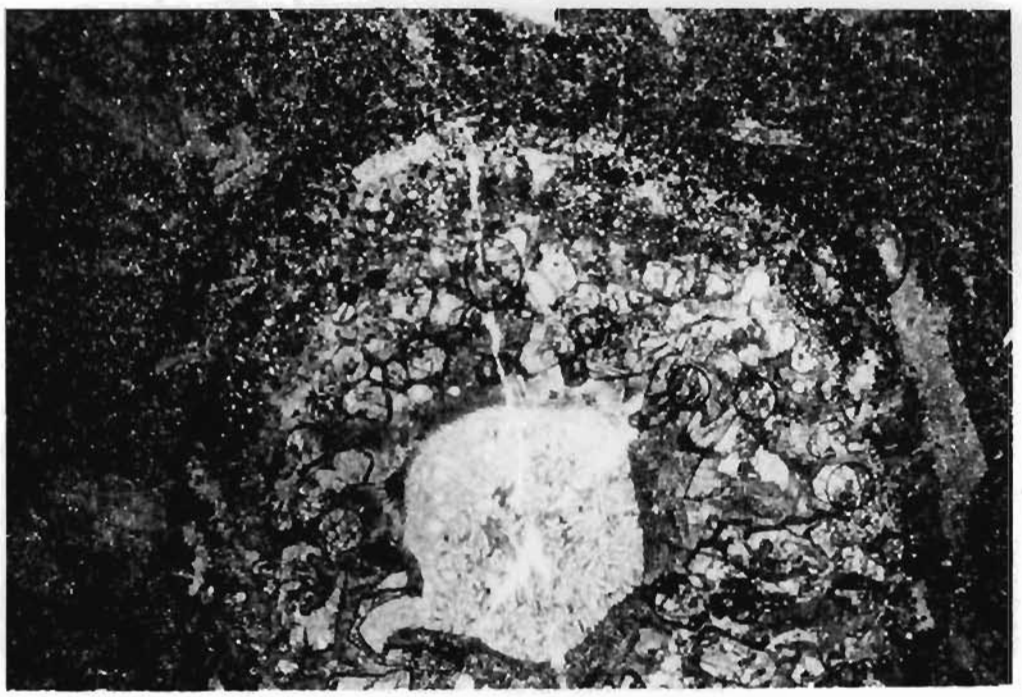

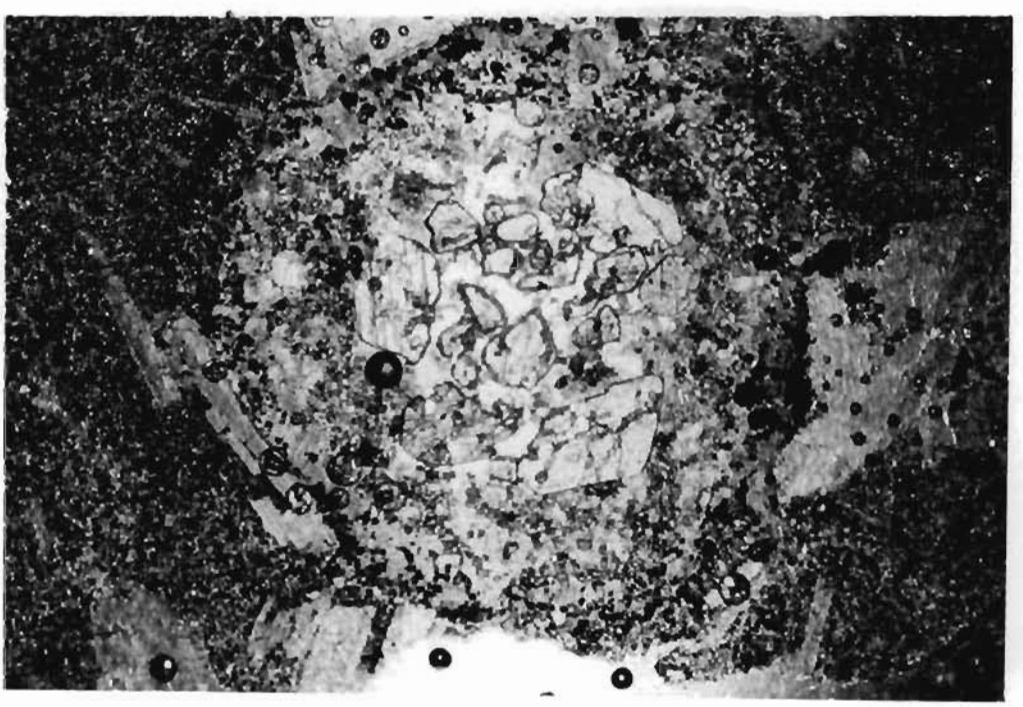

(J) Variation in pyroxene composition in the Komatipoort Intrusion

As noted in earlier sections, the compositions of the Ca-rich clinopyroxenes in the Komatipoort Intrusion, vary widely, ranging from $Ca_{39}Mg_{46}Fe_{15}$ to $Ca_{43}Mg_{4}Fe_{53}$. In Fig 15 , the compositions of these pyroxenes have been plotted in the pyroxene quadrilateral, allowing a generalised Ca-rich pyroxene crystallisation path to be defined. This closely approximates the generalised crystallisation path of the Ca-rich pyroxenes from strongly fractionated tholeiitic intrusions such as, for example, the Bushveld Complex, the Skaergaard Intrusion, and the Birds River Complex.

Examination of the Komatipoort trend in detail however, shows that the points representing Ca-rich pyroxenes have a tendency to cluster together in groups along, or adjacent to, the generalised crystallisation path. The Ca-rich pyroxenes of the olivine gabbro and the feldspathic gabbro plot above the crystallisation path for example, and appear to be slightly enriched in Ca compared with the augites of the clinopyroxene-plagioclase cumulate. Together they could be interpreted as defining a separate, short, mild iron-enrichment trend. It should be noted however, that comparisons of compositions of the pyroxenes from the olivine gabbro and the feldspathic gabbro are of limited value as the feldspathic gabbro pyroxene compositions are from one sample only. . The Ca-rich pyroxenes of the clinopyroxene-plagioclase cumulate and the most Mg-rich augites of the granophyric gabbro, on the other hand, may be interpreted as lying on a roughly parallel mild iron-enrichment trend, with a slightly lower Ca-content. This trend is relatively poorly defined, as insufficient analyses are available of the most Mg-rich ferro-augites from the granophyric gabbro.

The Ca-poor minimum in the generalised compositional path (see fig 15), lies approximately midway through the compositional range of the Ca-rich pyroxenes of the granophyric gabbro. In Table 31 , the

pyroxene represented by analysis no. 3 occurs as a mantle around a Ca-poor pyroxene with a composition represented by analysis 14 in the same table. This pyroxene (analysis 3) lies closest to the Ca-poor minimum in the generalised crystallisation path in fig 15 , of any of the analysed Ca-rich pyroxenes. Both the orientation of the tie-line joining the points representing analyses 3 and 14 (Table 31), and a comparison of the compositions of these two pyroxenes however, suggests they are unlikely to represent an equilibrium pair.

The rest of the Ca-rich pyroxenes of both the granophyric gabbro and the granophyre, plot in a group towards the Fe-rich end of the generalised crystallisation path. Some compositional overlap between the Ca-rich pyroxenes of the two rock types is suggested by similarities in both major and minor element composition, e.g. compare pyroxene analysis 1, from the granophyre (see Table 32 and fig 15), and the ferroaugites of the granophyric gabbro, (see Table 31 and fig 15). These compositional similarities plus textural considerations, however, suggest the possibility that this pyroxene (analysis 1 from the granophyre - see Table 31), represents a xenocryst from the granophyric gabbro, caught up in the granophyre. The rest of the analysed pyroxenes from these two rock types (see Tables 31 and 32), differ in major element chemistry as indicated by the fact that the granophyric gabbro pyroxenes are largely brown ferroaugites and the granophyre pyroxenes are mostly deeper brown ferrohedenbergites (see fig 15). As may be seen from fig 16 and fig 17 differences in minor element chemistry are present as well. If cognisance is taken of the relative degree of iron enrichment of these pyroxenes, it is found that the ferrohedenbergites of the granophyre, (excluding granophyre pyroxene analysis 1) are relatively enriched Ti and Al, compared with the ferroaugites of the granophyric gabbro, (compare Tables 31 and 32 , see fig 32).

There are certain textural similarities between the pyroxenes from these two rock types, namely, both show the presence of discontinuous

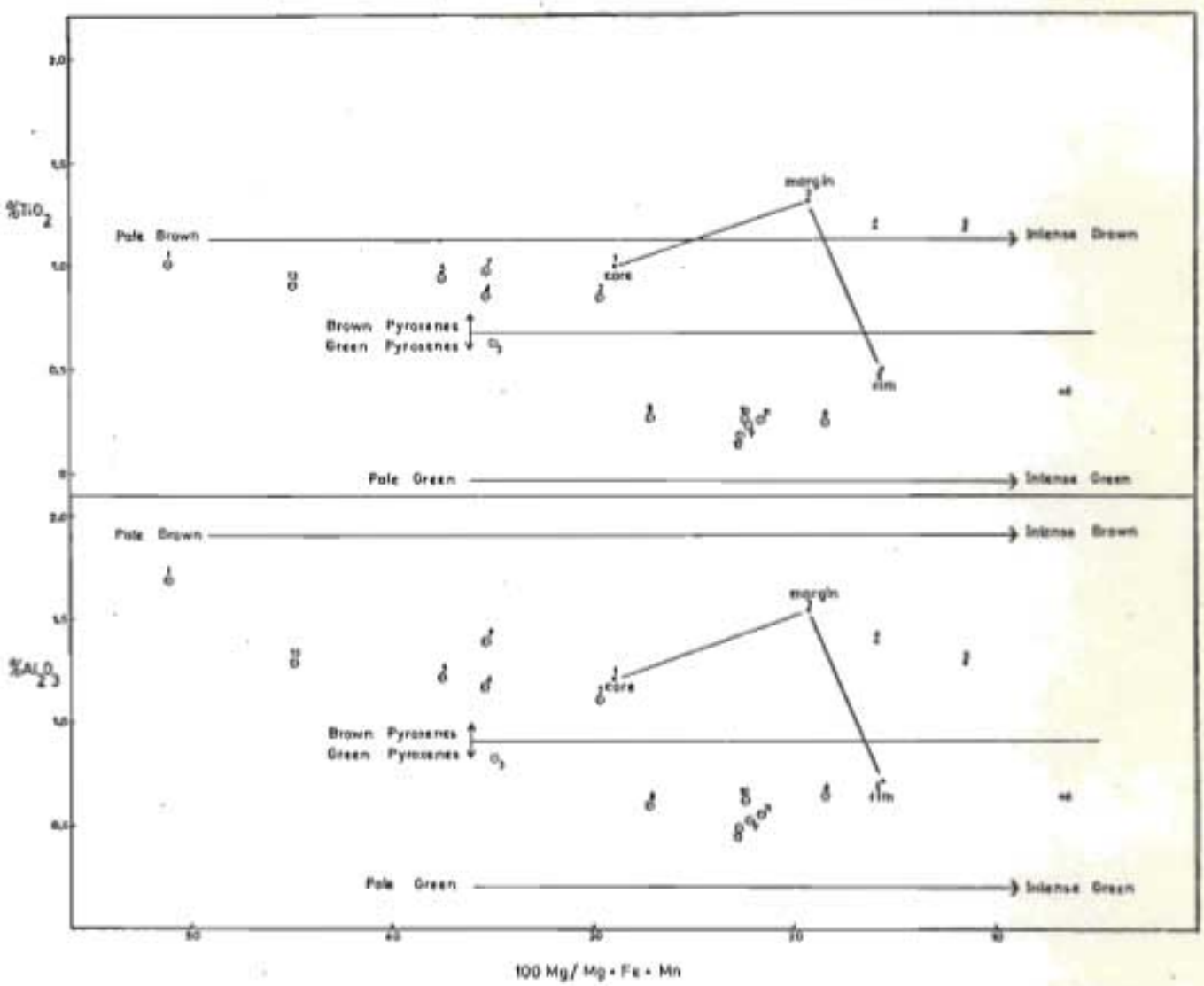

Figure 32. Variation in Al and Ti content with Mg Index for Pyroxenes of the Granophyric Gabbro and the Granophyre.

o Ca-rich pyroxenes from the granophyric gabbro
• Ca-rich pyroxenes from the granophyre

rims and marginal patches of a green pyroxene, which is itself, in places, rimmed by a green amphibole. Several of the pyroxene analyses in Tables 31 and 32 represent this marginal green pyroxene. As may be seen from fig 32, notable differences in minor element chemistry exist between the green and brown pyroxenes in both rock types. Specifically the green pyroxenes tend to have lower Ti and Al contents than the brown pyroxenes. Differences in major element composition include higher Ca, Si and Fe values in the green Ca-rich pyroxenes, (see Tables 31 and 32). The intensity of the colour of both green and brown pyroxenes diminishes with decreasing Fe content and pyroxene 3 from the granophyric gabbro, (see Table 31 and fig 32) is an intermediate greenish-brown colour.

Associated green and brown ferrohedenbergites have also been described from the Skaergaard Intrusion (Wager and Deer 1939, Brown and Vincent 1963, Nwe and Copley 1975), although these pyroxenes are on average far more Fe-rich than the pyroxenes discussed here. However with the exception of Fe-content they display differences in major and minor element chemistry, (Nwe and Copley, 1975) which parallel those present in the green and brown pyroxenes of the Komatipoort Intrusion, (see above). Some of the green pyroxene in the Skaergaard ferrodiorites have originated by inversion of ferrowollastonite, but this origin cannot be considered for the relatively Mg-rich, strainfield-free, green pyroxenes described here. If the green and brown ferroaugites and ferrohedenbergites are plotted as such, into the pyroxene quadrilateral, the green pyroxenes appear to define a separate crystallisation path,(fig 33), slightly enriched in Ca. This path lies close to the sub-solidus trend line defined by Nwe (1976), for Ca-rich pyroxene of the Skaergaard Intrusion, lying in the Fs-rich region of the pyroxene quadrilateral, which suggests that the green pyroxenes from the granophyric gabbro and the granophyre could also represent sub- solidus compositions. The sub-solidus pyroxenes determined by Nwe (1974), however showed exsolution lamellae of pigeonite, which became finer with increasing Fe content of the pyroxenes, making subsolidis compositions progressively more difficult to obtain.

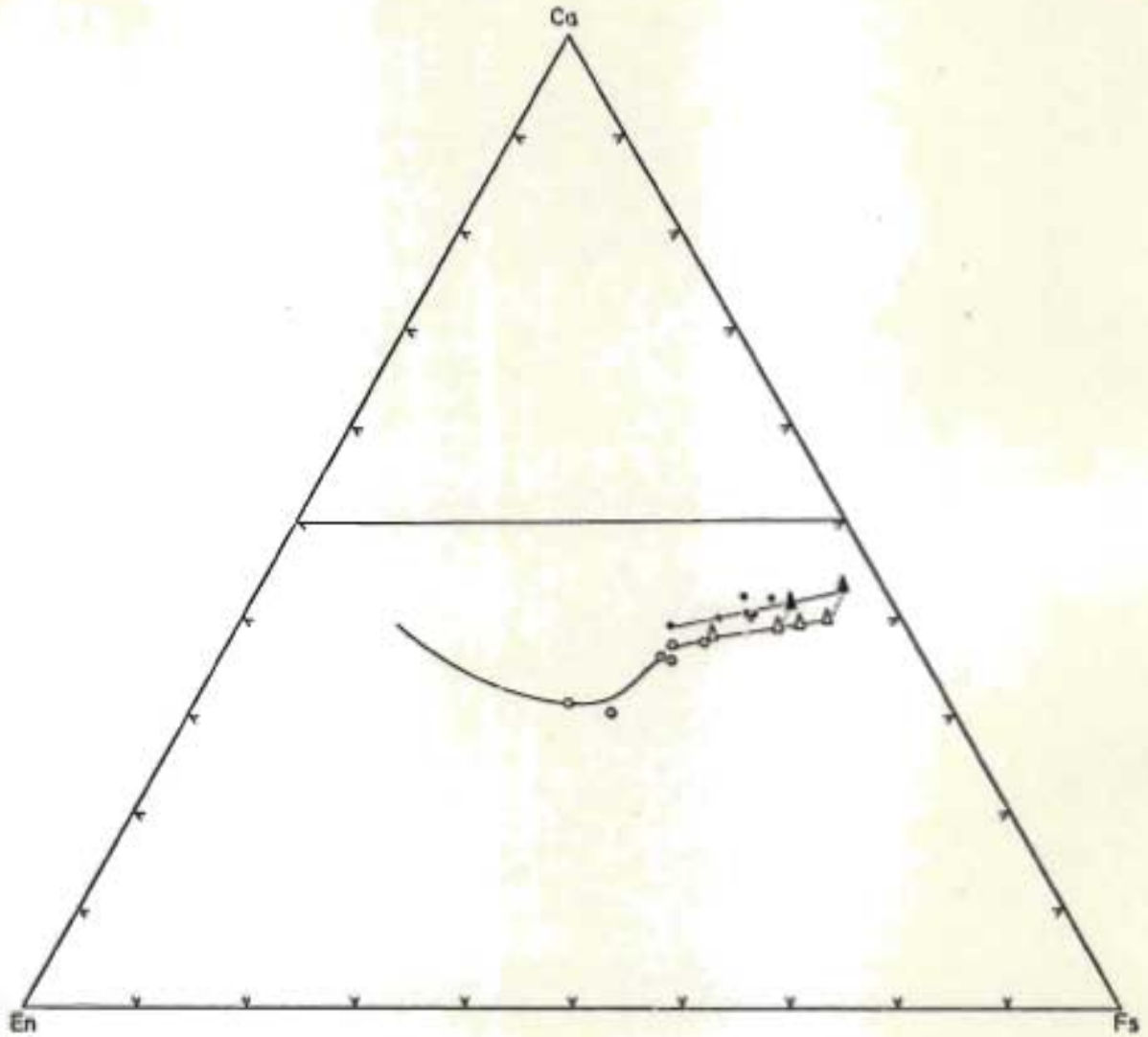

Figure 33. Generalised compositional trend for green pyroxenes and brown pyroxenes from the Granophyric Gabbro and Granophyre units of the Komatipoort Intrusion.

Granophyric Gabbro
- • Green pyroxenes
- o Brown pyroxenes

Granophyre
- ▲ Green pyroxenes
- △ Brown pyroxenes
- \ Tie lines

The green pyroxenes from the granophyre and the granophyric gabbro contain no microscopically detectable exsolution lamellae. If pigeonite lamellae of submicroscopic proportions were present, solidus rather than subsolidus compositions would be expected on analysis with a relatively diffuse microprobe beam, which again was found not to be the case. In addition, green and brown pyroxene representing pyroxene with and without exsolved pigeonite would be expected to lie on a coexisting pigeonite-augite tie line. From the orientation of the tie lines joining the brown and green ferrohedenbergites of the granophyre, (see fig 33), this does not appear to be the case.

Thus the green pyroxenes described here, for the reasons given above, do not appear to represent either the inversion product of a ferrowollastonite, or a subsolidus pyroxene produced by the exsolution of pigeonite.

Another possibility is suggested by the gradational nature of the transition from the brown to the green pyroxenes in the granophyric gabbro, and the apparent compositional relationship between a marginal green pyroxene and its brown counterpart, (see Tables 31 and 32, fig 32 and fig 33). These observations, together with the fact that the green ferroaugites of the granophyric gabbro tend to be enriched in iron relative to the associated brown ferroaugite, suggest that the green pyroxenes represent a sub-solidus re-equilibration product, resulting from interaction between a late stage, lower temperature residual fluid phase and the pre-existing Fe-rich pyroxenes in both the granophyre and the granophyric gabbro. This has produced a series of sub-solidus compositions. Differences in colour would be largely related to relative contents of Ti and Fe (see fig 32), although oxidation states may also be important.

(K) Major element chemistry of the Komatipoort Intrusion

(i) Unit 1 - The olivine gabbro

Chemical analyses of eight specimens of olivine gabbro are listed in Table 34 , p 225 . Five of these samples were collected along the Sihlangula Stream section, (see geological map). and encompass the full range of textures described from this part of the unit, (see section on petrography, p 117). The other three analysed specimens, collected along the Ngweti River section, represent typical olivine gabbro from the lower and middle parts of the unit, in this section. In general, the analyses of all these specimens show fairly low SiO_2, K_2O, P_2O_5 and to a lesser extent TiO_2, and relatively high MgO, Al_2O_3 and CaO. In Table 34 , p 225 , it may be seen that the average composition of the olivine gabbro in the Sihlangula Stream section of the Komatipoort Intrusion, closely resembles that of the average rock from the LZ_a of the Skaergaard Intrusion, (a plagioclase-olivine-cumulate). Differences in chemistry between the two averages could be explained largely in terms of differences in plagioclase content. When examined individually the analyses listed in Table 35 , p 226, show some fluctuation in Mg:Fe ratio ; this variation is caused largely by fluctuations in the relative proportions of olivine and pyroxene. The fine-grained, lineated, hornfels-textured rocks at the base of unit 1 on the Sihlangula Stream section, (analysis CL 1 , Table 34 , p 225), has a similar major element chemistry to the other analysed olivine gabbro samples, and this fact, coupled with the gradational variations in texture described in the section on petrography (see p 117), provides evidence that these lineated rocks should be regarded as the hornfelsed equivalent of the base of the olivine gabbro unit, rather than a metamorphosed olivine-rich basalt coincidentally interbedded with other basalts at the basal contact of the intrusion.

TABLE 34

MAJOR ELEMENT ANALYSES FOR EIGHT SPECIMENS OF OLIVINE GABBRO FROM THE KOMATIPOORT INTRUSION

	CL1[1]	CL2[1]	CL3[1]	CL4[1]	CL5[1]	CL35[2]	CL36[2]	CL49[3]
SiO_2	44,45	47,41	46,66	48,37	47,97	49,21	48,35	48,42
Al_2O_3	17,59	18,87	14,48	16,94	17,42	19,42	18,20	18,00
Fe_2O_3	2,49	2,23	1,22	2,18	1,03	7,69	10,40	9,92
FeO	10,80	8,06	12,30	9,28	6,76	nd	nd	nd
MgO	10,48	7,55	12,08	6,30	9,40	6,75	9,20	9,61
CaO	9,66	11,52	9,87	10,92	14,10	13,94	12,30	11,83
NaO_2	1,84	1,96	1,73	2,43	1,59	2,13	1,84	1,94
K_2O	0,14	0,28	0,23	0,32	0,12	0,19	0,28	0,3
H_2O^-	0,19	0,14	0,11	0,17	0,09	0,143	0,055	0,08
H_2O^+	1,16	1,09	1,07	0,93	0,88	nd	nd	nd
S	nd[5]	nd	nd	nd	nd	0,005	0,009	nd
CO_2	0,18	0,22	0,21	0,20	0,17	nd	nd	nd
LOI[6]	nd	nd	nd	nd	nd	0,005	0,000	0,007
TiO_2	1,00	0,90	0,48	1,06	0,52	0,44	0,57	0,65
P_2O_5	0,10	0,12	0,12	0,15	0,08	0,03	0,09	nd
MnO	0,16	0,15	0,21	0,18	0,13	0,11	0,14	0,11
TOTAL	100,24	100,50	100,77	99,43	100,26	100,063	101,434	100,867

- 1 Analyst - National Institute for Metallurgy
- 2 Analyst - University of Cape Town, Professor Erlank
- 3 Analyst - C. Logan
- 4 Total Fe expressed as Fe_2O_3
- 5 nd - not determined
- 6 LOI - loss on ignition

CL1 - CL5 Cross-section of the olivine gabrro in the Sihlangula Stream section (CL1 - Base, CL5 - Top)

CL35, CL36, CL49-

Table 35

Comparison of 1) Average rock (plagioclase-olivine-cumulate) from the Skaergaard Intrusion LZ_a with 2) Average olivine-gabbro from the Sihlangula Stream section of the Komatipoort intrusion, (average of analyses CL 1 to CL 5)

	1	2
SiO_2	45,48	46,97
Al_2O_3	16,41	17,06
Fe_2O_3	2,09	1,83
FeO	9,29	9,44
MgO	11,65	9,76
CaO	10,45	11,21
Na_2O	2,06	1,91
K_2O	0,27	0,22
H_2O^+	0,77	1,03
H_2O^-	0,26	0,14
TiO_2	0,94	0,80
P_2O_5	0,05	0,11
MnO	0,06	0,17
Total	99,79	100,65

(ii) Unit 2 - The clinopyroxene-plagioclase cumulate

Major element analyses of six samples of clinopyroxene-plagioclase cumulate are listed in Table 36 , p 228 . These analyses are representative of the lower and middle parts of unit 2 only, as specimens suitable for analysis were unobtainable from the upper part of the unit at the time that the geochemistry of the intrusion was investigated. Analysis CL 37 represents the composition of a sample of unit 2 collected close to the contact with the olivine gabbro. Samples at this point are contaminated with apparent xenocrysts and micro-xenoliths of olivine gabbro, as described in the section on petrography, (see p 142). The major element analysis of this rock, however, compares well with that of the typical clinopyroxene-plagioclase cumulate from the lower-middle parts of unit 2, (compare analyses CL 6 and CL 37 in Table 36). Analyses CL 38 and CL 39 represent magnetite-rich samples from the upper-middle parts of unit 2, and this enhanced magnetite content is reflected in the increased iron and titanium values in these analyses.

(iii) Unit 3 - The granophyric gabbro

Eight major element analyses of specimens of granophyric gabbro, are listed in Table 37 , p 229, and these form a cross-section of unit 3, collected along the course of the Komati River. The analyses show relatively mild enrichment in SiO_2 and Al_2O_3 and are actually slightly poorer in $FeO + Fe_2O_3$ than the analysed dolerites listed in Table 16 , p 51 . The presence of fairly low MgO contents however gives the rocks distinctly lower Mg:Fe ratios than the analysed dolerites from the Komatipoort area. In this sense the granophyric gabbro samples could be described as ferrogabbros. They show notable compositional similarities to the ferrogabbros from the Birds River Complex (Eales and Robey, 1976) listed in Table 38 for comparison, which are considered to have formed by the in situ differentiation of Karroo-age gabbro. A detailed comparison of the analyses in Tables 37 and 38, shows that the Komatipoort rocks in general tend to be lower in MgO and TiO_2 and higher in K_2O and P_2O_5, than the ferrogabbro from the Birds River Complex.

TABLE 36

MAJOR ELEMENT ANALYSES FOR SIX SAMPLES OF CLINOPYROXENE-PLAGIOCLASE CUMULATE FROM THE KOMATIPOORT INTRUSION

	CL6[1]	CL7[1]	CL37[2]	CL38[2]	CL39[2]	CL50[3]
SiO_2	50,53	49,90	50,52	47,21	47,29	50,8
Al_2O_3	13,94	15,40	13,95	11,24	11,34	12,75
Fe_2O_3	2.57	2,61	14,36[4]	20,65[4]	20,10[4]	14,60[4]
FeO	10,49	8,78	nd	nd	nd	
MgO	5,67	5,50	5,67	4,54	4,44	4,58
CaO	10,81	11,62	10,61	9,20	0,13	11,90
Na_2O	2,46	2,34	2,37	2,26	2,26	2,00
K_2O	0,76	0,46	0,79	0,93	0,98	0,88
H_2O^-	0,14	0,13	0,209	0,229	0,237	0,243
H_2O^+	0,89	0,93	nd	nd	nd	nd
S	nd[5]	nd	0,017	0,116	0,120	nd
CO_2	0,25	0,24	nd	nd	nd	nd
LOI[6]	nd	nd	0,017	0,000	0,000	0,015
TiO_2	1,61	1,56	1,51	3,34	3,41	1,65
P_2O_5	0,44	0,25	0,36	0,38	0,41	nd
MnO	0,23	0,20	0,23	0,29	0,28	0,28
TOTAL	100,79	99,92	100,613	100,385	99,997	99,698

1 - Analyst:- National Institute for Metallurgy
2 - Analyst:- University of Cape Town, Professor Erlank
3 - Analyst:- C. Logan
4 - Total Fe expressed as Fe_2O_3
5 - nd = not determined
6 - LOI = loss on ignition

CL6, CL7, CL50 - lower middle clinopyroxene-plagioclase cumulate unit
CL37 - lower contact of the clinopyroxene-plagioclase cumulate
CL38, CL39 - Upper middle clinopyroxene-plagioclase cumulate

TABLE 37

MAJOR ELEMENT ANALYSES FOR EIGHT SAMPLES OF GRANOPHYRIC GABBRO FROM THE KOMATIPOORT INTRUSION

	CL8[1]	CL9[1]	CL10[1]	CL24[1]	CL41[2]	CL42[2]	CL51[3]	CL52[3]
SiO_2	52,88	53,34	52,34	52,88	51,32	51,70	52,01	53,04
Al_2O_3	14,42	14,93	14,34	13,70	14,31	14,30	14,50	13,67
Fe_2O_3	3,81	4,55	4,49	4,38	16,18[4]	16,14[4]	15,98[4]	16,35[4]
FeO	8,86	8,35	9,62	9,79	nd[5]	nd[5]	nd[5]	nd[5]
MgO	1,72	1,51	1,75	1,94	1,87	2,08	1,76	1,63
CaO	7,06	7,23	7,67	7,95	7,18	7,62	8,40	7,42
Na_2O	2,85	2,85	2,82	2,91	2,81	2,86	2,98	2,78
K_2O	1,74	1,83	1,47	1,43	1,46	1,54	1,79	1,82
H_2O^-	0,43	0,31	0,44	0,42	0,469	0,452	0,28	0,39
H_2O^+	1,58	1,54	1,47	1,09	nd[5]	nd[5]	nd[5]	nd[5]
S	nd[5]	nd[5]	nd[5]	nd[5]	0,216	0,105	nd[5]	nd[5]
CO_2	0,45	0,52	0,84	0,20	nd	nd	nd[5]	nd[5]
LOI[6]	nd[5]	nd[5]	nd[5]	nd[5]	1,07	0,335	0,76	0,53
TiO_2	1,77	1,50	1,81	2,09	1,93	2,14	1,67	1,82
P_2O_5	0,79	0,62	0,69	0,88	1,01	0,92	nd[5]	nd[5]
MnO	0,23	0,24	0,28	0,26	0,24	0,25	0,23	0,24
TOTAL	98,59	99,32	100,03	99,92	100,065	100,442	100,36	99,69

1 - Analyst:- National Institute for Metallurgy
2 - Analyst:- University of Cape Town, Professor Erlank
3 - Analyst:- C. Logan
4 - Total Fe expressed as Fe_2O_3
5 - nd - not determined
6 - LOI - loss on ignition

TABLE 38

TWO SELECTED ANALYSES OF FERROGABBRO FROM THE BIRDS RIVER COMPLEX (from Eales and Robey, 1976)

	1	2
SiO_2	54,6	52,2
Al_2O_3	11,3	13,2
Fe_2O_3	9,8	4,6
FeO	6,0	10,1
MgO	2,3	3,2
CaO	5,0	7,7
Na_2O	2,78	2,99
K_2O	2,16	1,34
H_2O	2,4	0,8
CO_2	0,1	nd
TiO_2	2,0	2,4
P_2O_5	0,82	0,35
MnO	0,2	0,2
TOTAL	99,5	99,1

1 Birds River Complex - Fractionated derivative of the porphyritic suite. (Eales and Robey, 1976, p 104, Table 1, analysis 5)

2 Birds River Complex - Ferrogabbro with interstitial mesostasis. (Eales and Robey, 1976, p 104, Table 1, analysis 4)

(iv) Unit 4 - The Granophyre

Table 29, p 231, lists major element analyses of nine samples from unit 4. These include an analysis of the 'grey granophyre', mentioned in the section on petrography, (see p 189), and two samples of the finer-grained contact rocks present at the boundary between the granophyric gabbro and the granophyre. Together the analysed samples,which were collected along the bed of the Komati River, provide a cross-section of the granophyre. Major and trace element data suggest the grey granophyre may represent a metasomatised xenolith of granophyric gabbro, or possibly feldspathic gabbro caught up in the granophyre (see later) and the sample is listed as such in the index to Table 29, p 231. The granophyre of the Komatipoort Intrusion is in some respects, compositionally similar to the more siliceous differentiates of other tholeiitic intrusions. In terms of most major elements, it closely resembles certain differentiated rocks of the Birds River Complex, (i.e. those termed ' fractionated derivatives of the porphyritic suite' by Eales and Robey, 1976). Textural differences are apparent, however, between the Birds River Complex rocks and the Komatipoort intrusion granophyre, as the Birds River Complex differentiates have a glassy to microcrystalline groundmass.

Analyses of several differentiates from various basic intrusives are listed in Table 40, p 232, for comparitive purposes. The Komatipoort granophyre is clearly low in SiO_2 relative to other granophyres proper, and justification for terming the rock a granophyre must be given on textural rather than compositional grounds, as is the case also for the granophyric gabbro of unit 3. Despite generally lower SiO_2 contents, similarities are apparent in the analyses compared in these tables. Analysis 1, Table 40, (Birds River Complex), and analyses CL11 and CL23, Table 39, (Komatipoort intrusion), show strong similarities, as do analyses 3 and 4, Table 40, (Birds River Complex) and analyses CL12, Table 39, (Komatipoort intrusion).

Table 39

MAJOR ELEMENT ANALYSES OF NINE SAMPLES FROM THE GRANOPHYRE UNIT, KONATIPOORT INTRUSION

	CL11[1]	CL12[1]	CL32[1]	CL43[2]	CL45[2]	CL48[2]	CL53[3]	CL44[2]	CL23[1]
SiO_2	55,45	62,71	62,18	54,09	57,16	61,62	61,52	53,27	54,42
Al_2O_3	11,01	11,46	11,40	15,82	11,65	11,44	11,53	10,74	10,52
Fe_2O_3	4,81	4,79	3,63	13,37	15,67	14,00	14,37	19,75	4,67
FeO	10,77	6,98	8,49	nd[5]	nd[5]	nd[5]	nd[5]	nd[5]	12,98
MgO	0,96	0,48	0,40	1,12	1,15	0.48	0,51	1,30	1,50
CaO	5,27	3,81	4,17	6,63	4,55	4,05	4,06	5,70	6,18
Na_2O	2,76	3,35	2,86	3,12	2,93	2,77	2,81	2,16	2,59
K_2O	2,36	3,47	3,50	1,71	2,76	3,60	3,62	1,96	1,75
H_2O^-	0,50	0,27	0,06	0,247	0,500	0,249	0,35	0,400	0,41
H_2O^+	2,17	0,99	1,35	nd[5]	nd[5]	nd[5]	nd[5]	nd[5]	1,39
S	nd[5]	nd[5]	nd[5]	0,349	0,054	0,059	nd[5]	0,195	nd[5]
CO_2	1,38	0,22	0,20	nd[5]	nd[5]	nd[5]	nd[5]	nd[5]	0,33
LOI[6]	nd[5]	nd[5]	nd[5]	1,24	0,093	0,342	0,08	1,55	nd[5]
TiO_2	1,69	1,08	1,20	1,54	1,74	1,16	1,34	1,97	2,13
P_2O_5	0,47	0,20	0,23	0,56	0,57	0,28	nd[5]	0,72	0,80
MnO	0,30	0,26	0,28	0,24	0,262	0,25	0,28	0,20	0,35
TOTAL	99,90	100,07	99,95	100,036	99,089	100,30	100,47	99,915	100,02

1 - Analyst - National Institute for Metallurgy; 2 - Analyst - University of Cape Town, Professor Erlank; 3 - Analyst - C. Logan; 4 - Total Fe expressed as Fe_2O_3; 5 - nd - not determined; 6 - LOI - loss on ignition;

TABLE 40

ANALYSES OF FRACTIONATED ROCKS FROM SOME THOLEIITIC INTRUSIONS

	1*	2*	3	4	5	6*
SiO_2	57,5	66,5	55,10	57,30	64,39	65,0
Al_2O_3	11,0	11,8	9,90	11,13	12,37	11,8
Fe_2O_3			4,75	5,15	3,41	
FeO	15,1	9,1	15,14	11,75	6,74	10,4
MgO	1,5	0,7	0,13	0,81	0,31	0,7
CaO	6,1	3,5	7,76	4,83	3,67	4,3
Na_2O	3,3	3,5	3,86	3,51	4,30	3,0
K_2O	2,3	3,5	1,00	1,83	2,33	3,0
H_2O			1,12	1,42	1,36	
TiO_2	2,2	1,0	1,16	1,42	0,92	1,4
P_2O_5	0,8	0,2	0,24	0,35	0,09	0,2
MnO			0,14	0,28	0,21	
Other	0,2	0,2			0,2	0,2
TOTAL	100,0	100,0	100,3	99,78	100,30	100,0

* All Fe expressed as FeO and totals recalculated to 100% on H_2O and CO_2 - free basis by Eales and Robey (1976)

1) Birds River Complex - Porphyritic fayalite-bearing derivatives with microcrystalline to glassy groundmass,
2) (Eales and Robey, Table 2, p 105)
3 Transitional Granophyre, Sydtoppen, Skaergaard (Wager and Brown, 1968, p 158, 4489)
4 Ferrodiorite, Sandwich Horizon, Skaergaard, (Wager and Brown, 1968, p 158, 4330)
5 Melanogranophyre, U B G , Skaergaard, (Wager and Brown, 1968, 5264)
6 Fayalite Hedenbergite Granophyre, New Amalfi Sheet, (Poldervaart 1944)

These analyses effectively span the full range of compositional variation found in the granophyre of the Komatipoort intrusion.

The analysis of the 'grey granophyre', (Table 39 , p 232), is exceptional in that it differs from the other analysed Komatipoort intrusion granophyres in its noticeably higher Al_2O_3 and CaO contents, amongst other features. The major element composition of the 'grey granophyre' compares well with the most silica rich of the analysed granophyric gabbro samples listed in Table 37 , p 229 , (Analysis CL 9).

(v) Unit 5 - The feldspathic gabbro

A total of six analyses of the gabbro that composes unit 5 are shown in Table 41 , p 235 . Three of these analyses, (CL 14 , CL 26 , and CL 46 , Table 41), are of samples from the relatively fine-grained easterly margin of the unit, (described in the section on petrography, p 201), and one of the remaining analyses (CL 27 , Table 41) represents a specimen from what is considered to be a large xenolith of feldspathic gabbro, present at the contact between the granophyric gabbro and the granophyre. The remaining two analysed specimens were collected from the lower and middle part of unit 5, respectively. All of the analysed specimens were collected along a cross-section of the unit provided by the course of the Komati River, upstream from the Railway Bridge, (see geological map). An analysis of a feldspathic olivine gabbro from the Birds River Complex (Eales and Robey 1976), is also listed in Table 41 , p 234 , for comparitive purposes. There are similarities between this analysis and some of the analysed rocks of unit 5, (CL 27 and CL 40 , Table 41), despite the fact that the major rock forming minerals in the feldspathic gabbro from the Komatipoort intrusion show signs of alteration, (see section on petrography, p 201). Differences in chemistry between the Birds River Complex and Komatipoort analyses could be ascribed largely to variations in the amount of olivine, plagioclase and interstitial mesostasis

TABLE 41

MAJOR ELEMENT ANALYSES OF SIX SPECIMENS OF FELDSPATHIC GABBRO FROM THE KOMATIPOORT INTRUSION (A - F)

	A CL27[1]	B CL40[2]	C CL13[1]	D CL14[1]	E CL26[1]	F CL46[2]	G	
SiO_2	52,33	50,62	52,15	55,95	57,16	57,60	52,1	
Al_2O_3	19,27	17,36	16,10	18,22	17,70	15,13	17,0	
Fe_2O_3	1,63	12,59[3]	3,16	1,91	3,65	19,07[3]	1,6	
FeO	7,30	nd[4]	8,46	5,38	3,89	nd[4]	8,1	
MgO	1,78	2,75	2,20	1,57	1,68	2,40	4,9	
CaO	9,74	8,82	6,81	7,41	7,23	6,88	9,9	
Na_2O	3,21	2,97	3,17	3,40	3,02	3,26	2,27	
K_2O	1,29	1,29	2,56	2,12	2,59	3,00	0,76	
H_2O^-	0,26	0,209	0,31	0,35	0,36	0,228	) 1,5	
H_2O^+	1,24	nd[4]	1,68	2,07	1,20	nd[4]		
S	nd[4]	0,259	nd[4]	nd[4]	nd[4]	0,056	nd[4]	
CO_2	0,29	nd[4]	0,20	0,18	0,16	nd[4]	nd[4]	
LOI[5]	nd[4]	1,390	nd[4]	nd[4]	nd[4]	1,390	nd[4]	
TiO_2	1,23	1,60	1,71	1,00	1,01	1,01	1,4	
P_2O_5	0,31	0,43	0,58	0,34	0,28	0,32	0,30	
MnO	0,18	0,18	0,20	0,13	0,16	0,15	0,1	
TOTAL	100,06	100,48	99,29	100,03	100,09	100,49	99,93	

1 Analyst - National Institute for Metallurgy

2 Analyst - University of Cape Town, Professor Erlank

3 Total Fe expressed as Fe_2O_3

4 nd - not determined

5 LOI - loss on ignition

A Xenolith of medium grained feldspathic gabbro present near the eastern margin of the granophyric gabbro

B Medium grained feldspathic gabbro - near western margin of the feldspathic gabbro unit

C Medium grained feldspathic gabbro - near centre of the feldspathic gabbro unit

D Finer-grained feldspathic gabbro - 15 m from the eastern contact

E Finer-grained feldspathic gabbro - 5 m from the eastern contact

F Fine-grained feldspathic gabbro - at the eastern contact

G Feldspathic olivine gabbro, Birds River Complex (Eales and Robey, 1976, p 104)

present in the samples.

High levels of SiO_2 and K_2O are present in the analysed sample of the fine grained upper contact of the feldspathic gabbro unit, (CL 46 , Table 41), and it appears that this analysis is unlikely to represent the average composition the magma parental to the feldspathic gabbro. The explanation for the composition of the contact rock may be found in the partial hybridization of the upper contact rocks with a younger granophyric microgranite intrusive described in a previous section, (see p 205), and much of the glassy interstitial material present in the analysed contact rocks is likely to represent infiltrated granophyric microgranite magma.

(vi) Variation Diagrams

Variations in major element chemistry in the rocks of the Komatipoort intrusion have been illustrated using several variation diagrams: an AFM diagram, major oxides versus position in the intrusion, major oxides versus the index $\frac{2K_2O}{Na_2O + K_2O} + \frac{FeO + Fe_2O_3}{MgO + FeO + Fe_2O_3}$ which is recommended for rocks exhibiting relative enrichment in both alkali and iron by Eales and Robey (1976).

(a) The AFM diagram

In figure 34 , p 236, the analysis of rocks from the Komatipoort intrusion have been plotted in an AFM diagram, in terms of weight percentages. The use of this diagram for the portrayal of petrogenetic relations has been criticised by Wright (1974), however Barker (1978), has suggested that AFM diagrams can provide certain types of information when used with judgement and in conjunction with other projections. In the present instance the diagram is used mainly for comparitive purposes since the AFM diagram has been

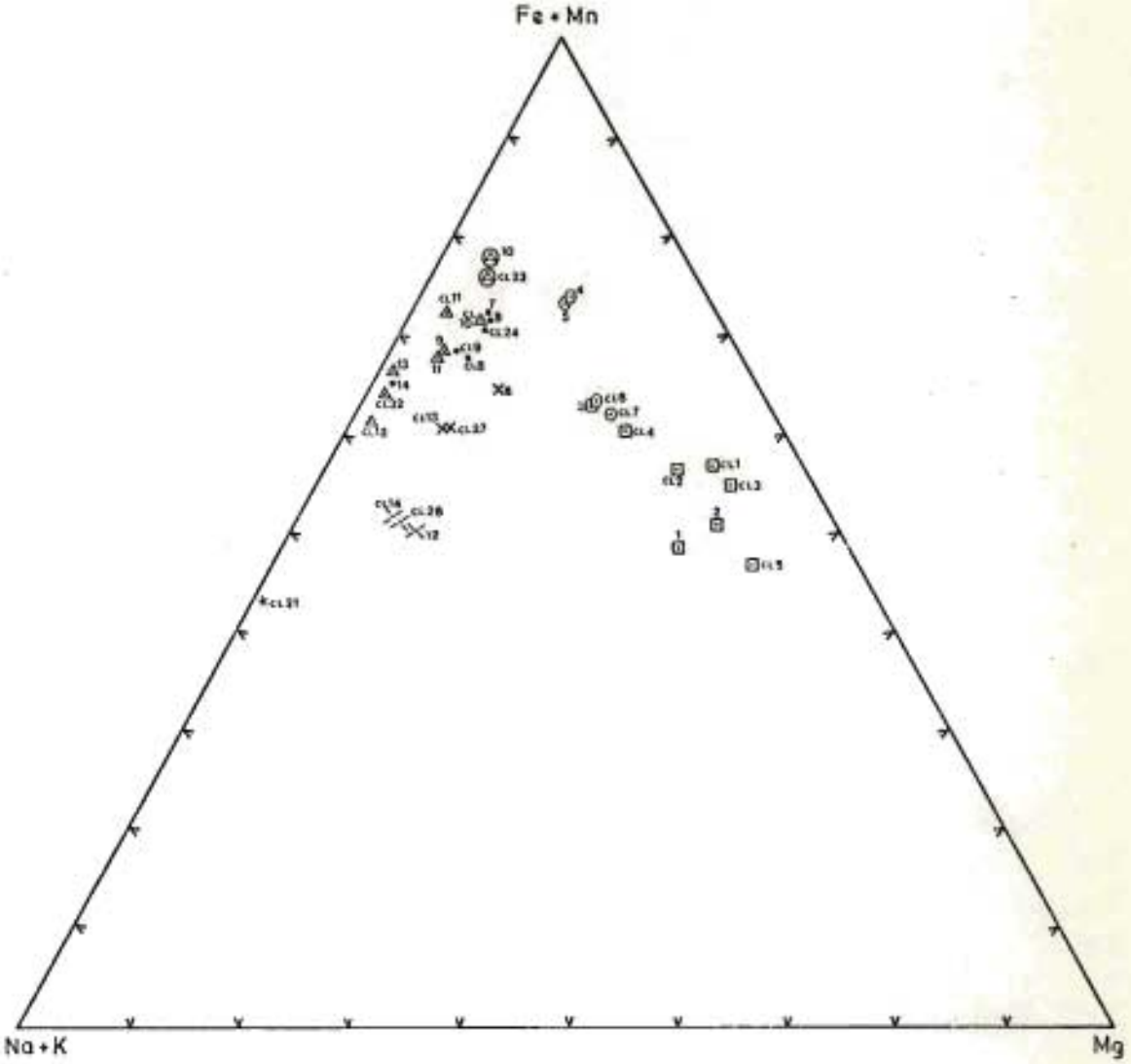

Figure 34. A.F.M. diagram for rocks of the Komatipoort Intrusion.

- ⊞ Olivine Gabbro
- ⊙ Clinopyroxene Plagioclase Cumulate
- • Granophyric Gabbro
- △ Granophyre
- × Feldspathic Gabbro
- ⊛ Granophyre - Granophyric Gabbro Contact
- ⋇ Feldspathic Gabbro - Upper Contact Zone
- * Rhyolitic Extrusive

1-14 are CL sample numbers 35 - 48

used extensively to portray major element variation in igneous rock series.

It is apparent from figure 34 , that the analyses presented here follow a typical, tholeiitic, moderate Fe-enrichment trend, roughly comparable to that of the Bushveld Complex (Wager and Brown, 1968, Fig 217, p 402), and the Skaergaard (Wager and Brown, 1968, Fig 116, p 173), intrusions. The analyses of samples of olivine gabbro and clinopyroxene-plagioclase-cumulate, amongst others, do not represent liquid compositions, as these rocks contain high proportions of cumulus phases. Several of the granophyre analyses on the other hand are likely to represent liquid compositions, and the trend as shown in fig. 34, is a product of both liquid and cumulate rock compositions.

Several features that are apparent on this diagram can be confirmed using other diagrams. These include the alkali-rich nature of the analysed fine-grained contact rocks of the feldspathic gabbro (unit 5), which plot closer to the reference point provided by the rhyolitic extrusive analysis, also plotted in this diagram, than the analysed feldspathic gabbro samples from the interior of the intrusions. Further the Fe-rich nature of the analysed samples from the contact between the granophyre and the granophyric gabbro is apparent, although perhaps over emphasized, in figure 34.

(b) Major-oxides versus position within the intrusion

Major oxide weight percentages have been plotted against position within the intrusion in fig.35, p 238. It should be noted that olivine gabbro samples from the Sihlangula River section only have been plotted to obviate difficulties over the assignment of the relative positions of samples collected in different parts of the intrusion. Further, the analysed sample of a granophyre dyke intruding the granophyric gabbro (CL 48) and the analysis of the sample of grey granophyre, (granophyric gabbro xenolith), CL 43 ,

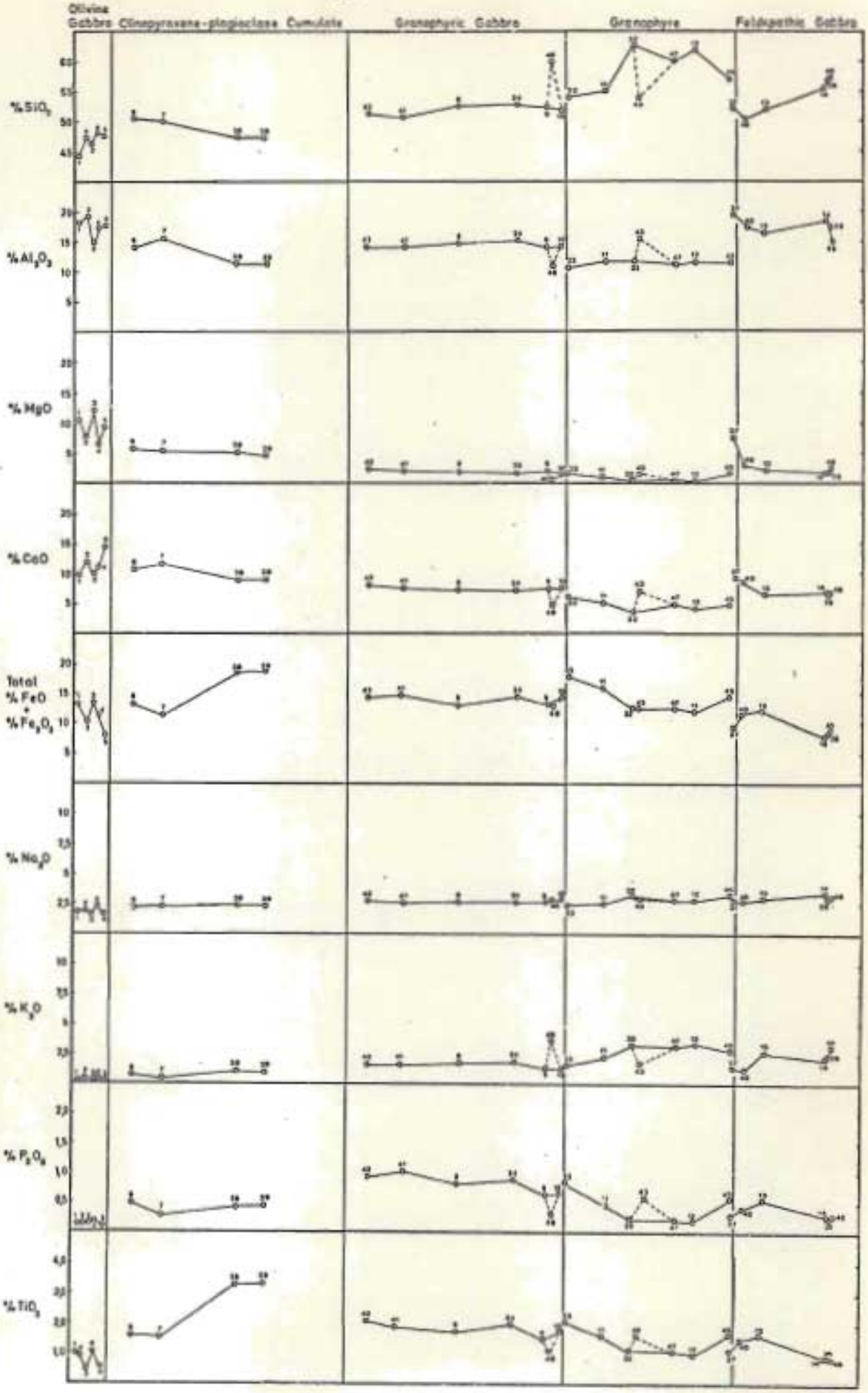

Figure 35. Major oxides plotted against the position of the sample within the Kangerlussuaq intrusion.

are joined to the main trend by dotted lines, in this diagram.

I The olivine gabbro

Most of the major elements show irregular fluctuations in concentration within the olivine gabbro, and these fluctuations appear to result largely from variations in the proportions of the discrete olivine and plagioclase crystals and the ophitic pyroxene plates.

II The clinopyroxene-plagioclase cumulate

Variations in major element content between samples of the clinopyroxene-plagioclase cumulate are dominated by differences between the magnetite poor, (low FeO + Fe_2O_3 and TiO_2) and magnetite-rich samples, (high FeO + Fe_2O_3 and TiO_2). No meaningful generalised trends in terms of the other major elements could be detected across the zone. Samples from the upper third of the zone, which displays a sharp increase followed by a slow decline in olivine content from west to east across the unit, were however, not available for analysis.

III The granophyric gabbro

The granophyric gabbro samples in general appear relatively homogeneous, although very slight decreases in P_2O_5, TiO_2, CaO and MgO from east to west across the zone may be discerned. These decreases are accompanied by equally slight increases in K_2O, Al_2O_3 and possibly SiO_2. The analysed sample of the granophyre dyke intruding the granophyric gabbro (CL 48), shows obvious similarities in major element content to the analysed granophyre samples from near the centre of the granophyre unit.

Compared with the adjacent clinopyroxene-plagioclase cumulate the granophyric gabbro shows a marked increase in SiO_2 and P_2O_5

and a smaller increase in Al_2O_3, Na_2O and K_2O. The amount of TiO_2 and $FeO + Fe_2O_3$ present in the granophyric gabbo is noticeably less than that in the magnetite-rich samples from unit 2, but represents an increase compared to the magnetite-poor clinopyroxene-plagioclase cumulate samples. The MgO and CaO contents of the granophyric gabbro are slightly less than that of the clinopyroxene-plagioclase cumulate samples. The interpretation of these compositional differences is complicated by the large gap between the last analysed clinopyroxene-plagioclase cumulate sample and the first analysed granophyric gabbro sample.

IV The granophyre

In general major element oxide concentrations vary roughly symmetrically, or in some cases slightly unsymmetrically about the approximate centre of the unit. Oxides such as Al_2O_3, Na_2O and possibly CaO appear exceptional in this regard in that Al_2O_3 and Na_2O show a tendency to increase slightly from east to west across the unit while CaO shows a tendency to decrease in concentration. Samples collected from near the centre of the zone do, however, contain less CaO than any of the other analysed granophyre samples.

The oxides MgO, $FeO + Fe_2O_3$, P_2O_5 and TiO_2 increase in concentration at either margin. SiO_2 shows a well-defined maximum near the centre of the unit and decreases in concentration fairly rapidly towards the margins. The K_2O content tends to increase across the whole unit from west to east, although there is some suggestion of a local high near the centre of the granophyric unit.

The contact of the granophyre with the granophyric gabbro could be discerned in the field only with difficulty due to the similarity in the appearance of the two rock types. In terms of major

element geochemistry the transition is sharply defined with marked increases in the granophyre in SiO_2 and $FeO + Fe_2O_3$, and to a lesser extent in TiO_2, P_2O_5 and K_2O. Relative to the granophyric gabbro, the granophyre is notably depleted in Al_2O_3, and to a smaller degree in CaO and Na_2O.

Strong similarities in major element oxide content between the 'grey granophyre' (granophyric gabbro xenolith) and the granophyric gabbro analyses (see Table 27, p228), are apparent in this diagram, (fig 35). In several respects the analysis (CL 43), resembles some of the analysed feldspathic gabbro samples, however Al_2O_3, MgO and possibly CaO contents are significantly lower than might be expected.

V The feldspathic gabbro

In examining variations in the major element oxide content of the feldspathic gabbro it is necessary to discriminate between samples from the contact of the zone and those from the interior of the feldspathic gabbro unit. Unfortunately, relatively small numbers of analyses of these rocks are available.

Some possible variation trends may be discerned in the interior of the unit if the feldspathic gabbro xenolith from the granophyric gabbro (CL 27), is regarded as the most westerly representative of this unit 5. These include a tendency for Al_2O_3, MgO and CaO to decrease from west to east and simultaneously for $FeO + Fe_2O_3$, K_2O, P_2O_5, TiO_2 and to a lesser extent Na_2O to increase from west to east. SiO_2 shows a smaller fluctuation in concentration.

The three analysed specimens of the fine grained contact rocks also show a distinct variation trend. SiO_2, K_2O and $FeO + Fe_2O_3$ increase towards the contact whereas Al_2O_3 shows a noticeable decrease. MgO, CaO, TiO_2 and P_2O_5 contents show little variation. Petrographic evidence described earlier, (see p 201), provides

evidence of the intrusive relationship that exists between the granophyre of unit 4 and the feldspathic gabbro of unit 5. This relationship is reflected in the large differences in the chemistry of the two rock types adjacent to their mutual contact. The feldspathic gabbro show much higher Al_2O_3, MgO and CaO contents and lower SiO_2, $FeO + Fe_2O_3$, K_2O, P_2O_5 and TiO_2 with no suggestion of a gradational transition between the two zones.

(c) Major oxides versus the index $\frac{2K_2O}{Na_2O + K_2O} + \frac{FeO + Fe_2O_3}{FeO + Fe_2O_3 + MgO}$

I The olivine gabbro

In this diagram (fig 36, p 244) the major element oxides such as SiO_2, Al_2O_3, MgO and CaO show a scattering similar to that observed in the previous diagram, (major oxides versus position). K_2O, TiO_2, P_2O_5 and to a lesser extent $FeO + Fe_2O_3$ and Na_2O increase as the index employed here increases, possibly reflecting the concentration of several of these elements in the interstitial mesostasis, present in minor but variable amounts in these rocks.

II The clinopyroxene-plagioclase cumulate

As in the previous diagram (fig 35) compositional variations are dominated by the large diffferences in $FeO + Fe_2O_3$ and TiO_2, resulting from differences in magnetite and ilmenite content between the analysed samples of this unit.

III The granophyric gabbro

The granophyric gabbro analyses show a small range of variation in general, however many of the major element oxides do show a systematic change in concentration with an increase in the index employed here. Further, plots of several of the major element

FIGURE 36.

For figure 36, see insert in pocket at the end of this thesis.

oxides versus the fractionation index fit fairly closely to a straight line. SiO_2, Al_2O_3 and K_2O show a distinct increase with increase in the fractionation index, apparently in response to variations in the concentration of the K-feldspar bearing interstitial micropegmatite. Corresponding decreases occur in the concentration of CaO, TiO_2, FeO + Fe_2O_3 and P_2O_5, although in respect of the last-mentioned oxide, analyses CL10 and CL24 are anomalous. The grey granophyre, (granophyric gabbro xenolith), plots together with the granophyric gabbro analyses with respect to most elements, although the P_2O_5 content of this sample is somewhat lower than would be expected.

IV The granophyre

Analysis of a sample of a rhyolitic extrusive has been plotted in this diagram for reference purposes (see fig 36). The majority of the analyses of the granophyre have major oxide contents which plot close to a straight line trending in the direction of the point representing this reference rhyolitic extrusive in the fractionation index diagram, (fig 36). K_2O, SiO_2 and to a markedly lesser extent Al_2O_3 and Na_2O tend to increase with increasing fractionation index, and MgO, CaO, TiO_2, P_2O_5 and FeO + Fe_2O_3 decrease as the fractionation index increases.

The MgO contents of the analysed granophyre samples continue the trend of the granophyric gabbro samples as do, slightly less exactly, the P_2O_5, TiO_2, Na_2O, CaO and the K_2O contents. The SiO_2 values of the granophyre plot along a straight line with a distinctly different slope to the corresponding line which can be drawn through the points representing the analysed granophyric gabbro samples. For both Al_2O_3 and FeO + Fe_2O_3 the points representing the analysed granophyre samples define trends apparently unrelated to the corresponding trends shown by the granophyric gabbro analyses in the same diagram. The Al_2O_3

values in the granophyre analyses are lower than those of the granophyric gabbro analyses and rise only slightly with increasing fractionation index.

The granophyre resembles the granophyric gabbro in terms of $FeO + Fe_2O_3$ in that the sum of the oxides decreases with increasing fractionation index, however, the $FeO + Fe_2O_3$ contents of the granophyre sample with the lowest fractionation index considerably exceeds the $FeO + Fe_2O_3$ content of the most fractionated granophyric gabbro.

The analysed sample of the granophyre dyke which crosscuts the granophyric gabbro (CL 48), plots close to the most fractionated granophyre in the fractionation index diagram (fig 36), demonstrating its chemical affinity with the granophyre.

V The feldspathic gabbro

Two of the analysed feldspathic gabbro samples from the interior of the unit have almost identical fractionation indices, and little meaningful information can be derived from this diagram concerning these rocks. The fractionation indices of the fine-grained contact rocks on the other hand show large differences, but there is no indication of a systematic variation in major element content with fractionation index in these rocks.

(vii) Average Composition

By means of weighted averages, the mean composition of four of the units of the Komatipoort intrusion have been estimated. These are shown in Table 42 , p 248 .

It should be noted , however, that insufficient analyses of the feldspathic gabbro are available for a reasonably reliable average

to be estimated and in addition it is possible that its chemical composition has been affected by the metamorphism it has suffered.

In Table 42 , p 248, an estimate of the average composition of the initial magma that may have produced the clinopyroxene-plagioclase-cumulate and the granophyric gabbro is shown. Proportions for this weighted average were obtained from measurements of areas covered by the two rock types indicated on the geological map, and although it is acknowledged that these measurements may not give true relative abundances of the various types, they provide the only available guide.

Listed in Table 43 , p 249 , for comparitive purposes, are the estimated average compositions of the Karroo dolerites (from Walker and Poldervaart, 1949, Table 17), and the average composition of the Komatipoort tholeiite basalts, calculated from the analyses presented in this work. The relatively high differentiation index of the estimated average composition of the clinopyroxene-plagioclase cumulate - granophyric gabbro magma as compared with that of the average Karroo dolerite, may be evidence that the average presented in Table 42 is unrealistic. The average Komatipoort tholeiite listed in the same table however has a differentiation index of 72,28 compared with 76,5 for the Average Magma. There are strong similarities in the compositions of the two averages, but a major difference lies in the TiO_2 contents of the two averages, the average Komatipoort tholeiite having a higher TiO_2 content. Cox, et al (1966), found similar differences between the TiO_2 contents of the major intrusives and the volcanics of the Nuanetsi area, and this difference, in the present context, may not be of great significance. The major objection to the Komatipoort intrusion average presented in Table 43 , however, is its relatively low MgO content, although a dolerite with a similar MgO content is listed in Table 16 , p 51 .

TABLE 42

Composition of average rocks from zones 1,2,3, and 4 of the Komatipoort Intrusion, (calculated using weighted averages of selected analyses presented in this study).

	Average olivine gabbro,(Unit 1).	Average clinopyroxene-plagioclase cumulate (Unit 2)	Average granophyric gabbro (Unit 3)	Average granophyre (Unit 4)	Komatipoort Intrusion Average Magma for Units 2 and 3
SiO_2	47,60	50,20	52,90	58,54	51,40
Al_2O_3	16,90	14,70	14,66	11,22	14,68
Fe_2O_3	1,70	2,60	4,30		3,35
FeO	9,10	9,60	8,90	*15,66	9,28
MgO	8,80	5,60	1,70	0,85	3,87
CaO	11,60	11,20	7,30	4,72	9,47
Na_2O	1,90	2,40	2,80	2,78	2,58
K_2O	0,30	0,60	1,70	2,88	1,09
TiO_2	0,70	1,60	1,70	1,54	1,64
P_2O_5	0,12	0,35	0,70	0,47	0,51
MnO	0,17	0,22	0,25	0,27	0,23
H_2O^+	1,00	0,91	1,53	1,48	1,19
H_2O^-	0,13	0,20	0,40	0,34	0,29
CO_2	0,20	0,25	0,60	0,57	0,41
$\frac{FeO + Fe_2O_3}{FeO + Fe_2O_3 + MgO}$	55,10	68,50	88,60	101,32	76,5

* Total Fe expressed as Fe_2O_3

TABLE 43

Comparison of the estimated average composition of units 2 and 3 of the Komatipoort Intrusion with that of the average Karroo dolerite (from Walker and Poldervaart, 1949), and the estimated average Komatipoort tholeiite, (from analyses presented in this study).

	Komatipoort Intrusion average magma for units 2 and 3	Average Komatipoort tholeiite	Average Karroo dolerite*
SiO_2	51,4	50,62	51,9
Al_2O_3	14,68	12,88	15,5
Fe_2O_3	3,35	3,56	1,0
FeO	9,28	10,34	10,7
MgO	3,87	5,33	8,2
CaO	9,47	9,46	9,7
Na_2O	2,58	2,37	1,8
K_2O	1,09	0,98	0,7
TiO_2	1,64	2,36	1,1
P_2O_5	0,51	0,54	0,1
MnO	0,23	0,23	0,2
H_2O^+	1,19		
H_2O^-	0,29		
CO_2	0,41		
$\frac{FeO + Fe_2O_3}{FeO + Fe_2O_3 + MgO} \times 100$	76,5	72,28	58,79

*Walker and Poldervaart (1949) Table 17.

(viii) Summary

In general the major element analyses representing the rock types forming the various units of the Komatipoort Intrusion tend to form clusters in the variation diagrams rather than defining one continuous series. In addition, within cross-sections of units such as the granophyric gabbro and to a lesser extent the clinopyroxene-plagioclase cumulate, there is little systematic variation with position in the intrusion. The granophyric gabbro , in fact, appears to form a relatively homogeneous unit. These observations suggest that the various units originated as separate intrusions.In the variation diagrams, however, smooth curves can be drawn through points representing the olivine gabbro, the clinopyroxene-plagioclase cumulate, and the granophyric gabbro. Thus although these units may not represent an intrusion fractionated in situ, they could be representatives of a fractionation sequence developed at depth, and intruded separately at their present site. The granophyre resembles the more extreme fractionation products of differentiated tholeiitic intrusives in terms of major element chemistry, however differences in Al and Fe contents provide evidence that the granophyre is unlikely to have formed part of the same fractionation sequence as units 1,2 and 3, (see fig 37). The granophyre could however, represent an extreme differentiate of a separate tholeiitic fractionation sequence. Some of the evidence is suggestive of a hybrid origin for the granophyre, since in figs 36 and 37 the granophyre analyses plot close to a straight line trending towards a reference rhyolitic extrusive analysis. The fact that none of the other rocks of the Komatipoort Intrusion have a composition suitable to constitute the other component in the hybridising process, suggests the granophyre in the Komati River section may be a multiple intrusion.Field evidence does not support this possibilty.The remaining unit, the feldspathic gabbro, appears to form a separate intrusion.

(L) Trace element chemistry of the Komatipoort Intrusion

Fourteen samples representative of the major rock types from the Komatipoort Intrusion have been analysed for 14 different trace elements in addition to major elements. The results of the trace element analyses are listed in Table44 A and B. Variations in trace element

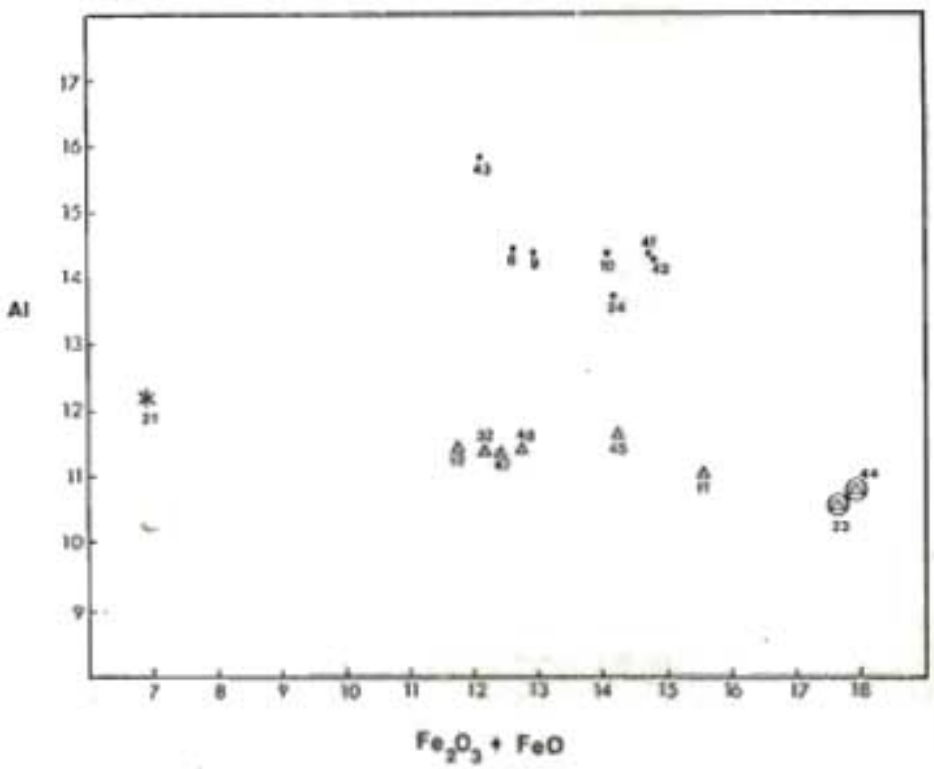

Figure 37 Al versus total Fe oxides for granophyres (△) granophyric gabbros (•) and mutual contact rocks (⊗) of the Komatipoort Intrusion.
* Reference acid volcanic analysis
All numbers are CL sample numbers

TABLE 44 A

TRACE ELEMENT ANALYSES FOR SEVEN SAMPLES FROM THE KOMATIPOORT INTRUSION (expressed as p.p.m)
(corresponding major element analyses are listed in Tables 34,36,37,39, and 41).

Analyst: University of Cape Town, Professor Erlank.

	CL35 * 1	CL36 2	CL37 3	CL38 4	CL39 5	CL40 6	CL41 7	
Ba	64	106	316	394	412	421	601	CL35 - Olivine gabbro- near western margin
Sr	301	264	339	354	357	467	435	
Rb	2,5	4,9	19,5	21,0	21,7	28,9	34	CL36 - Olivine gabbro- near eastern margin
Y	9,7	12,8	35	44	45	37	67	
Zr	27,5	63	226	306	320	298	494	CL37 - cpx-plag-cumulate - western margin
Nb	2,8	3,5	14,7	19,0	19,8	16,3	33	CL38 - cpx-plag-cumulate - centre
Zn	36	61	102	156	160	95	161	
Cu	24,4	80	109	87	83	113	117	CL39 - cpx-plag-cumulate - centre
Co	46	67	45	48	52	31	26,3	CL40 - feldspathic gabbro - base
Ni	93	181	67	22,8	19,6	27,4	3,1	
V	139	115	186	68	40	159	34	CL41 - granophyric gabbro - middle
Cr	103	310	152	5,3	3,8	30,0	6,6	
Th	nd[1]	0,74±0,17	2,1 ±0,2	3,0 ±0,2	3,1 ±0,2	3,4 ±0,3	5,6 ±0,2	
U	nd[1]	0,13±0,08	0,46±0,07	0,45±0,06	0,46±0,06	0,79±0,09	0,82±0,07	

nd - not detected

* - Sample numbers as given in several of the diagrams.

TABLE 44 B

TRACE ELEMENT ANALYSES FOR SEVEN SAMPLES FROM THE KOMATIPOORT INTRUSION (expressed as p.p.m)
(corresponding major element analyses are listed in Tables 34,36,37,39 and 41)

Analyst:University of Cape Town, Professor Erlank

	CL42 *8	CL43 9	CL44 10	CL45 11	CL46 12	CL47 13	CL48 14
Ba	621	831	807	1025	753	871	1243
Sr	439	480	295	286	401	225	315
Rb	37	42	53	69	72	88	99
Y	64	63	89	91	54	101	101
Zr	510	534	741	887	534	1057	1055
Nb	36	36	54	61	42	74	71
Zn	159	136	270	180	100	198	211
Cu	121	46	56	38	128	21,2	22,9
Co	25,2	175	18,6	18,1	57	8,0	7,7
Ni	3,6	3,5	2,5	2,2	62	2,1	2,1
V	60	14,9	4,9	10,7	51	4,4	5,2
Cr	6,9	5,5	6,3	4,5	103	4,4	4,9
Th	5,5 ± 0,2	5,4±0,2	7,9±0,3	9,1±0,3	7,4±0,3	11,6±0,3	11,6±0,3
U	0,89±0,05	1,2±0,1	1,7±0,1	1,5±0,1	1,3±0,1	2,0±0,1	2,1±0,1

CL42 - granophyric gabbro - eastern margin

CL43 - grey granophyre (granophyric gabbro xenolith)

CL44 - granophyre-granophyric gabbro contact rock

CL45 - granophyre - eastern margin

CL46 - feldspathic gabbro fine-grained eastern contact

CL47 - granophyre - western margin

CL48 - granophyre vein cross-cutting the granophyric gabbro

* - Samples numbers as listed in several of the diagrams.

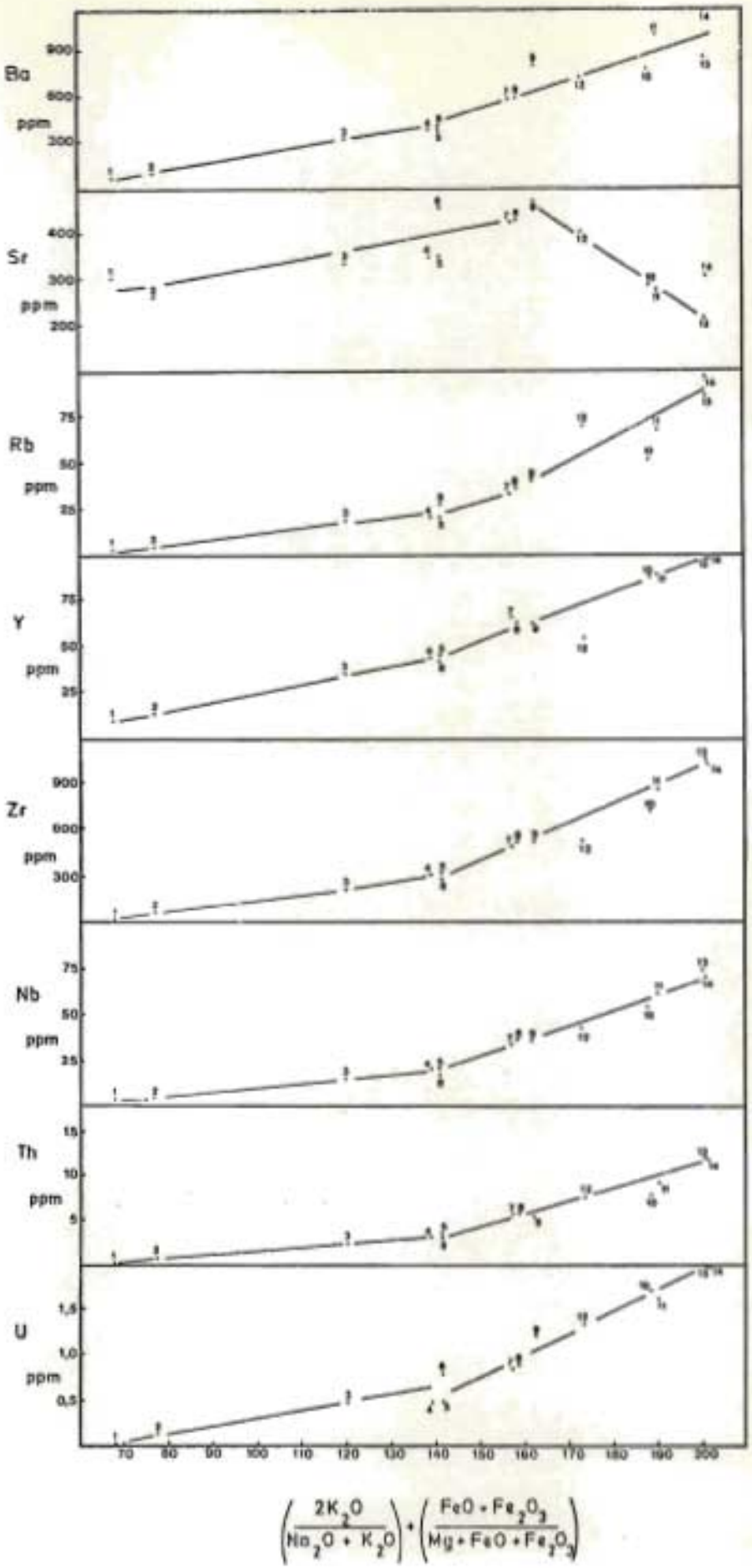

Figure 38A. Variation in trace element content of rocks of the Komatipoort Intrusion with a Fractionation index. (Numbering as in Table 44A-B p 252-3)

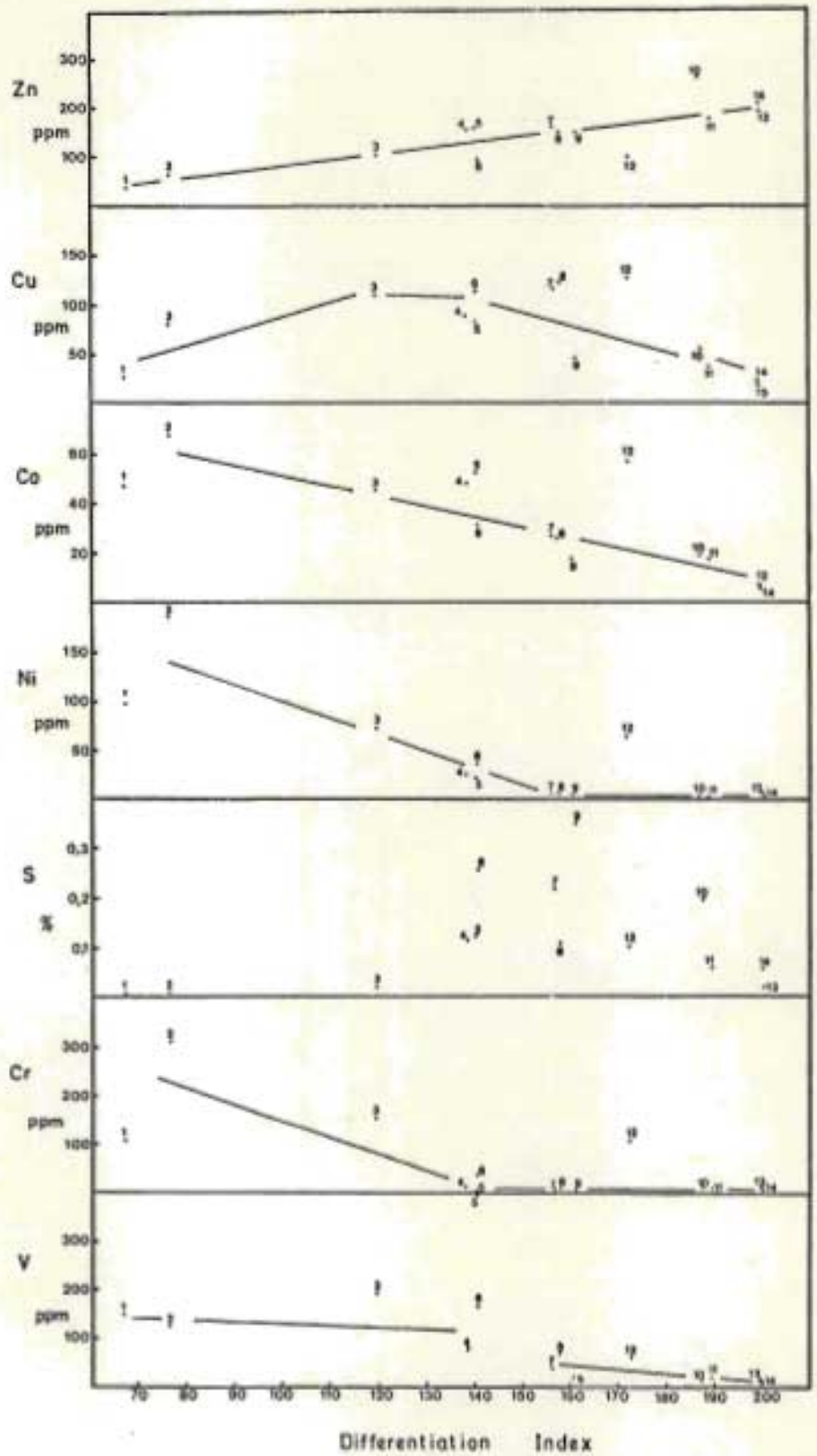

Figure 38B. Variation in trace element content of rocks of the Komatipoort Intrusion with a Fractionation Index. (Numbering as in Table 44 A-B, p.252-3).

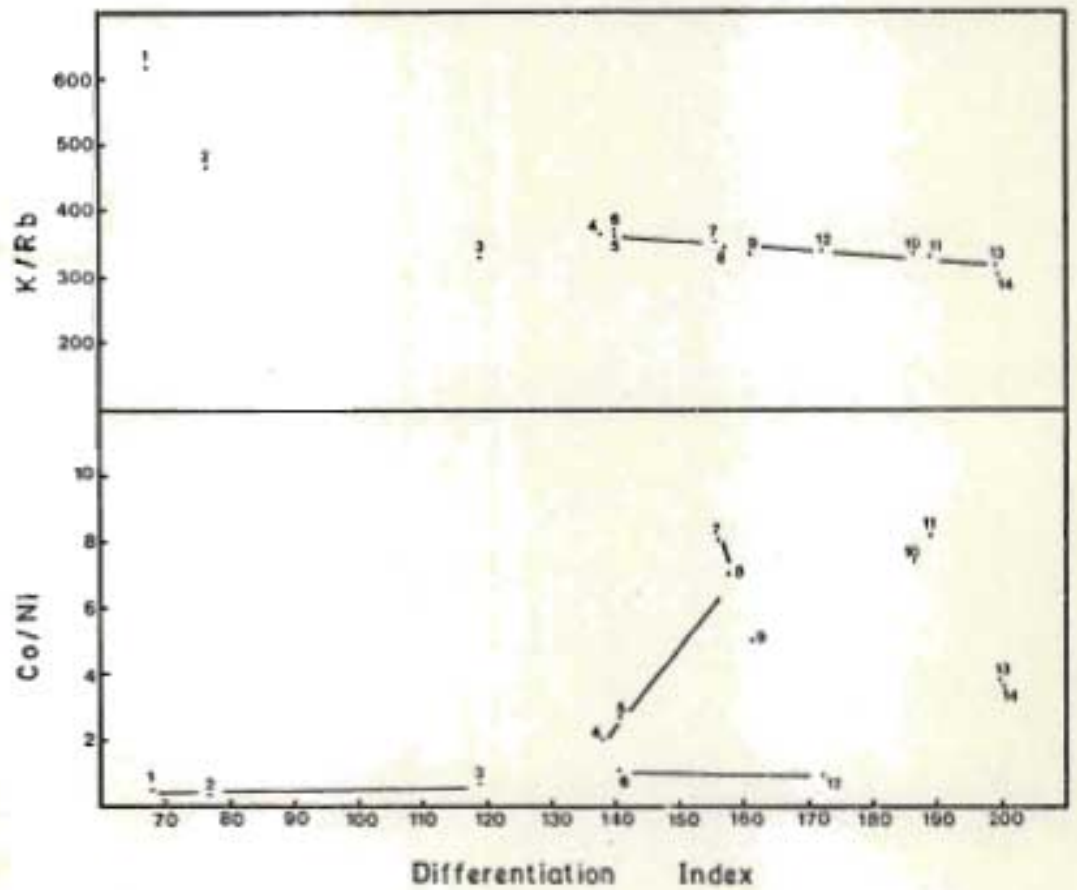

Figure 39. Variations in Co/Ni and K/Rb of rocks of the Komatipoort Intrusion. (Numbering as in Table 44A-B p. 252 - 253).

content of these rocks in relation to fractionation index

$$\frac{2K_2O}{Na_2O + K_2O} + \frac{FeO + Fe_2O_3}{MgO + FeO + Fe_2O_3} \quad \% \quad \text{(Eales and Robey 1976)}$$

are illustrated in fig 38 A and B . In addition, variations in the Co/Ni ratio , and the K/Rb ratio are shown in fig 39 .

Ba, Rb, Y, Zr, Nb, Th and U in general display the same type of variation with increasing fractionation index. This involves a slow increase in concentration of the trace element concerned, from rocks with a relatively low fractionation index, (olivine gabbros) to samples with a moderate fractionation index (feldspathic gabbro and clinopyroxene-plagioclase cumulate), followed by a relatively rapid rise in trace element content in passing to rocks with higher fractionation indices, such as the granophyric gabbro and the granophyre, (see fig 38 A and B). This trend, in the case of several of the elements mentioned above is largely the result of the 'residual' character of the element concerned, (e.g. Rb, Zr, Th, U). These residual elements tend to be excluded from early formed crystals in tholeiitic basaltic magma, and instead are preferentially concentrated in the residual fraction.

Variations in the K/Rb ratio are shown in fig 39 . Highest values are present in the sample of olivine gabbro with the lowest fractionation index, but the ratio drops rapidly with increase in the fractionation index of the various samples. The initial high K/Rb ratios are associated with olivine gabbro samples that contain extremely small amounts of interstitial micropegmatite. This interstitial micropegmatite is likely to be the normal repository of much of the Rb and K present in a rock of this nature. A similar correlation between high K/Rb ratios and low concentrations of interstitial micropegmatite has been reported by Eales and Robey (1976), from the Birds River Complex. It is reported by these authors, that in some cumulates, mesocumulus, adcumulus and heterad-

cumulus growth results in the expulsion of the interstitial residue to varying degrees. Where little interstitial micropegmatite remains, whole rock K/Rb ratios will, in effect, be determined by the K/Rb ratio of the plagioclase present in the rock. This is because K and Rb contents of other minerals present in rocks such as the olivine gabbro, are too low to have a major influence on the whole rock K/Rb ratio. Eales and Robey (1976), note that according to Murthy and Griffin (1970), and Goodman (1972), K/Rb ratios of plagioclase are usually higher than their corresponding whole rock values. Thus the high K/Rb ratios determined in samples from the lower part of the olivine gabbro unit, may result from the very small quantities of interstitial micropegmatite present in these rocks.

Variations in micropegmatite content may then provide an explanation for the variation in concentration of Rb (and all the 'residual' elements) with fractionation index in the rocks of the Komatipoort Intrusion.

In rocks with a higher fractionation index than the olivine gabbro, there appears to be a small drop in K/Rb ratio as the fractionation index increases. This is in accord with the conclusions of Prinz (1967) who found that the K/Rb ratio decreases in more highly fractionated rocks, due to the Rb concentration in the residual magma increasing at a rate slightly in excess of that of K. Increases in absolute quantities of K, Rb and other 'residual' elements with similar variation curves, are however, as noted above, a response to significant increases in the amount of micropegmatite present in rocks with higher fractionation indices.

Although Nb has been shown by Eales and Robey (1976) to concentrate in the opaque oxides in rocks of the Birds River Complex, in the Komatipoort Intrusion these opaque oxides are themselves a late interstitial phase for the most part, and often occur associated with interstitial micropegmatite. Probably for this reason the Nb here

here has a distribution similar to that of the 'residual' elements.

Prinz (1967) and Wager and Brown (1968) both suggest that Ba increases with differentiation of basic rocks. The variation curve for Ba in the Komatipoort Intrusion is similar, but distinctly flatter than the curves for the 'residual' elements. Ba distribution is complicated by a tendency for this element to be preferentially incorporated in plagioclase of certain compositions. Thus plagioclase in the range oligoclase-labradorite contains more Ba than plagioclase with a more anorthite or albite-rich composition, (Prinz 1967). The plagioclase in the olivine gabbro may have a composition as basic as bytownite whereas the rocks of intermediate fractionation index contain abundant labradorite. This difference is likely to produce an enrichment in Ba in the rocks of intermediate fractionation index, that is additional to the increase caused by a rise in the interstitial micropegmatite contact of these rocks. This additional increase in the Ba content of the rocks with intermediate fractionation indices may be sufficient to produce the observed flattening of the variation curve.

Yttrium is also considered by Prinz (1967) and Wager and Brown (1968) to increase in the late fractionation stage. This element has a slightly flattened variation curve similar to that of Ba. The flattening in this case is likely to result from the presence of relatively large amounts of pyroxene in the rocks of intermediate fractionation index as this mineral is known to contain significant amounts of Y (Prinz 1967, Eales and Robey 1976).

Strontium shows a variation trend distinctly different to that of the 'residual' type elements because it is preferentially concentrated in plagioclase of an anorthite-rich nature. This results in enrichment of Sr in rocks containing abundant plagioclase, such as the feldspathic gabbro and the clinopyroxene-plagioclase cumulate, and relative depletion in rocks of higher fractionation index which contain increasing amounts of K-feldspar and albite-rich plagioclase.

Elements Co, Ni, Cr and to a lesser extent V, show a broad similarity in variation trend. The resemblance between the variation trends of Ni and Cr are particularly marked. This is a consequence of a tendency for Ni to be incorporated in early formed olivine and to a lesser extent, clinopyroxene crystals, and for Cr to occur either in early formed pyroxenes (particularly augites), or as Cr-spinels included in early olivines. This results in the enrichment of these elements in early formed cumulate minerals and a corresponding depletion of the residual magma, (Prinz 1967).

Cobalt, on the other hand enters the same minerals as Ni, but in smaller amounts (Prinz 1967), producing a relatively gradual decline in Co content of the more fractionated rock types, compared to the rapid decline in Ni, (see fig 38).

In fig 38 it may be seen that the variation in the Co/Ni ratio with fractionation index appears to follow two distinct trends. In samples of the olivine gabbro, the ratio is low, and the feldspathic gabbro samples have a Co/Ni ratio of a similar order, (see fig 38). The clinopyroxene-plagioclase cumulate samples appear to have distinctly higher Co/Ni ratios than the feldspathic gabbro of equivalent fractionation index and the Co/Ni ratio rises sharply again in the granophyric gabbro, to produce another trend. These trends are to some degree obscured by the points representing samples CL 43, 44, 45, 47, and 48 , however these samples have Ni contents below the detection limit of the analytical method used. Thus they could plot closer to the higher clinopyroxene-plagioclase cumulate - granophyric gabbro trend if true Ni contents rather than detection limits were used to calculate the Co/Ni ratios.

Vanadium enters magnetite and to a lesser extent pyroxene (Prinz 1967) during the middle stages of fractionation and is therefore enhanced in rocks of moderate fractionation index and depleted in rocks of higher fractionation index. A distribution similar to that observed on the Komatipoort Intrusion was found in the rocks

of the Skaergaard Intrusion by Wager and Brown (1968).

Sulphur distribution is controlled by two factors. First a tendency to concentrate in the residual magma and secondly, when the concentration is high enough in relation to other variables, a tendency to form an immiscible liquid which settles out of the basic magma. The solubility of S in the magma is affected by the concentration of Fe_2O_3 in the magma, the fS_2 and fO_2, (Haughton, Roeder and Skinner, 1974).

Sulphur concentration in rocks of the Komatipoort Intrusion is low in the olivine gabbro, rises in the rocks of moderate fractionation index and decreases in the rocks of highest fractionation index. Scatter of the points is extremely wide however, presumably in response to the complex variables controlling the S distribution.

Copper variation is to some extent correlated with that of S, but this relationship is disturbed first by the presence of abundant Cu-free Fe-sulphides and secondly by a tendency for Cu to be incorporated in other minerals such as pyroxenes. Wager and Brown (1968) studied the distribution of Cu in the rocks of the Skaergaard Intrusion and found that Cu tended to increase in the residual magma until the late stages of crystallization. In the Komatipoort Intrusion rocks, Cu content rises until rocks of an intermediate fractionation stage are reached, and then decreases in the most highly fractionated rocks. There is a marked scatter however, possibly in part as a result of an association between Cu and S.

Zinc shows a steady increase with increasing fractionation index throughout the entire range of samples. At higher fractionation indices scatter increases. Wager and Brown (1968) suggest that Zn may be concentrated to some extent in magnetite. If this is the case for the Komatipoort Intrusion rocks, the nature of the occurrence of the opaque oxides has allowed a mild increase in the concentration of Zn in the residual magma, as was suggested for Nb.

(i) Factor Analysis and Trace Element Content

Prinz (1967) used factor analysis to study the trace element content of 267 basalts from localities with a world-wide distribution. By this means he showed that 90 per cent of the variation in proportions of trace elements in these basalts could be accounted for by four end members. These end members are calculated for each basalt analysis using the same thirteen trace elements, weighted by four series of (thirteen) different factors. The end members are dominated respectively by 1) Sr, 2) Cr (and Ni), 3) Ba (with V and Zr), 4) V (with Ba and Zr). Appropriate factors are supplied by Prinz (1967) to permit conversion of any new analysis of these thirteen elements into its corresponding four end members, (Prinz 1967, p 315, Table V). Using the four end members each analysis can be plotted in a tetrahedron, which, as indicated by Prinz (1967), produces a diagram well suited for portraying trends.

Analyses of only ten of the thirteen elements used by Prinz (1967) are available for the rocks of the Komatipoort intrusion. These are Ba, Sr, Rb, Y, Zr, Cu, Co, Ni, V and Cr. Ga, Li and Sc were also used by Prinz, but these three elements contribute on average only 5 per cent to each of the end members. They are thus not of great significance in accounting for the variations in the proportions of trace elments in the rocks studies by Prinz (1967).

In view of the basaltic character of many of the rocks of the Komatipoort intrusion, the four end members proposed by Prinz (1967) were calculated for the Komatipoort intrusion analyses, making allowances for the absence of the three elements mentioned. The points representing the various analyses were then plotted in a tetrahedron, using the four end members as corners. The projections of these points onto the four triangular faces of the tetrahedron are shown in fig 40 . Three dimensional modelling of the tetrahedron showed that the real distribution of most points within the tetrahedron is best represented by the projection of the points into

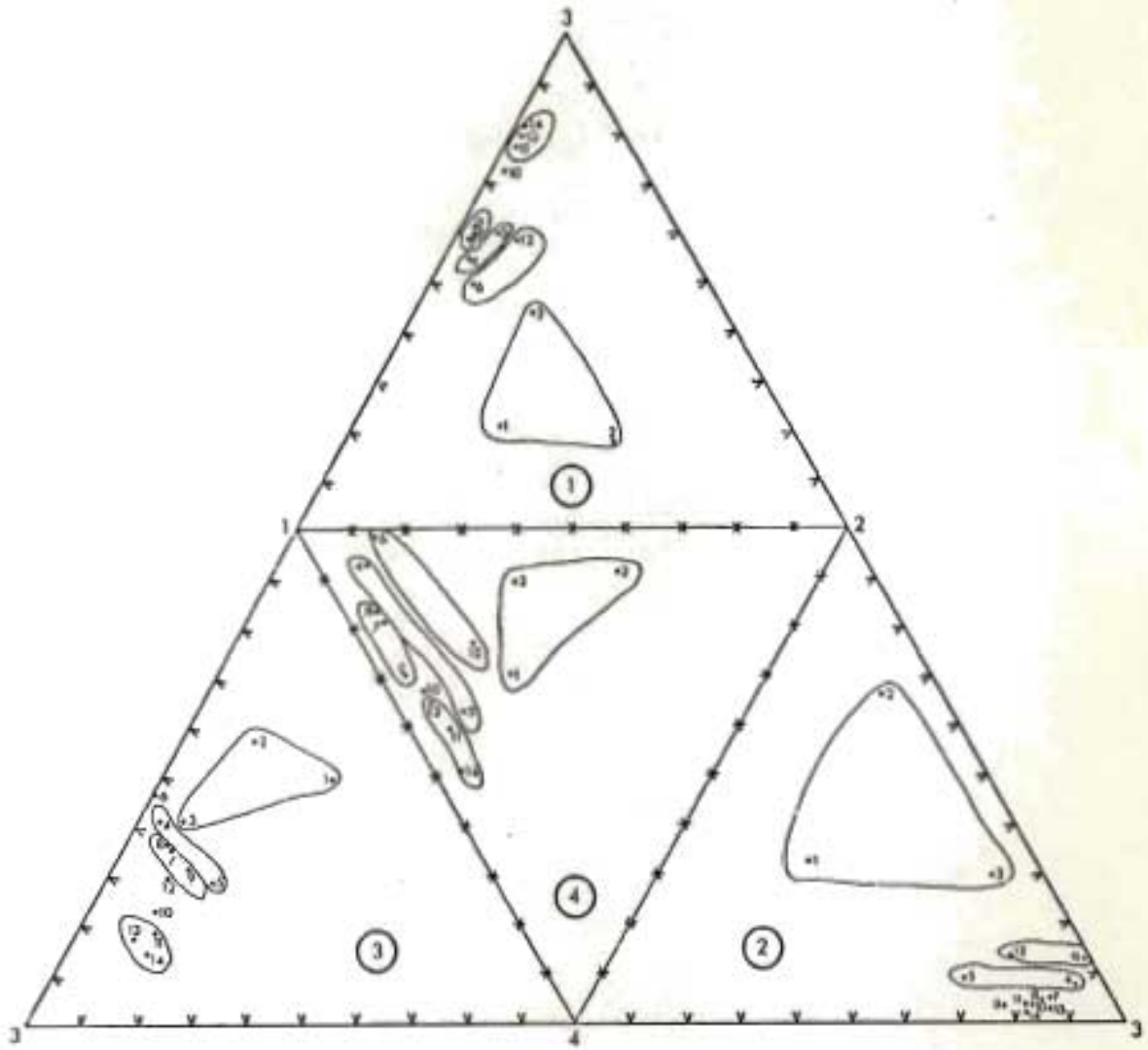

Figure 40. Tetrahedral plot of trace elements of rocks of the Komatipoort Intrusion with trace elements expressed in terms of four end members. (Equivalent CL sample numbering in Table 44A-B, p. 252 - 253).

triangle 1 in fig 40(factors 1, 2 and 3). This is because the majority of the points lie fairly close to a plane parallel to the tetrahedron face represented by triangle 1 fig 40 . Confirmation of this is provided by inspection of the distribution of points in triangle 3, fig 40 . Relationships between points representing the granophyres, the granophyric gabbro analyses, and to a lesser extent the clinopyroxene-plagioclase cumulates only, are, on the other hand best portrayed in triangle 3, fig 40 . The points representing the analyses of those rock types lie almost completely within a single plane that is parallel to triangle 3 (end members 1, 2 and 4) and very close to it, as may be seen by inspection of triangle 1, fig 40 .

Points representing analyses of the same rock type, not unexpectedly, tend to cluster together. It is of some significance however that the analysis of the 'grey granophyre' (CL 43,Table 32) plots within the granophyric gabbro 'field' and the sample of the granophyre dyke intrusive into granophyric gabbro, (CL 48, Table 32), lies in the granophyre 'field'.

In addition to this clustering effect, the points projected into Triangle 1, fig 40 appear to be distributed along two distinct trends. The first of these trends extends from the middle of the triangle, away from corner 2, (see fig40 , triangle 1), towards the upper-middle part of side 1-3, in a direction virtually parallel to side 2-3 of the same triangle. From the middle of the triangle where points representing the olivine gabbro plot, the trend passes successively through the feldspathic gabbro 'field', then the clinopyroxene-plagioclase 'field' and finally the granophyric gabbro 'field'. This suggests a drop in end-member 2 (Cr and to a lesser extent Ni) and an increase in end-members 3, (Ba and Zr mostly) passing from the olivine gabbro, through the feldspathic gabbro and clinopyroxene-plagioclase cumulate, to the granophyric gabbro.

The second trend lies along side 1-3 in Triangle 1 fig 40, and again in Triangle 3, indicating an enrichment in end-member 3 (Ba and Zr largely) and a corresponding depletion in end member 1, (Sr), passing from the granophyric gabbro to the granophyre. The first of these trends is likely to result from an observed decrease in olivine content and in some cases pyroxene content, with increasing fractionation index in the analysed samples of olivine gabbro, clinopyroxene-plagioclase cumulate and feldspathic gabbro. In addition it is probable that the Cr and Ni contents of the pyroxenes in these rocks decreases with increasing fractionation index. Simultaneously, the interstitial micropegmatite content increases, leading to an increase in end member 3, dominated by Ba and Zr, and effectively representative of the 'residual' type elements. The second trend, an increase in end member 3, in passing from the granophyric gabbros to the granophyres apparently reflects a marked increase in the interstitial micropegmatite content of these rocks, producing a rise in the 'residual element concentration'. This increase is accompanied by a corresponding decrease in end member 1 (Sr), as the plagioclase content of the rocks decreases antipathetically with rising micropegmatite content.
Thus much of the variation in trace element content displayed in both diagrams discussed here (fig 3 and fig 40) can be explained by the removal or accumulation of trace elements in cumulus crystals of olivine, pyroxene, plagioclase, magnetite and to a lesser extent apatite and zircon, or the accumulation of trace elements in the residual magma during the fractionation of one or more of the same crystal phases.

(M) The origin of the Komatipoort Intrusion.

The igneously laminated clinopyroxene-plagioclase cumulates of unit 2 which dip at around 25^{o} to the east provide the only available direct evidence of the attitude of any of the units comprising the Komatipoort intrusion. If the other units present in the intrusion

are assumed to have a similar attitude to unit 2, the sequence of rock units from west to east across the Komatipoort intrusion (olivine gabbro, clinopyroxene-plagioclase cumulate, granophyric gabbro, granophyre, feldspathic gabbro), on initial inspection, is suggestive of a cross-section of a tholeiitic sheet which has fractionated in situ by crystal settling. It is apparent however, from the preceding account, that the Komatipoort intrusion is a composite body. The origin of each of the five major units and their genetic relationships is therefore discussed briefly below. The crystallisation history of the complex is described later, (see p 274).

(i) Unit 1 - The olivine gabbro

Several lines of evidence are available to suggest the importance of cumulus processes in the formation of the olivine gabbro. These include the similarities in major element composition between the olivine gabbro and olivine-plagioclase cumulates from the Skaergaard intrusion, (see Table 35), the ophitic textures described in the section on petrography and in addition the troctolitic modal compositions of some specimens from unit 1. If the finer-grained specimen described from near the southern extremity of the unit (see p 125), (which contains large olivine and smaller, oscillatory zoned plagioclase phenocrysts), is regarded as a marginal phase of this unit, it is apparent that plagioclase and olivine phenocrysts were present in some abundance in the parental magma at the time of its emplacement. Both modal concentrations of the major rock forming minerals and major element oxides show apparently random fluctuations along cross-sections across the unit and there is thus no evidence of concentration of phenocrysts by flowage differentiation. The olivine gabbro appears therefore to have originated initially by the settling of olivine and plagioclase phenocrysts from a relatively phenocryst-rich magma-body,(probably with a sheet like form), accompanied by crystallisation of the residual magma.

The random orientation of the plagioclase crystals suggests they may have settled, in part at least, as glomeroporphyritic aggregates.

Petrographic evidence from samples collected along the Sihlangula Stream section suggest recrystallisation in response to high temperature contact metamorphism has occurred subsequent to the formation of the olivine gabbro. The absence of lower temperature mineral assemblages towards the interior of the Komatipoort intrusion, coupled with the presence of such assemblages in the adjacent basalts, suggests that the temperature gradient responsible for the metamorphism, increased towards the interior of the intrusion. Possible confirmation of this is provided by the nature of the variation in mineral textures along the Sihlangula Stream cross-section. As is apparent from the section on the petrography of the olivine gabbro, (p 117), and that on mineralogy, (p 126), each of the major rock-forming minerals in unit 1 are first affected by recrystallisation processes at different points in the cross-section. Thus olivine only is affected in the most easterly parts of the unit, however in the middle of the unit plagioclase also shows signs of recrystallisation. Finally in the most westerly parts of the unit pyroxene is recrystallised in addition to the other two major rock forming minerals. This sequence, olivine, plagioclase, pyroxene, corresponds to the order of crystallisation that may be deduced from the textures present in the un-metamorphosed olivine gabbro. Available evidence suggests therefore, that in the most easterly part of unit 1, conditions were such that only the highest temperature mineral, (olivine), was affected and the lower temperature minerals, plagioclase and pyroxene, were stable in their igneous form. Under the conditions prevailing near the middle of the unit both the olivine and the intermediate temperature plagioclase were unstable, and only the relatively low temperature pyroxene was stable in its igneous configuration. Finally at the western contact the entire igneous assemblage was unstable under prevailing conditions. In view of the relatively short distance over which these textural changes take place, and the initially relatively homogeneous nature of the olivine gabbro, noted in other parts of the unit, it is considered likely that differences in temperature, rather than other factors such as pressure, volatile

concentration, PO_2 etc., are responsible for the observed textural variations. Since the temperature range over which each of the major rock forming minerals, (olivine, plagioclase and pyroxene), is stable, is likely to be related to their temperature of crystallisation, the observed textures are considered to indicate that the olivine gabbro in the Sihlangula Stream section was recrystallised under the influence of a temperature gradient rising from around 700°C (pyroxene hornfels facies at low pressures), at the western contact to yet higher temperatures at the eastern contact of the unit with the clinopyroxene-plagioclase-cumulate. These higher temperatures were apparently still below those required for partial melting of the olivine gabbro.

(ii) Unit 2 - The clinopyroxene-plagioclase cumulate

Abundant evidence of a cumulus origin is available for unit 2, the clinopyroxene-plagioclase-cumulate, in the form of the widespread igneous lamination and the gravity stratified units described in the section on petrography, (see p 142). The relatively fine-grained, seriate textured rocks described from the contact with the olivine-plagioclase-cumulate, (see p 142), contain what appear to be partially resorbed xenocrysts derived from the olivine-plagioclase cumulate, suggesting the contact between unit 1 and unit 2 is unlikely to be gradational. Instead the textural evidence suggests an intrusive contact between a younger magma, of which the clinopyroxene-plagioclase-cumulate is a derivative, and a pre-existing olivine gabbro. Intrusion of this magma after the formation of the olivine gabbro, could, in addition provide an adequate heat source for the contact metamorphic effects observed in the olivine gabbro in the Sihlangula Stream section.

(iii) Unit 3 - The granophyric gabbro

An important factor in considering the origin of the granophyric gabbro is the relationship of this unit to the other units in the intrusion. Dykes of granophyre have been observed cross-cutting

the granophyric gabbro and the 'grey granophyre' described earlier, has been interpreted here as a xenolith of granophyric gabbro in the granophyre. The granophyric gabbro is thus considered to be older than the granophyre. Xenoliths of feldspathic gabbro were found in the upper part of the granophyre and the feldspathic gabbro is therefore considered to be older than the granophyric gabbro. Thus the granophyric gabbro can have a direct genetic relationship only with the olivine gabbro or the clinopyroxene-plagioclase-cumulate. The granophyric gabbro however shows no signs of the contact metamorphic effects noted in places in the olivine gabbro of unit 1, which are to be expected if unit 2 had an intrusive relationship with the granophyric gabbro. It appears probable therefore that the granophyric gabbro could be directly related by fractionation processes only to unit 2 the clinopyroxene-plagioclase-cumulate. The granophyric gabbro shows a distinct resemblance to the mildly fractionated tholeiitic rocks of the Birds River Complex, as described in a previous section, (see p 227). This similarity, together with the position of the granophyric gabbro just to the east of the easterly dipping clinopyroxene-plagioclase cumulate, suggest that the granophyric gabbro could represent the upper more acid component of a single intrusive tholeiitic unit, which fractionated by crystal settling to produce both units 2 and 3. No direct evidence is available as to the nature of the contact between the granophyric gabbro and the clinopyroxene-plagioclase-cumulate, because of the lack of exposures, mentioned in the section on the lithology of these rocks, (see p 140). There is however, other indirect evidence which provides some support for a direct genetic relationship between the two rock types. This includes:-

1) The Ca-rich pyroxene compositional variation trend is reasonably continuous from the clinopyroxene-plagioclase-cumulate to the granophyric gabbro.
2) The plagioclase in the upper part of the clinopyroxene-plagioclase-cumulate is similar in composition and zoning to some of the plagioclase in the granophyric gabbro.
3) Chemical and mineralogical variations between the two units in general appear compatible with such a genetic relationship.

4) The similarity in the distribution of the two rock types.

Other features however, suggest a more complex origin for the granophyric gabbro, namely:-

1) The widespread reaction and resorbtion textures coupled with the presence of mechanically deformed grains of pyroxene and plagioclase (see p 160), suggest a possible hybrid origin for the granophyric gabbro.

2) Major elements, when plotted against the fractionation index (see fig 36), tend to approximate a straight line, again suggesting a hybridization process.

3) A relatively SiO_2-rich average composition is obtained if the exposed portions of these rock types are assumed to represent the actual abundance of the two rock types and are used to calculate the average composition of a magma parental to units 2 and 3, (see Table 42),

In view of the small number of available analyses of both minerals and rocks from the Komatipoort intrusion, no attempt has been made to use quantitative modelling to assess the relative merits of crystal fractionation and hybridisation processes responsible for the genesis of units 2 and 3. Examination of the Cr contents of the rocks of the Komatipoort intrusion, recorded in Table 32 , however, shows that both the clinopyroxene-plagioclase-cumulate samples and the granophyre samples have Cr values higher than that of the granophyric gabbro analyses, suggesting that the granophyric gabbro is unlikely to have originated by hybridization of the clinopyroxene-plagioclase-cumulate by magma similar in composition to the granophyre.

A further point which should be taken into consideration, is that, for reasons already given, none of the other rock units in the

in the Komatipoort intrusion could represent the upper more acid component from which the cumulus phases which constitute bulk of unit 2 have been removed.

In general therefore, the available evidence appears to favour the interpretation that units 2 and 3 represent the lower and upper portions of a single fractionated tholeiitic sheet. The evidence suggest however that the granophyric gabbro either suffered later partial hybridization by a relatively small quantity of intrusive acid magma, or, more likely, at a late stage in the crystallisation history of the unit, a tectonic event effected a redistribution of late stage interstitial fluids, producing the hybrid and deformation textures noted in the granophyric gabbro.

(iv) Unit 4 - The granophyre

Clear evidence is available for an intrusive origin for the granophyre of unit 4. This evidence includes an intrusive contact between the granophyric gabbro and the granophyre, (exposed in the Komati River), and the presence of xenoliths of feldspathic gabbro near the upper contact of the granophyre. In addition, north of the Crocodile River the granophyre occurs together with the feldspathic gabbro only. Further evidence of its intrusive nature is provided by the frequently symmetrical variation of major element oxide concentrations about the centre of the unit.

No unequivocal evidence was found for the form or attitude of the granophyre unit, however its constant position between the feldspathic gabbro and the granophyric gabbro, both of which are here interpreted as sub-concordant sheets, suggests that the granophyre may be of a similar nature.

(v) Unit 5 - The feldspathic gabbro

As exposed in the Komati River, the feldspathic gabbro unit has a fairly well exposed, intrusive, upper contact with the basalts,

and this contact, in places appears to be dipping towards the east at a moderate angle. The nature of this upper contact combined with evidence provided by the variations in texture and modal proportions in the feldspathic gabbro unit, are considered to indicate that the feldspathic gabbro is a sub-concordant sheet which has suffered mild fractionation by crystal settling.

Xenoliths of the feldspathic gabbro are found in the granophyre and the granophyric gabbro, and the granophyric gabbro and the clinopyroxene-plagioclase-cumulate are considered to have a common origin, as described earlier. The feldspathic gabbro is therefore considered to be older than units 2, 3 and 4. Thus the only unit which could have a direct genetic relationship with the feldspathic gabbro is the olivine gabbro of unit 1. Various similarities between the olivine gabbro and the feldspathic gabbro are present, and suggest the possibility that the olivine gabbro may represent the base of the feldspathic gabbro unit, enriched in cumulus olivine and plagioclase. The similarities include the large plagioclases present in both units (size, composition, oscillatory zoning) trace element contents, (especially Ni, - see Table 44A,B), pyroxene composition, (although the feldspathic gabbro pyroxene compositions were determined in only one sample)and textures present in some of the rocks.

Important differences, include the high olivine content of the olivine gabbro and the absence of olivine in the feldspathic gabbro. Small quantities of olivine were noted in the feldspathic gabbro unit near the Crocodile River however. The most significant difference between the two units appears to lie in the fine grained marginal rocks. The finer grained marginal rocks from the southern extremity of the olivine gabbro contain large olivine phenocrysts and smaller oscillatory zoned plagioclase phenocrysts, (see p 125). These phenocrysts are completely absent from the upper contact rocks of the feldspathic gabbro. The large differences in the composition of upper and lower contact rocks of what would in effect be a relatively

thin sheet suggests that the olivine gabbro and the feldspathic gabbro are unlikely to be related in terms of simple crystal fractionation. It is possible however that they may be derived from a common source. There is no direct indication of the relative ages of units 1 and 5, the only indication is provided by the absence of any evidence of two phases of contact metamorphism in unit 1, the olivine gabbro, which suggests the olivine gabbro is younger than the feldspathic gabbro.

(vi) Summary

The available evidence is here interpreted as suggesting that the formation of the Komatipoort intrusion involved:-

1) Intrusion and fractionation by crystal settling of magma parental to the feldspathic gabbro of unit 5. The unit probably has the form of a sub-concordant sheet.

2) Intrusion of magma parental to the olivine gabbro below unit 5, again in the form of a sub-concordant sheet, following by settling out of the cumulus olivine and plagioclase present in the magma.

3) Intrusion of tholeiitic magma between units 1 and 5 followed by fractionation (crystal settling) to produce units 2 and 3. These units also form sub-concordant sheets.

4) Intrusion of the granophyre of unit 4, as a sub-concordant sheet.

(N) Petrogenesis of the Komatipoort Intrusion

(i) Unit 5 - The feldspathic gabbro

The available evidence, slight though it may be, (described in a preceding section) suggests that the feldspathic gabbro may be the oldest member of the heterogeneous group of intrusives comprising the Komatipoort Intrusion. Formation of the Komatipoort intrusion is therefore assumed to have been initiated by the emplacement of the magma responsible for the formation of the feldspathic gabbro unit. Variations in modal composition, texture, and to a lesser extent geochemistry (owing to the small number of available analyses), from east to west across the feldspathic gabbro unit are considered important evidence that the intrusion was formed by the emplacement of a horizontal sheet of gabbroic magma, which subsequently suffered mild differentiation by crystal fractionation, (predominantly of plagioclase). Differences in the modal variation curves (see fig 31 , p 208), between the Sihlangula section and the Railway Bridge Section may be explained largely by the fact that the thinner, southern portion of the sheet, cooled relatively rapidly, and thus crystal settling was not as effective as in the northern portion of the sheet. With a thickness of only 100 meters, even the northern part of the sheet would probably cool fairly rapidly and it is proposed that relatively high concentrations of volatiles may have been present to reduce viscosity and promote crystal settling. Some evidence for this low viscosity is available, at the upper contact of this unit, where veinlets of feldspathic gabbro 3 - 4 cms in width, penetrate the country basalt along joint planes for distances of up to 10 m. Further the widespread alteration of the major rock forming minerals to albite,epidote, chlorite etc., even in the feldspathic gabbro outcropping in the Sikwawa River a few kms east of the Komatipoort intrusion, suggests possible alteration of the feldspathic gabbro by late-stage, low temperature fluids.

Available evidence indicates that plagioclase with a composition of the order of An_{65} crystallised alone initially, and settled out to accumulate at the base of the intrusion, initially together with more basic plagioclase phenocrysts present in the magma of the time of its emplacement. The composition of the magma was such that pyroxene did not commence crystallisation until the temperature of the magma had dropped significantly, and thus in the lowest parts of the intrusion, in the railway bridge section, pyroxene occurs as sub-ophitic to ophitic plates enclosing the plagioclase crystals. The pyroxene at this point is therefore, considered to be an intercumulus phase.

At a slightly later stage in the crystallisation history of the intrusion, when the magma temperature within the main body of the intrusion had dropped sufficiently, pyroxene joined plagioclase, as a cumulate phase. These minerals accumulated to form the rocks comprising the lower-middle part of the sheet, and it is here that faint igneous lamination and a slight preferred orientation of the plagioclase crystals within the plane of the layering, are developed. The latter orientation may be evidence for the presence of weak convection currents at this stage of development of the sheet. In the upper two thirds of the sheet there is no evidence of settling of individual crystals, although possibly some fractionation may have been effected by settling of glomeroporphyritic aggregates. The mild differentiation produced by the process described above, as indicated in the relevant section of geochemistry has resulted in a slight upward decrease in alumina, magnesium and calcium and an increase in titanium, potassium, phosphorus and iron content. The calcium and alumina concentration at the base is interpreted as resulting from the accumulation of plagioclase. The upward increase in iron content is probably due to the fact that magnetite did not crystallise as a cumulus phase. The late crystallisation of magnetite may in turn be explained as a result of the effect of relatively low PO_2 amongst other factors, according to studies by Osborn (1959 and 1962), Roeder and Osborn (1966), Hamilton and

Anderson (1968) and Haughton, Roeder and Skinner, (1974),however a low fO_2 appears unlikely in view of the probable high H_2O levels present. The fine grained upper contact rocks show some noteworthy geochemical features, including an increase in the concentration of oxides such as SiO_2, $FeO + Fe_2O_3$ and K_2O and a decrease in Al_2O_3 content, as the upper contact of the feldspathic gabbro unit with the country basalts is approached. In addition the single specimen of a fine grained contact rock for which trace element data is available, (CL 46), appears unusually rich in Ni, Co and Cr in relation to its fractionation index (see fig 37A,B)Most of the features of the geochemistry of these contact rocks commented on here, are in one way or another a reflection of the concentration of pink glassy interstitial material present in these rocks. The concentration of this interstitial mesostasis increases towards the upper contact, and in view of the presence of an acid intrusive along the upper contact, and the tendency of this intrusive to form hybrid rocks locally, (see description p 205), it appears possible that these contact rocks represent an initial stage in a hybridisation process. Textural features of these rocks do provide some support for this proposal. The pink mesostasis may therefore be considered to represent infiltrating, hybridising acid magma. Introduction of increasing amounts of this magma would account for the variations in major element oxide concentrations and, by raising the fractionation index, account for the apparently abnormal trace element concentrations.

(ii) Unit 1 - The olivine gabbro

Following the emplacement of the feldspathic gabbro, the magma responsible for the formation of the olivine gabbro is considered to have been intruded. Finer grained rocks from the southern extremity of the unit here interpreted as rapidly cooled marginal phases, contain phenocrysts of olivine and smaller oscillatory zoned phenocrysts of plagioclase, suggesting the magma contained such phenocrysts in suspension on intrusion.

The presence of less basic second generation plagioclase crystals and mantles of a similar composition around the oscillatory zoned first generation crystals, in the coarser-grained olivine gabbro samples, indicates that shortly after intrusion plagioclase of this composition crystallised, both as new crystals and around the pre-existing phenocrysts. The rounded form of some of the olivine crystals could indicate that olivine crystallisation ceased either before or directly after emplacement of the magma, but some metamorphism of the olivine grains may have occurred. Textures of the olivine gabbros are interpreted as indicating the settling out of the olivine and plagioclase grains followed by crystallisation of the intercumulus pyroxene plates and albite-rich rims to the plagioclase crystals. As temperatures dropped further hypersthene was formed by inversion of clinopyroxene. The bulk of the major element oxide variation and some of the trace element variation in the unit is thus controlled by fluctuations in the proportions of the two cumulus phases, olivine and plagioclase, on the one hand and the abundance of the intercumulus minerals, largely pyroxene, on the other. The abundance of other major elements and 'residual' trace elements are controlled more directly by the abundance of trapped intercumulus liquid present in the rock.

A possible objection to this origin for the olivine gabbro unit could be found in the relatively thin nature of the unit (15m), if it has the concordant sheet-like form proposed here. The slight thickness of the unit would imply, either that the concentration of phenocrysts in the magma at the time of emplacement was unusually high, or that evidence of a former more extensive upper portion of the unit has been destroyed by later igneous activity. Petrographic evidence suggested the presence of an intrusive contact between the olivine gabbro and the clinopyroxene-plagioclase-cumulate, (see p 142), and during the emplacement of unit 2, the upper part of unit 1 could have been eliminated by stoping,or if unit 1 was still in the process of crystallising, by simple mixing of the two magmas. Evidence of the intrusive nature of the contact

between unit 1 and unit 2, includes the presence of microxenoliths of olivine gabbro in the lower part of the clinopyroxene-plagioclase-cumulate. The presence of these microxenoliths indicates that at least the lower part of the olivine gabbro unit was completely crystalline at the time of the intrusion of the magma from which the clinopyroxene-plagioclase cumulate was derived.

In the Sihlangula River section, the olivine gabbro appears to have suffered high temperature contact metamorphism. Because of the direction in which the metamorphic temperature gradient increases and in addition, because of the high-grade nature of the metamorphism, (i.e. pyroxene hornfels at the lower contact of unit 1, rising into the interior of the unit), the heat source is considered to have been the relatively thick layer of magma, parental to the clinopyroxene-plagioclase-cumulate, and known to be intrusive into the olivine gabbro. The absence of contact metamorphic effects in other parts of the olivine gabbro unit then requires comment, and it is suggested here, may be accounted for by differences in water content of the olivine gabbro along the length of unit 1, or possibly by variations in the temperature gradient along the length of unit 1, resulting in turn from variations in the attitude or shape of the lower contact of the intruding magma body.

(iii) Units 2 and 3 - The clinopyroxene-plagioclase-cumulate and the granophyric gabbro

After the consolidation of the lower part at least, of the olivine gabbro unit, the magma parental to the clinopyroxene-plagioclase-cumulate and the granophyric gabbro is considered to have been intruded, again in the form of a sub-concordant sheet. It is apparent from the petrographic evidence of the contact rocks (see p 142) that clinopyroxenes and plagioclase of a more fractionated composition than those present in the olivine gabbro were the initial phases to crystallise out of this magma. It is also clear from these contact rocks that a proportion of xenocrysts and

microxenoliths derived from the olivine gabbro were caught up in this magma on intrusion. Sporadic large rounded olivine crystals that occur in the lower part of unit 2 are considered to have originated in this fashion, and the initial pulse of magma from which unit 2 is derived, was possibly, olivine-free prior to intrusion. The igneous lamination present even in the lowest parts of this unit provides evidence of settling of the crystallising plagioclase and clinopyroxene, and in places particularly in the upper portion of the unit, magnetite joins the silicates as a cumulus phase.

In the lower half of unit 2 in particular, the clinopyroxene and plagioclase crystals commonly contain well-defined cores of a slightly different composition. For the pyroxenes, the compositional differences are usually in terms of Mg-Fe content, and to a lesser extent, Ca-content. The cores may be regarded as phenocrysts present in the magma at the time of its emplacement, however there does not appear to be any evidence of a phenocryst population in the lower contact rocks between units 1 and 2. Rather it is suggested, they provide evidence of the influx of a second pulse of magma after the onset of crystallisation in the first. This second pulse of basic magma could also have been an important factor in determining the homogeneous character of the lower two thirds of unit 2, since it would result in basification of any fractionated residue produced by earlier crystal settling.

The upper third of unit 2 is marked by the appearances of abundant fayalitic olivine, and it is suggested that this provides evidence suggestive of a gradual evolution of the residual magma to more highly fractionated iron-rich compositions. Rapid settling of the crystals of both plagioclase and clinopyroxene, which were apparently crystallising from the magma continuously led to an Fe-enriched residual liquid, and ultimately, in the upper third of the unit, cumulus magnetite makes its appearance in some abundance.

From the study made of the rhythmic gravity stratified units, it appears that cooling conditions at the top of the magma chamber allowed the development of concentrations of plagioclase, pyroxene and magnetite crystals, which, possibly by a process similar to that described by Wager and Brown, (1968), formed magmatic density currents considered responsible for the development of the gravity stratified rhythmic layers. Evidence provided by grain size measurement however, suggests that crystallisation of plagioclase at least, continued within the density current.

It has been suggested earlier that the granophyric gabbro represents the acid residuum of the original tholeiitic magma sheet, after removal of the cumulate crystals present in the clinopyroxene-plagioclase-cumulate. As noted earlier, however, if this is the case, the homogeneous nature of the granophyric gabbro, and the deformation effects present in the major rock-forming silicates in this unit, coupled with the reaction textures commonly found in these rocks, suggest that the granophyric gabbro may have been disturbed and to some extent mixed by a tectonic event late in its crystallisation history. An alternative possibility is that the granophyric gabbro has been hybridised by its own late stage acid derivatives migrating up-dip during the eastward tilting which has occurred in this area. A similar up-dip migration of acid differentiated has been proposed by Ernst (1960), for the Endion Sill. Effectively however, differences between the two proposals are small and the granophyric gabbro still represents the upper fractionated portion of a differentiated tholeiitic sheet.

(iv) Unit 4 - The granophyre

Evidence of granophyre dykelets cross-cutting both the granophyric gabbro and the feldspathic gabbro, indicates that the granophyre was emplaced between two solidified sheets, and the presence of abundant xenocrysts and xenoliths along both margins of the granophyre suggests that this intrusion was of a forceful nature. Some

of the alteration present in the feldspathic gabbro may be ascribed to the effects of the granophyre, although similar features are not developed in the granophyric gabbro. This is because the feldspathic gabbro lies above the granophyre and any escaping volatiles may be expected to pass upwards from the intrusion through the feldspathic gabbro, particularly since much of the shattering and cracking present in the feldspathic gabbro could have been produced during earlier igneous activity. Thus relatively free passage may have been available for volatiles and these may be in part responsible for the sericitisation of plagioclase in the feldspathic gabbro, the mild degree of alteration of the pyroxenes and, the development of zeolites. The granophyre is relatively thin and may, in any case, have been intruded at a fairly low temperature thus effects on the granophyric gabbro could have been largely deformational.

The distribution of mineralogical and chemical features along the cross-section of the granophyre, is in most cases, symmetrical or slightly assymmetrical about the centre of the unit. In part this appears to be governed by the distribution of xenocrysts, however it is likely that in addition crystallisation occurred simultaneously from both margins inwards. The presence of occasional xenocrysts and xenoliths of feldspathic gabbro at the western contact of the unit suggest that settling of aggregates of the crystals may have occurred and that slight crystal fractionation may also have played a part.

There are similarities in modal abundances of major mineral phases and major element chemistry, between the granophyre of the Komatipoort intrusion and the fractionated rocks forming the upper acid differentiates of fractionated tholeiitic sheets.

In view of the strong evidence of an intrusive relationship between the granophyric gabbro and the granophyre, the granophyre cannot however be an <u>in situ</u> fractionation product unless subsequent auto-

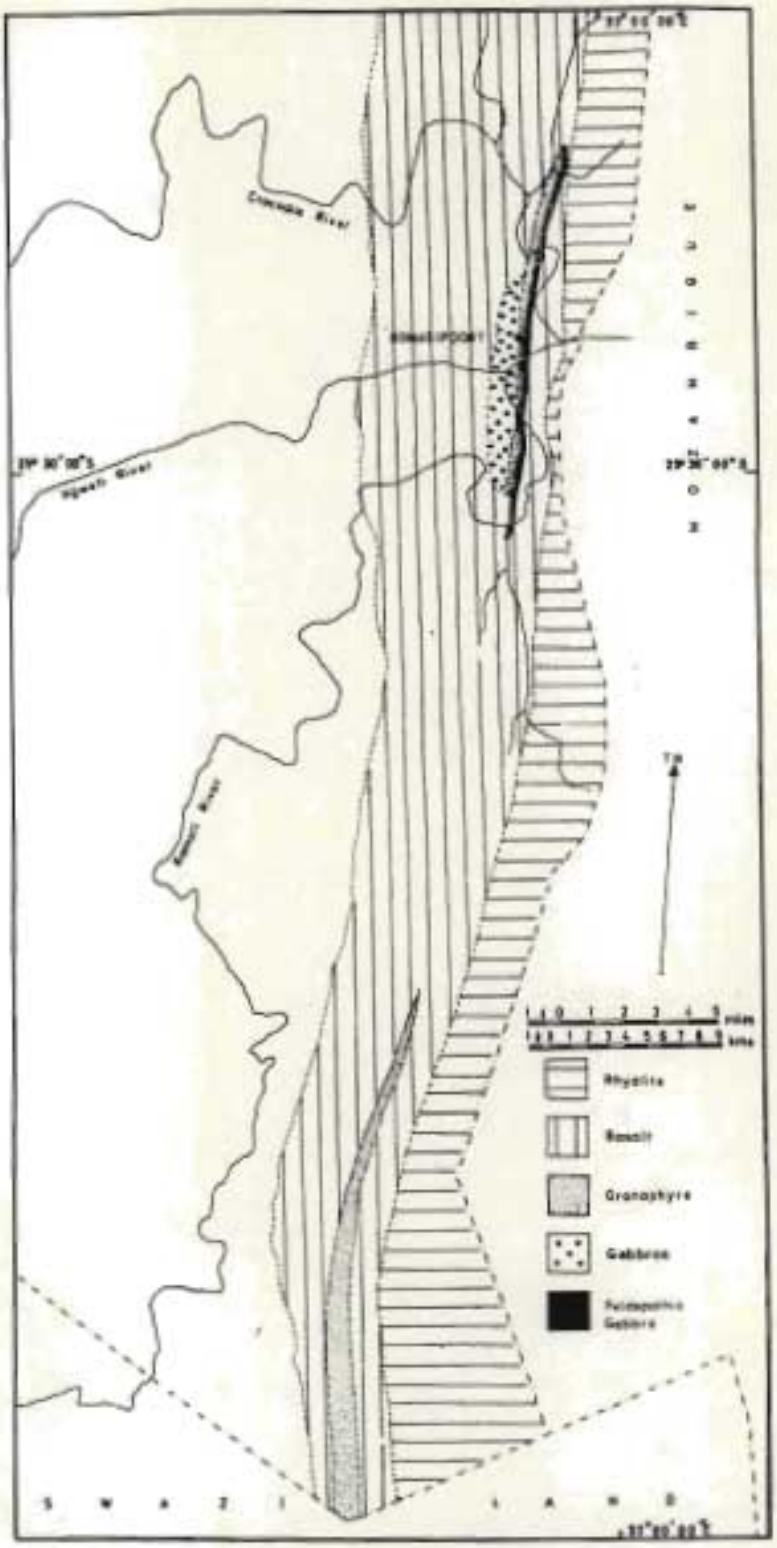

Figure 41. Distribution of granophyre bodies in the Western portion of the Lebombo belt between Komatipoort and Swaziland.

intrusion has occurred. The down-dip extent of the intrusion is unknown and equally well the volume of rock now eroded off may have been of considerable size. Tectonic movements during the final stages of development of other parts of the intrusion may therefore have resulted in the separation of a granophyric fraction and its intrusion between the feldspathic gabbro and differentiated series rocks. No conclusive evidence is available, however, and it may be significant that other larger bodies of granophyre have intruded the basalts at roughly the same stratigraphic height as the Komatipoort granophyre, also cropping out in a manner which suggests a sheet-like form (see map in fig 41, p 283). Similarly,in the Nuanetsi Province, the main granophyre is known to form an extensive granophyre sheet and these granophyres, may therefore represent a widespread related, intrusive event in the Lebombo. Little quantitative data is available, for these intrusives at this juncture, but their presence does provide additional evidence that the granophyre at Komatipoort may have an origin independent of the other Komatipoort intrusion rocks.

The above discussion applies to the southern granophyre mass, as all available analyses are from the southern mass. In the northern part of unit 4, there is both field and petrographic evidence that the additional textural variations present result largely from the intrusion of several smaller acid dykes into the main granophyre body. The petrogenesis of the granophyre unit of the Komatipoort Intrusion is discussed further in the section on the origin of the acid volcanics, (see p 320).

5.8 THE GEOCHEMISTRY OF THE KARROO VOLCANICS IN THE KOMATIPOORT AREA

5.8.1 INTRODUCTION

Excluding analyses of samples from the major intrusives, (described earlier), twelve new analyses of volcanic rocks have been presented. Amongst these are two olivine-rich basalts, three olivine-poor basalts, (including one intermediate type), one olivine-rich dyke rock, four dolerites and two rhyodacites. Results are shown in Tables 5, 8, 10, 13 and 16.

5.8.2 GEOCHEMISTRY OF THE BASALTS OF THE KOMATIPOORT AREA

The tholeiitic character of both olivine-poor basalts and olivine-rich basalts is indicated by the large amount of hypersthene present in their norms, and is confirmed by the Murato diagram shown in fig 42 , p 285 , on which the basalt and dolerite analyses have been plotted. All of the basic volcanics fall into the tholeiitic field, the boundary of which, in fig 42 , p 285 , is defined by the line ABCD.

Cox, et al (1965) subdivided the tholeiitic basalts of the Nuanetsi area into two genetically distinct, differentiated series, namely a high magnesium series with an Fe/Mg index $\left(\frac{FeO + Fe_2O_3}{FeO + Fe_2O_3 + MgO}\right)$, of less than 50, and a low magnesium series with an Fe/Mg index greater than 50. The presence of these two rock series has been subsequently confirmed in general in other studies. Examination of the analyses of the Komatipoort Volcanics reveals only one analysis that could be classified as a high Mg basalt, that is sample C1 25, an olivine basalt, (see Table 5 , p 16).

Variations in geochemistry have been illustrated by means of several variation diagrams including a Niggli diagram, an AFM triangular

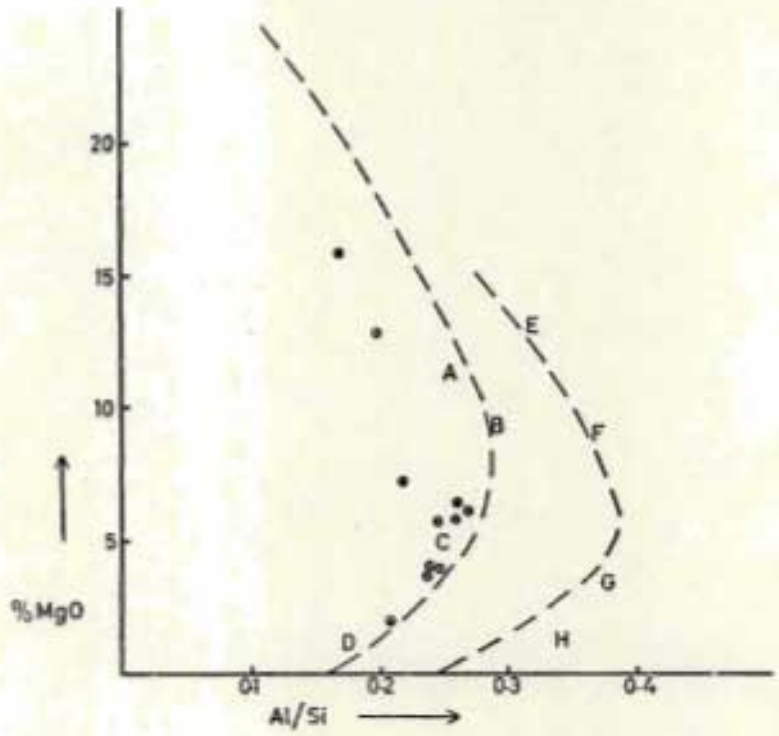

Figure 42. Murato diagram for basic volcanics of the Komatipoort Area. The line ABCD defines the field in which tholeiitic basalts plot.

variation diagram, a Harker diagram and a mafic index versus major element diagram,(see figs 43, 44, 45, 46, pgs 287, 288, 289, 290). although in view of the small number of available new analyses the results will be treated with caution.

Recently criticism has been levelled against Harker diagrams, in which major elements are plotted against SiO_2 on the grounds that because the SiO_2 value represents part of the rock analysis some regularities in variation would be expected even in unrelated rock types , (Chayes, 1967). The criticism appears valid and similar arguments could be directed against several of the diagrams used in the present work, however, for purposes of comparison it was found convenient to use the diagrams listed above. Plotting of the major elements against the index suggested by Chayes, (1967), to circumvent this objection, produces slightly more scattering but essentially the same trend. Objections to the other diagrams have been mentioned earlier, (see p 236).

(A) Variations in Geochemistry

The Niggli diagram and the mafic index diagram both show a well-developed fairly continuous variation trend, which in the case of the Niggli diagram closely approaches a straight line (see figs 43, 46, pgs 287, 290). A similar continuous differentiation series is apparent in the mafic index diagram of the same type prepared by Cox and Hornung,(1966), for Nuanetsi basalts. These show a reasonably good correspondence in the variation occurring in the basalt series from the two areas.

SiO_2 content increases slightly in basalts of higher differentiation index and Al_2O_3 shows a gradual but distinct increase from low to high differentiation index rocks. $FeO + Fe_2O_3$, although displaying some scatter is enriched at the low magnesia end of the series. MgO shows a steady and marked decrease throughout the series and TiO_2 displays a similar, although weaker, trend. CaO initially increases

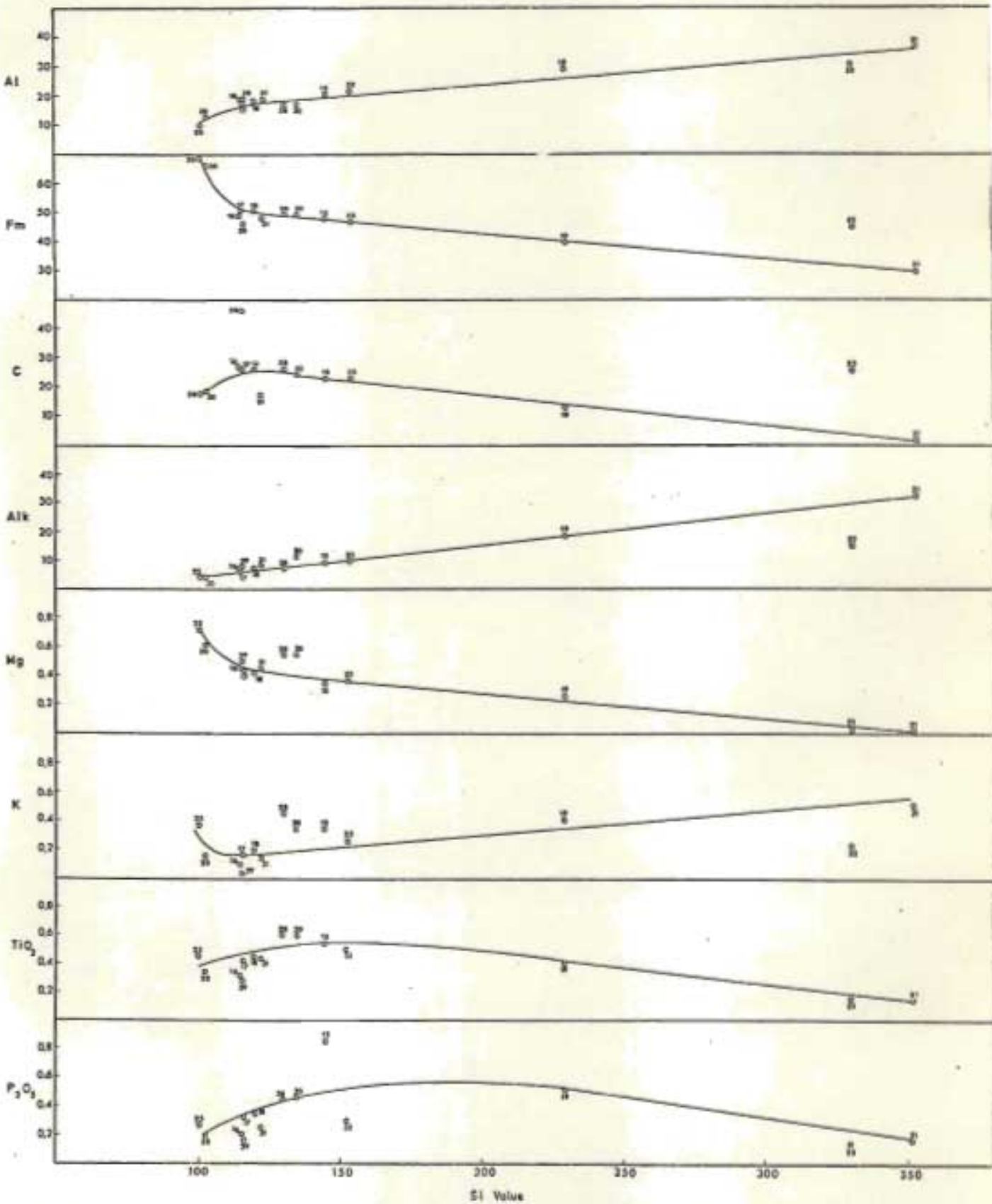

Figure 43. Niggli Variation Diagram for extrusives and intrusives from the Komatipoort area

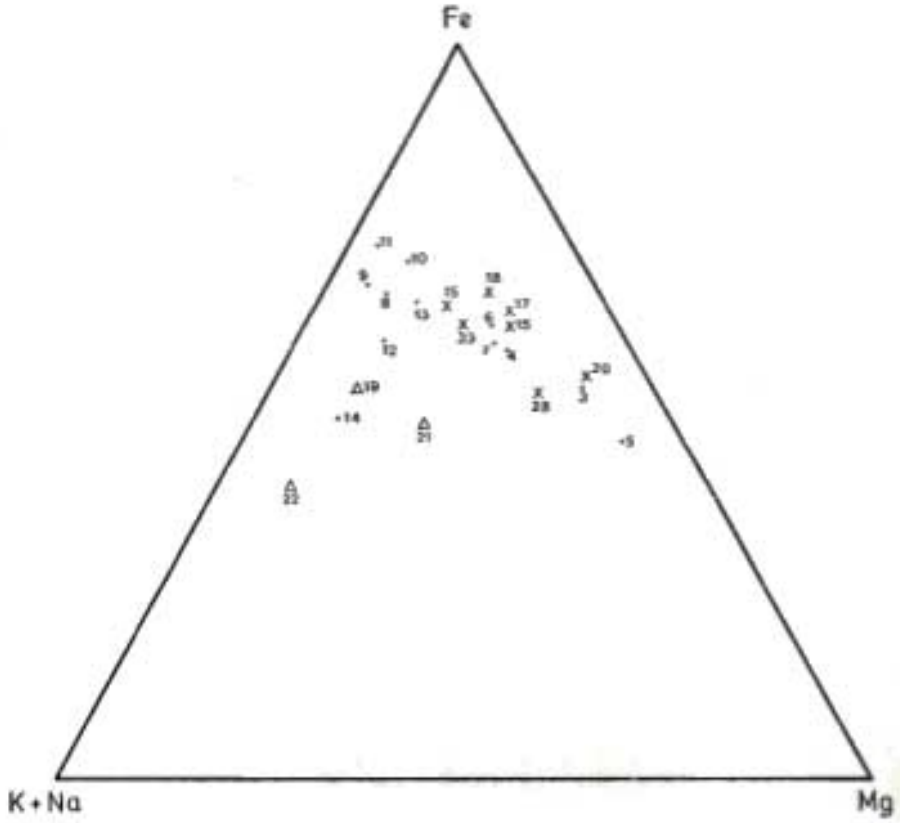

Figure 44. AFM diagram for basic volcanics of the Komatipoort area.

△ Intermediate to acid extrusives

× Dolerites and basalts

· Komatipoort Intrusion rocks

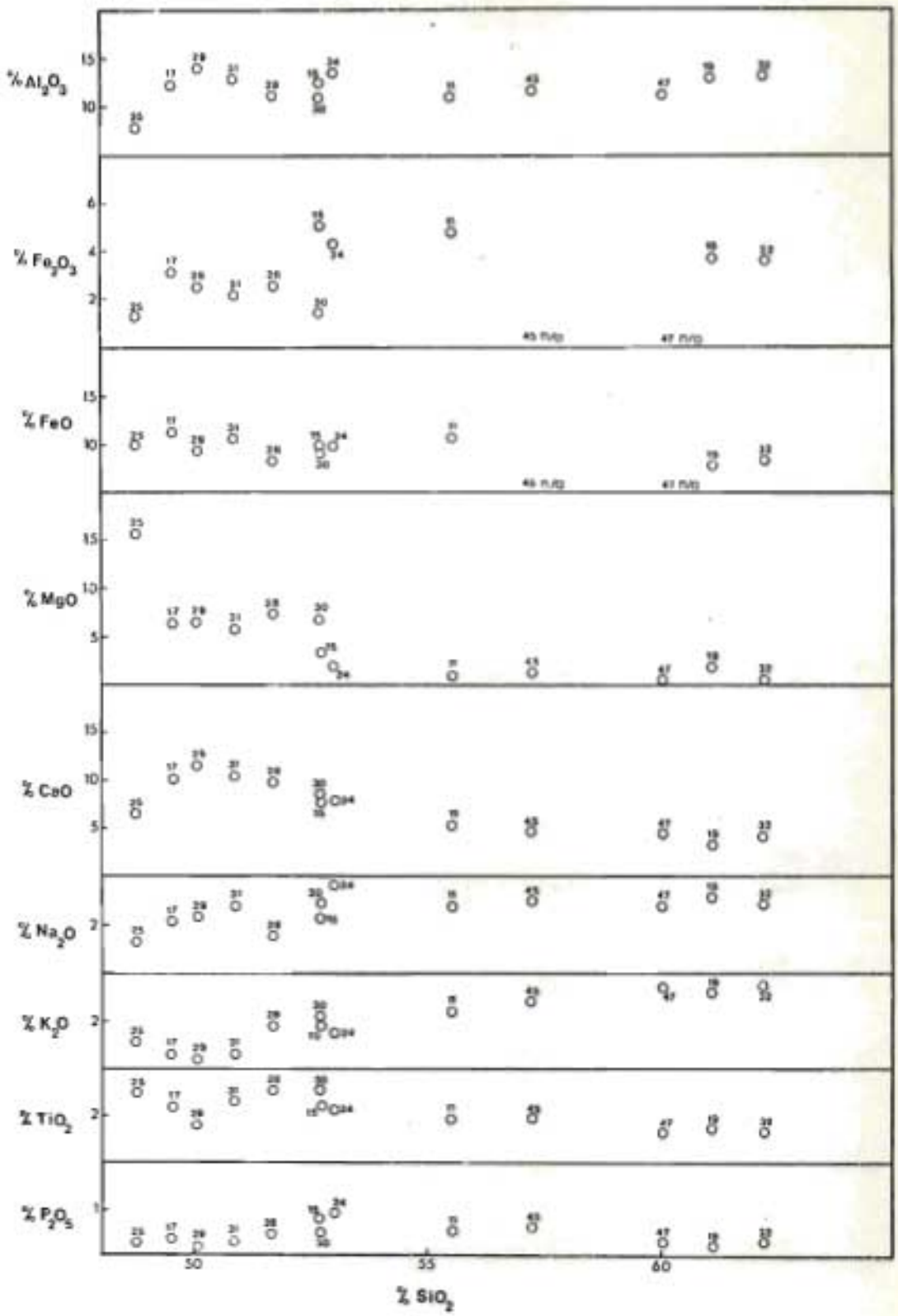

Figure 45. Harker diagram for the basic volcanics of the Komatipoort area. (Sample numbers are CL numbers).

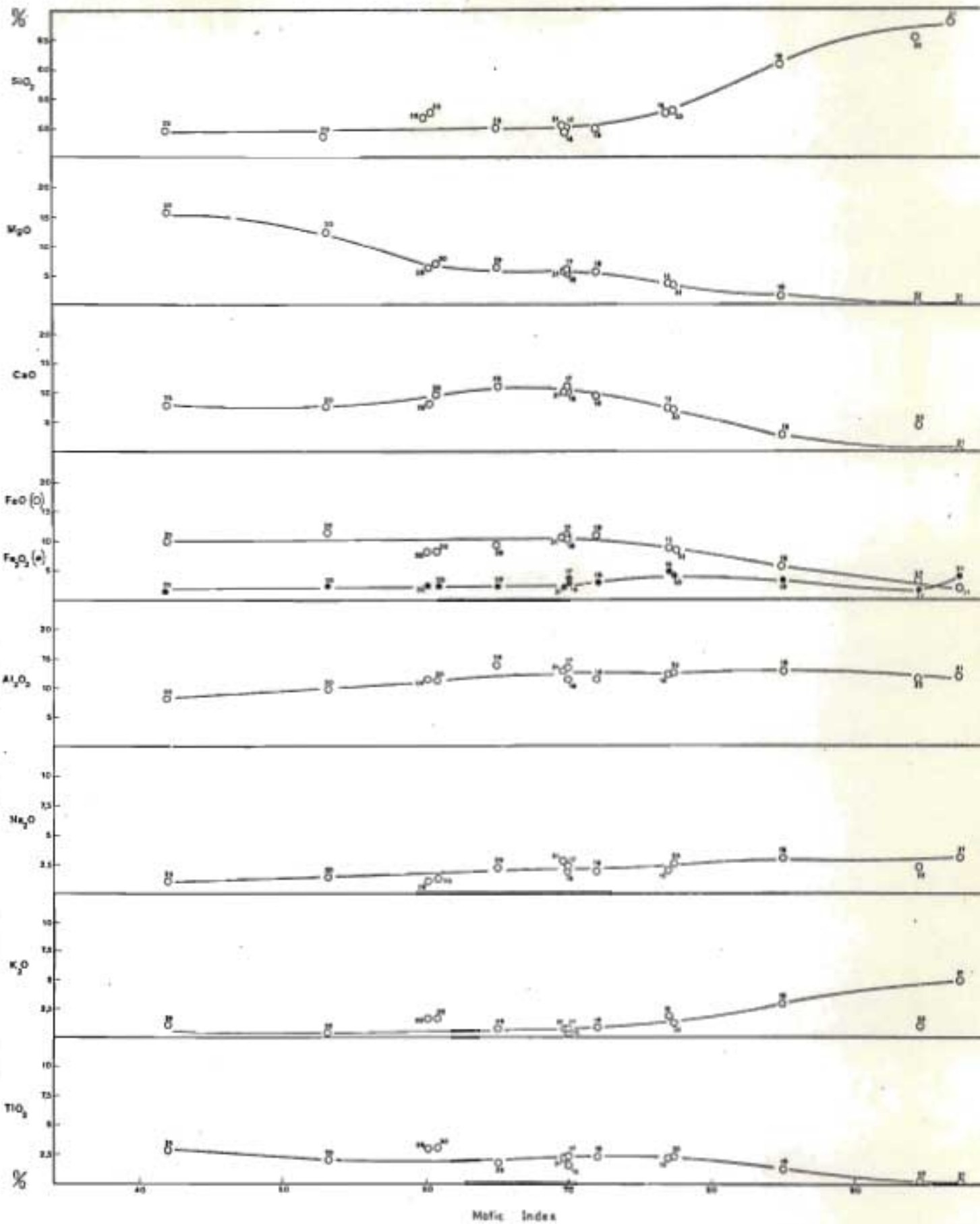

Figure 46. Matic Index versus major elements for the basic volcanics of the Komatipoort area. (All numbers are CL sample numbers)

from the high magnesia into the low magnesia rocks but a noticeable decrease occurs amongst the less-magnesium rich members of the low magnesia series. Na_2O shows a gradual but steady increase through the series.

The fractionation trend of the basaltic magma is frequently illustrated by means of the triangular AFM variation diagram, and in fig 44, p 288 , the analyses to the tholeiitic rocks from the Komatipoort area have been plotted on this diagram. For comparitive purposes, the differentiation trend displayed by the rocks of the Komatipoort Intrusion and a line joining the points representing Daly's average basalt, andesite, dacite and rhyolite have been included in the diagram. The relatively small number of analyses appear to define a distinct moderate iron enrichment curve, although at least two of the analyses fall off this line and instead lie fairly close to the curve representing Daly's average volcanics.

This mild iron enrichment trend is again shown by the diagrams in fig 47, p 292 , in which mafic index has been plotted against SiO_2 content and total iron oxides have been plotted against the same oxide. Comparisons with diagrams of Osborne (1959) again suggest that the trend indicates a mild degree of iron enrichment.

(B) Comparison of the Komatipoort Tholeiites with other Karroo Basalt Sub-Provinces

Initial direct comparison of the average chemical compositions of the Nuanetsi, Olifants River, Komatipoort, Swaziland, Drakensberg and Victoria Falls areas (Table 45 , p 293), confirm a previously known southward variation in the chemistry of the basic volcanics, (Cox, et al., 1967). In fig 48 , p 294 , the averages are compared with the Komatipoort trend. TiO_2 K_2O and to a lesser extent, P_2O_5 decrease southward while Al_2O_3 increases in general. These changes are similar to the differences found by Cox, et al., (1965), to exist between the Nuanetsi basalts and the Karroo dolerites. The

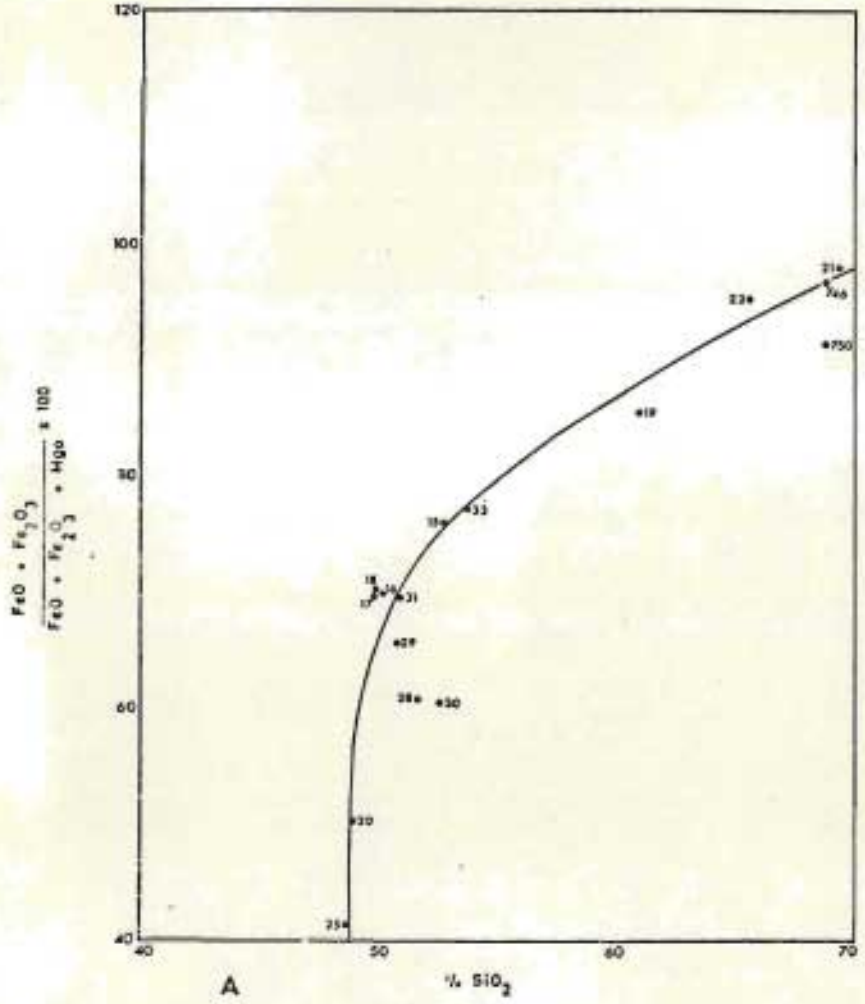

Figure 47A. Matic Index versus SiO_2 content for the basic volcanics in the Komatipoort area.

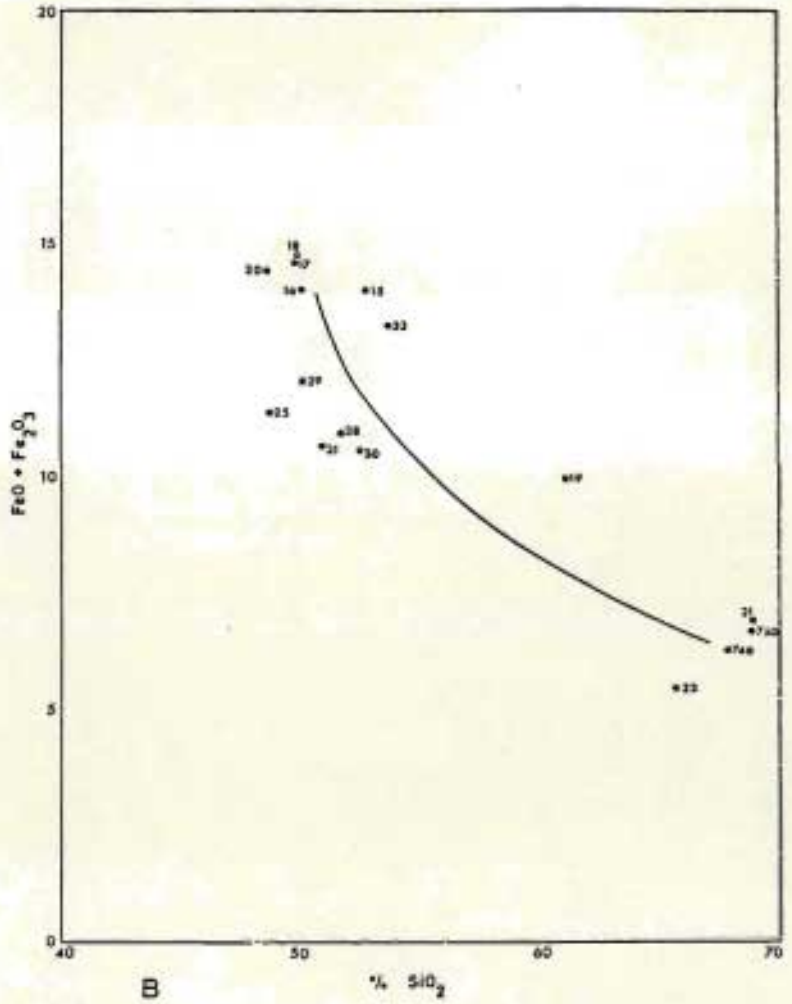

Figure 47B. Total Fe oxides versus SiO_2 content for the basic volcanics in the Komatipoort area.

TABLE 45

Comparison of average Komatipoort tholeiites with average tholeiites from other parts of the Karroo Province

	1 Drakensberg	2 Swaziland	3 Komatipoort	4 Nuanetsi	5 Average Upper Lebombo Basalt	6 Victoria Falls
SiO_2	51.80	50.47	50.62	51.63	51.89	50.53
TiO_2	1.13	1.64	2.36	2.45	2.69	2.98
Al_2O_3	14.18	15.19	12.88	13.46	12.58	13.99
Fe_2O_3	3.92	4.18	3.56	4.35	4.32	3.32
FeO	7.26	6.32	10.34	8.49	10.12	9.27
MnO	0.17	0.13	0.23	0.16	0.23	0.18
MgO	7.10	4.61	5.33	5.63	6.58	5.43
CaO	10.57	9.04	9.46	9.75	9.03	10.93
Na_2O	2.40	2.85	2.37	2.54	2.04	1.37
K_2O	0.74	0.91	0.98	1.15	0.63	0.76
P_2O_5	0.13	0.23	0.54	0.33	0.27	0.50
Number of analyses	21	5	5	5	4	5
$\frac{FeO + Fe_2O_3}{FeO + Fe_2O_3 + MgO} \times 100$	61.15	69.54	72.28	69.52	68.70	69.87

1. Cox and Hornung (1966) Table 2 Analysis 'A'
2. Urie and Hunter (1963) Table 1
3. Present work, including two analyses from de Assunção, et al.,(1961).
4. Cox, et al. (1965) Table 35 Analysis 1
5. de Assunção, et al., (1961).
6. Cox, et al. (1965) Table 35 Analysis 2.

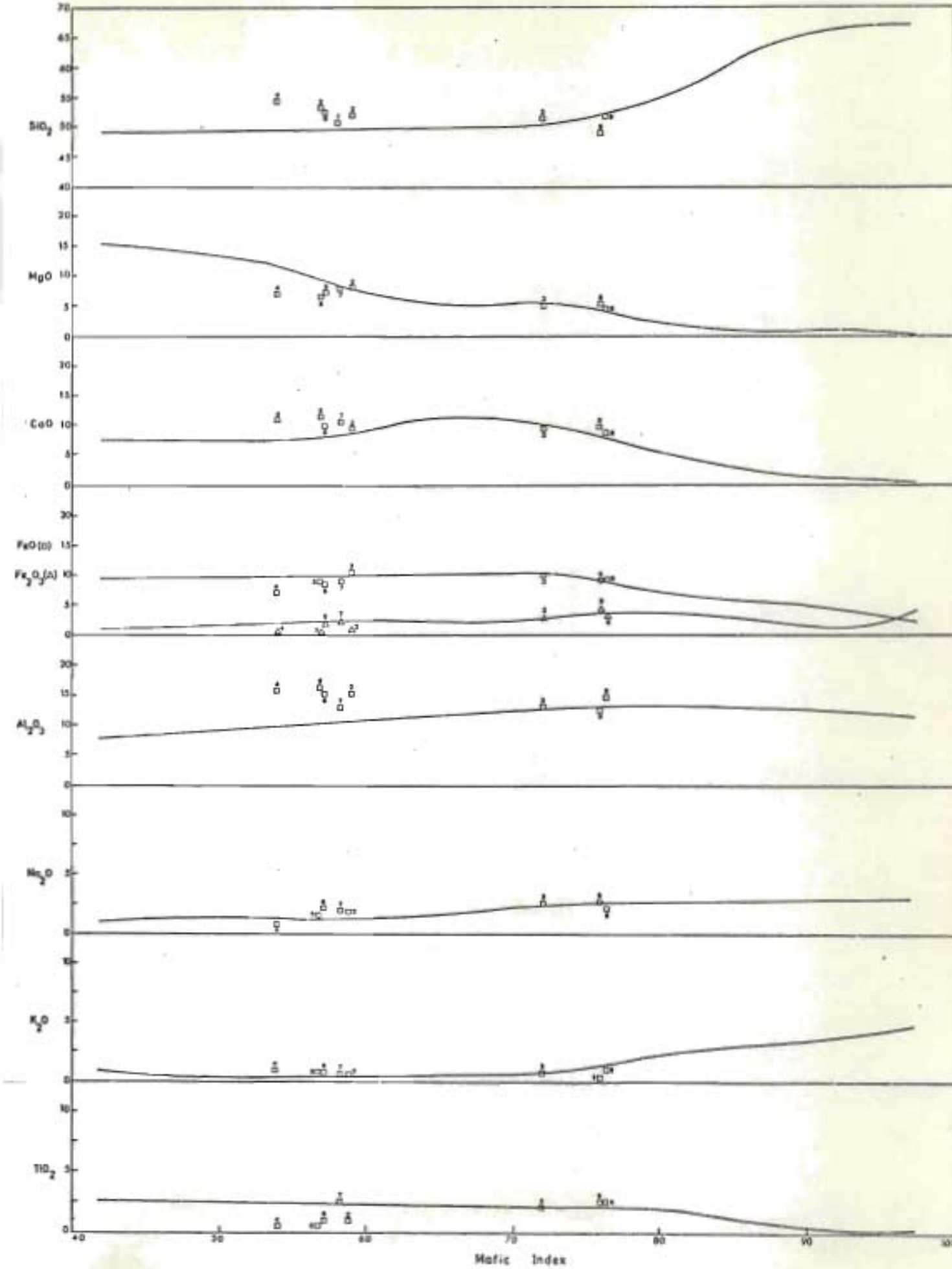

Figure 48. Comparison of the Komatiepoort basalt variation trend with average compositions from other provinces. (Numbering as in Table 46, p 297).

southward changes in basalt composition within the Lebombo have been further illustrated in a series of plots of K_2O versus MgO, TiO_2 versus MgO, and Al_2O_3 versus MgO, (fig 49, p 296). Again there is some suggestion of a southward decrease in TiO_2 and K_2O and a possible increase in Al_2O_3 as suggested by Cox et al., (1965).

(C) Comparison of the Komatipoort Tholeiites with other Tholeiitic Basalt Provinces

In Table 46 and fig 48 estimated average compositions of eight tholeiite provinces are compared with a calculated average and the trend for the Komatipoort rocks. A comparison of these compositions suggest that the Komatipoort tholeiites resemble in bulk chemistry both the Deccan and the Iceland tholeiite averages both of which have similar Fe/Mg indices to the Komatipoort rocks. The Iceland tholeiite average is somewhat lower in K_2O than the Komatipoort average. Inspection of the other averages shows that the Komatipoort average tend to be enriched in TiO_2 compared with several of the other provinces, particularly those of Antarctica and Tasmania. The U.K. Tertiary basalts bear a fairly strong resemblance to the Komatipoort rocks, but are somewhat higher in Al_2O_3 and SiO_2, and the Hawaiian rocks are extremely high in MgO when compared with the basic Komatipoort volcanics.

(D) Discussion of Major Element Variation

Comparison of the three analyses of olivine-rich volcanic rocks (Tables 5 , p 16 and 13 , p 42), reveals several differences in the geochemistry of the three samples. Although the differences between sample CL28 and sample CL 25 are those that would be expected from the disparity in their differentiation indices, and could largely be explained by the fractionation of olivine (see section on Petrogenesis of Basalts) sample CL 25 displays compositional differences of another type when compared with sample CL20 . Despite its lower differentiation index sample CL25 has a higher TiO_2 content,

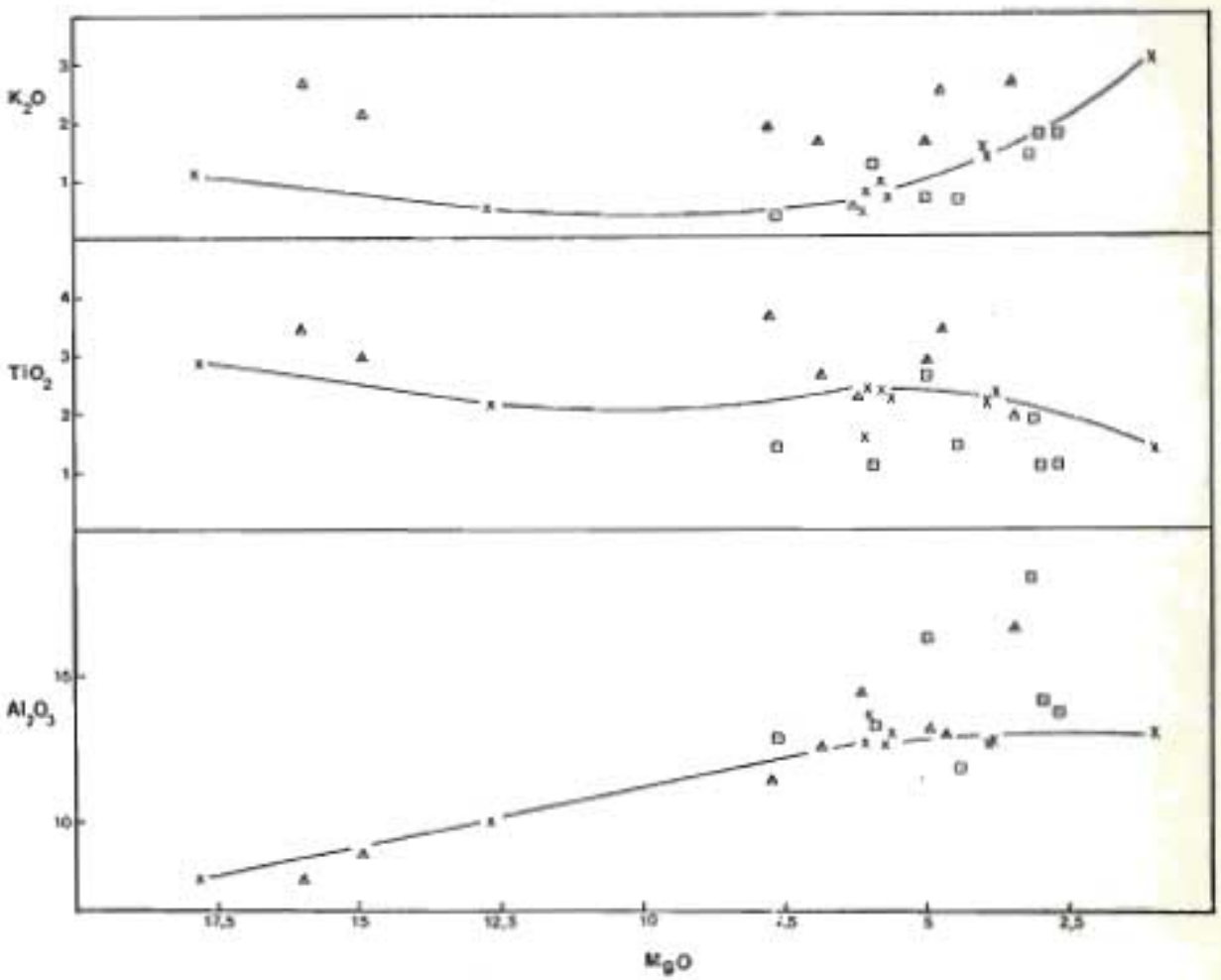

Figure 49. MgO versus K_2O, TiO_2 and Al_2O_3 for the Lebombo basalts.

x Komatipoort area analyses
▲ Nuanetsi area analyses (Cox et al, 1965).
□ Swaziland area analyses (Urie and Hunter, 1963).

TABLE 46

Comparison of average Komatipoort tholeiite with average chemical composition of rocks from eight tholeiite provinces

	Komatipoort 1	Karroo 2	Deccan 3	Antarctica 4	Tasmania 5	Palisadan 6	Hawaiian 7	U.K. 8	Thingmuli Iceland 9
SiO_2	50.62	51.9	51.50	54.00	53.3	52.2	50.89	51.6	48.75
TiO_2	2.36	1.1	2.37	0.7	0.6	1.3	2.79	2.7	2.85
Al_2O_3	12.88	15.5	13.47	16.1	16.4	15.4	13.22	15.0	13.12
Fe_2O_3	3.56	1.0	3.10	0.8	0.5	1.6	2.03	3.4	4.64
FeO	10.34	10.7	10.51	7.4	8.3	8.7	9.12	9.6	9.61
MnO	0.23	0.2	0.18	0.1	0.2	0.1	0.14	0.2	0.25
MgO	5.33	8.2	5.28	7.0	6.7	7.3	8.02	4.9	5.46
CaO	9.46	9.7	9.79	11.1	11.5	10.0	10.56	8.9	9.71
Na_2O	2.37	1.8	2.68	1.8	1.6	2.4	2.17	2.4	2.85
K_2O	0.98	0.7	0.81	1.0	0.9	0.8	0.43	1.1	0.49
P_2O_5	0.54	0.1	0.31	-	-	0.2	0.27	0.2	0.48
Number of analyses	6	6*	18***	2**	6**	4*	32****	32**	10*****
$\frac{FeO + Fe_2O_3}{FeO + Fe_2O_3 + MgO} \times 100$	72.28	58.79	72.04	53.94	56.78	57.12	58.16	72.62	72.29

* Walker and Poldervaart 1949 Table 17

** Walker (1964) Table 2

*** Sukheswala and Poldervaart (1958) Table 3 number 2

**** Kuno, et al. (1959) Table 10. number 1.

***** Carmichael, (1964) Table 2

a higher K_2O content and a higher P_2O_5 content and cannot be related to CL20 by a process of simple crystal fractionation of olivine, plagioclase, orthopyroxene or clinopyroxene. Comparison of analysis C120 with those of the olivine-poor basalts listed in Table 8, p24 shows a relationship by crystal fractionation may exist between sample CL20 and the olivine-poor basalts.

This suggests the presence of representatives of the two distinct differentiated series initially described by Cox, et al., (1965) from the Nuanetsi area. Cox, et al., originally divided these basalts into a high magnesia series, with an Fe/Mg index less than 50, and a low magnesia series with an Fe/Mg index greater than 50. This, from the analyses presented here does not appear to provide an altogether satisfactory criterion for distinguishing the two series, since it is clear that rock types such as sample CL28, which has an Fe/Mg index of 60 may possibly form by simple crystal fractionation on Cox's high magnesia type basalt magma. Such a process would produce a continuous differentiation series analogous with, but unrelated to, the low magnesia series. If this distinction is not made, a considerable amount of scatter may be expected to be shown by the low magnesia tholeiites, and Cox, et al., (1965, p187), report that the low magnesia tholeiites show a much more irregular behaviour than the high Fe/Mg index basalts. Representatives of the high Mg series which have been compositionally modified by high level fractionation do not appear to be common in other parts of the Lebombo. This is shown diagrammatically in fig 50,p 299, in which K_2O has been plotted against MgO for a number of rock analyses. From this it may be seen that in the Nuanetsi area, a series of basalts with compositions that plot relatively close to the trend of the low Mg basalts of the Komatipoort area, are present.

In fig 50, p299, in which K_2O has been plotted against MgO for a number of rock analyses, the two distinct trends (high and low Mg), have been defined for both the Komatipoort basic volcanics, and those of the Nuanetsi area. Also plotted on the diagram are the points representing samples CL25 and CL28, the latter sample falling relatively

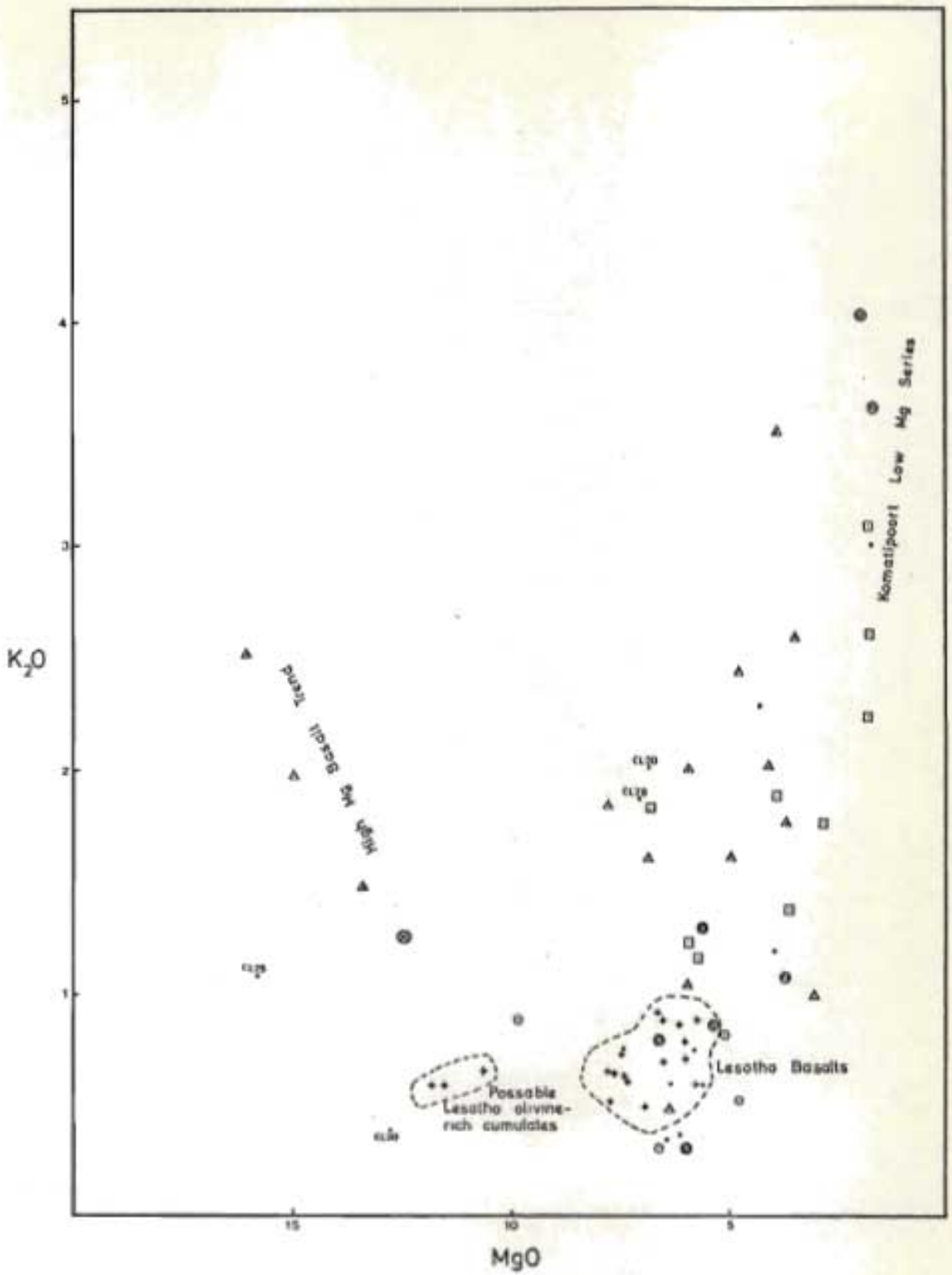

Figure 50. MgO versus K_2O for the basic rocks of the Lebombo Belt.

Location and source of Basalt Analyses

△ Nuanetsi - Cox et al, 1965.

• Lesotho Basalts - Cox and Hornung, 1966.

□ Olifants River, Lebombo - Saggerson and Logan, 1970.

⊗ Northern Lebombo - Cox et al, 1965.

◎ Komatipoort Upper Basalts - H. Wachendorf, 1971.

○ Lebombo Upper Basalts - De Assunção et al, 1962.

· Komatipoort Basalts - Present work.

close to the low magnesium series trend, although as indicated above, does not appear that it could be related to this series by crystal fractionation. Sample CL20 occupies an ambiguous position, lying close to the admittedly poorly defined, high magnesium Komatipoort trend and yet at the same time possessing a composition which could be related to the low magnesium tholeiites by normal fractionation processes. Perhaps significantly, the olivine-rich rock types from the basalts in Lesotho (Cox and Hornung 1966), plot in the same area of the diagram. Cox and Hornung also experienced some difficulty in assigning an origin of these rocks, but concluded that they were olivine cumulates, although this has subsequently been questioned by O'Hara (1968), (see section on petrogenesis).

(E) Trace Element Content of the Basaltic Rocks

Trace element content of the basic volcanics were not studied in detail, and values for Cu and Cr were determined in only four of the basaltic rocks, as shown in Table 47 , below.

TABLE 47

Cu and Cr contents of four specimens of basaltic volcanics rocks

Sample no.	Rock type	%Cu	%Cr	Fe/Mg Index
CL 25	Olivine normative basalt	0.01	0.16	41.92
CL28	Quartz normative basalt	0.01	0.045	60.8
CL31	Quartz normative basalt	0.02	0.034	69.79
CL33	Quartz normative basalt	0.01	0.017	77.58

(i) Cu

Clearly few, if any, conclusions can be based on so small a number of determinations, but it is of interest to note that the Cu distribution shown is in accordance with that reported by Prinz (1967), in that a quartz normative tholeiite has the highest Cu value.

Regarding the mineralogical distribution of Cu, Prinz has quoted the 1957 results of Wager and others. who determined the partition coefficient of Cu between sulphide and silicate liquids in the Skaergaard intrusion. Here, although the original magma contained 50 p.p.m. Cu, separation of olivine, pyroxene, plagioclase and iron ores containing even smaller amounts of Cu, led to an accumulation of Cu in the liquid until a concentration of 200 p.p.m. was reached. At this stage the Cu sulphide liquid began separating, initially showing strong concentrations of Cu. A rapid decrease in the partition ratio with the silicate liquid occurs, however, with continued fractionation. Similar results were obtained by Gunn, (1971), on Hawaiian basalts, which on differentiating by the separation of olivine only, show a steady increase in Cu content with advancing differentiation. In addition Prinz (1967), has reported a median value of 100 p.p.m. for 156 analyses of basaltic rocks, and by comparison the concentrations found in the Komatipoort rocks do not appear to be abnormal. This is in contrast to the Nuanetsi area volcanics where Cox, et al. (1965), found anomalously high concentrations of Cu in the gabbroic intrusions.

Few analyses of other Lebombo basic volcanics are available for comparison although Saggerson and Logan (1970) presented Cu data for basic volcanics from the Olifants River area. Two basalts are included, with Cu contents of 0.009% and 0.015% respectively, i.e. of a similar order of magnitude to the Komatipoort rocks. Analyses of one limburgite and one melanephelinite show relatively high concentrations, i.e. 0.068% and 0.023% respectively; highest concentrations thus occur in the limburgite.

(ii) Cr

The Cr content of the basic volcanics shown in Table 47 , p 300 , varies inversely with differentiation index, showing a marked relationship between fractionation stage and Cr content.

High proportions of Cr are commonly present in early formed olivine and pyroxene and fractionation of these minerals reflects a depletion in Cr content of the magma with rise in differentiation index. The Cr results form the Komatipoort area are thus consistent with an origin by fractionation of basalt by crystal settling, or by varying degree of partial melting of the olivine-rich mantle rocks, or by accumulation in the extrusive magma of variable amounts of early formed olivine crystals. Prinz, (1967), in summarising work on the average Cr content of basaltic rocks records a median value of 140 p.p.m. for 245 analyses. The Cr values, however, show large dispersion. Cr values in the Komatipoort rocks by comparison appear to be slightly high, even if the 0.16% recorded for the olivine basalt which contains a high proportion of olivine phenocrysts, is ignored.

5.8.3 GEOCHEMISTRY OF THE ACID VOLCANICS

Relatively few analyses of the acid volcanics are available from the Komatipoort area; those presented consist of the two new analyses, an analysis of the Causeway Dyke from Lombaard (1952), and two from the adjacent area in Mozambique (from de Assuncão, et al., 1961, see Tables 10, 19, p 34 and p 58 . These rocks have been plotted on several variation diagrams.

In fig 45 , p 289 , major oxides have been plotted against SiO_2, together with the analyses of the basaltic rocks, useful for reference purposes. Variations observed are essentially similar to those described by Cox, et al. (1965) involving decreases in CaO, Na_2O, Al_2O_3, TiO_2, Fe_2O_3 + FeO, MgO and P_2O_5 and increases in K_2O, with increasing SiO_2. From its position in relationship to other analyses, sample CL22 is anomalous in several respects. It contains abnormally low K_2O and to a lesser extent NaO_2 and abnormally high CaO, possibly as a result of thermal metamorphism by an adjacent intrusive, not observed in the field.

These analyses have also been plotted on the AFM diagrams described in the section on the geochemistry of the basic rocks fig 44 , p 288), and as may be seen from the diagram they continue the mild iron enrichment trend of the basalts down towards the K + Na corner of the triangle in the familiar pattern of other differentiated rocks series. For comparison the acid rocks analyses by de Assuncão, (1961), have been plotted on a similar diagram and show (fig 51 , p 304), a better defined but essentially similar trend. In both diagrams there is a distinct gap at the point where the trend swings towards the Na + K corner of the diagram. Comparing this with the trend of the Komatipoort Intrusion rocks, (fig 34 , p 237), it is found that to some extent, this gap is occupied by the granophyres from the Komatipoort Intrusion.

Southward variations in the geochemistry of the Lebombo acid volcanics are more difficult to detect than was the case for the basic rocks, but

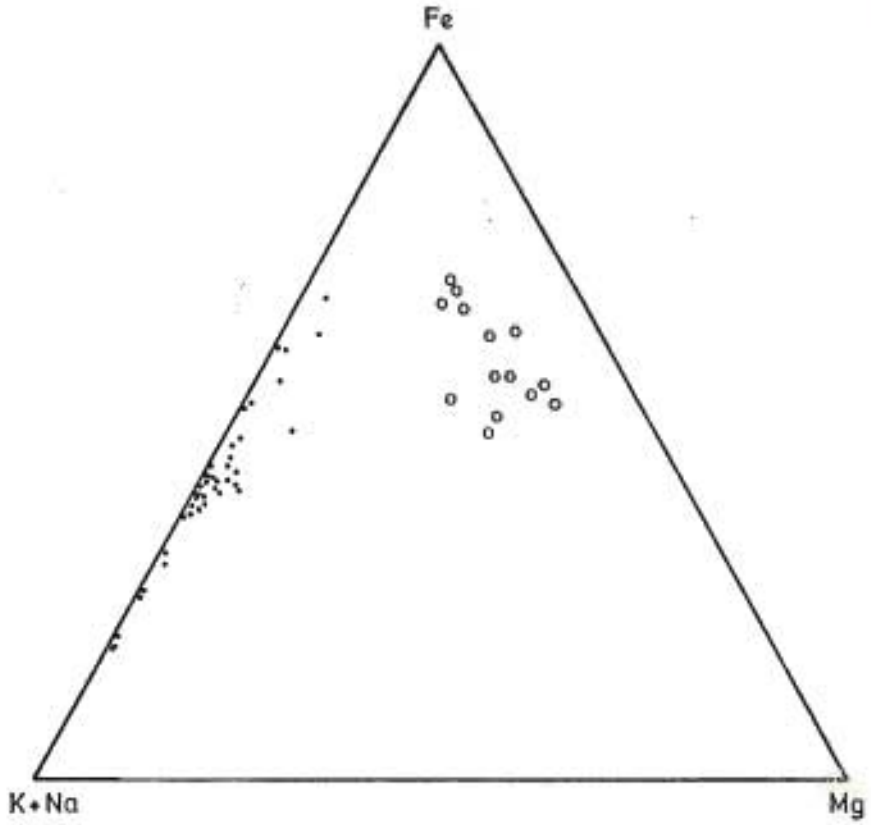

Figure 51. AFM diagram for the Lebombo volcanics of Mozambique, (De Assunção et al, 1962).

- Acid volcanics
- o Basic volcanics

Cox et al. (1965), have suggested that the acid volcanics display a southward decrease in K_2O and have provided averages to confirm this. In fig 52 , p 306 , groups of analyses from various points along the Lebombo have been plotted on diagrams illustrating variation of K_2O, TiO_2 and P_2O_5 with SiO_2 content, and from these it would appear that, in rocks containing more than 60% silica, there is a southward decrease in K_2O and P_2O_5 contents but not in TiO_2. Other major elements display no recognisable variation pattern when plotted on the same type of diagram.

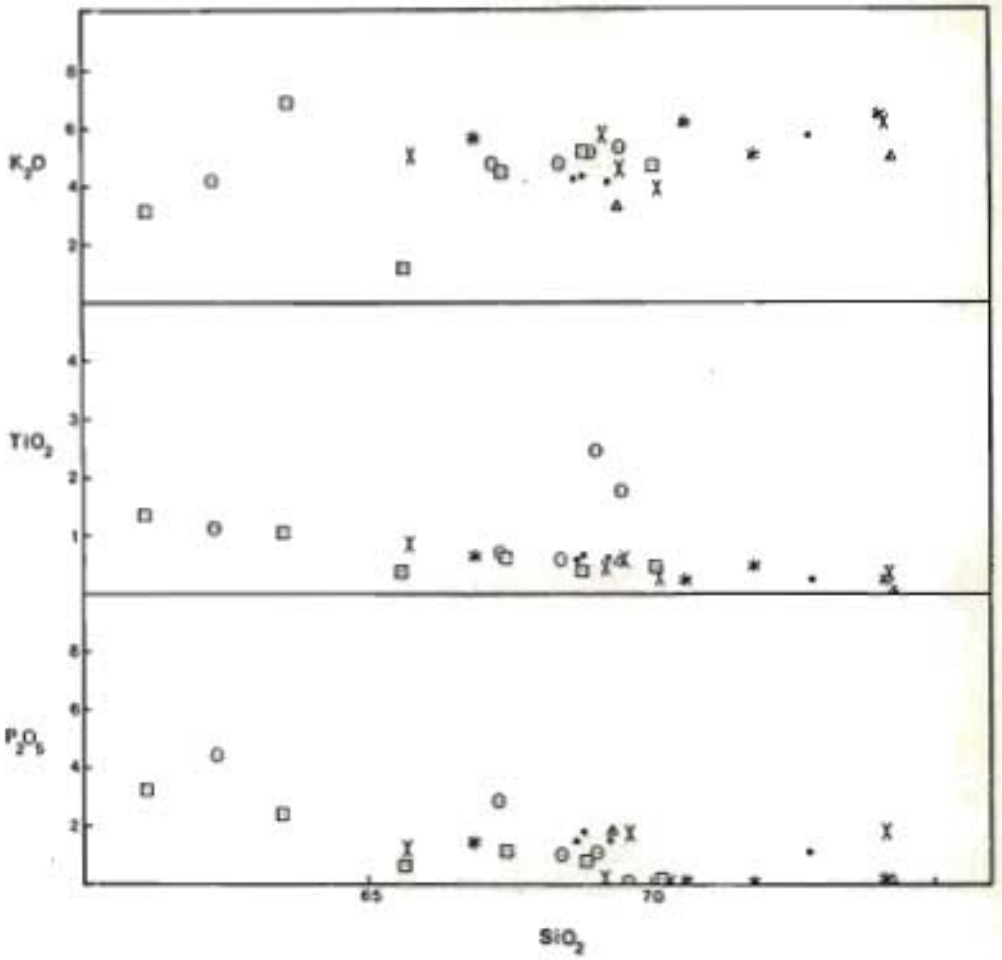

Figure 52. Variation of K_2O, TiO_2 and P_2O_5 with SiO_2 contents in the acid volcanics from different parts of the Lebombo.

- O Northern Lebombo samples (De Assunção et al, 1962).
- • Swaziland samples (Urie and Hunter, 1963).
- X Southern Lebombo samples (De Assunção et al, 1962).
- * Nuanetsi area samples (Cox et al, 1965).
- △ Natal Lebombo samples (De Assunção et al, 1962).
- □ Komatipoort area samples.

6 PETROGENESIS OF THE KARROO VOLCANICS

6.1 Introduction

Although the main object of this work has been a petrological study of the Komatipoort intrusion, and relatively little data has been collected on the extrusive volcanics themselves, it is of interest to consider the signifance of available information on the Komatipoort rocks in relation to the petrogenesic models that have been proposed for the Karroo and more specifically the Lebombo volcanics. The problem of the petrogenesis of the Karroo volcanics in the Komatipoort area should however, be viewed in the context of its position, not only in the Lebombo belt, but on the broader scale of its relationship to the African rift system and its associated volcanism, since Maud (1962) and Vail (1968), have both pointed out that structurally, the Lebombo belt may be regarded as a southerly extension of this rift system. More recently, age measurements (Wooley and Garson 1970), on alkaline volcanics from the Lupata and Chilwa provinces, suggest that these provinces, together with those of Nuanetsi and the Lebombo, are part of a broadly synchronous period of vulcanicity (Karroo). Thus, on a large scale, the southward decrease in the abundance of alkaline rocks, noted in the Karroo volcanics of the Lebombo itself, is repeated as the tectono-volcanic rift system extends from the Chilwa alkaline province of Malawi into Rhodesia and the Republic of South Africa. Within the Lebombo belt, the gradual southward elimination of the basal alkaline and olivine-rich rock types, is accompanied by the well-known southward decrease in K, Ti, P and less certainly Mg, coupled with a possible increase in Al content in the low-Mg tholeiite series, (see section of Geochemistry). Only the acid volcanics appear to show relatively insignificant southward compositional variations.

An explanation is therefore required for the observed lateral petrological variations in the Lebombo and in the rift system as a whole, as well as for the origin of the three major rock groups (viz. olivine-alkaline, tholeiitic, rhyo-dacitic), and for the tectono-volcanic environment in which they occur.

6.2 Previous Hypotheses for the origin of the Lebombo volcanics

A number of workers have interested themselves in the origin of the Lebombo belt and its volcanic rocks, and several theories have been proposed to account for the known petrological associations. Early workers on the Lebombo (Du Toit 1929, and E. and V. Gorsky in Frankel, 1960), were disturbed by the absence of closely spaced vents to account for the extensive areas covered by what appeared to be rhyolitic flows, which would presumably have been extremely viscous on eruption. More recently, others (Urie and Hunter 1963, Stratten 1965, and Cox et al.1965), have concluded that the bulk of the acid lavas were extruded as ignimbrites and subsequently, petrogenetic aspects of the volcanics have received more attention. Theories proposed for the origin of the belt and its volcanic rocks, in approximate chronological order, are as follows:

1. Du Toit (1929) postulated that the diverse rock types of the Lebombo belt, have originated by simple differentiation of basaltic magma combined with a process of acidification of the magma by assimilation of granitic crustal material.

2. E. and V. Gorsky in Frankel, (1960), in order to overcome the problem of extrusion of viscous, acid lava, which apparently formed continuous flows over wide areas, suggested that the rhyo-dacites had resulted from the metasomatic alteration of an originally extensive, basic extrusive sequence. The presence of interbedded tholeiitic basalts amongst the rhyolites, which would require a selective metasomatic process and the presence of acid dykes within the basalt sequence, are a few of several objections that may be raised to this theory.

3. Stratten (1965) has postulated an origin essentially similar to that suggested by Du Toit (1929), involving some differentiation of basaltic magma, coupled with contamination and melting of granitic crystal rocks.

4. Cox et al.(1965) argue that neither the vast volume of rhyolitic material nor the chemical variation found in the analysed mafic rocks from Nuanetsi, can be explained by differentiation of a single magma in terms of crystal settling by the observed phenocrysts. In particular, the transition from the high Mg basalt series (olivine-rich) to the low Mg series requires a separating phase extremely rich in magnesium and containing about 4 % total alkalis.

The necessity for the removal of relatively large amounts of alkalis renders the observed phenocrysts, olivine and clinopyroxene, unlikely as the separating mineral phases. Suggestions of contamination by sialic matter as a a source of potash in the high Mg basalts are countered with the argument that although the high Mg basalts are considerably richer in alkalis than Karroo dolerites of the same Fe/Mg index, there is no significant difference in the SiO_2 content. They consider the low magnesia tholeiite equally unlikely as a parental magma, as the high magnesia tholeiites would have to be considered as cumulative differentiates, which would be at variance with the known age relations between the high and low magnesia types.

Cox et al. (1965), and Johnson (1966), and again Cox (1972), have therefore, proposed the idea of the Karroo volcanic cycle, with a symmetrical variation in rock types ranging from early alkaline rocks through olivine basalts and tholeiites, to rhyolites, finally returning to tholeiitic and alkaline lavas once more.

In Cox's 1972 version of the Karroo volcanic cycle in south east Africa, the cycle begins with a body of potassium-rich picritic magma rising from a depth of at least 500 km. This magma provided the source for the Karroo volcanics in the northern part of the Karroo Province. The rising body also generated a peripheral zone of tholeiitic magma which gave rise to some of the northern rocks and most of the southern rocks, including the Karroo dolerites and the basalts of Lesotho and Swaziland. The early volcanic products were followed by

primitive picritic lavas in the 'culminating' stage of the cycle and this in turn, was followed by the 'steady state' phase in which uniform, moderately fractionated basalts were extruded. Subsequently a 'waning' stage produced the more salic rocks of the Chilwa province and Lupata and finally, the Cretaceous kimberlites of Southern Africa could represent a terminal stage.

5. Manton (1968) determined the strontium isotope ratios of both basic and acid Lebombo volcanics in a series of ten samples covering the entire Nuanetsi-Lebombo province. The results of this work he found, favour a mantle origin for the acid magma as well as the basic magma. The initial ratios of the Nuanetsi acid and basic magmas differ, however, and Manton has suggested one of the following three mechanisms may account for these differences.

   (i) Derivation of the acid magma from a heterogeneous upper mantle.
   (ii) Deep seated contamination of a large body of lava.
   (iii) The existence of acid magma at depth, for some time before extrusion.

6. Saggerson and Logan (1970) have noted the southward decrease in the quantity of the early alkaline Lebombo lavas and have attempted to account for this by suggesting that initial deep fracturing associated with down-warping of the cratonic margins would probably be required for the melting of mantle rocks, which they considered necessary for the production of the parental magma of alkaline and olivine basalts. The southward decrease in the intensity of rift faulting, then matches the gradual southward elimination of the of the alkaline lavas.

7. Woolley and Garson (1970) in proposing a petrogenetic scheme for the Lebombo-Nuanetsi-Sabi-Lupata-Chilwa provinces have suggested that in South Africa, magma generation was restricted to high mantle levels, producing a single rock series of tholeiitic

affinities. Further to the north deeper faulting associated with rifting tapped both lower and higher levels in the mantle and two, or possibly three, primary magmas and associated differentiation products made their way to the surface. They recognise the problem of the large volume of rhyolites and postulate some degree of crustal melting to account for the calc-alkaline rhyolites. For the origin of the rarer hyperalkaline rhyolites differentiation of the more alkaline basalts is proposed.

8. Wachendorf (1971) has suggested an upper mantle origin for the basalts and derivation of the felsic volcanics from basalt magma by crystal fractionation. The roughly equal proportions in which the acid and basic lavas occur, he explains by assuming contamination of the fractionating basalt with crustal material.

9. Cox and Jamieson (1974), in a paper on the detailed petrography of the olivine-rich basaltic rocks from the Nuanetsi area, suggest that compositional variations in the lavas are controlled either by a polybaric fractionation process involving the removal of olivine and orthopyroxene crystals at pressures in the range of 6 - 12 kb. Alternatively the variations in liquid composition may have been produced during equilibration of the liquids with excess harzburgite wall-rock over the same pressure range. Largely on account of difficulties encountered in explaining the simultaneous fall of K with Mg in this rock series, the wall-rock equilibration model is preferred by Cox and Jamieson.

6.3 Origin of the Komatipoort Basalts

In their investigations on the origin of the New Georgia Group Basaltic rocks, Cox and Bell (1972) recast their analyses in terms of normative diopside, olivine, plagioclase and quartz, and subsequently plotted these values in a simple tetrahedral phase diagram for dry tholeiitic magma at one atmosphere.

Similar values have been calculated for the Komatipoort basic volcanics, and projections of the points representing the Komatipoort analyses into the pseudo-quaternary system Ol- Cpx - Pl - Qz are shown in fig 53 , p 313 . The method used for converting normative values into plotting co-ordinates is that of Cox and Hornung (1966)(although here no standard Fe-oxidation factor is used) , and includes on average, 80% of the original hydrous analyses. The 3-phase surfaces that form the boundaries of the primary phase field of the phase from which the projection is made, shown in figure 53 , a, b and c are from Cox and Bell (1972) and the primary phase fields shown where they intersect the Ol - Cpx - Pl plane in Fig 2, (d), are from the same source.

Three dimensional modelling of the distribution of the points in the tetrahedron shows that the majority of points, excluding those representing samples 33, 15 and 19, lie close to the Di, Fo, Pg face of the tetrahedron, and their distribution is therefore, well illustrated by the projection from the quartz coign, (53 , B). In this projection samples 20 and 25, the olivine basalts, are displaced towards the olivine corner of the diagram, suggesting control by simple segregation or accumulation of olivine. Sample 28 lies close to the Ol + Cpx + L surface and adjacent samples also plot close to this

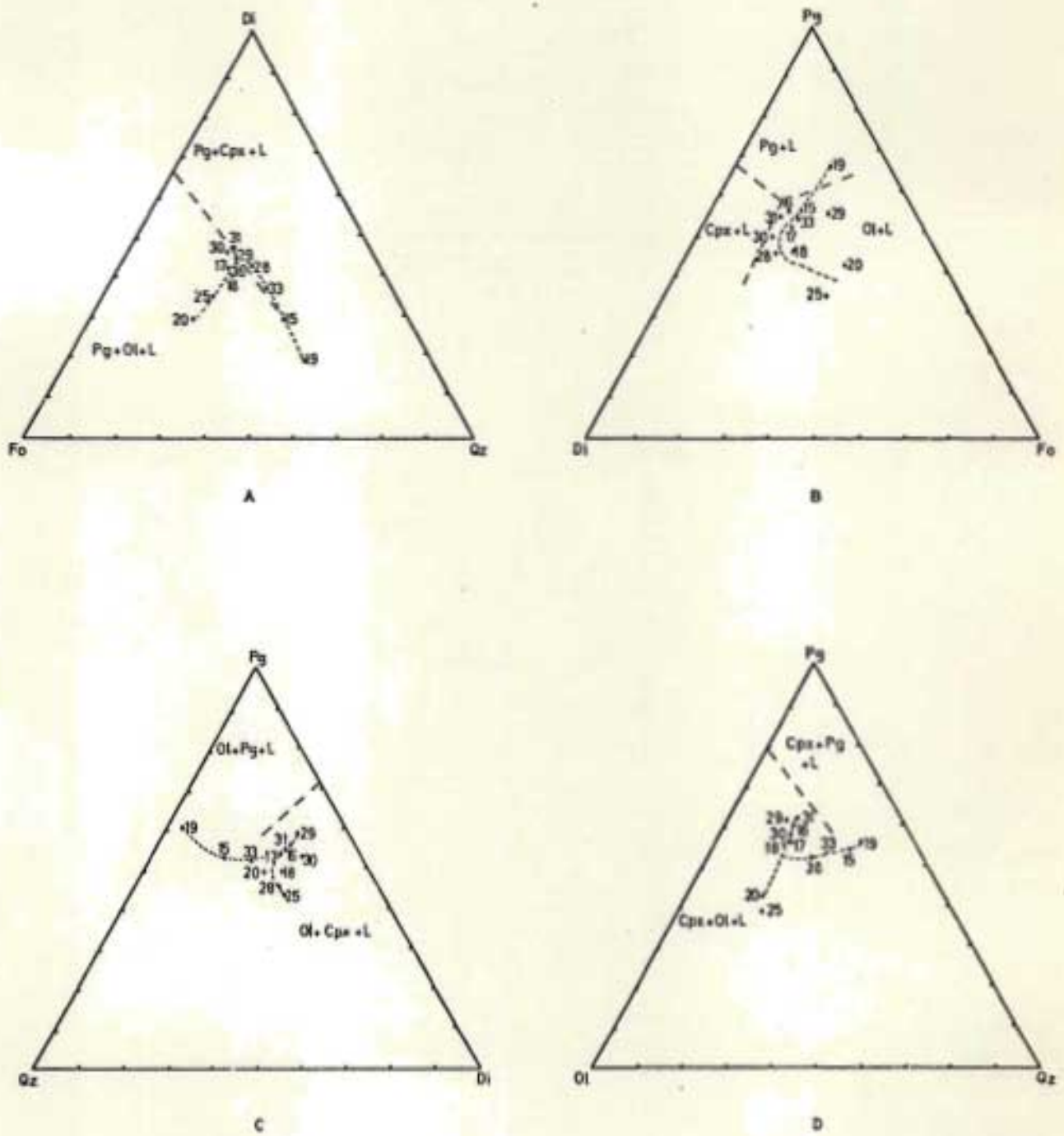

Figure 53. Plot of the Komatipoort basic volcanics (recast in terms of normative diopside, olivine, plagioclase and quartz), in a simple tetrahedral phase diagram for dry tholeiitic magma at one atmosphere.

Dolerites - CL15, CL16, CL17, CL18
Andersite - CL19
Olivine Basalt - CL20, CL25
Olivine-rich Dyke Rock - CL28
Olivine-free Gabbro - CL29
Olivine-bearing Gabbro - CL30
Basalts - CL31, CL33

surface but progressively closer to the low pressure cotectic. This is broadly suggestive of a compositional variation trend in the basic volcanics, controlled initially by the segregation of olivine until the Ol + Cpx + L surface is reached and subsequently by olivine plus pyroxene until the low-pressure cotectic is attained.

The relative positions of samples 33, 15 and 19 on the other hand is best illustrated in the projection from the Fo coign (53 , C) and points representing these samples may be seen to lie on a slightly curved trend extending from near the low-pressure cotectic to the Qz - Pg side of the triangle. This trend could be produced by the fractionation of pyroxene, initially together with minor amounts of plagioclase. These results then suggest that although plagioclase is a common phenocryst phase in these volcanics their compositional variation trend was controlled by the fractionation of olivine and pyroxene, which are far less abundant as phenocrysts in these rocks. This abundance of plagioclase phenocrysts in many of the basic volcanics could however, be related to the relatively small density contrast which was probably present between the plagioclase and its parental magma, which could lead to relatively low settling velocities for the plagioclase crystals.

The near-cotectic compositions of many of the low-Mg basalts may be evidence of a relatively low-pressure origin for these basalts in view of the non-coincidence between cotectic liquid compositions at high and low pressures. The significance of the coincidence in basalt composition with the low-pressure cotectic has been widely debated in the literature and

O'Hara (1968) in discussing the Lesotho basalts, has raised the possibility of the derivation of the parental tholeiite liquid by olivine fractionation at high pressures, in magma produced by deep-seated partial melting. This magma, he suggests, could by coincidence reach a composition in the equilibrium clinopyroxene-olivine-plagioclase-liquid at a pressure of less than 8 kb, and then be erupted after slight olivine gabbro fractionation.

Evidence for the latter possibility is found in the work of Jamieson (1966) who described the olivine-rich basalts of the Nuanetsi area, which although clearly primitive in character by comparison with the olivine-poor Lebombo basalts, have a composition in part, similar to that of the low pressure cotectic liquid.

Difficulties arise however, in explaining the high concentrations of incompatible elements in certain of the Lebombo volcanics, as well as the southward decrease along the Lebombo in the incompatible element content of the low-Mg basaltic rocks. One possible answer to these problems lies in postulating variable amounts of eclogite fractionation at high pressures which effectively increases only the incompatible element content of a partial melt. This process however should produce a melt significantly depleted in heavy rare earth elements and little evidence for its presence has been detected in the study of other basaltic rock series.

Jamieson and Clarke (1970) have concluded "that the processes leading to evolved contents of K and associated elements are partly independent of the processes leading to evolved major oxide compositions". Cox (1972) has embodied this in his Karroo Volcanic Cycle in which the high-Mg, K-rich series has a separate origin from the low-Mg series, and southward variations in incompatible elements in the low-Mg series, are explained by some mixing of these two magmas. Cox and Jamieson (1974) have described phenocrysts of orthopyroxene jacketed by clinopyroxene, from the olivine basalts in the Nuanetsi area, and those orthopyroxenes are considered to have a high pressure origin. Similar-

looking jacketed orthopyroxenes were noted, in the present work, in the olivine-free gabbro of the Basal Intrusion, in the Komatipoort area. This rock belongs to the low-Mg series and the presence of the jacketed orthopyroxenes in these rocks suggested either possible mixing of Cox's postulated two magma series, (low and high-Mg), or derivation of the one series from the other. A more detailed study of these phenocrysts (see p 103), indicated however, that they are unlikely to have a similar origin to those described from Nuanetsi by Cox and Jamieson, (1974). Further, since these jacketed phenocrysts apparently may have more than one origin, care should be taken to discriminate between these origins. Thus it is not possible from the present work to suggest a high pressure origin for the low-Mg series or a common origin for the low and high-Mg basaltic rock series.

An examination of fig 50 , p 299 , (MgO versus K_2O diagram), suggests that only four of the analysed Komatipoort rocks could have affinities with the high-Mg series. Two of these, the olivine basalts CL20 and CL25 show strong similarities to the high-Mg series rocks, but the other two, CL30, the olivine bearing gabbro of the basal intrusion and CL 28, the olivine rich dyke rock, plot in a position intermediate between the high-Mg and low-Mg treads. Differences of a similar nature are noted between the two pairs of samples, in 53 (d), in which the points representing the two olivine basalts are displaced towards the olivine corner of the diagram, whereas CL28 and CL30 plot closer to the low-Mg series rocks, and the low-pressure cotectic.

The olivine basalt analysis CL 20, plots close to the olivine-rich basalts of Lesotho in fig 50 , and could in fact represent a low-Mg series basalt enriched in cumulus olivine. The second olivine basalt, CL 25, however, shows chemical characteristics typical of the high-Mg series. The other two analyses with possible high-Mg series affinities have relatively high SiO_2 values, (see Table 13 , p 42 and Table 22 , p 101) which combined with the other characteristics just discussed suggests several possible modes of origin which could account for their intermediate nature. These are:-

1. Contamination of high-Mg series magma by crustal rocks.
2. Hybridisation of a fairly strongly fractionated low-Mg series magma by a high-Mg series liquid
3. Accumulation of cumulus olivine in fairly strongly fractionated low-Mg series basalts.
4. Fractionation of high-Mg series magma by removal of olivine crystals.

Contamination of high-Mg series magma by crustal rocks appears unlikely in view of the high CaO content and low FeO + Fe_2O_3 content of the two samples, (CL28 and CL 30). Their CaO contents are higher and their FeO + Fe_2O_3 contents are lower than many of the high-Mg series lavas analysed by Cox and Jamieson (1974, Table 9 , p 280). Contamination by SiO_2-rich crustal rocks, which may be expected to be low in CaO and in some cases (e.g. andesitic compositions) high in FeO + Fe_2O_3, therefore appears unlikely. Hybridisation of a fairly strongly fractionated low-Mg series magma by a high-Mg series liquid (origin 2, above) appears impossible for similar reasons.

Accumulation of olivine crystals in a fractionated low-Mg series basalt or fractionation of a high-Mg series basalt may therefore be considered. As a result of the small number of available analyses it is not possible to determine trends in variation diagrams reliably and relate these to the major phenocryst control lines. Instead the effect of the extraction or addition of various proportions of olivine on the composition of the analysed olivine-bearing gabbro sample, from the Basal Intrusion was calculated. The olivine composition used in this calculation was that of the olivine from the olivine-free gabbro from the Basal Intrusion, (see Table 21). Two of the more reasonable results of this calculation are listed in Table 48, together with the olivine-bearing gabbro analysis, (CL 30).

TABLE 48

Effect of addition or subtraction of olivine on analysis CL30*

	1 Addition of 20% olivine	2 CL 30	3 Subtraction of 5% olivine
SiO_2	49,25	52,56	53,44
Al_2O_3	9,00	11,25	11,84
Total Fe as FeO	10,36	8,12	7,53
MgO	14,39	6,88	4,90
CaO	6,82	8,42	8,84
Na_2O	2,33	2,91	3,06
K_2O	1,72	2,15	2,26
TiO_2	2,47	3,08	3,24
P_2O_5	0,34	0,42	0,44

* Note:- H_2O^+, H_2O^-, MnO, CO_2 have not been included in this calculation

Examination of the results listed in Table 48 suggests that the olivine-bearing gabbro is unlikely to have originated by olivine accumulating in, or being added to a fractionated low-Mg liquid. Removal of only 5 per cent olivine from the olivine-bearing gabbro analysis produces a composition depleted in iron and enriched in calcium, with respect to the calculated SiO_2 content. Subtraction of clinopyroxene, the only other observed phenocryst phase present in the olivine-bearing gabbro, improves the situation as far as calcium is concerned, but reduces the iron content yet further.

Addition of 20 per cent olivine to the olivine-bearing gabbro analysis on the other hand produces a composition that closely approximates that of the Mg-rich series lavas, (compare with Cox and Jamieson,1974, Table 9, p 280).

Thus fractionation of olivine in Mg-rich series lavas appears to provide an adequate mechanisim for the production of magmas with a composition similar to that of the olivine-bearing gabbro.

To summarise, the close correspondence between the composition of the low-Mg series basalts and the low pressure cotectic, coupled with the presence of the phenocryst assemblage noted in these rocks, may be explained by an origin involving in situ melting of the low velocity zone followed by some low pressure crystal fractionation, as proposed by Cox, (1972) and Cox and Jamieson, (1974). One of the analysed olivine basalts could represent either a cumulus-olivine enriched, low-Mg series basalt or an extreme representative of the high-Mg series trend. The other olivine basalt clearly belongs to the high Mg-series lavas, which Cox and Jamieson (1974), have suggested originated by a process involving partial melting of mantle peridotite followed by a slow rise from depth, equilibration of these melts with harzburgite wall rock through a pressure range of 6 - 12kb, and then rapid eruption of magmas without further fractionation. Two of the analysed specimens from Komatipoort that belong to the high-Mg series, are considered to show signs of fairly extensive olivine fractionation, suggesting, that in the Komatipoort area, eruption of some of the high-Mg liquids, was not as sudden as in Nuanetsi area, and that continuous crystallisation and fractionation of olivine may have occurred during a slower rise to the surface, producing magma with a composition approximating the low pressure cotectic.

Other analysed basic rocks from the major intrusives in the Komatipoort area appear to belong to the low-Mg basaltic series and therefore to have originated in the same manner as the low-Mg series basalts.

6.4. ORIGIN OF THE ACID VOLCANICS

In general three possible origins have been considered for the acid volcanics:

(i) Simple differentiation of basic magma.
(ii) Partial melting of mantle material.
(iii) Partial melting of lower crustal material or of a heterogeneous upper mantle.

Simple differentiation of basic magma has been suggested by several authors for the origin, at least in part, of the acid volcanics and some of the available evidence does provide support for this hypothesis. For example, the rhyolites tend to form a continuous series above a silica content of 61% as indicated in the section on geochemistry, and generally there appears little reason why this series of rocks should not have originated by the fractionation of the known phenocryst phases. Acid volcanics derived by crystal fractionation of the same basic magma that gave rise to the basaltic rock series could reflect similar longitudinal variations in chemical composition, and as noted earlier, there is a slight suggestion of a southward decrease in K_2O content. In addition the work of Manton (1968), mentioned earlier, suggests a mantle origin for the acid magma.

Some fairly strong objections may be raised to this hypothesis, however. It has been suggested that the volume of acid magma is too great to have been generated by crystal fractionation and that there is a lack of a corresponding volume of basic rocks, particularly towards the southern end of the Lebombo where tholeiitic basalts only, occur. On a global scale the restriction of rhyolitic outpourings (and granitic intrusions) to continental environments may be interpreted as evidence against an origin by differentiation. More detailed objections are the lack of a longitudinal variation in TiO_2 content to compliment that shown by the Lebombo basalts (although fractionation of ilmenite or titaniferous magnetite may account for this), and the fact that Manton (1968), found an initial difference in strontium isotope ratios between the acid and basic volcanics. The last point according to Manton, discounts the

possibility of any continuous differentiation process involving a basic parent magma producing and erupting successively more acid differentiates, and led Manton to suggest the possibility of deriving the acid material from a heterogeneous upper mantle. Alternatively he suggested deep-seated contamination of a large body of magma could explain the difference in isotope ratios and finally, he proposed that the acid magma may have existed at depth for some time before extrusion.

It appears therefore, that, in general, the acid volcanics were not generated by the simple differentiation of basic magma. In addition, the evidence of very slight variations only, in the strontium isotope ratios of rhyolite samples collected from widely separated points along the length of the Lebombo (Manton 1968) suggests the rhyolites could not have originated by partial melting of heterogeneous lower crustal rocks. Thus it is considered likely that the rhyolites have originated by partial melting of either a heterogeneous upper mantle or a relatively homogeneous portion of the lower crust. Little positive evidence is available for the existence of either of these structures, although the Lebombo-Nuanetsi monocline parallels the margin of the Mozambique mobile belt and it is conceivable that during the course of the considerable tectonic activity associated with the formation and the subsequent history of the mobile belt, that the base of the crust may have been melted and solidified several times over a long period of time, to fulfil one of Manton,s requirements; that the acid magma may have existed at depth over a long period of time in order to equilibrate strontium isotope ratio distribution throughout the length of the Lebombo. Compositional variations which are present in the rhyodactic series could be produced either by variations in degree of partial melting of such a layer, followed by crystal fractionation, or contamination, or by some combination of these processes.

A major feature of the geochemistry of acid-basic volcanic provinces such as the Iceland province is the bi-modal distribution of SiO_2 in representative analyses of the volcanic series. The Lebombo province is no exception in this regard and analyses with

an SiO_2 content in the range 57-61 per cent, are, to the authors knowledge, unknown from the Lebombo. The Komatipoort Intrusion is thus exceptional in that rocks with an SiO_2 content in this range do occur. Analysis CL 46,(Table 41, p 235), an analysis of the upper margin of the feldspathic gabbro unit has, for example, an SiO_2 content of 57,6 per cent. As described earlier, however, (see p 276), there is evidence that the upper margin of the feldspathic gabbro has suffered partial hybridisation during the emplacement of a minor body of acid magma along the upper contact of the feldspathic gabbro subsequent to the consolidation of this unit, (see p 205). These particular intermediate rocks are thus considered to have originated by simple hybridisation.

A more significant occurrence of rocks with intermediate SiO_2 contents may be found in the granophyre unit of the Komatipoort intrusion. The analysed granophyre samples have SiO_2 contents extending from around 53 per cent to about 63 per cent. A more detailed examination of those analyses shows an absence of samples with SiO_2 contents between 57,16 and about 60,2 per cent. This gap may be a reflection of the relatively low number of samples of granophyre analysed during this investigation, but there are also other differences between the two groups of samples. The high SiO_2 granophyre samples show little variation in chemistry whereas in the low SiO_2 granophyres much greater variability in chemistry is present. Further the low SiO_2 granophyres occur at the margins of the granophyre unit. There is therefore a possibility that the granophyre unit could represent a multiple intrusion, and indeed in the northern granophyre mass there is evidence of several intrusive acid phases. The analyses presented here are however, all from the Komati River cross-section of the southern granophyre mass and apart from the geochemical differences, there is little evidence for the presence of multiple granophyric intrusives. Further, an origin by multiple intrusion would require the coincidental juxtaposition, in the Komatipoort Intrusion, of the most and the least SiO_2-rich representatives of the basic and acid portions of the bimodal volcanic series. Similarities in the geochemistry of the two granophyres, such as the uniformly low Al_2O_3 content would also require explanation. The low SiO_2 samples, (see discussion in the section on the petrogenesis of the granophyre unit, p. 280), are

therefore considered to have formed largely by inward crystallisation from the margins of the unit. Thus the low SiO_2 granophyres need not be considered to represent liquid compositions, but an early marginal crystallisate of the granophyre unit magma. This magma, in turn, may be represented by the high SiO_2 granophyres. Support for this proposal is provided by the fact that those granophyres are extremely constant in composition and secondly by the fact that the analysis of a granophyre vein intruding the granophyric gabbro, (CL 48, Table 39), falls into the high SiO_2 group.

The tendency of the granophyres to plot on a straight line in the variation diagram described on p 245, therefore could be explained by multiple hybridising intrusions of magma of intermediate compositions, but this tendency could also possibly result from the compositional relationship between an early marginal, (relatively high temperature), crystallisate and the residual magmatic liquid. It is possible that continuation of this marginal crystallisation or hybridisation of the early crystallisate by the residual magma could produce rocks with an SiO_2 content between 58 and 60 per cent, and these may be present in the Komatipoort Intrusion. As discussed above, it is considered unlikely that these rocks would represent liquid compositions.

An alternative origin for the two types of granophyre present in the Komatipoort Intrusion is suggested by differences in their major element chemistry, which resemble those characterising coexisting immiscible silicate liquids,(McBirney, 1975, Phillpots, 1978, Visser and Koster van Groos, 1979). These differences include the relatively high levels of total Fe-oxides, P_2O_5 and TiO_2 present in the low SiO_2 granophyres and the relatively high alkalies present in the high SiO_2 group. If an overall mean chemical composition is calculated from the average composition of each group, an average granophyre composition with a silica content of 58,55 is obtained. That is, a composition with a silica content almost in the centre of the gap in the bimodal silica distribution shown by the Lebombo volcanics, (57-61%). Thus if the two varieties of Komatipoort granophyre did originate by a process involving liquid

immiscibility, it appears possible that the absence of rocks with an intermediate silica content could be explained by liquid immiscibility, where such intermediate magmas were generated. These magmas need not necessarily have been abundant in the Lebombo, since it is likely they would represent relatively strongly fractionated basic magma. In these magmas elements such as K, Fe, Ti and P tend to reach relatively high concentrations simultaneously, as is apparent from the descriptions given in the section on the geochemistry of both the Komatipoort basalts and the Komatipoort Intrusion, (p 284 and p 224). This would tend to favour the development of liquid immiscibility. As Visser and Koster van Groos, (1979), have indicated, P_2O_5 and TiO_2 distribution patterns are unlikely to be able to distinguish liquid immiscibility from crystal fractionation. Nevertheless, it is possible that the Komatipoort granophyres could provide direct evidence of liquid immiscibility in the Lebombo, and further work appears justified to ascertain whether the two granophyre types have originated as immiscible liquids. Two possible aspects that may be worth investigating are the distribution coefficients and the fact that the basic and acid immiscible components would be expected to show isotopic evidence of a common, (mantle), origin.

The bimodal silica distribution in the Lebombo volcanics suggests that the andesitic rocks discussed in the previous section,(CL 19, Table 8, p 24), with an SiO_2 content of just over 61 per cent should be discussed with the acid volcanics. In terms of its major element chemistry however, it is not possible to eliminate an origin by the fractionation of basic magma. Compared with the available analyses of acid volcanics from the Komatipoort area it appears high in Al_2O_3, MgO and possibly Na_2O and K_2O, but as more data becomes available, this analysis may prove to be less unusual than it appears at present.

In fig 36, p 244, analysis CL 22, an acid volcanic from the Komatipoort area, (Table 10, p 34), has been plotted, and

this analysis tends to lie on or close to the extension of the straight line along which the Komatipoort Intrusion granophyres plot. This in turn suggests that this rock could have originated by a continuation of the process that produced the variation in chemistry of the Komatipoort granophyres.

Sample CL 21, (Table 10, p 34), on the other hand displays a distinctly different chemistry, containing higher levels of SiO_2, Al_2O_3, total Fe oxides, Na_2O and K_2O, and lower levels of MgO and particularly CaO. TiO_2, P_2O_5 and MnO values are similar. It is apparent from this that these two rock types could not be derived from each other or a common parental magma by fractionation of the usual phenocyst phases such as quartz, feldspar magnetite or Fe-rich pyroxene. It could, however, be derived from the andesitic rock represented by analysis CL 19 Table 8, by fractionation of several of the commonly observed phenocryst phases. This rock, as suggested above, could be derived by fractionation of representatives of the basaltic rock series. There is thus some suggestion of more than one origin for the acid volcanics in the Komatipoort area, however very few analyses of these rocks were available during this study and these conclusions must be regarded as speculative.

Concluding Remarks.

The Komatipoort area lies approximately mid-way along the Lebombo volcanic belt and it is apparent from the description given here of the rock types from this area, that there is a gradual transition from the alkali and olivine basalt, tholeiitic basalt, rhyolite succession of the northern Lebombo to the tholeiitic basalt, rhyolite sequence present in the southern Lebombo. The high-Mg series basalts not only decrease in abundance, southwards from the Nuantsi area, but there appears to be a change in their nature as well, since fractionated representatives of this series are considered to be present in the Komatipoort area. These do not appear to have been described from the northern Lebomob and could result from a slower rate of progress of the high-Mg series lava to the surface, allowing time for fractionation.

The bulk of the basic rocks in the Komatipoort area are representatives of this series which have suffered fractionation at low pressures. Despite the relative abundance of plagioclase as a phenocryst phase in the basalts, compositional variation in the low- Mg series appears to have been controlled by the separation of olivine and pyroxene, and only in the more highly fractionated examples does it appear likely that plagioclase has played a significant role. The crystallisation sequence in the low-Mg series basalts according to the one-atmosphere phase diagram is olivine, pyroxene, plagioclase, as the composition of the magma gradually evolves towards the low-pressure cotectic, presumably while the lava moves towards the surface. If this is accepted it becomes clear that plagioclase may only have appeared as a crystalline phase relatively late in the crystallisation history of the low-Mg volcanics, and that this coupled with the low density contrast between the plagioclase and the magma, could provide an explanation for both of the features, i.e. for the relative abundance of phenocryst plagioclase in these rocks and for its absence during fractionation of most of the low-Mg basalts. Thus in the fractionation of the low-Mg basalts also, the rate of movement of the magma to the surface may have been a significant

factor.

If plagioclase is a relatively unimportant phase in the production of the low-Mg basalt factionation sequence, it would appear unlikely that this fractionation occurred in high-level intrusive bodies such as the Komatipoort Intrusion in which plagioclase is an early crystalline phase in all units. J. Bristow, (personal communication), has suggested the Crocodile River Intrusion may be a more likely site. The crystallisation sequence in the Crocodile River Intrusion has here been shown to be olivine, orthopyroxene, clinopyroxene, plagioclase, closely resembling that expected in the fractionating low-Mg basalts. In addition the Crocodile River Intrusion is the southern-most representative of an extensive line of basic intrusive masses which volumetrically and in regard to their geographical distribution, appear adequate to have made a significant contribution to the production of the low-Mg series basalts of the northern Lebombo. Thus the Crocodile River Intrusion may provide an example of the nature of the environment in which the fractionation of the low-Mg series basalts has occurred.
If so these intrusive masses may be expected to show the southward decrease in K_2O, TiO_2 and possibly MgO displayed by the basic lavas, which in turn may be a reflection of mantle inhomogeneity.

The rhyolitic volcanics in the Karoo province are restricted to the western and eastern margins of the African sub-continent. This restriction of the rhyolites to the continental margins provides some evidence that the generation of the rhyolitic magma could be associated with the fragmentation of Gondwanaland. Rising temperatures in the lower continental crust could be initiated by downwarping of the continental margin or upwelling of mantle material at the point of separation of Africa and Antarctica. Upwelling of mantle material could also lead to partial melting of this upper mantle material and thus alternative modes of generation of the rhyolitic magma are possible.

A more detailed examination of the distribution of the Lebombo rhyolites shows, however, that spatially they are closely associated with the Lebombo tectonic - volcanic belt, rather than the present margin of Africa. In the Nuanetsi area for example

the Lebombo is some 500 to 600 kilometers from the edge of the continental shelf. The Lebombo belt, however, represents the southern end of the African Rift System which has developed along the lines of pre-existing, much older crustal structures, (Wooley and Garson, 1970), and it appears possible that this structure has controlled the geographic distribution of the Lebombo rhyolites by providing a relatively easy mode of access to the surface.

Along the west coast of the sub-continent, similar rock types have been produced, but as a result of the absence of a structure analogous to that of the southern end of the African rift system the structure and distribution of these volcanics differs widely from those forming the Lebombo belt.

REFERENCES

ADAMS, F.D. 1910. An experimental investigation into the action of differential pressure on certain minerals and rocks, employing the process suggested by Professor Kick. J.Geol., 18, pp. 489-525.

BARKER, D.S. 1978. Magmatic trends on alkali-iron-magnesium diagrams. Am. Mineralogist, 63, pp.531-534.

BELOUSOV , V.V. 1962 Basic problems in geotectonics. Mcgraw-Hill Book Company Inc.,New York and London.

BHATTACHARJI, S. 1967. Mechanics of flow differentiation in mafic and ultramafic sills. Jour. Petrol., 75, p101.

BHATTACHARJI, S. and SMITH,C.H. 1964. Flowage differentiation. Science, 145, pp. 150 153.

BIDYUT, B. 1967. Mechanical properties of rocks at high temperatures and pressures. Inst. of Geol. and Devel. of Min. Res., Moscow. English trans., Fitzsimmons,J.P., Consultants Bureau, New York.

BOWEN, N.L. and SCHAIRER, J.F. 1935. The system Mgo-FeO-SiO_2. Am. J. Sci., 229, pp. 151-217.

BOYD, F.R. 1971. Anatomy of a mantled pigeonite from Oceanus Procellarum. Carnegie Inst. Washington Year Book, 69, pp. 511-543.

BROWN, G.M. 1957. Pyroxenes from the early and middle stages of fractionation of the Skaergaard Intrusion,East Greenland. Mineral. Mag., 31, pp.511-543.

BROWN, G.M. and VINCENT, E.A. 1963. Pyroxenes from the late stages of fractionation of the Skaergaard Intrusion. Jour. Petrol., 4, pp. 175-197.

BUDDINGTON, A.F. 1936. Gravity stratification as a criterion in the interpretation of the structure of certain intrusives of the north-western Adirondacks. Rept. 16th Internat. Geol. Congr. Washington.

CAMPBELL, I.H. 1978. Some problems with cumulus theory. Lithos, 11, pp.331-373.

CAMPBELL, I.H. and BORLEY, G.D. 1974. The geochemistry of pyroxenes from the lower layered series of the Jimberlana Intrusion, Western Australia. Contrib. Mineral. Petrol., 47, pp. 281-297.

CARMICHAEL, I.S.E. 1964. The petrology of Thingmuli, a Tertiary volcano in Eastern Iceland. J. Petrol.,5, pp. 435-460.

CARMICHAEL, I.S.E., NICHOLLS, J., and SMITH, A.L. 1970. Silica activity in igneous rocks. Am. Mineralogist, 55, pp. 246-263.

CAWTHORN, R.G. and O'HARA, M.J. 1976. Amphibole fractionation in calc-alkaline magma genesis. Am. J. Sci., 276, pp 309-329.

CHAYES, F. 1967. On the graphical appraisal of the strength of assosciations in petrographic variation diagrams. Researches in Geochemistry, Abelson, P.H., J. Wiley and Sons, New York.

*COHEN, E. 1875. Erlauternde Bemerkungen zu der Routenkarte einer Reise von Lydenburg nach der Goldfeldern und von Lydenburg nach der Delagoa Bai im östlichen Sd-Afrika. Jahresber. d. geog., Hamburg, pp. 244-299.

COOK, E.F. 1955. Nomenclature and recognition of ignimbrites. Geol. Soc. America Bull., 66,p. 1544.

COX, K.G., JOHNSON, R.L., MONKMAN, L.J., STILLMAN, C.J., VAIL, J.R., and WOOD, D.N. 1965. The geology of the Nuanetsi Igneous Province. Phil. Trans. roy. Soc. Lond.,Ser. A, 257, pp. 71-218.

COX, K.G. 1970. Tectonics and volcanism of the Karroo Period and their bearing on the postulated fragmentation of Gondwanaland. African Magmatism and Tectonics, Clifford,T.N., and Gass, I.G. Oliver and Boyd, Edinburgh. pp. 211-235.

COX, K.G. 1972. The Karroo Volcanic Cycle. Jl. geol. Soc. Lond., 128, pp.311-336.

COX, K.G. and HORNUNG,G. 1966. The petrology of the Karroo Basalts of Basutoland. Am. Mineralogist, 51, pp.1414-1432.

COX, K.G.,MACDONALD,R. AND HORNUNG, G. 1967. Geochemical and petrographic provinces in the Karroo Basalts of Southern Africa. Am. Mineralogist, 52, p. 1451.

DE ASSUNCÃO, A.F.T., COELHO, A.V.P., and ROCHA, A.T. 1962. Petrologia das lavas dos Lebombo. Mem. Junta Invest. Ultramar, (Lisbon), 99, 74pp.

DU TOIT, A.L. 1929. The Volcanic Belt of the Lebombo - a region of tension. Trans. roy. Soc. S. Afr., 18, 189pp.

DU TOIT, A. L. 1954. Geology of South Africa, 3rd Edition. Oliver and Boyd, Edinburgh.

DONALDSON, C.H. 1975. Ultramafic inclusions in anorthite megacrysts from the Isle of Skye. Earth Planet. Sci. Lett., 27, pp. 251-256.

DRAKE, M.J. 1976. Plagioclase-melt equilibria, Geochim. Cosmochim. Acta, 40, p457.

EALES, H.V. and ROBEY, J. VAN A. 1976. Differentiation of tholeiitic Karroo magma at Birds River, South Africa. Contrib. Mineral. Petrol., 56, pp. 101-117.

ERNST, W.G. 1960. Diabase-granophyre relations in the Endion Sill, Duluth, Minnesota. Jour. Petrol., 1, pp. 286-302.

FAIRBAIRN, H.W. 1942. Structural petrology of deformed rocks. Addison and Wesley, Cambridge, Mass.

FRANKEL, J.J. 1960. Late Mesozoic and Caenozoic events in Natal, South Africa. Trans. N. Y. Acad. Sci., 22, pp. 565-577.

GOODMAN, R.J. 1972. Distribution of Ga and Rb in coexisting groundmass and phenocryst phases of some basic volcanic rocks. Geochim. Cosmochim. Acta, 36, pp. 303-317.

GRIGGS, D.T., TURNER, F.J., and HEARD, H. 1960. Deformation of rocks at 500 - 800°C. Geol. Soc. Amer., Mem. 79.

GRIGOR'EV, D.P. 1965. Ontogeny of minerals. Israel program for Scientific Translations, S. Monson, Jerusalem.

GUNN, B.G. 1962. Differentiation in Ferrar Dolerites, Antartica. N.Z.J. Geol. Geophys., 5, pp. 820-863.

GUNN, B.G. 1971. Trace element partition during olivine fractionation of Hawaiian basalts. Chem. Geol., 8, pp. 1-13.

HAMILTON, D.L. and ANDERSON, G.M. 1968. Effects of water and oxygen pressure on the crystallisation of basaltic magmas. In 'Basalts'. Poldervaart, A., and Hess,H., 2, pp. 573-622. J. Wiley and Sons, New York.

HAUGHTON, S.H. 1963. The stratigraphic history of Africa South of the Sahara. Oliver and Boyd, Edinburgh and London.

HAUGHTON, D.R., ROEDER, P.L., and SKINNER, B.J. 1974. Solubility of sulfur in mafic magmas. Econ. Geol., 69, pp. 451-467.

IRVINE, T.N. 1963. Origin of the ultramafic complex at Duke Island, Southeastern Alaska. Min. Soc. Amer. Special Paper 1, 36-45.

IRVINE, T.N. 1965. Sedimentary structures in igneous intrusions with particular reference to the Duke Island Ultramafic Complex. Soc. Econ. Palaeontol. Mineral. Special publ. 12, pp. 220-232.

JACKSON, E.D. 1961. Primary textures and mineral assosciations in the ultramafic zone of the Stillwater Complex, Montana. U.S. Geol. Surv. Prof. Paper, 358, pp. 1-106.

JAMIESON, B.G. 1966. Evidence on the evolution of basaltic magma at elevated pressures. Nature, 212, pp. 243-246.

JAMIESON, B.G. and CLARKE, D.B. 1970. Potassium and assosciated elements in tholeiitic basalts. Jour. Petrol., 11, part2, pp. 243-246.

JOHNSON, R.L. 1966. The Shawa and Dorowa carbonatite complexes, Rhodesia. Carbonatites, Tuttle, O.F., and Gittins, J. Interscience Publishers, New York, London, and Sydney.

KING, L.C. 1962. Morphology of the Earth. 1st Edition. Oliver and Boyd, Edinburgh and London.

KRETZ, R. 1961. Some applications of thermodynamics to coexisting minerals of variable composition. Examples: orthopyroxene - clinopyroxene and orthopyroxene - garnet. J. Geol., 69, pp. 361-387.

KRETZ, R. 1963. Distribution of magnesium and iron between orthopyroxene and calcic pyroxene in natural mineral assemblages. J. Geol., 71, pp. 773-785.

KUSHIRO, I. 1960. Si-Al relations in clinopyroxenes from igneous rocks. Am. J. Sci., 258, pp. 548-554.

KUNO, I. 1959. Origin of Cenozoic petrographic provinces of Japan and surrounding areas. Bull. Vulcanologique, ser. II, 20, pp.37-76.

KYNASTON, H. 1907. The geology of the neighbourhood of Komatipoort. Trans. geol. Soc. S. Afr., 9, p. 18.

LE BAS, M.J. 1962 The role of aluminium in igneous clinopyroxenes with relation to their parentage. Am. J. Sci., 260, pp. 267-288.

LOMBAARD, B.V. 1952 Karroo dolerites and lavas. Trans. geol. Soc. S. Afr., 55, pp. 175-198.

LONGHI, J., WALKER, D., and HAYS, J.F. 1975. Fe-Mg distribution between olivine and lunar basaltic liquids,EOS. Trans. Am. Geophys. Union,56, p. 471.

MARSHALL, P. 1935. Acid rocks of the Taupo-Rotorau volcanic district. Trans. roy. Soc. N.Z., 164, pp. 323-366.

MANTON, W.I. 1968. The origin of assosciated basic and acid rocks in the Lebombo-Nuanetsi Igneous Province, Southern Africa, as implied by Strontium Isotopes. Jour. Petrol. 9, pp. 23.

MAUD, R.R. 1961.A preliminary review of the structure of coastal Natal. Trans. geol. Soc. S. Afr., 54, pp. 247-256.

MCBIRNEY, A.R. 1975. Differentiation of the Skaergaard Intrusion. Nature, 253, pp. 691-694.

MCDOUGALL, I. 1962. Differentiation of the Tasmanian dolerites, Red Hill dolerite - granophyre assosciation. Geol. soc. America Bull., 73, pp. 279-416.

MOLENGRAAFF, G.A. 1897. Report of the State Geologist, S.A.R., English Translation, p. 138.

*MUGGË, O. 1898. Ueber Plasticität und verwandte Erscheinungen in Kristallen. Nues Jahrb., 1, pp. 102-108.

MURTHY, V.R. and GRIFFIN, W.L. 1970. K/Rb fractionation by plagioclase feldspars. Chem. Geol., 6, 265-271.

MYSEN, B.O. 1974. The oxygen fugacity as a variable during partial melting of peridotite in the upper mantle. Carnegie Inst. Washington Year Book, 73, pp. 237-240.

NASH, W.P. 1976. Fluorine, Chlorine and OH-bearing minerals in the Skaergaard Intrusion. Am. J. Sci., 276, pp. 546-557.

NWE, Y.Y. 1976. Electron-probe studies of the earlier pyroxenes and olivines from the Skaergaard Intrusion, East Greenland. Contrib. Mineral. Petrol., 55, pp. 105-126.

NWE, Y.Y. and COPLEY, P.A. 1975. Chemistry, subsolidus relations and electron petrography of pyroxenes from the late ferrodiorites of the Skaergaard Intrusion, East Greenland. Contrib. MIneral. Petrol., 53, pp.37-54.

O'HARA, M.J. 1963. Distribution of iron between coexisting olivines and pyroxenes in peridotite, gabbros and other magnesian environments. Am. J. Sci., 261, pp. 32-46.

O'HARA, M.J. 1968. The bearing of phase equilibria studies in synthetic and natural systems on the origin and evolution of basic and ultrabasic rocks. Earth-Sci. Rev., 4, pp. 69-133.

OSBORNE, E.F. 1959. Role of oxygen pressure in the crystallisation and differentiation of basaltic magma. Am. J. Sci., 257, pp. 609-647.

OSBORNE, E.F. 1962. Reaction series of subalkaline igneous rocks based on different oxygen pressure conditions. Am. Mineralogist, 47, pp. 211-226.

PETTIJOHN, I.J. 1957. Sedimentary Rocks, Second Edition. Harper Brothers, New York. 718 pp.

PHILPOTTS, A.R. 1978. Textural evidence for liquid immiscibility in tholeiites. Min. Mag.. 42, pp.417-425.

POLDERVAART, A. 1944. The petrology of the Elephants Head dike and the New Amalfi sheet. Trans. roy. Soc. s. Afr. , 30, pp.85-119.

PRINZ, M. 1967. Geochemistry of basaltic rocks. Trace Elements. In 'Basalts', Poldervaart,A. and Hess, H., 1, J. Wiley and Sons, New York, London and Sydney.

RALEIGH, C.B. and TALBOT, J.L. 1967. Mechanical twinning in naturally and experimentally deformed diopside. Am. J. Sci., 265, p.151.

RAMBERG, H. and DE VORE, G.W. 1951. Distribution of Fe^{++} and Mg^{++} in coexisting olivines and pyroxenes. J. Geol., 59, pp.193-210.

ROEDER, P.L. 1974. Activity of iron and olivine solubility in basaltic liquids. Earth Planet. Sci. Lett., 23, p.397.

ROEDER, P.L. and EMSLIE, R.F. 1970. Olivine-liquid equilibrium. Contrib. Mineral. Petrol., 29, p. 275.

ROEDER, P.L. and OSBORNE, E.F. 1966. Experimental data for the system $MgO-FeO-Fe_2O_3-CaAl_2Si_2O_8-SiO_2$ and their petrological implications. Am. J. Sci., 264, pp. 428-480.

ROOBOL, M.J. 1972. Size-graded igneous layering in an Icelandic intrusion. Geol. Mag., 109(5), pp. 393-404.

SAGGERSON, E.P. and LOGAN, C.T. 1970. Distribution controls of layered and differentiated mafic intrusions in the Lebombo Volcanic Sub-Province. Symposium on the Bushveld Igneous Complex and other Layered Intrusions. Geol. Soc. S. Afr., Special Publication,1.

SPRY, A. 1969. Metaphorphic Textures. Pergamonn press, Oxford.350 pp.

STEINER, J.C., JAHNS,R,H. and LUTH, W.C. 1975. Crystallisation of alkali feldspar and Quartz in the haplogranite system $NaAlSi_3O_8$-$KAlSi_3O_8$-SiO_2-H_2O at 4 Kb. Geol. Soc. America Bull., 86, pp. 83-98.

STRATTEN, T. 1965. The pyroclastic and assosciated igneous rocks of the Lebombo Mountain Range south of the Great Usutu River, Zululand. Unpublished Thesis, Potchefstroom Univ.

SUKHESWALA, R.N.and POLDERVAART, A. 1958. Deccan basalts of the Bombay Area, India. Geol. Soc. America Bull., 69, pp.1476-1491.

TRUSWELL, J.F. 1967. A critical review of stratigraphic terminology as applied in South Africa. Trans. geol. Soc. S. Afr., 70, pp. 81-116.

TURNER, F.J., and VERHOOGEN,J. 1960. Igneous and metamorphic petrology. Mcgraw-Hill, New York.

URIE, J.G. and HUNTER, D.R. 1963. The geology of.the Stormberg Volcanics. Bull. geol. Surv. Swaziland, 3.

VAIL, J.R. 1968. The southern extension of the East African Rift System and related igneous activity. Geol. Rdsch., 57, p. 601.

VENTER, J. 1954. Geology of the Komatipoort Coalfields. Unpublished Report of the Geol. Surv. S. Afr., Pretoria.

VISSER, H.N. and VERWOERD, W.J. 1960. The Geology of the country North of Nelspruit. Explan. Sheet 22, Geol. Surv., Dept.Min., S. Afr.

VISSER, W. and KOSTER VAN GROOS, A.F. 1979. Effects of P_2O_5 and TiO_2 on liquid-liquid equilibria in the system K_2O-FeO-Al_2O_3-SiO_2. Am. J. Sci., 279, pp. 970-988.

WACHENDORF, H. 1971. Die Rhyolithe und Basalte der Lebombos im Hinterland von Lorenco Marques,(Mozambique). Geotekt. Forsch., 40, pp. 1-86.

WADSWORTH, W.J. 1961. The ultrabasic rocks of South-west Rhum. Phil. Trans. Roy. Soc. Lond., Ser. B, 244, pp. 21-64.

WAGER, L.R. 1968. Rhythmic and cryptic layering in mafic and ultramafic plutons. In 'Basalts', Poldervaart, A. and Hess, H., 2, pp. 573-622. J. Wiley and Sons, New York.

WAGER, L.R. and BROWN, G.M. 1968. Layered igneous rocks. Oliver and Boyd, Edinburgh and London.

WAGER, L.R. and DEER, W.A. 1939. Geological investigations in East Greenland, Pt. III, The petrology of the Skaergaard Intrusion, Kangerdlugssuaq, E. Greenland. Meddr. Grønland, 105, no. 4.

WALKER, F. 1964. A comparitive survey of four tholeiitic magma provinces. Krishnan Memorial Volume, Indian Geophys. Un., pp. 309-326.

WALKER, F. and POLDERVAART, A. 1949. Karroo dolerites of the Union of South Africa. Bull. geol. Soc. Amer. 60, pp. 591.

WOOLLEY, A.R. and GARSON, M.S. 1970. Petrochemical and tectonic relationship of the Malawi carbonatite-alkaline province and the Lupata-Lebombo volcanics. African Magmatism and Tectonics, Clifford, T.N. and Gass, I.g. Oliver and Boyd, Edinburgh, pp. 237-260.

WRIGHT, T.L. 1974. Presentation and interpretation of chemical data for igneous rocks. Contrib. Mineral. Petrol., 48, pp. 233-248.

* - Not consulted in the original.

Acknowledgements

The author would like to express his thanks to Professor E.P. Saggerson of the University of Natal for his continued interest and encouragement during the preparation of this thesis, and for many useful discussions, which directly influenced several of the conclusions reached here.

Thanks are also due to Professors Schreiner and Verbeek of the Chemistry Department of the University of Natal, for their aid with the atomic absorption techniques employed for several of the rock analyses.

In addition, the author is indebted to the Geological Survey, the National Institute for Metallurgy and Professor Erlank of the University of Cape Town, for the majority of the chemical analyses. The National Institute for Metallurgy, and in particular, Dr. S.A. Hiemstra and Mr. E.A. Viljoen are thanked for the electron-microprobe analyses of minerals and for help with various other aspects of the work.

The assistance of my wife, Margaret, with the diagrams was of considerable value and is greatly appreciated.

In the final stages of preparation of the thesis, Mr. A. de Sousa provided help in the preparation of some of the photographs and Miss L. Haig assisted in proof-reading the thesis, which is gratefully acknowledged.

APPENDIX

1. Experimental Methods

1.1. Mineralogical Determinations

Election microprobe analyses of selected mineral grains were made by the National Institute for Metallurgy using an A.R.L. microprobe analyser with wavelength dispersive crystal spectrometers. Several points on each grain were analysed and averaged to obtain the final analysis in most cases. The electron microprobe data was processed using the program developed by Rucklidge and Gasparrini, (1969).

Optical estimates of plagioclase, pyroxene and olivine compositions were made using standard determinative methods. In the case of pyroxene, the methods described by Hess (1960) were followed and for plagioclase both refractive indices and the universal stage techniques described by Slemmons (1962), were employed. Plagioclase twin laws were also determined from the charts supplied by Slemmons, (1962). Where the structural state of the plagioclase is mentioned, this has been determined by the plotting of optic elements on the relevant diagram given by Marfunin, (1966, Figure 51). All refractive index measurements were made in sodium light, using standard Cargille liquids, the refractive index of which was checked on a refractometer, both before and after use.

Estimates of composition from these optical properties were made, where possible, using the curves recommended by Brown (1967). These include Deer et al., (1963, vol. 1. Figure 11, vol 2, Figure 10) and Brown and Vincent (1963, Figure 5). In places, however, the curves of Poldervaart (1950) and Hess, (1949) were used.

In some instances divine compositions were identified using the X-ray diffraction method recommended by Jambor and Smith,(1964).

1.2. ANALYTICAL METHODS

Whole rock analyses for major elements were performed on a Tectron AA3 atomic absorption spectrophotometer using techniques

developed by the Department of Chemistry, University of Natal, Pietermaritzburg and the Coronation Brick and Tile Company, Durban,R.S.A. All analyses were performed in duplicate, and analyses totalling less than 99 per cent or greater than 102 per cent were rejected.

1.2.1. Dissolution

Two solutions of each sample were made per analysis, one a sodium hydroxide fusion that was analysed for SiO_2 only, and the other a hydrofluoric acid-perchloric acid process, that was analysed for all other required elements. A standard amount of lanthanum oxide was added to each solution to act as a suppressant.

1.2.2. Determinations

Quantitative determinations were made by two methods:

(a) Plotting of unknown sample readings on curves prepared from a series of standards of known composition. (G1, W1, U.S. Geological Survey Standards, B.C.S. 269 Firebrick Standard).

(b) The method of standard additions.

In addition the relative proportions of FeO and Fe_2O_3 were determined by a potassium dichromate titration.

Whole rock analyses performed by the National Institute for Metallurgy were made using standard X-ray fluorescence and wet chemical methods.

1.3. STAINING TECHNIQUE

Where clouding prevented the identification of feldspars, (particularly in the acid volcanics), potassium feldspars were distinguished from plagioclase by staining of both polished slabs and thin sections, using the techniques described by Bailey and Stevens, (1960).

1.4. NORMS AND NIGGLI VALUES

Calculations of norms and niggli values for many of the analyses presented was performed by Dr. J.W. von Backström on an I.B.M. S/360 model 40G computer using a program developed by Van Niekerk and Von Backström, (1966).

REFERENCES

BAILEY, E.H., and STEVENS, R. 1960. Selective staining of k-feldspar and plagioclase on rock slabs and thin sections. Am. Mineralogist, 45, pp. 1020-1025.

BROWN, G.M. 1967. Mineralogy of basaltic rocks. Basalts, Poldervaart, A., and Hess, H., I.J. Wiley and Sons, New York, London and Sydney.

BROWN, G.M., and VINCENT, E.A. 1963. Pyroxenes from the late stages of fractionation of the Skaergaard intrusion. Jour. Petrol., 4, pp. 175-197.

DEER, W.A., HOWIE, R.A., AND ZUSSMAN, J. 1963. Rock forming minerals. Longmans, London, 1, 2, 4.

HESS, H.H. 1949. Chemical composition and optical properties of common clinopyroxenes, Pt. 1. Am. Mineralogist, 34, pp. 621-666.

HESS, H.H. 1960. Stillwater Igneous Complex, Montana: a quantitative mineralogical study. Mem. Geol. Soc. Amer., 80, 230pp.

JAMBOR, J.L., and SMITH, C.H. 1964. Olivine composition determination with small diameter X-ray powder cameras. Min. Mag., 1964, 33, pp 730-741.

MARFUNIN, A.M. 1966. The feldspars. Israel Program for Scientific Translations, Jerusalem. 317pp.

POLDERVAART, A. 1950. Correlation of physical properties and chemical composition in the plagioclase, olivine, orthopyroxene series. Am. Mineralogist, 135, pp. 1067-1079.

RUCKLIDGE, J.C., and GASPARRINI, E.L. 1969. Specifications of a complete program for processing electron microprobe data: EMPADR VII. Circular, Dept. of Geology, University of Toronto, Canada.

SLEMMONS, D.B. 1962. Determination of volcanic and plutonic plagioclases using a 3 or 4 axis universal stage. Geol. Soc. America, Special Paper 69, 64pp.

VAN NIEKERK, H., and VON BACKSTRÖM, J.W. 1966. A Fortran IV computer code for calculation of C.I.P.W. norms and niggli values. Atomic Energy Board Report PEL 126, Pelindaba, Republic of South Africa.